50272-101

REPORT DOCUMENTATION PAGE	1. REPORT NO. NCEER-92-0031	2.	3. PB93-198315
4. Title and Subtitle: Evaluation of Seismic Retrofit of Reinforced Concrete Frame Structures: Part II - Experimental Performance and Analytical Study of a Retrofitted Structural Model			5. Report Date: December 8, 1992 6.
7. Author(s): J.M. Bracci, A.M. Reinhorn and J.B. Mander			8. Performing Organization Rept. No.
9. Performing Organization Name and Address: Department of Civil Engineering State University of New York at Buffalo Buffalo, New York 14260			10. Project/Task/Work Unit No. 11. Contract(C) or Grant(G) No. (C) BCS 90-25010 (G) NEC-91029
12. Sponsoring Organization Name and Address: National Center for Earthquake Engineering Research State University of New York at Buffalo Red Jacket Quadrangle Buffalo, New York 14261			13. Type of Report & Period Covered: Technical Report 14.

15. Supplementary Notes
This research was conducted at the State University of New York at Buffalo and was partially supported by the National Science Foundation under Grant No. BCS 90-25010 and the New York State Science and Technology Foundation under Grant No. NEC-91029.

16. Abstract (Limit: 200 words)
This report is Part II of a two part series on the evaluation of seismic retrofit methods for concrete frame structures. It deals with the behavior of the entire structural system when several retrofit techniques are applied to individual components. An analytical and an experimental study was done on a scaled model of a structure and several retrofit techniques were evaluated. Part I describes the evaluation of individual components retrofitted and tested with cyclic loading, that provided the base for modeling of the entire structure presented in this report. In this report the evaluation of three retrofit techniques, i.e., concrete jacketing method, masonry jacketing method, and partial frame masonry infill, is presented based on an analytical study of retrofitting a typical lightly reinforced frame designed according to ACI 318-89 only for gravity loads (1.4D + 1.7L). The jacketing technique is further evaluated based on an experimental and analytical study using a 1:3 scale structural model subjected to simulated earthquake motion supplied by the seismic simulator (shaking table) at SUNY/Buffalo. The (jacketing) technique was applied only to selective portions of the structure, and it achieved the limited improvement of strength and damage control as required in moderate seismicity areas and as anticipated. This selected retrofit required only minimal structural interference and may prove to be economically attractive. The analytical modeling, based on component information (obtained from the study presented in Part I of this report series), shows that the overall response of retrofitted structures can be adequately estimated, if good information is available for the components.

17. Document Analysis a. Descriptors

b. Identifiers/Open-Ended Terms
Reinforced concrete frames. Retrofitting. Shaking table tests. Masonry infill. Concrete jacketing. Masonry jacketing. Scale model tests. Strong column weak beams. Gravity load design. Local member damage. Global failure mechanisms. Beam column joints. Added slab fillets. Earthquake engineering.

c. COSATI Field/Group

18. Availability Statement	19. Security Class (This Report)	21. No. of Pages
Release Unlimited	Unclassified	204

PB93-198315

NATIONAL CENTER FOR EARTHQUAKE ENGINEERING RESEARCH

State University of New York at Buffalo

Evaluation of Seismic Retrofit of Reinforced Concrete Frame Structures:

Part II — Experimental Performance and Analytical Study of a Retrofitted Structural Model

by

J.M. Bracci, A.M. Reinhorn and J.B. Mander

Department of Civil Engineering
State University of New York at Buffalo
Buffalo, New York 14260

Technical Report NCEER-92-0031

December 8, 1992

This research was conducted at the State University of New York at Buffalo and was partially supported by the National Science Foundation under Grant No. BCS 90-25010 and the New York State Science and Technology Foundation under Grant No. NEC-91029.

NOTICE

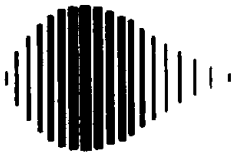

Evaluation of Seismic Retrofit of Reinforced Concrete Frame Structures:

Part II - Experimental Performance and Analytical Study of a Retrofitted Structural Model

by

J.M. Bracci[1], A.M. Reinhorn[2] and J.B. Mander[3]

December 8, 1992

Technical Report NCEER-92-0031

NCEER Project Numbers 89-1001A, 90-1001A and 91-3111B

NSF Master Contract Number BCS 90-25010
and
NYSSTF Grant Number NEC-91029

1 Research Associate, Department of Civil Engineering, State University of New York at Buffalo
2 Professor, Department of Civil Engineering, State University of New York at Buffalo
3 Assistant Professor, Department of Civil Engineering, State University of New York at Buffalo

NATIONAL CENTER FOR EARTHQUAKE ENGINEERING RESEARCH
State University of New York at Buffalo
Red Jacket Quadrangle, Buffalo, NY 14261

PREFACE

The National Center for Earthquake Engineering Research (NCEER) was established to expand and disseminate knowledge about earthquakes, improve earthquake-resistant design, and implement seismic hazard mitigation procedures to minimize loss of lives and property. The emphasis is on structures in the eastern and central United States and lifelines throughout the country that are found in zones of low, moderate, and high seismicity.

NCEER's research and implementation plan in years six through ten (1991-1996) comprises four interlocked elements, as shown in the figure below. Element I, Basic Research, is carried out to support projects in the Applied Research area. Element II, Applied Research, is the major focus of work for years six through ten. Element III, Demonstration Projects, have been planned to support Applied Research projects, and will be either case studies or regional studies. Element IV, Implementation, will result from activity in the four Applied Research projects, and from Demonstration Projects.

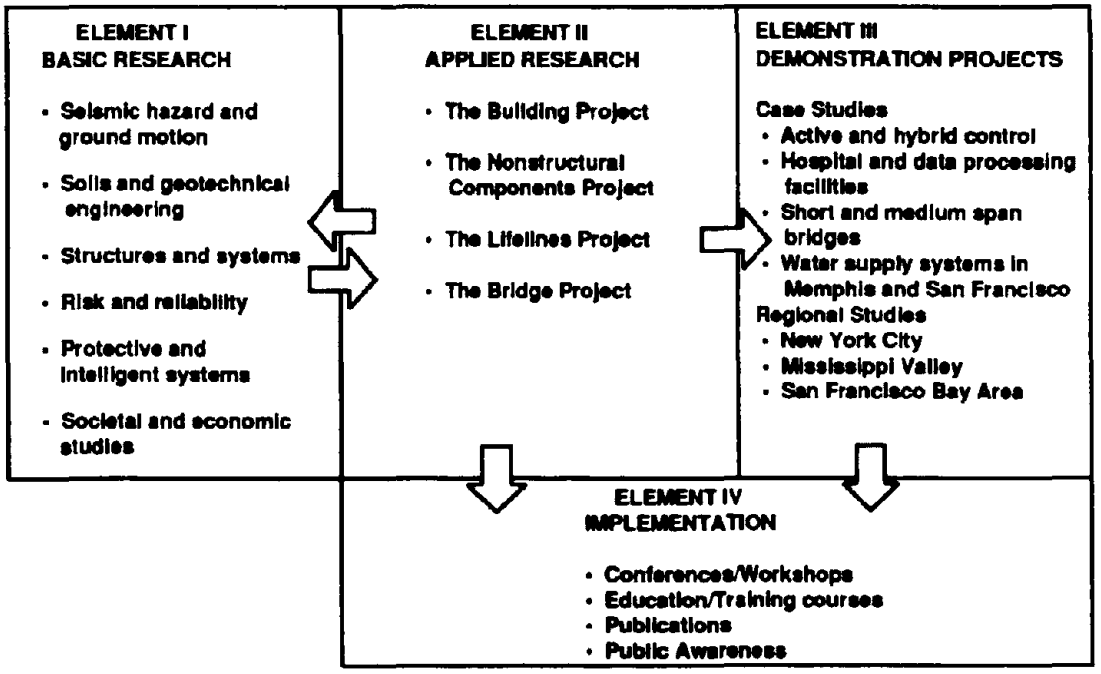

Research in the **Building Project** focuses on the evaluation and retrofit of buildings in regions of moderate seismicity. Emphasis is on lightly reinforced concrete buildings, steel semi-rigid frames, and masonry walls or infills. The research involves small- and medium-scale shake table tests and full-scale component tests at several institutions. In a parallel effort, analytical models and computer programs are being developed to aid in the prediction of the response of these buildings to various types of ground motion.

Two of the short-term products of the **Building Project** will be a monograph on the evaluation of lightly reinforced concrete buildings and a state-of-the-art report on unreinforced masonry.

The **structures and systems program** constitutes one of the important areas of research in the **Building Project**. Current tasks include the following:

1. Continued testing of lightly reinforced concrete external joints.
2. Continued development of analytical tools, such as system identification, idealization, and computer programs.
3. Perform parametric studies of building response.
4. Retrofit of lightly reinforced concrete frames, flat plates and unreinforced masonry.
5. Enhancement of the IDARC (inelastic damage analysis of reinforced concrete) computer program.
6. Research infilled frames, including the development of an experimental program, development of analytical models and response simulation.
7. Investigate the torsional response of symmetrical buildings.

This report is the second of a two-report series summarizing research on the retrofit of reinforced concrete buildings that had been designed only for gravity loadings. The first report is concerned with reduced-scale column, beam-column, and beam-column-slab specimens which were retested after retrofit. This report describes analytical and shake-table studies of a three-story building model which was first tested to near failure level loads. The retrofit of the damaged building included concrete jacketing and post-tensioning of the columns and slab fillets around the columns. The failure mechanism was successfully changed to a desirable weak-beam and strong-column failure.

ABSTRACT

This report is Part II of a two part series on the evaluation of seismic retrofit methods for concrete frame structures. It deals with the behavior of the entire structural system when several retrofit techniques are applied to individual components. An analytical and an experimental study was done on a scaled model of a structure and several retrofit techniques were evaluated. Part I describes the evaluation of individual components retrofitted and tested with cyclic loading, that provided the base for modeling of the entire structure presented in this report.

In this report the evaluation of three retrofit techniques, i.e., concrete jacketing method, masonry jacketing method, and partial frame masonry infill, is presented based on an analytical study of retrofitting a typical lightly reinforced frame designed according to ACI 318-89 only for gravity loads (1.4D + 1.7L).

The jacketing technique is further evaluated based on an experimental and analytical study using a 1:3 scale structural model subjected to simulated earthquake motion supplied by the seismic simulator (shaking table) at SUNY/Buffalo.

The (jacketing) technique was applied only to selective portions of the structure, and it achieved the limited improvement of strength and damage control as required in moderate seismicity areas and as anticipated. This selected retrofit required only minimal structural interference and may prove to be economically attractive.

The analytical modeling, based on component information (obtained from the study presented in Part I of this report series), shows that the overall response of retrofitted structures can be adequately estimated, if good information is available for the components.

ACKNOWLEDGEMENTS

Funding for this work was provided through the National Center for Earthquake Engineering Research (NCEER) Contract No. 891001A, 901001A, and 913111B under the National Science Foundation Master Contract No. ECE-86-07591 and the State of New York. The support is gratefully acknowledged.

The authors also acknowledge the assistance and contributions of Paul Reifler, Inc. (Mr. Tom Tallman and Mr. Bill Haas) and Master Builders, Inc. (Mr. Jim Shea) for materials toward the construction of the model building. Their devoted assistance was key to the success of the project.

The authors are grateful for the collaboration and assistance of Profs. Richard N. White and Peter Gergely of Cornell University throughout the duration of this study.

A special thanks is expressed to the laboratory technicians, Dan Walch, Mark Pitman, Dick Cizdziel, Xiaoqing Gao, and Paul Pattarroyo for their help and expertise during the construction and testing of the model. Thanks are also extended to John Valente and to all the undergraduate students who took an active part in the construction of the model. Their dedication to this project is gratefully acknowledged.

TABLE OF CONTENTS

TABLE OF CONTENTS (cont.)

LIST OF FIGURES

LIST OF FIGURES (cont.)

LIST OF FIGURES (cont.)

LIST OF TABLES

SECTION 1

INTRODUCTION

1.1 Background

The study presented herein is part of a comprehensive research program sponsored by the National Center for Earthquake Engineering Research (NCEER) on the seismic damage assessment and performance evaluation of buildings in zones of low seismicity, such as in the Eastern and Central United States. Buildings in such zones are typically designed only for gravity loads (U = 1.4D + 1.7L, herein referred to as GLD) according to the non-seismic detailing provisions of the code. These building are also termed lightly reinforced concrete (LRC) structures throughout this study. Although such structures are designed without consideration of lateral loads, they still possess an inherent lateral strength which may be capable of resisting some minor and moderate earthquakes. However the deficient detailing of members can lead to inadequate structural performance during seismic activity.

Two main parts from the current study (i) a seismic performance **Evaluation** of gravity load designed R/C Frame Buildings and (ii) an evaluation of seismic **Retrofit** of R/C frame structures. The first part will be mentioned as **Evaluation** and the second as **Retrofit**.

A research program on the **Evaluation of the seismic performance of gravity load designed R/C frame buildings** was developed and carried out according to the plan outlined in Fig. 1-1.

Based on a survey of typical building construction practices in the Eastern and Central United States (Lao, 1990 and El-Attar et al., 1991a and 1991b), a one-third scale model was constructed and tested on the shaking table in the State University of New York (SUNY) at Buffalo Earthquake Simulation Laboratory. The prototype design, model construction and similitude, initial dynamic characteristics, shaking table testing program along with the simulated ground motions, and the elastic response of the model from minor base motions are presented in Part I of the Evaluation Report Series (Bracci et al 1992b). Based on this report, analytical models can be developed and used to predict the inelastic response of the model building during more severe earthquakes.

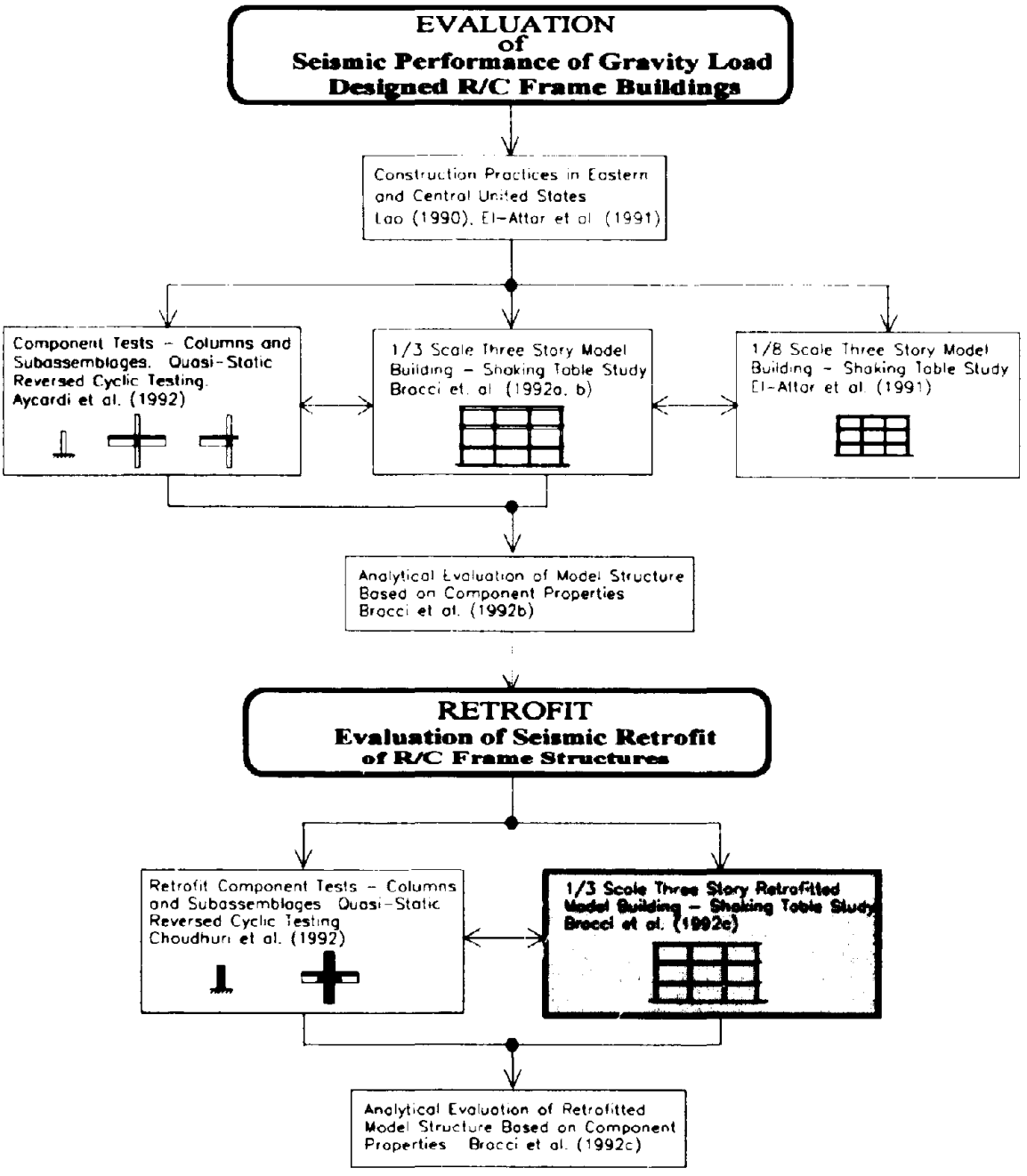

Fig 1.1 Research Context - Seismic Performance of Gravity Load Designed Reinforced Concrete Frame Buildings

Companion reduced scale slat-beam-column subassemblages were also constructed with the same materials in conjunction with the construction of the one-third scale model building are presented in Part II of the Evaluation Report Series (Aycardi et al., 1992). The components were tested under quasi-static reversed cyclic loading and conducted prior to the testing of the model building. The results of the component tests were used to identify the behavior of localized members and subassemblages of the structure and the member properties for predicting the overall response of the model building with analytical tools.

The experimental and analytical performance of the model building during moderate and severe shaking is presented in Part III of the Evaluation Report Series (Bracci et al., 1992b). The analytical predictions of the model building during these earthquakes are presented based on member behavior developed from engineering approximations and component tests. Some of the conclusions of the evaluation study are that the response of the model is governed by weak column - strong beam behavior and large story drifts develop under moderate and severe earthquakes. A one-eighth scale model of the same prototype building was also constructed and tested at Cornell University by El-Attar et al. (1991b) as part of a collaborative study with SUNY/Buffalo. A comparison of the response behavior between the two scale models is also presented.

A second part of this research program was conducted to evaluate various **seismic retrofit techniques for R/C frame structures** typically constructed in low seismicity zones (see Fig. 1-1). Based on the seismic behavior of the one-third scale model from the previous study, a series of retrofit schemes were proposed for improved seismic resistance and presented in this report which is Part II of the Retrofit Report Series.

In Part I of the Retrofit Report Series (Choudhuri et al., 1992) of this research program, a capacity analysis and redesign method for seismic retrofitting of R/C structures is developed and tested. Retrofit using an improved concrete jacketing technique was selected and first performed on companion components. The retrofitted components were then tested under quasi-static reversed cyclic loading and used to identify the behavior of the individual members. Retrofit of the components was also performed to verify the constructability of the retrofit technique for the model building.

The work done in Part I of the Retrofit Report Series is used as base to evaluate and model the member properties of the beam column components with the concrete jacketing technique and is used further for predicting the response of the overall retrofitted model building with analyses

presented in this report, which is Part II of the Retrofit Report Series. Based on analytical estimates, a global seismic retrofit for the one-third scale model building was proposed and constructed. An experimental and analytical shaking table study of the retrofitted model building was then conducted and the response behavior is presented. The main conclusions from this study are that seismic retrofit of gravity load designed R/C frame buildings: (i) can be designed to successfully enforce a strong column - weak beam behavior; and (ii) is a viable economic and structural alternative as compared to demolition and reconstruction of another.

1.2 Overall Objectives of Research Program

The objectives of the overall research program are summarized below along with the corresponding NCEER publications from Table 1-1:

1. Investigate the performance and principal deficiencies of typical LRC frame buildings during earthquakes through shaking table testing of a one-third scale model under minor, moderate, and severe earthquakes. (*Seismic Resistance of R/C Frame Structures Designed only for Gravity Loads: Parts I and III*, Evaluation report series, by J.M. Bracci, A.M. Reinhorn, and J.B. Mander)

2. Identify the potential collapse mechanisms for typical LRC frame buildings. (*Seismic Resistance of R/C Frame Structures Designed only for Gravity Loads: Part III*, Evaluation report series, by J.M. Bracci, A.M. Reinhorn, and J.B. Mander)

3. Determine the behavior and material properties of individual members and subassemblages of the structure. (*Seismic Resistance of R/C Frame Structures Designed only for Gravity Loads: Part II*, Evaluation report series, by L.E. Aycardi, J.B. Mander, and A.M. Reinhorn)

4. Determine the contribution of components in the overall response of the structure near collapse. (*Seismic Resistance of R/C Frame Structures Designed only for Gravity Loads: Parts II and III*, Evaluation report series, by J.M. Bracci, L.E. Aycardi, A.M. Reinhorn, and J.B. Mander)

TABLE 1-1 NCEER Publications Summarizing Current Study

EVALUATION SERIES:
Seismic Resistance of R/C Frame Structures Designed only for Gravity Loads
Part I: Design and Properties of a One-Third Scale Model Structure (by J.M. Bracci, A.M. Reinhorn, and J.B. Mander), NCEER-92-0027
(i) Identification of deficiencies of current engineering practice. (ii) Scale modeling. (iii) Experimental identification of structural characteristics. (iv) Ground motions for structural evaluation and experimental program. Note: This report serves as bare material for evaluation of analytical tools.
Part II: Experimental Performance of Subassemblages (by L.E. Aycardi, J.B. Mander, and A.M. Reinhorn), NCEER-92-0028
(i) Identify behavior and deficiencies of various components in structures. (ii) Identify member characteristics for developing analytical models to predict the seismic response of the one-third scale model structure. Note: This report serves as evaluation of structural characteristics to be incorporated in the evaluation of the entire structural system.
Part III: Experimental Performance and Analytical Study of Structural Model (by J.M. Bracci, A.M. Reinhorn, and J.B. Mander),NCEER-92-0029
(i) Investigate the performance and principal deficiencies of typical gravity load designed frame buildings during earthquakes through shaking table testing of a one-third scale model under minor, moderate and severe earthquakes. (ii) Identify the potential collapse mechanisms for such typical frame buildings. (iii) Compare the measured response of the model building with that predicted by analytical models developed from (1) engineering approximations, (2) component tests, and (3) an experimental fit using a non-linear time history dynamic analysis. Note: This report emphasizes the structural behavior, collapse margins via damage, and efficiency of predictions using component properties evaluated from tests.

RETROFIT SERIES:
Evaluation of Seismic Retrofit of R/C Frame Structures
Part I: Experimental Performance of Retrofitted Subassemblages (by D. Choudhuri, J.B. Mander, and A.M. Reinhorn), NCEER-92-0030
(i) Presentation of retrofit techniques. (ii) Identify constructability and behavior of retrofitted components. (iii) Identify retrofitted member characteristics for developing analytical models to predict seismic response of the retrofitted model building.
Part II: Experimental Performance and Analytical Study of Retrofitted Structural Model (by J.M. Bracci, A.M. Reinhorn, and J.B. Mander), NCEER-92-0031
(i) An analytical seismic evaluation of retrofitted gravity load designed frame buildings using various local and global retrofit techniques. (ii) Shaking table testing of one of the proposed retrofit techniques on the 1/3 scale model under minor, moderate, and severe earthquakes. (iii) Verify a change in formation of the potential collapse mechanism under ultimate load from an undesirable column-sidesway/soft-story mechanism to a more desirable beam-sidesway mechanism. (iv) Compare the measured response of the retrofitted model building with that predicted by analytical models developed from engineering approximations and component tests using a non-linear time history dynamic analysis.

5. Compare the measured response of the model building with that predicted by analytical models developed from engineering approximations or from component tests using a non-linear time history dynamic analysis. (*Seismic Resistance of R/C Frame Structures Designed only for Gravity Loads: Part III*, Evaluation report series, by J.M. Bracci, A.M. Reinhorn, and J.B. Mander)

6. Investigate appropriate local and global retrofit techniques for improving the seismic performance of LRC buildings. (*Evaluation of Seismic Retrofit of R/C Frame Structures: Part II*, Retrofit report series, by J.M. Bracci, A.M. Reinhorn, and J.B. Mander)

7. Investigate the seismic performance of the retrofitted model building and compare the measured response with the response of the original (unretrofitted) model from the same earthquakes. (*Evaluation of Seismic Retrofit of R/C Frame Structures: Part II*, Retrofit report series, by J.M. Bracci, A.M. Reinhorn, and J.B. Mander)

8. Determine the behavior and material properties of the retrofitted members and subassemblages of the structure. (*Evaluation of Seismic Retrofit of R/C Frame Structures: Part I*, Retrofit report series, by D. Choudhuri, J.B. Mander, and A.M. Reinhorn)

9. Determine the contribution of retrofitted and unretrofitted components in the overall response of the structure near collapse. (*Evaluation of Seismic Retrofit of R/C Frame Structures: Part I*, Retrofit report series, by D. Choudhuri, J.B. Mander, and A.M. Reinhorn)

10. Compare the measured response of the retrofitted model building with that predicted by analytical models developed from engineering approximations or from component tests using a non-linear time history dynamic analysis. (*Evaluation of Seismic Retrofit of R/C Frame Structures: Part II*, Retrofit report series, by J.M. Bracci, A.M. Reinhorn, and J.B. Mander)

1.3 Background to Present Study

The ensuing sub-sections provide a brief summary of some of the previously tested retrofit techniques for R/C structures.

1.3.1 Epoxy Injection Repairs

A form of repair for R/C members damaged by minor to moderate earthquakes is the epoxy repair technique. Two suitable techniques for repairing cracks are (i) the epoxy impregnation and (ii) pressure injection methods. Wolfgram-French et al. (1990) showed that both methods can restore member stiffnesses to about 85% of the original stiffness and the member strengths can be fully restored to the original strength capacity. It was also shown that both methods can restore the energy dissipation capacity and rebar bond strength of the damaged member specimens.

Although both of these methods can locally restore the stiffness and strength to members of the structure, the overall structural response still remains the same in event of future strong ground motions, similar to the one that caused the existing damage. Therefore, an upgrade (retrofit) for seismic protection of the structure can not be accomplished by using the epoxy injection techniques to the damaged R/C members.

1.3.2 Steel Jacketing

Circular and rectangular steel jacketing can be used to increase the flexural strength, ductility, and shear capacity of existing vulnerable columns. Chai et al. (1991) performed experimental cyclic tests on 0.4 scale models of circular bridge columns retrofitted by encasing the critical hinge regions with a steel jacket and bonded with concrete grout. Experimental verification of the increased flexural strength, ductility, and energy dissipation was achieved by the additional confinement from the jacket.

Beres et al. (1992) performed experimental cyclic testing using a steel jacketing retrofit of full scale interior and exterior joints with discontinuous bottom beam reinforcement and without a slab. The retrofit of the interior joints was directed at preventing pull-out of the bottom beam reinforcement. The resulting damage was transferred from the embedment zone to elsewhere in the joint panel. Whereas the retrofit of the exterior joint was directed at preventing splice failure in the column, spalling of the concrete cover of the joint, and pull-out of the bottom beam reinforcement. The resulting plastic hinge formed in the joint panel zone near the top of the beam. The steel jacketing schemes were proposed for zones of moderate seismicity.

1.3.3 Concrete Jacketing

Concrete jacketing has been widely used in repairing, strengthening, and improving the ductility capacity of damaged reinforced concrete columns: Bett et al. (1985); Iglesias (1986); Stoppenhagen and Jirsa (1987); Krause and Wight (1990); and many more. An existing vulnerable column is encased in a concrete jacket with additional longitudinal and closely spaced transverse reinforcement (for shear and confinement) to satisfy the required bending moment, shear force, and ductility demands. Mander et al. (1988a and 1988b) showed that substantial enhancements of compressive strengths can be achieved in heavily loaded columns with adequate confining steel.

Bett et al. (1985) performed several forms of concrete jacketing retrofit to short columns. Their general results were similar to those described above.

Stoppenhagen and Jirsa (1987) constructed a 2/3 scale model of a moment resisting frame with deep spandrel beams and short, slender columns. The frame was insufficient for ductility capacity and for strength under seismic loads. Concrete jacketing was used to increase the lateral strength capacity and to force the hinging into the beams. Under reversed cyclic loads up to 1.6% drift: (i) a ductile failure mechanism developed with hinging in the beams and small damage to the columns; and (ii) the lateral capacity of the retrofitted frame was 5 times greater than the original.

Krause and Wight (1990) constructed a 2/3 scale model of a 2 story R/C frame with a column jacketing retrofit. Under quasi-static reversed cyclic loading, the retrofit improved the strength and ductility of the columns, ductility of the beam-column joints, and hysteretic behavior of the frame. The energy dissipation capacity was increased and the failure mode was a ductile strong column - weak beam failure mechanism.

1.4 Concluding Previous Studies on Retrofit Techniques

The previous section provides a brief summary of some of the previously tested retrofit techniques for R/C structures. The appropriate seismic retrofit techniques for low-rise gravity load designed R/C frame structures would need to upgrade the structural strength and ensure life safety during seismic events. Epoxy repair techniques can not provide the required strength capacities to properly retrofit structural systems to resist earthquakes. Steel jacketing techniques, mainly used for increasing the member shear and ductility capacities, can only provide some local strength capacity increases, which may be insufficient for such structures. Deficiencies associated with the beam-column joints would also need appropriate retrofit considerations and

may generate problems using steel jacketing techniques. Concrete jacketing of columns in a structural system can be used to adequately increase the member strength capacities and effectively resist the forces generated by earthquakes. However constructability problems associated with the tightly spaced added transverse reinforcement may arise.

In this study, a global retrofit of the structural system using an improved concrete jacketing technique is applied only to selected columns. This method uses post-tensioning of the jacketed column and is accompanied by a beam-column joint strengthening.

1.5 Scope of Study in this Report

This report is Part II of a two part series on the evaluation of seismic retrofit techniques for reinforced concrete frames. In this report, several local and global retrofit techniques are proposed for repair and enhanced seismic resistance of gravity load designed reinforced concrete frame structures to ensure life safety during a future seismic event. An analytical seismic evaluation is performed for each retrofit alternative on the existing damaged model based on member properties from engineering approximations. One global retrofit alternative is selected for the structure based on the analytical seismic performance and retrofit constructibility. The retrofitted model was then tested on the shaking table under the same moderate and severe earthquakes previously performed. It is shown the retrofitted model performed adequately and was governed by a desirable strong column - weak beam behavior during the shaking.

Analytical modeling is based on integrating the identified member properties from original and retrofitted component tests and is used to interpret and predict seismic response of retrofitted model buildings. An analytical damage evaluation of the retrofitted model is also performed to assess structural integrity after the induced ground motions in terms of damage states.

The performance evaluation of the selected technique is done using the performance of individually retrofitted components studied in Part I of this report series. An analytical study was done using the information from individual components.

The following outlines the contents in each section of Part II of Retrofit Report Series (this report):

Section 2 summarizes the assessment of seismic damage states for typical R/C frame structures, followed by a discussion of the seismic local member damage versus global failure mechanisms.

Several local and global retrofit methods for GLD frame structures are presented. An analytical evaluation of the seismic response of the model with the various global retrofit alternatives is presented.

Section 3 summarizes the selected retrofit method and shaking table testing schedule for the model according to the analytical evaluation. The initial dynamic characteristics of the retrofitted model are also presented and compared with the previously damaged state of the model before retrofit.

Section 4 details the experimental performance of the retrofitted model during moderate and severe earthquakes. A corresponding damage evaluation and identification of the ensuing dynamic characteristics is presented. Analytical modeling, with member behavior developed from the component tests (from Part I of Retrofit Report Series), is used to predict the seismic response of the retrofitted model. Comparisons with the experimentally measured response are shown. An analytical quantification of damage from the earthquakes and an elastic analysis to identify the corresponding equivalent strength ratios from inelastic response are also presented. Finally, a summary of the maximum story response and dynamic characteristic history of the retrofitted model from the earthquakes is presented along with the concluding remarks on the seismic excitation of the retrofitted model.

Section 5 provides a summary of the experimental and analytical studies and concluding remarks concerning seismic retrofit of gravity load designed R/C structures.

SECTION 2

RETROFIT OF GLD R/C FRAME STRUCTURES

2.1 Introduction

Many gravity load designed (GLD) reinforced concrete frame structures, not specifically designed to withstand earthquakes, have survived minor, moderate, and severe magnitude earthquakes (Armenia, Turkey, Loma Prieta, and Mexico City). Their survival is because they have some inherent strength for resisting lateral forces. However, this inherent strength can not be regarded as sufficient for resisting all moderate or major type earthquakes, since earthquakes vary in magnitude, frequency content, and striking direction. In many areas, however, questions are repeatedly asked: Should a structure be retrofitted to adequately resist the large seismic forces of an earthquake? Or is the probability for occurrence of a strong ground motion too small to warrant retrofitting? The seismic retrofit (upgrade) of an undamaged structure to adequately absorb the seismic forces of an unexpected future earthquake can potentially be an expensive proposition. In the Eastern United States and other low seismicity zones, it may be very difficult to convince owners and/or government officials to invest in such retrofit of structures, except possibly for special structures. To address this dilemma, the study herein focuses primarily on relatively inexpensive retrofit techniques that can be applied to either damaged or undamaged structures in low to moderate seismicity areas. The same structural retrofit may also be required to guard against other hazards which produce large lateral loads such as hurricanes, tornados, and blasts.

2.2 Assessment of Seismic Damage States for R/C Structures

Following an earthquake, an engineering inspection and assessment of damage for most structures, including buildings, bridges, retaining walls, homes, apartment buildings, etc., may be required for further serviceability and for safety to the community. In this study, consideration will only be given to R/C frame structures and the damage which typically occurs in these structures from earthquake forces. The following classifications define damage states and limits along with a descriptive condition of a structure following an earthquake:

(a) ***minor damage - "serviceable" condition***. For this classification, the extent of damage to the structure may vary from no damage to slight cracking of the R/C members and should allow the structure to remain operational. Non-structural components may also have developed some minor cracking. However, no retrofit would be required with the exception of some patching (possibly epoxy injection which is described later) of the minor cracks in the structure.

(b) ***moderate damage - "repairable" condition***. The structure would be in need of repairs to regain a serviceable condition. The damage would be in the form of cracking in both the structural and non-structural elements. During the repair, the structure, or part thereof, may or may not be temporarily closed depending on the severity and location of the damage. The existing damaged structure must also be classified as either safe or unsafe from collapse in event of a future strong ground motion (possibly an after-shock), with the later meaning the temporary closure of the structure until a retrofit can be completed. Obviously, economics would play a vital role in the decision of whether to repair the existing damage or demolish the structure and possibly construct another. Nevertheless for a moderately damaged state, it is assumed that the retrofit of the structure is possible and more economically beneficial.

(c) ***severe damage - "irrepairable" condition***. The structure can be regarded as unsafe and in need of major restorations. Damage would result in the form of widespread cracking and spalling of the R/C structural and non-structural members. The onset of the resulting failure mechanism may be evident. The damage would initiate danger to the occupants of the structure and nearby individuals from the possibility of falling debris and the risk of collapse. Since the costs for repair could be considerable, the structure may be classified as irrepairable and thereby force immediate closure and demolition. However, it should be emphasized that such a damage state is expected for a very strong earthquake, when life safety is the greatest concern.

(d) ***partial or full collapse***. For completeness, the final damage state would be visually obvious and catastrophic. A separation area from the structure may be required

for the safety of the local residents in case of falling debris until total demolition could be completed. This damage state may well cause loss of life and therefore should be avoided in new design and retrofit of existing structures.

The previous descriptions categorized the damage states of R/C structures subjected to strong ground motions as either minor, moderate, severe, or collapse. Herein the retrofit of structures excited by seismic loads with a moderate (repairable) assessment of structural damage will be focused, in particular related to the one-third scale three story R/C frame model described in the preceding sections.

In general after strong shaking, all structures should be thoroughly inspected by an engineer and if necessary analyzed for the capability of resisting future ground motions. Next if required and desired, several retrofit schemes should be considered and analyzed to repair the induced structural damage. Since the repair might be very costly, a rigorous retrofit design should be considered to improve the structural response for any future strong ground motions (although this may not be a design criterion in low seismicity zones). This design must comply to a target damage state. In low seismicity areas, the target damage state for design is within the irrepairable damage state (near collapse, but not collapse).

2.3 Local Member Damage versus Global Failure Mechanisms

Researchers and engineers have gained tremendous knowledge from past earthquakes by studying the local and global damage of various typical structural members and components of R/C buildings, especially in moderate seismicity zones where some major earthquakes caused widespread damage and collapse of non-seismically designed structures (Armenia 1990).

The following discussions are related to the expected damage in R/C structures, not designed to withstand seismic loadings (GLD structures). Some of the ***local member damage concentrations (or failures)*** that can develop in GLD R/C structures from strong ground motions are outlined below, along with their impact on the overall (global) structural response.

(a) Beams:

(i) *Flexural failure* from steel yielding and concrete crushing, which is desirable in a global failure mechanism.

(ii) *Shear failure* from beam hinging due to minimal transverse reinforcement. This corresponds to a loss of moment capacity in the beams which can lead to large floor displacements under seismic as well as service loading.

(b) Columns:

(i) *Flexural failure* from steel yielding and concrete crushing, which is undesirable in a global failure mechanism.

(ii) *Transverse steel (hoop) fracture or buckling of the longitudinal steel in the columns* may occur due to inadequate shear and/or confining steel. The inadequate shear and confining steel results in a lack of member ductility, which can result in the development of an undesirable local column failure (hinging).

(iii) *Lap splice failure* may occur from critical stress concentrations from lateral loads in the splice zone (above story slab). This leads to loss of moment resistance and thus may promote a soft-story mechanism.

(iv) *Cover spalling* which leads to compression failure and an undesirable column failure.

(c) Beam-Column Joints:

(i) *Pull-out of the discontinuous positive beam reinforcement in the beam-column joints* from the unexpected positive moments. This localized failure results in an overall structural stiffness degradation that leads to large story deformations in event of future ground motions.

(ii) *Joint shear failure* may occur due to lack of or inadequate joint shear reinforcement. The global consequences are similar to (i).

(iii) *Sliding bond failure* of the beam reinforcement in the joints from localized crushing of the concrete due to repeated inelastic cycling.

(iv) *Spalling of the concrete cover in the exterior beam column joints*. The spalling of the concrete cover can lead to a column failure due to depreciating axial load capacity. The cover spalling may be indicative to the lack of anchorage for bars within the joint, which result also in a structural stiffness degradation.

In addition to the various local damages, ***global structural failures or collapse mechanisms*** can develop. These are major causes for partial or total collapse of structures. The possible basic collapse mechanisms for R/C structures are shown in Fig. 2-1 and are outlined below:

(a) *Column-Sidesway/Soft-Story Collapse Mechanism*
(b) *Beam-Sidesway Collapse Mechanism*
(c) *Hybrid Collapse Mechanism* - combination of (a) and (b)

Note that although mixed (hybrid) mechanisms are a possibility, the discussion is continued only to the basic mechanisms listed above as (a) and (b). For a typical gravity load designed R/C framed building excited by strong ground motions, laterally induced shear forces develop in the columns from the inertial loads causing large bending moment demands on the columns. The gravity load design column moments are relatively small since the beam design moments on each side of the column face tend to cancel. The columns are essentially constructed with minimum size and reinforcement. Such non-seismic detailing practice results inherently in a weak column - strong beam construction. Due to low strength, lack of member ductility resulting from a lack of seismic detailing, and the high degree of seismically induced bending moment, local hinging can develop in the columns. Such local column hinging can lead to the undesirable development of a *structural column-sidesway/soft-story (Fig. 2-1a) collapse mechanism*. These global failure mechanisms are well documented from past earthquakes and result in a brittle (non-ductile) sudden collapse of structures. A beam-sidesway mechanism is ideally the preferred mechanism since energy is dissipated more efficiently by plastic hinges in the beams, Park and Paulay (1975), and the vertical loads can still be transfer through the undamaged columns.

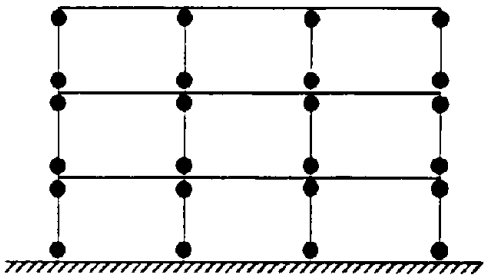

(a) Column-Sidesway/Soft Story (apparent in previous testing)

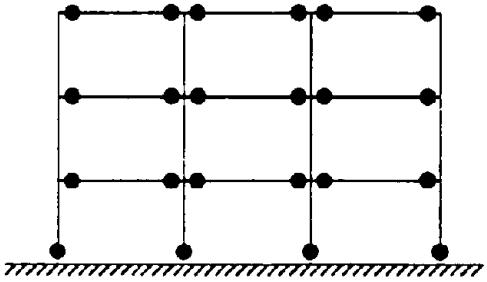

(b) Beam-Sidesway (desirable)

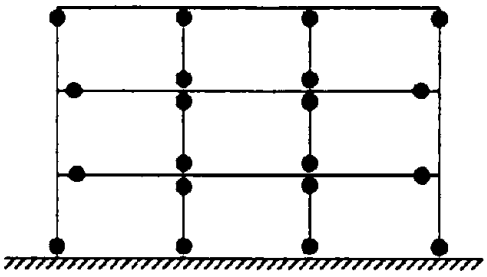

(c) Possible Hybrid

FIG. 2-1 Collapse Mechanisms for the Model Structure

2.4 Concerns and Expected Seismic Damage of GLD R/C Frame Structures

Some of the concerns of gravity load designed R/C frame buildings during earthquakes are: (i) Insufficient strength to stay within a functional stage and avoid large inelastic deformations; (ii) Danger of severe loss of life due to non-structural damage, such as windows, blocks, ceiling tiles, etc., due to large deformations; and (iii) Small margin of safety against total structural collapse.

It was shown in a previous report (Bracci et al., 1992b) that the columns of the low-rise GLD R/C frame model building were heavily damaged, ranging from moderate to severe damage states, from the simulated shaking table ground motions. An incipient column-sidesway/soft-story collapse mechanism was evident in the response during the simulated motions. This type of damage is also expected to occur in prototype low-rise buildings that have similar structural details during severe seismic events. In high-rise buildings where the columns in the lower stories carry large amounts of gravity loads and are appropriately designed, a desirable strong column - weak beam behavior inherently exists. However the columns in the upper stories of high-rise buildings contain smaller amounts of gravity loads and can be vulnerable to weak column - strong beam behavior during seismic activity, as the behavior in low-rise buildings.

In zones of low to moderate seismicity, the probability of occurrence of a severe earthquake is very small. Due to the concerns and expected (or actual) seismic damage in GLD frame buildings, seismic retrofit should focus on strengthening the columns such that they are stronger than the beams to enforce a more desirable beam-sidesway mechanism (Fig. 2-1b) and avoid the more dangerous soft-story mechanism (Fig. 2-1a). This retrofit will force the local damage from the vulnerable columns to be distributed into a larger number of beam and slab components of the structure. Since the beam-sidesway mechanism consists of a large number of hinges in the beams and only a few at the base columns, the resulting mechanism has a larger safety margin against collapse due to the larger rotational capability and energy dissipation capacity of the beam hinges as compared to the columns in a soft-story mechanism. Column strengthening would also result in a stiffer structure which should imply better control of the story displacements under the influence of large lateral loads. However, column stiffening may have an adverse effect on the response, as additional accelerations may result in larger base shear demands. In such cases, larger shear and moment demands are imposed on individual components. Therefore the local retrofit should be carefully designed and balanced in the overall (global) structural context.

2.5 Local and Global Retrofit Methods for GLD R/C Structures

In Section 1, several local repair and retrofit (upgrade) techniques previously performed and tested were identified in a literature survey. In this section, several local retrofit methods are proposed along with a summary of the design process. These methods are analyzed and compared in the context with the three story model structure presented in this study. The integration of the local retrofit in a structural system is further discussed and the results of testing one of the solutions is presented in Section 4.

2.5.1 Improved Concrete Jacketing

An improved concrete jacketing method, shown in Fig. 2-2, is proposed to satisfy some of the deficiencies of columns integrated in a gravity load designed R/C frame building. This retrofit technique is outlined below:

1. *Encase existing columns in a concrete jacket with additional longitudinal and transverse reinforcement.* For the upper columns of the structure where an increased strength is the main retrofit objective, the increased column size and added reinforcement would be such that the retrofitted columns have greater moment capacities than the corresponding adjacent beam (overstrength) capacities. However at the base columns, the retrofit objective is not to increase moment strength but to increase the shear and ductility capacities, since the foundation is presumed to be relatively weak. Therefore the reinforcement is not anchored in the foundation to avoid transmission of any additional stresses to the foundation. Another constructive reason for discontinuing the added rebars is that plastic hinges should form at the base columns in the desirable beam-sidesway mechanism (see Fig. 2-1b). Therefore instead of strengthening these sections and possibly altering the desirable mechanism, a hinge can always form at the base by the discontinuation of these rebars. Proper confinement is necessary to provide rotational ductility to these hinges. To deter any shear failure in the base columns, the additional transverse reinforcement should also provide a dependable shear strength for the most adverse combination of column end moments.

2. *Post-tension the longitudinal high strength column reinforcement.* The required longitudinal reinforcement in the column is housed in a sleeve from the mid-height of the first story to the roof and unbonded to the concrete. Below the mid-height of the first story, the longitudinal reinforcement is bonded to the concrete for anchorage. The

longitudinal reinforcement is post-tensioned vertically. The bonded reinforcement from the foundation to the mid-height of the first story (or higher) is to provide the required anchorage reaction to the applied prestressing force. Post-tensioning the added high strength reinforcement has the following beneficial aspects on the composite section:

(a) Enhances the shear capacity of the column and beam-column joint zone from the increased axial load by ensuring the structural behavior is always in the elastic regime.

(b) Provides an initial strain in the new composite section of existing concrete and added grout to ensure compatibility of the section.

(c) Provides a compressive pressure on the discontinuous positive beam reinforcement to deter pull-out.

3. *Provide a reinforced concrete fillet in the unreinforced beam-column joints for: (a) enhanced joint shear capacity; and (b) anchorage for the discontinuous beam reinforcement.* In addition to providing increased joint shear capacity with the concrete fillet, the negative bending moment capacity of the beams at the column face would also be increased due to the added compressive width from the confined concrete in the web of the beam from the fillet. The weak link is therefore forced to the end of the fillet. Since the development length of the positive beam reinforcement is also increased, the full positive moment strength of the beam section would be able to develop without pull-out occurring at the column face. Therefore by ensuring strong column - weak beam behavior and providing a fillet, the critical beam hinge would be forced away from the column face to a point near the end of the fillet with moment strengths of the unretrofitted beam section. The dimensions of the fillet are designed from the required development length of the discontinuous beam reinforcement and the designated hinge locations in the beams.

The relocation of the potential beam plastic hinges from the face of the columns was studied by Paulay and Bull (1979) and by Park and Milburn (1983). It was suggested from their studies to move the potential beam hinge the smaller distance of either the beam height or 500 mm. from the column face. Buchanan (1979) reported on the construction of New Zealand's tallest concrete building which uses spandrel beams with the potential beam hinges moved toward the center of the span. Paulay and Priestley

(1992) also summarized some of this work. Al-Haddad and Wight (1986) analytically studied the effects of moving the plastic hinge locations in beams. According to their conclusions, it is suggested to locate the potential plastic hinges in the beams approximately one beam depth away from the column face. This enables the joint core to remain elastic and provides a longer anchorage length for the beam bars.

Application of the above mentioned retrofit procedures to the three story frame model is outlined below:

Choudhuri et al. (1992) (see Part I of the Retrofit Report Series) quasi-statically tested a retrofitted companion interior sub-assemblage component of the model (column-beam-slab) using the improved concrete jacket retrofit for the column to determine construction feasibility and capacity limits of components (see Section 1 for details). It was observed that the column stiffnesses, strengths, and ductilities were dramatically increased. Severe damage was transferred to the beams and slab with primarily elastic behavior in the columns. Thus the desirable beam-sidesway mechanism developed in the sub-assemblage under large lateral cyclic loads.

Since appropriate column strength, ductility, and a desirable failure mechanism had resulted in this component test using the concrete jacketing method, a similar retrofit scheme was adopted in this study. The scheme was selectively applied to columns of the model by increasing the existing 4 in. square section to a 6 in. square section using the same concrete as in the component test. Fig. 2-3 shows the details of the improved concrete jacketing technique in a typical retrofitted column of the model. The added reinforcement consists of high strength 3/8 in. diameter threadbars (f_y = 120 ksi) housed in a plastic sleeve above the bottom half of the first story and post-tensioned at the root with a total force of about 31 kips (0.7 f_{pu}). The column section at the foundation has discontinuous added longitudinal reinforcement without prestressing and is considered as a regular reinforced concrete section.

From manufacturer (Master Builders, Inc.) specifications and tests conducted on the material during retrofit on 2 in. cubes, it is found that the concrete used in the jacket (Set-45) has characteristic properties of low shrinkage, high strength (28-day cylinder strength of about 8.0 ksi), modulus of elasticity of 5,250 ksi, and superior bond adhesion to the existing concrete columns. Since the special high strength concrete provides good bond to the existing concrete column, the retrofitted section can be idealized as a 6 in. square reinforcement concrete section with four layers of steel, two existing and two prestressed. For a conservative design, a

homogeneous concrete strength of 5.0 ksi is used for idealizing the composite section. Since initial stresses also exist in the added threadbars from prestressing, the yield strengths are appropriately adjusted for tensile and compressive strength capacities with a corresponding prestressing force applied to the section. Under ultimate load, the strains in the post-tensioned threadbars are assumed to be proportional with the strain profile in the concrete. Fig. 2-4a shows the interaction diagrams for the section with an applied prestressing force in the added reinforcement to 70% of the ultimate strength (31 kips total) and with the same bars without prestressing. It should be noted that since the interaction development considers the initial strains in the concrete and steel from prestressing, the axial load in the interaction diagram refers to additional axial loads only. It can be observed that the tensile capacities with and without prestressing are identical. However the compressive capacity and moment capacity at the corresponding dead loads for the prestressed section are smaller due to the applied compressive forces from prestressing. Although the effective capacity is somewhat smaller in the prestressed columns, the additional column and joint shear capacity, the uniformity of strains, and improved bond of the rebars in the joint are important benefits of retrofit.

From the prestressed section in Fig. 2-4a, it can be observed that the moment capacity of the retrofitted section without any axial load is about 110 kip-in, which is precisely the moment capacity observed in the component test, Choudhuri et al. (1992). Considering prestressing with the additional axial force from the dead loads (total of about 45 kips), the moment capacity is determined to be about 130 kip-in (for a first story upper interior column). It was shown by Bracci et al. (1992a and 1992b) that a first story interior column had an over-strength capacity of about 44.0 kip-in. Therefore, the bending moment strength of retrofitted column is increased about 200% with the concrete jacketing method. The nominal strength of the retrofitted columns of a first story interior beam-column joint section is about 59% stronger than the corresponding beams considering slab steel contributions from the full slab width and no pull-out effects (99 kip-in and 65 kip-in for the negative and positive beam moments, respectively). Due to disproportionate distributions of moments during higher mode response of frame buildings, ACI-318 requires a 20% increase in factored design column strength as compared to the design strength capacity of the beams. This corresponds to nominal column strengths of about 71% stronger the beam capacities with a strength reduction factor ϕ_c = 0.7 and 115% stronger if beam overstrength is considered. Therefore the column retrofit may not be adequate for a new design. For investigating the adequacy of a minimum retrofit, a lower bound retrofit solution was considered in this study appropriate for a low seismicity zone.

The interaction diagram of the base column, with discontinuous longitudinal reinforcement and a dead load of about 15 kips, is shown in Fig. 2-4b. It is developed based on a 6 in. square section with only the two existing layers of steel. It can be observed that a moment capacity of the base column is 70 kip-in. In comparison with the unretrofitted base column, the bending moment strength of this retrofitted column is increased about 59%.

Since the columns with the exception of the lower first story columns are retrofitted to remain primarily elastic, the non-seismically detailed beam-column joints must also remain elastic to avoid an undesirable joint shear failure. The existing interior columns of the model have no shear reinforcement in the joints. Therefore according to ACI-318 for an axial compression member, the code based shear capacity of the concrete, V_c, is defined as:

$$V_c = 2\left(1 + \frac{N_u}{2000A_g}\right)\sqrt{f'_c}\, b_w d \qquad (2.1)$$

where N_u = Factored axial load normal to the cross section

f'_c = specified compressive strength of concrete

b_w = web width

d = distance from extreme compression fiber to centroid of longitudinal tension reinforcement

Therefore using Eq. (2.1), the unretrofitted joint shear capacity from the concrete according to ACI-318 is 2.6 kips. Since this is expected to be inadequate for retrofit, a concrete fillet is used with additional joint reinforcement for added shear strength and confinement of the joint. Also since the development length of the positive reinforcement in the beams is inadequate for developing the full moment capacity, the concrete fillet can be designed to provide the additional development length required for this reinforcement.

The design of the fillet stems from basic mechanics. Paulay (1989) showed that the required joint shear reinforcement is equal to the sum of the forces from the positive and negative reinforcing steel in the beams. Fig. 2-5 shows a free body diagram of a column with maximum stresses in the positive and negative beam reinforcement due to applied shear forces in the columns. From equilibrium, the shear forces in the column can be solved as follows:

$$V' = |(C_t + T_t) - (C_b + T_b)| \cdot \frac{1}{2} + |(C_t + T_t) + (C_b + T_b)| \cdot \frac{z_d}{2l_c} \qquad (2.2a)$$

$$V = [(C_b + T_b) - (C_t + T_t)] \cdot \frac{1}{2} + [(C_t + T_t) + (C_b + T_b)] \cdot \frac{z_d}{2l_c} \qquad (2.2b)$$

where C_t, C_b = internal rebar compression forces, top and bottom, respectively

T_t, T_b = internal rebar tension forces, top and bottom, respectively

z_d = Distance between positive (bottom) and negative (top) beam reinforcement

l_c = Distance between story mid-heights

V' = Shear force at mid-height of the top column

V = Shear force at mid-height of the bottom column

Note that for symmetrically reinforced beams, V = V'.

The maximum shear force occurring in the joint, V_{joint}, can be described as follows:

$$V_{joint} = [(C_b + T_b) + (C_t + T_t)] \cdot \frac{1}{2} + [(C_t + T_t) + (C_b + T_b)] \cdot \frac{z_d}{2l_c} \qquad (2.3)$$

The dependable concrete shear strength, V_c, from ACI-318 for prestressed members is the smaller of V_{cw} and V_{ci} below:

$$V_{cw} = \left(3.5\sqrt{f'_c} + 0.3f_{pc}\right)b_w d \qquad \text{for uncracked sections} \qquad (2-4a)$$

$$V_{ci} = 0.6\sqrt{f'_c}\,b_w d + \frac{V_i M_{cr}}{M_{max}} \qquad \text{for cracked sections} \qquad (2-4b)$$

but not less than:

$$V_c \geq 1.7\sqrt{f'_c}\,b_w d \qquad (2-4c)$$

where V_i = factored shear force at section due to externally applied loads occurring simultaneously with M_{max}

M_{cr}, M_{max} = cracking moment and maximum factored moment at section

f_{pc} = compressive stress in the concrete due to prestressing and applied axial loads

The required joint steel shear capacity in the fillet, V_{sh}, can be represented in terms of the maximum joint shear force and the dependable concrete shear strength as follows:

$$V_{sh} = V_{joint} - V_c \tag{2.5}$$

The required joint steel area in the fillet, A_{sh}, can be determined as follows:

$$A_{sh} = \frac{V_{sh}}{f_{yh}} \tag{2.6}$$

where f_{yh} = transverse hoop yield strength

For the model structure, the internal beam compression and tension forces in the beam are:

$$T_t = 3A_s f_s = C_b \tag{2.7a}$$
$$T_b = 2A_s f_s = C_t \tag{2.7b}$$

where A_s = area of a D4 rebar (0.04 in.^{2})

f_s = beam steel stress at overstrength, taken as 1.25 f_y (1.25*68 ksi = 86 ksi)

C_b = force contribution from concrete and steel for equilibrium

Therefore inserting Eqs. (2.7a) and (2.7b) into Eqs. (2.2a) and (2.2b), the column shears can be represented as follows:

$$V' = A_s f_s + \frac{5A_s f_s z_d}{l_c} \tag{2.8a}$$

$$V = -A_s f_s + \frac{5A_s f_s z_d}{l_c} \tag{2.8b}$$

The maximum shear force which can occur in the beam-column joints of the model is described as:

$$V_{joint} = 5A_s f_s - \frac{5A_s f_s z_d}{l_c} \tag{2.9}$$

Therefore the maximum required joint shear capacity is about 15.2 kip (note the unretrofit joint shear capacity is 2.6 kips). Considering a total axial force of about 45 kips from dead and

prestressing loads and b_w = 14 in., the dependable concrete shear capacity from Eq. (2.4) is 6.2 kips. Therefore using Eqs. (2.5) and (2.6), the required area of the added reinforcement (unannealed D4 hoops with A_s = 0.04 in.^{2} and f_y = 82 ksi) in the fillet is calculated as: A_{sh} = 0.11 in^2 (2.75 legs). Therefore the provided joint reinforcement used for retrofit of the model is two (4 legs) unannealed D4 rebars fully around the fillet (see Fig. 2-3). A similar interior joint reinforcement detail was recently presented by Paulay and Priestley (1992) for a well-detailed joint section.

For the transverse reinforcement for the retrofitted columns, the required spacing of the added transverse hoops can be determined from ACI-318 as follow:

$$s_{req} = \frac{2A_{sh}f_{yh}d}{V_s} \tag{2.10}$$

where d = distance from the outermost compression fiber to the center of the longitudinal reinforcement in the beam

A_{sh} = area of added hoop reinforcement

f_{yh} = yield strength of the added hoop reinforcement

V_s = required shear strength

In the analytical study in the next sub-section, it is shown that the base shear capacity for the model from a shake-down analysis is about 22 kips (about 100% larger than unretrofitted). Since the moment of inertia of the retrofitted column is about 4 times the unretrofitted columns, the retrofitted column shear is estimated as 1/5 of total base shear from the ratio of total column stiffnesses in the model. Therefore from Eq. (2.10) with a column shearing force of 4.4 kips (1/5 of total base shear) and using ga. 11 black hoop reinforcement (see Bracci et al., 1992a for properties), the required spacing for the shear reinforcement in the base columns with no prestressing is obtained as 1.6 in. The provided spacing is 1-1/2 in. (1.5 in.). In the prestressed section, no shear reinforcement is required.

Some comments can be made about the construction and aesthetic characteristics of the concrete jacketing techniques:

(a) Drilling holes through the slabs and beams are required for pouring the concrete into the columns and continuity of the longitudinal reinforcement. Construction process requires formwork and is relatively easy, although drilling through the beam reinforcement should be avoided if possible.

(b) Closure of the structure would only be located in areas of retrofit, provided the structure has enough reserve strength to resist a near future earthquake. Therefore each story of the structure, or part thereof, would temporarily be closed only when the retrofit of that story is being worked on.

(c) Small reductions in the clear span widths would result for the retrofitted bay.

(d) Minimal amount of retrofit material, including transverse reinforcement, is required.

2.5.2 Masonry Block Jacketing

Similar to the concrete jacketing method, a masonry block jacketing method can be used for repairing and strengthening an existing damaged column. Fig. 2-6 shows a detail of a typical retrofitted column using the masonry jacketing technique. An existing damaged column can be strengthened by encompassing the existing section with masonry blocks. Some additional space between the existing concrete column and the new masonry blocks can be filled with grout and used for additional shear capacity and for addition of confining steel reinforcement to the existing column.

Additional longitudinal reinforcement, either prestressed or regular reinforcement, is provided in the jacketed zone extending continuously through the slabs. In this study, a prestressed reinforced concrete and masonry section is considered. The advantages of prestressing for this method are: (i) an increased shear capacity in the columns and joints; (ii) an initial uniform strain is obtained in the existing concrete and the new masonry blocks (for compatibility and for counteracting the stress losses from creep in the masonry joints); and (iii) a compressive pressure on the discontinuous positive beam reinforcement which would deter pull-out.

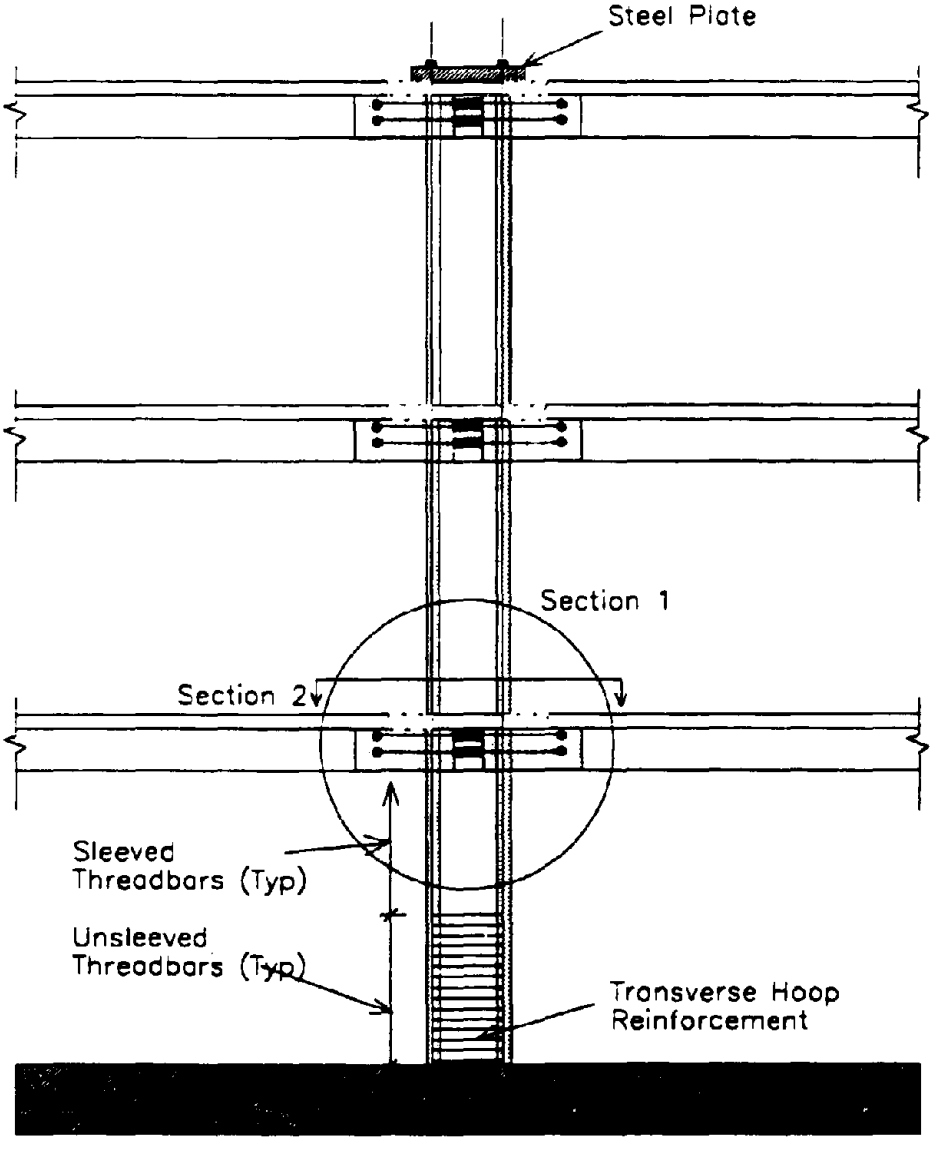

Elevation

FIG. 2-2a Improved Concrete Jacketing Technique

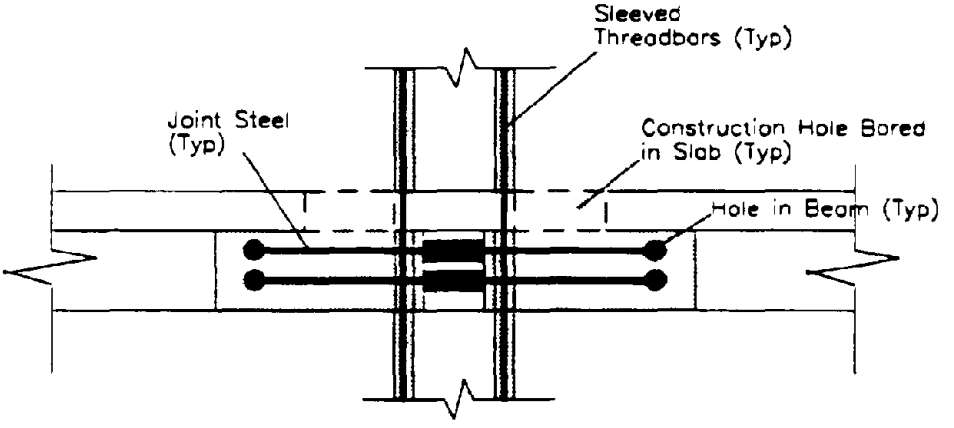

Section 1

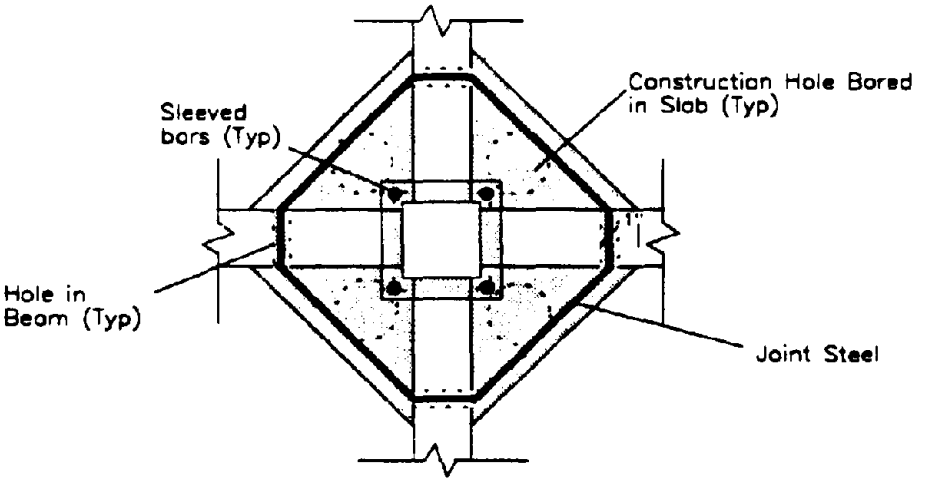

Section 2

FIG. 2-2b Improved Concrete Jacketing Technique (Cont'd)

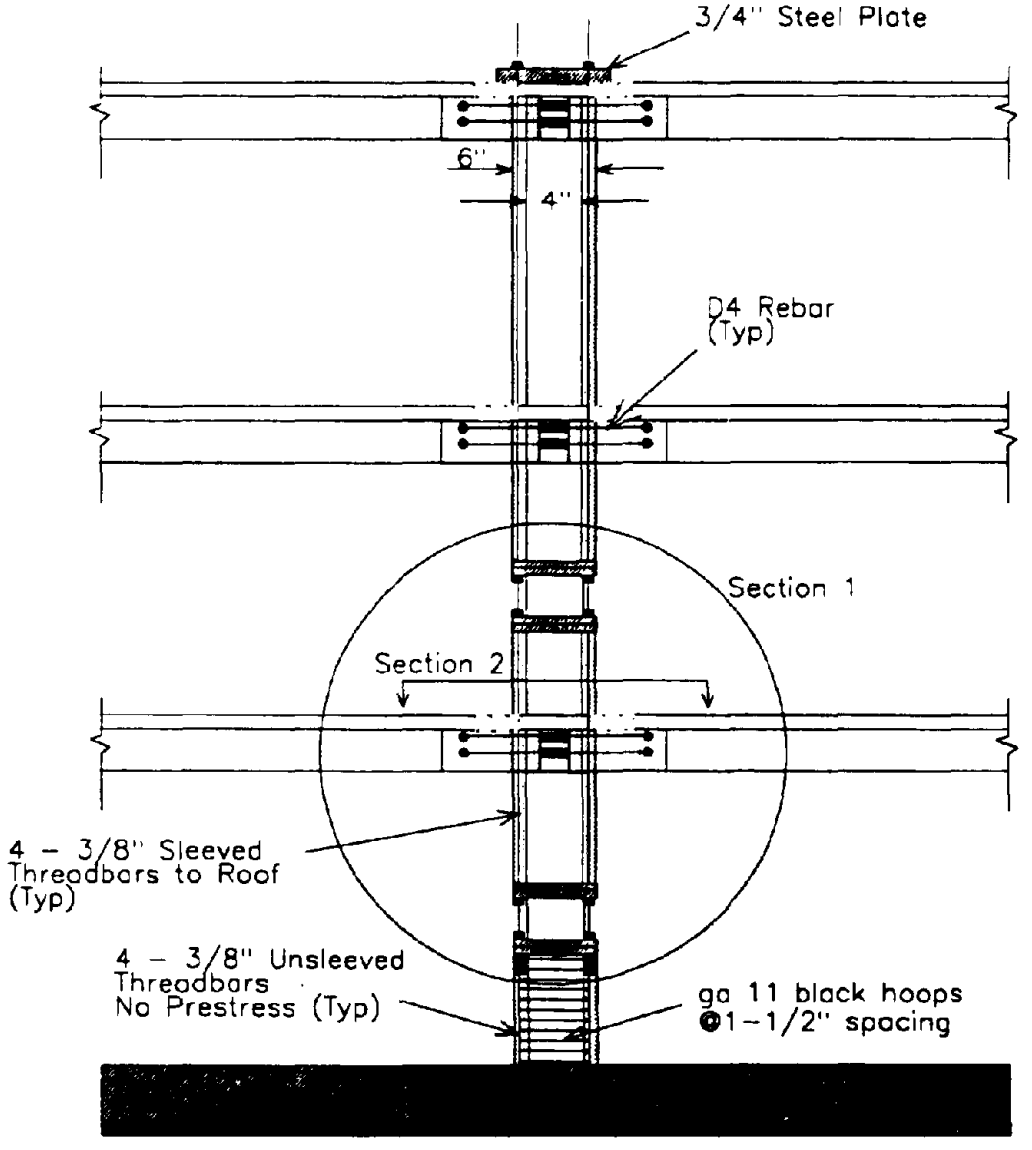

Elevation

FIG. 2-3a Improved Concrete Jacketing Technique for the Model

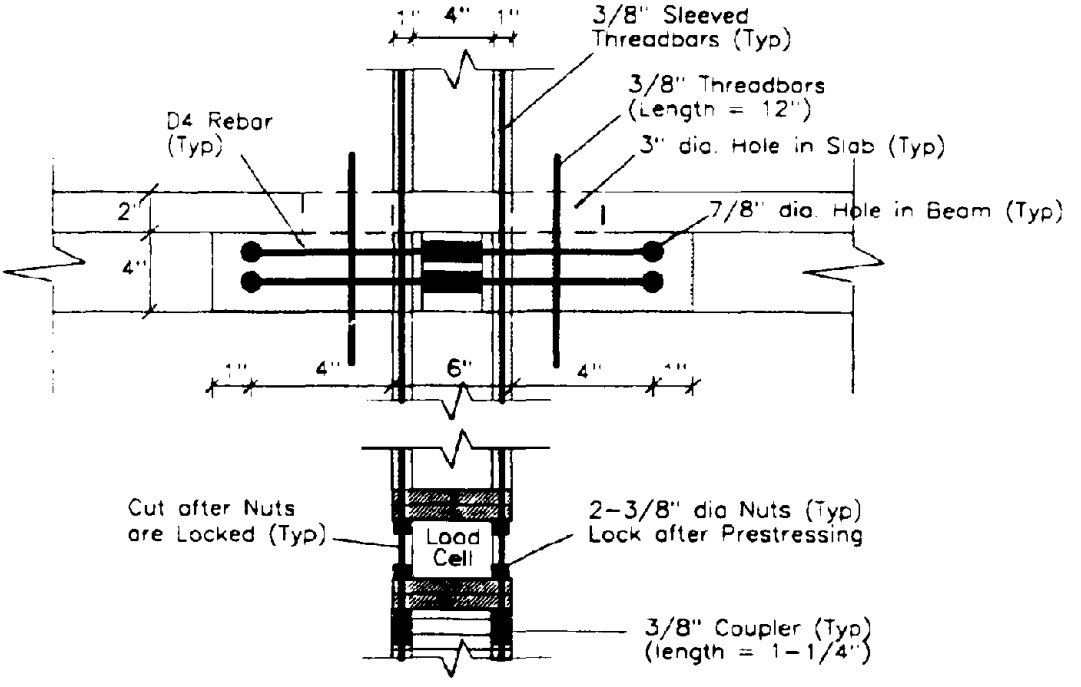

Section 1

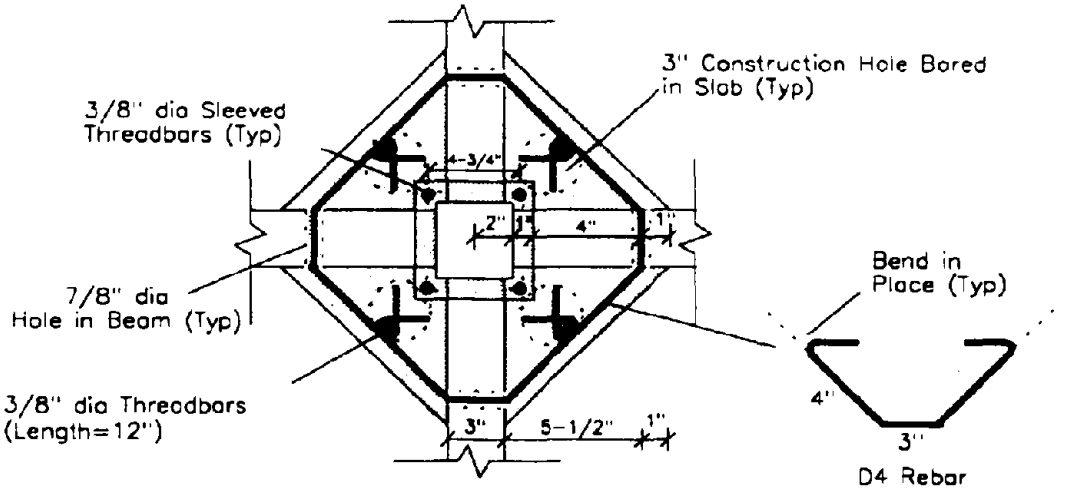

Section 2

FIG. 2-3b Improved Concrete Jacketing Technique for the Model (Cont'd)

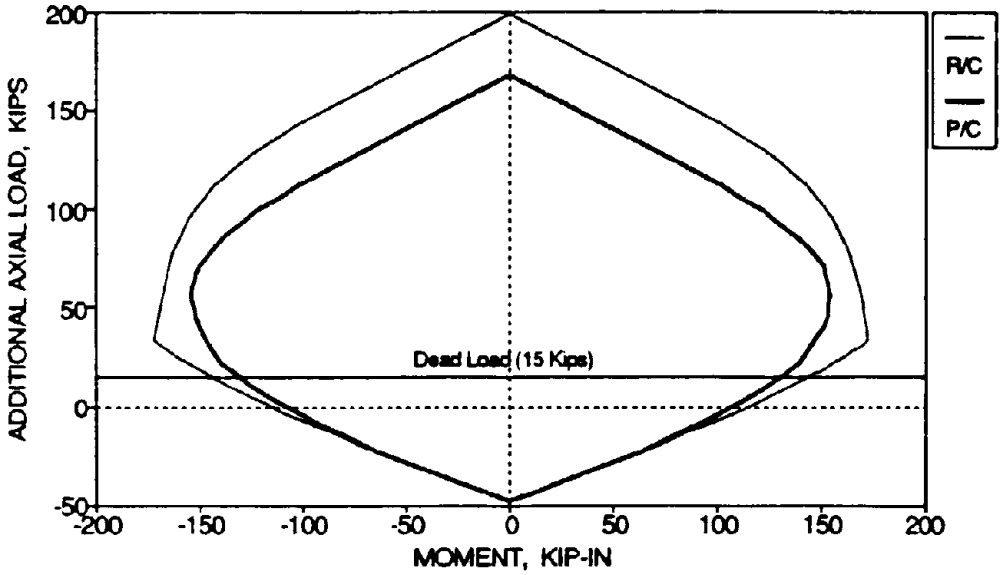

(a) Prestressed/Non-Prestressed Section

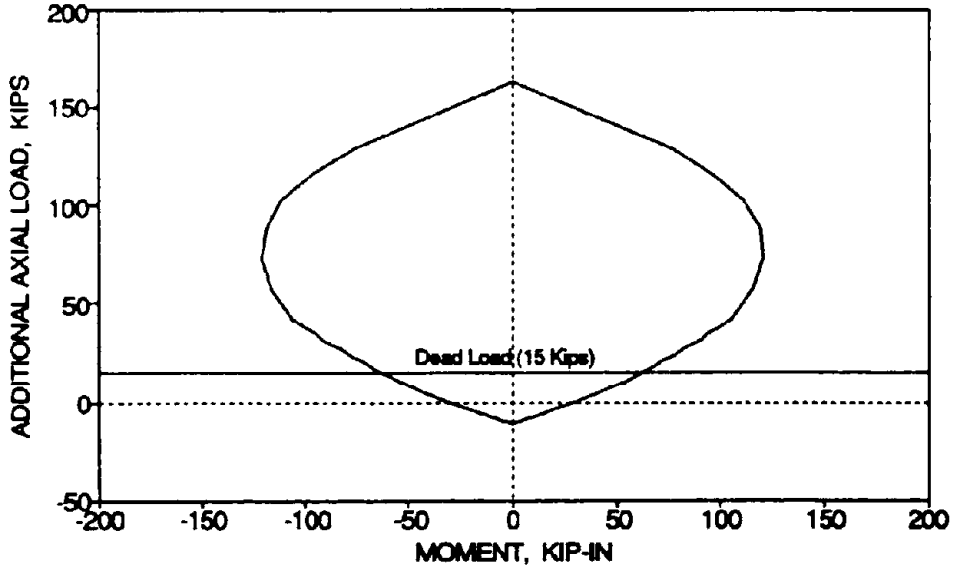

(b) Base Section

FIG. 2-4 Interaction Diagram for the Columns using the Concrete Jacketing Technique

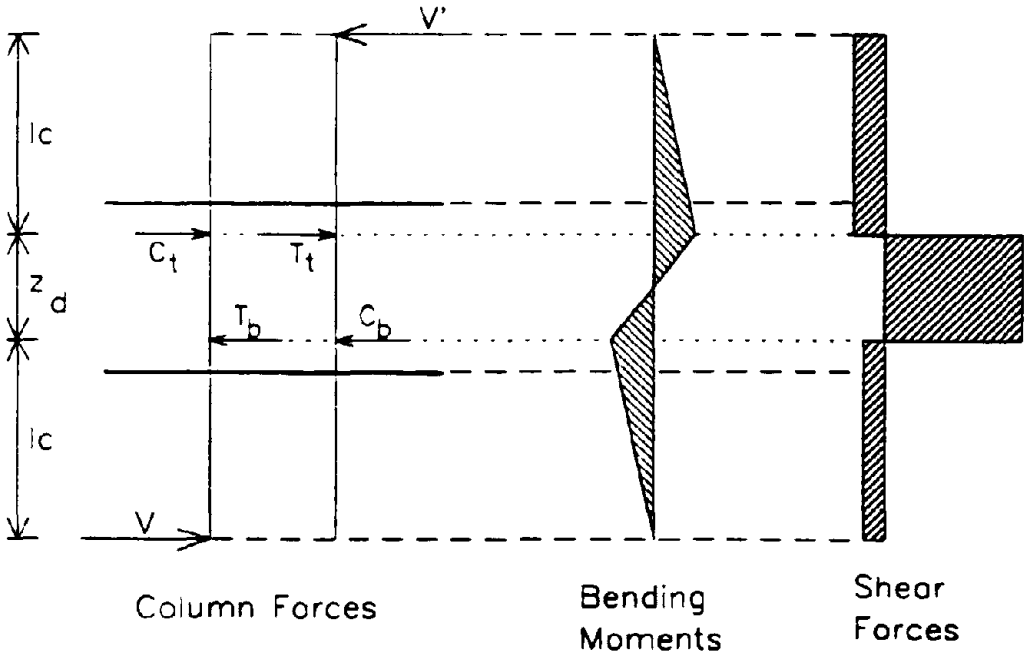

FIG. 2-5 Free-Body Diagram for a Joint with Maximum Shearing Forces

Since the lower first story columns are primarily located in the plastic hinge zone for a beam-sidesway mechanism (see Fig. 2-1b), transverse reinforcement is required in the section between the masonry blocks and the existing concrete columns for added shear strength and confinement as shown in Fig. 2-6. A thin wire mesh can be provided in the block layers to prevent shear cracking in the bed joints and ensure continuity of the masonry and existing concrete column section.

For the scaled model structure presented in this study, the existing 4 in. square damaged columns can be increased to a 9-1/3 in. square section by encompassing the column with the one-third scale of 6 in. masonry blocks. The strength of both materials, concrete and masonry, are considered in an interaction diagram ($f_m' = 1.2$ ksi, $f_c' = 4.0$ ksi) based on the compression depth at a particular load. It should be noted that the strength of the composite section will be governed by the quality of the work by the contractor. However, conservative estimates of material strengths are used for design. The suggested additional longitudinal reinforcement is 3/8 in. diameter threadbars with a yield strength of 120 ksi. Note that the added reinforcement and total prestressing force (32 kips) used for the masonry jacketing is identical with the one for the suggested concrete jacketing method. Accordingly, the tensile and compressive strengths of the reinforcement are appropriately adjusted. Under ultimate load, the strains in the prestressed reinforcement are assumed proportional with the strain profile in the concrete. Fig. 2-7a shows the interaction diagram for the masonry jacket column retrofit based on the composite section of masonry blocks and the existing reinforced concrete section with a prestressing force of 32 kips. With the prescribed axial dead loads of 15 kips for a first floor interior column, the predicted moment strength of the column with a masonry jacket retrofit is about 160 kip-in, which is about a 250% increase in strength from the original column. The retrofitted column strengths at a first story interior beam-column joint are about 95% stronger than the beams nominal capacity, which is more than required by the ACI-318 for design (71%). At the base column with discontinuous longitudinal reinforcement and without prestressing, the moment capacity can be observed as 80.0 kip-in from Fig. 2-7b, which is about an 80% increase in strength from the original column.

For the beam-column joints, the added thin wire mesh and transverse reinforcement in the block joints may be designed to adequately resist the shear forces in the joint from seismic loads. If these shear forces can not be resisted, a concrete fillet with joint reinforcement can be used for additional shear strength and confinement of the joint, similar to the one in the concrete jacketing.

Since the positive and negative beam reinforcement remain the same, the joint steel design would be identical to the improved concrete jacketing method. Thus the same concrete fillet design for the beam-column joints can be used for the different retrofit methods.

Some construction and aesthetic characteristics of the masonry jacketing method can be mentioned:

(a) The construction requires drilling of holes through the existing slabs and beams for pouring the concrete into the columns and fillet (if needed) and for continuity of longitudinal reinforcement. The construction process is relatively easy.

(b) Since the masonry block themselves are used as formwork for the grout, no additional formwork, except for the fillet (if needed), is required for the retrofit.

(c) Access in the structure would be limited only in areas of retrofit. Therefore each story of the structure should be temporarily closed when retrofit of that story columns are being worked on;

(d) The method leads to small reductions of the clear span (5-1/3 in.) for the retrofitted bay of the model. This span reduction, quantified above for the model, corresponds to a 16 in. (1'-4") span reduction of a 18 ft. bay in the prototype building.

2.5.3 Partial Masonry Infill

Masonry and R/C infill walls have been widely tested at universities/research institutions and constructed in practice for increasing the stiffness and strength of structures to control story displacements from high wind loads and other natural forces, including seismic loads. Some of these investigators include: Benjamin and Williams (1958); Stafford Smith and Carter (1969); Esteva (1966); Fiorato, Sozen, and Gamble (1970); Klingner and Bertero (1976); Kahn and Hanson (1976); Parducci and Mezzi (1980); Priestly (1980); Bertero and Brokken (1983); Krause and Wight (1990); and many more. Most new low to medium rise construction of R/C buildings in the Eastern and Central United States have such walls. Infill walls can also be constructed to retrofit an existing damaged (or undamaged) R/C building for improved structural stiffness and strength, thereby reducing story displacements. High shear is placed on the columns and beam-column joints potentially leading to a premature snap-through failure in an existing column. An architectural disadvantage of using an infill wall retrofit for an existing building is the loss of space and access in the building near the wall.

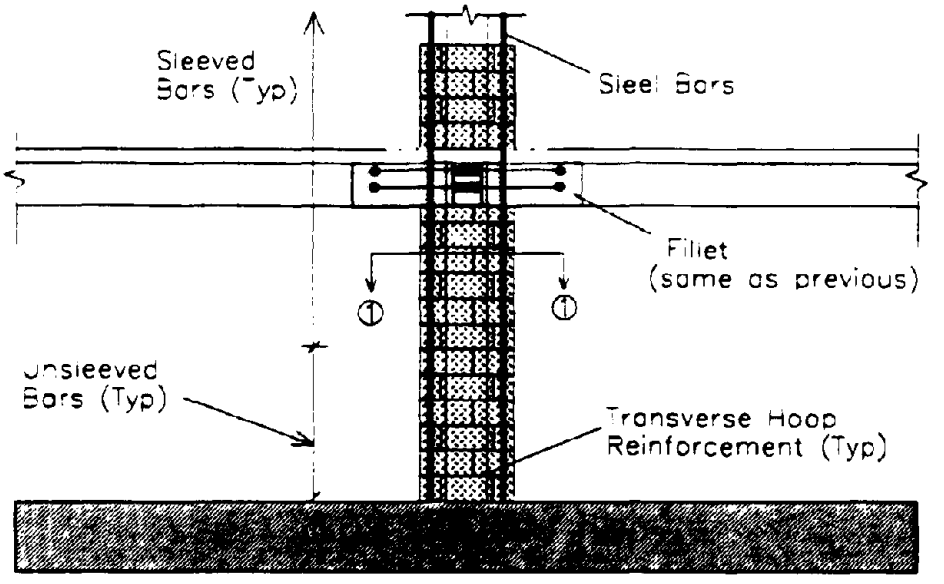

Elevation

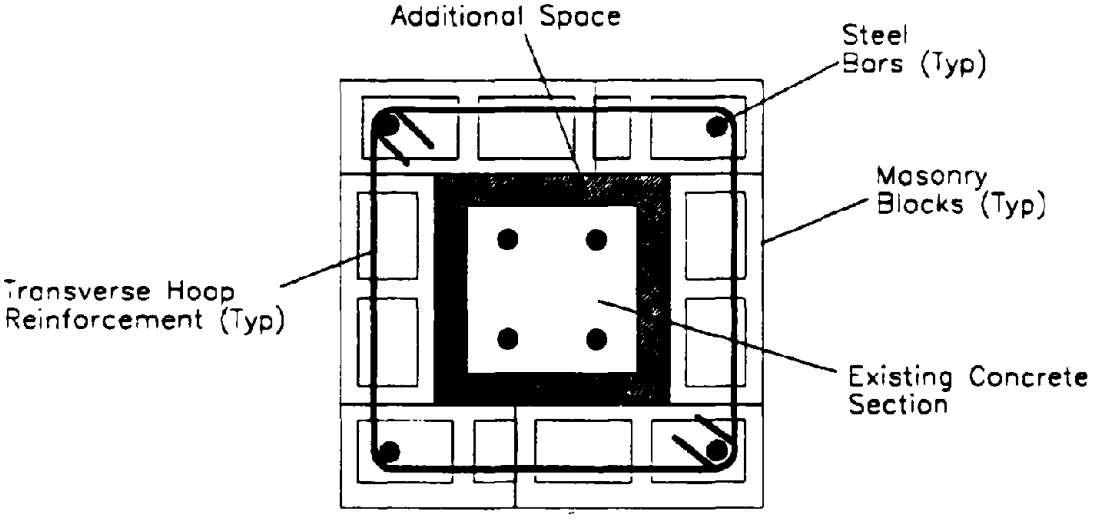

Section 1-1

FIG. 2-6 Masonry Jacketing Technique

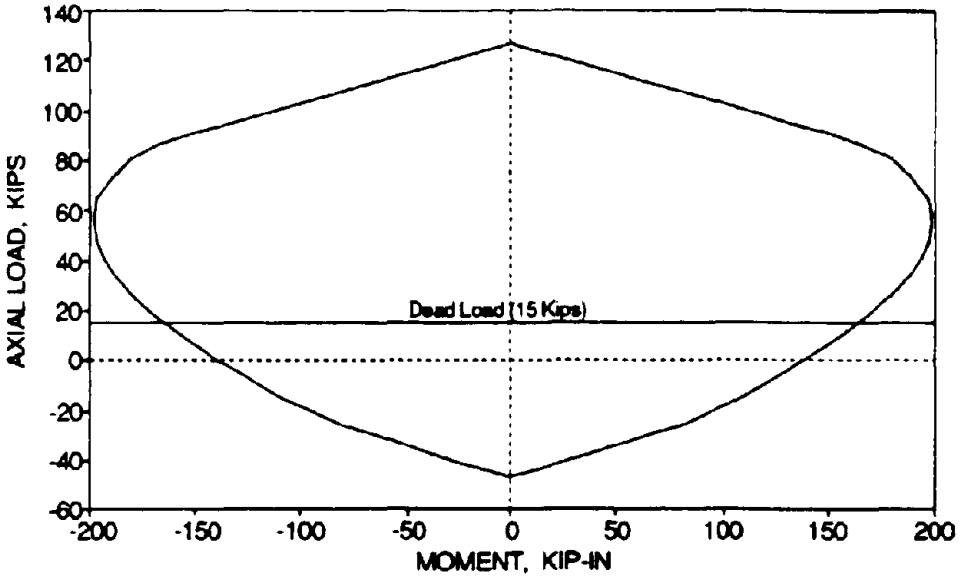

(a) Prestressed Section

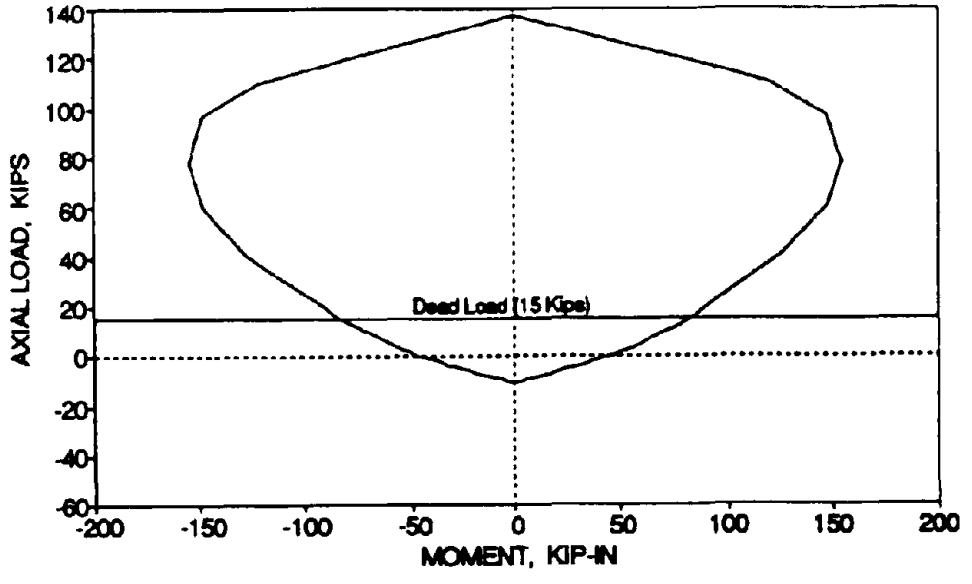

(b) Base Section

FIG. 2-7 Interaction Diagram for the Columns using the Masonry Jacketing Technique

To maintain an almost full passageway between bays and still enhance the critical column strengths, another method of retrofit can be suggested for low to moderate seismicity zones. A partial masonry infill wall can be constructed on each side of selected columns of the structure. Fig. 2-8 shows a detail using partial masonry infill walls on each side of the column for retrofit. It can be observed that the partial wall should extend not more than a few blocks from the existing column face. The number of blocks required in each partial infill wall may vary based on the desired column strength, but will be generally governed by the required development length of the discontinuous positive beam reinforcement. Longitudinal reinforcement in the masonry walls extends continuously through the story slabs for continuity of the wall. In this solution, post-tensioning can also be used to provide the benefits discussed earlier. Since the lower first story columns are primarily located in the plastic hinge zone for a beam-sidesway mechanism (see Fig. 2-1b), adequate transverse reinforcement should be provided in the masonry joints of this zone to resist the large shear forces from the seismic loads. Continuous transverse reinforcement should also be provided in the section between the masonry blocks around the existing concrete columns for added shear strength and confinement, as shown in Fig. 2-8.

For the scale model considered in this study, the existing 4 in. square damaged columns are strengthened using one-third scale 8 in. masonry blocks. The additional reinforcement is 3/8 in. diameter threadbars with a yield strength of 120 ksi. Note that the total prestressing force used for the partial infill method is identical as in the other methods. However since the reinforcement provided is twice the other methods, the prestressing force per bar is only half of the other methods. Fig. 2-9a shows the interaction diagram for the partial masonry infill retrofit based on the composite section of one-third scale 8 in. masonry blocks and existing R/C column with a total prestressed force of 32 kips. Therefore with the prescribed axial dead loads, the partial infill retrofitted columns for the first story of the model have a bending moment strength of 450 kip-in, which is about 10 times stronger than of the existing column. The column strengths at an interior beam-column joint are about five times stronger than the beams, which is well in excess of that required by the ACI-318. It is important to note that the moment strengths of the retrofitted columns assumed adequate transverse reinforcement so that the full moment strength of the section could be achieved. Also note that the column sections are intentionally designed to have a high moment capacity to force a beam-sidesway mechanism. At the base column with discontinuous longitudinal reinforcement and without prestressing, the moment capacity can be observed as 190.0 kip-in from Fig. 2-9b, which is about 330% stronger than of the existing column. However this may be excessive for the foundation.

To guard against beam-column joint failure, holes can be drilled through the beams and additional .ransverse reinforcement can be designed for the joint to adequately resists the shear forces from seismic loads. The masonry blocks can be cut in place to encompass the joint.

Some construction and aesthetic characteristics of the partial masonry infill method can be mentioned:

(a) The construction require holes cut through the slab for pouring of concrete grout and continuity of reinforcement. Construction process is very simple and economically beneficial.

(b) No formwork is required for the retrofit, since the masonry block themselves can be used as formwork for the grout.

(c) Access in the structure would be limited only in areas of retrofit. Therefore each story of the structure would temporarily be closed when retrofit of that story columns are being worked on;

(d) A clear span reduction of 16 in. (1'-4") for the retrofitted model bay. This span reductions corresponds to a 48 in. (4 ft.) span reduction of a 18 ft. bay in the prototype building.

2.5.4 Summary of Design Process

This sub-section summarizes the aforementioned design methodologies developed in Part I (Choudhuri et al., 1992) of the Retrofit Report Series. Note that in each scenario there is a parallel set of steps that progress through the design process.

CONVENTIONAL CAPACITY DESIGN	CAPACITY ANALYSIS AND REDESIGN
Step 1: Longitudinal Beam Reinforcement	
D.1 Flexural design of beams:	**R.1 Flexural check of beam strength distribution:**
Beams are designed and proportioned for moments which are a result of applying the moment redistribution process to the elastic design code actions. Beam plastic hinges are	The anchorage of the positive reinforcement at the beam-column joint connections should be particularly considered. If the bottom bars are

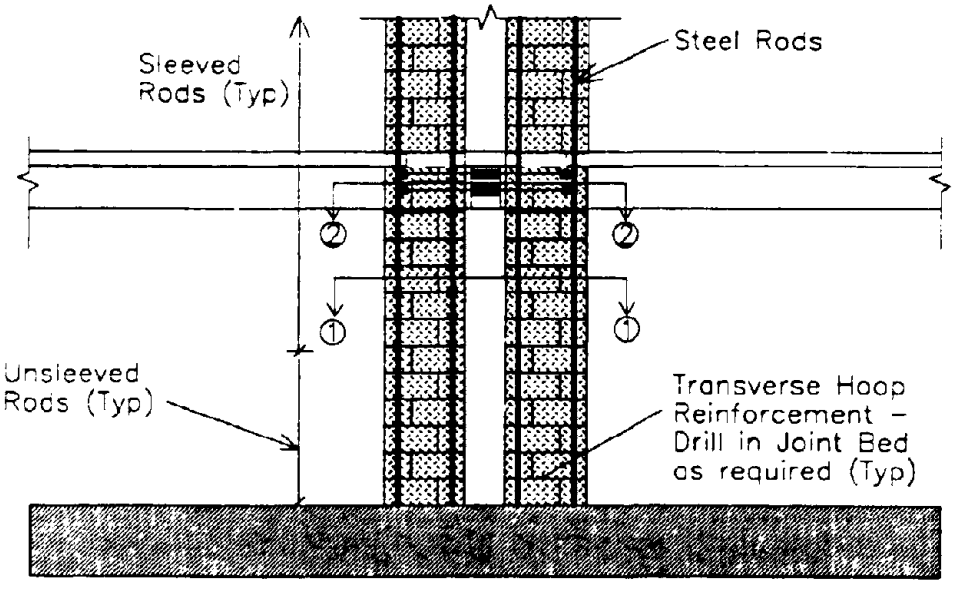

Elevation

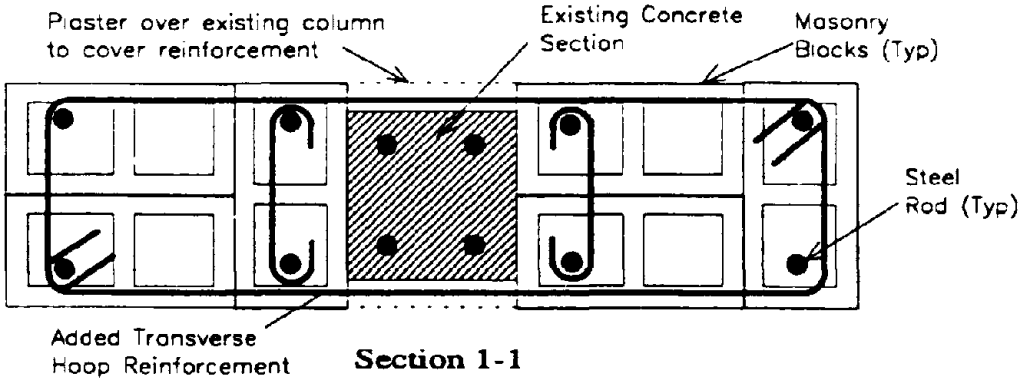

Section 1-1

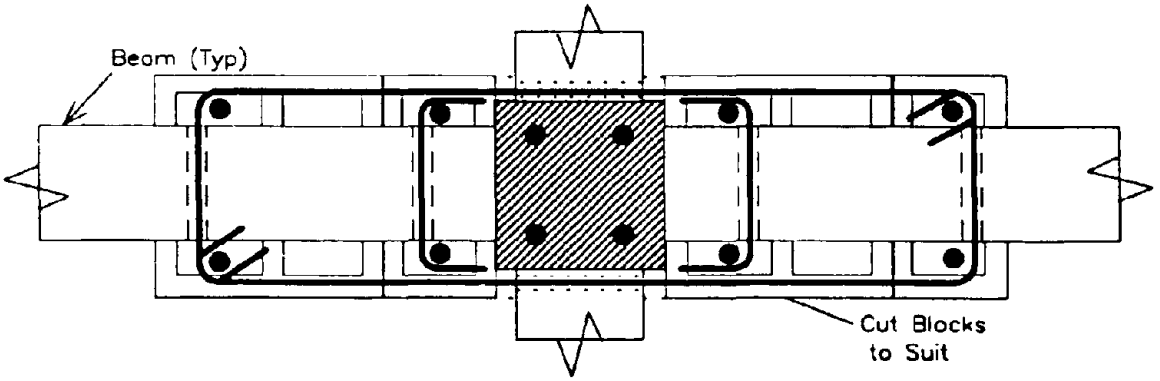

Section 2-2

FIG. 2-8 Partial Masonry Infill Technique

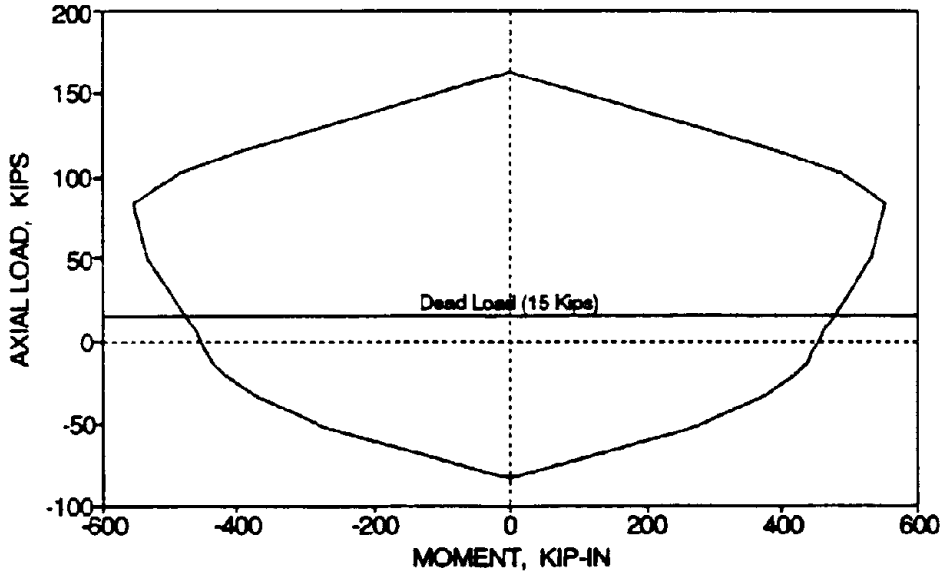

(a) Prestressed Section

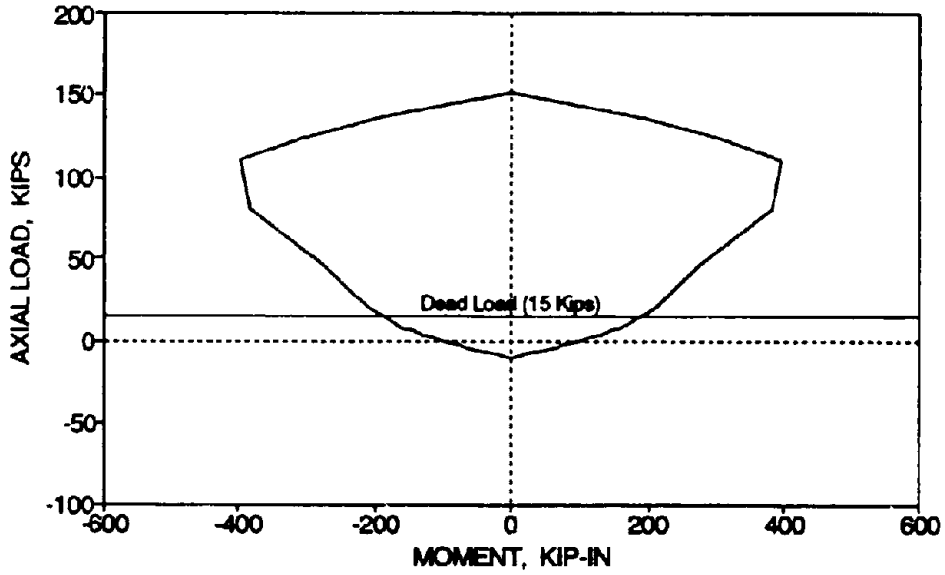

(b) Base Section

FIG. 2-9 Interaction Diagram for the Columns using the Partial Masonry Infill Technique

generally located at the column face and adequately detailed for ductility. From the actual reinforcement provided, the beam flexural overstrength capacity is assessed. This is used in beam shear and column strength design.

discontinuous, then a means of providing dependable positive moment capacity needs to be devised for enhancing seismic resistance. A beam-column joint fillet is a recommended solution. From the actual reinforcement provided, the beam flexural overstrength capacity is assessed. This should include the full effects of the floor slab steel on the negative moment capacity.

Step 2: Transverse Beam Reinforcement

D.2 Shear design of beams:

This is achieved by providing shear strength for the entire beam to be greater than the shear corresponding to the maximum possible flexural strength at the plastic hinge region of the beam. The underlying premise being that inelastic shear deformations do not provide the essential characteristics for energy dissipation.

R.2 Check of shear strength:

It may not be the intent to bring beam shear capacity up to code strength for new design. However, critical regions such as potential plastic hinge zones and the centers of beams which may have little or no shear reinforcement should be assessed for shear strength and supplementary stirrups provided, if necessary.

Step 3: Longitudinal Column Reinforcement

D.3 Flexural strength design of columns:

The nominal flexural strength of the columns is computed by considering the beam overstrengths. This ensures a weak beam - strong column failure mechanism. It should be mentioned that the beam flexural overstrengths are determined and then an additional allowance is made to account for possible higher-mode structural response. From the actual longitudinal reinforcement

R.3 Flexural strength redesign of columns:

The required flexural strength of the columns is computed from the assessed beam overstrengths. The optimum axial load ratio is computed, which helps size the column section. The lower story column is designed as a conventional R/C section. If the imposed axial load due to gravity for the upper story columns is less than the optimum amount, prestressing can be applied to the

provided, the flexural capacity is assessed. This is used in the next step for column shear design.

upper story columns. The cracking surface for the prestressed columns is plotted on a column interaction diagram and the reserve capacity is computed. The ultimate shear to be resisted by the columns should be calculated for the transverse reinforcement design.

Step 4: Transverse Column Reinforcement

D.4 Transverse reinforcement detailing for the columns:

From the most adverse combination of column end overstrength moments, the maximum possible shear force in the columns is computed. Transverse shear reinforcement is provided over the entire column height. Additional shear steel and/or confinement or antibuckling steel is generally required in the potential plastic hinge zone.

R.4 Transverse reinforcement detailing for the redesigned columns:

For the lower story R/C columns, step D.4 applies for the shear steel design. For the upper story PSC columns, use the prestressed concrete code equations to determine the shear resisted by the concrete. Generally the intrinsic shear strength of the compressed concrete would be greater than the ultimate shear to be resisted, else provide supplementary transverse shear steel.

Step 5: Beam-Column Joint Reinforcement

D.5 Detailing of the beam-column joint:

The beam-column joint is a poor source of energy dissipation and thus needs to be detailed to resist the high shear input from the beam and column actions. In this step, the designer should attempt to keep the joint elastic by reducing, if not eliminating, any inelastic deformation due to the joint shear forces and bond deterioration.

R.5 Detailing of the beam-column joint:

Check that there is adequate longitudinal beam bar anchorage through the joint core. Since the length of the joint fillet has been decided in step 1 of the redesign, the designer should attempt to detail the fillet reinforcement in this step. The joint may be considered to behave in an elastic manner and the shear resisted by the concrete in elastic joints is computed. If the input shear

forces from the beams and columns exceed that resisted by the concrete via strut action, provide the necessary reinforcement.

2.6 Global Retrofit of R/C Structures - Analytical Evaluation

The retrofit solutions outlined in the previous sub-sections provide local retrofit measures to columns, joints, beams, and components. However, the effectiveness of integrating these local retrofit schemes in a structure is not entirely obvious. Application of certain retrofit measures may not be beneficial to the overall performance of the structure. Therefore a global verification of integrating the local retrofit schemes is performed analytically using IDARC, Kunnath et al. (1990), with structural parameters described from engineering approximations to obtain an assessment of the effectiveness of integrating "the parts into the whole".

The objective of the analytical study is to first evaluate the seismic response of the existing model to another strong ground motion. If the seismic performance is not acceptable, evaluate the seismic response of the retrofitted model with the proposed concrete jacketing, masonry jacketing, and partial masonry infill alternatives. The control parameters for selecting the optimal global retrofit scheme for the model under strong ground motion are: story displacements (inter-story drifts); base shear demands and capacities; stress demands in members; and the apparent global collapse mechanism.

2.6.1 Analytical Evaluation of Original (Damaged) Model

It was shown by Bracci et al. (1992b) in Part III of the Evaluation Retrofit Series that a considerable amount of inelastic deformation and damage formed in the model during the moderate and severe ground motions. It was also shown that the analytical modeling using IDARC adequately predicts the response characteristics obtained in the experimental tests performed on the model. IDARC, therefore, is used again as an analytical tool to evaluate the strength of the model to resist another strong ground motion with further member stiffness deterioration. Consecutive runs of the moderate (0.20 g), severe (0.30 g), and another future severe (0.30 g) earthquakes are used to capture the hysteretic degradation in the model.

Table 2-1 shows the initial first period of the model, the base shear demands and capacities (from a shakedown analysis at 2% structure drift limit), the inter-story drifts, and the bending

moment demands and capacities for the beams and columns obtained in the analytical study. The nominal column to beam strength ratios are also tabulated in Table 2-1. Fig. 2-10 outlines the calculation of the nominal column to beam strength ratios for an interior and exterior subassemblage and for a story subframe. The experimental structural response from the previous shaking table test (TFT_30) are presented along with: (i) the analytically calculated structural response for this test; and (ii) the analytically predicted structural response for a future occurrence of severe ground motion. For comparative evaluations, the Taft N21E component, scaled for a PGA of 0.30 g, is used to simulate the future severe demands. Note that this magnitude may be excessive for low seismicity zones. However it is considered that a more straight forward evaluation can be made for an extreme event and then compared with the observed performance. It can be observed that good agreement exists between the experimental response and the analytical response for TFT_30 (also see Bracci et al., 1992b). From the future severe ground motion analysis, increases in inter-story drifts are observed, which can be attributed to the softening of the model. The base shear demand is greater than the analytical base shear capacity from a shakedown analysis based on a 2% drift limit. This will almost ensure severe damage or collapse in a future shaking. The bending moments are also increasing. Note that the nominal column to beam strength ratios for an interior subassemblage and a story are 0.60 and 0.75, respectively (weak column - strong beam behavior). With increasing story displacements, base shears, and moments in the members up to full capacities for a future severe ground motion, further damage would be expected in the model with strong probability of collapse occurring. If constructed in an area of high seismicity, this structure would be rated unserviceable and subject to closing.

2.6.2 Analytical Evaluation with Proposed Retrofit Methods

Since the model was assessed as a moderately damaged structure (Bracci et al., 1992b), repair and retrofit is required before serviceability could be reinstated. An analytical study of the suggested local retrofit methods, presented in the previous sub-section, integrated in the model are presented using IDARC with the Taft N21E PGA 0.30 g ground motions. Since many members make up the structural system of the model, a few options of retrofitting the members of the structure existed. With induced seismic excitation, the interior columns would be more critical than the exterior since larger demand bending moments, shear forces, and axial loads will develop (Bracci et al., 1992b). El-Attar et al. (1991b) observed failure in the first story interior columns of the 1/8 scale model replica under a very large base motion. Therefore it was determined to evaluate the global response for retrofitting: (i) only the interior columns;

and (ii) all the columns for each bay for both the concrete and masonry jacketing methods. Since a partial masonry infill wall could not extend beyond the existing exterior facade of the structure, the stiffening of only the interior columns for each bay is examined.

In addition to the various retrofit techniques for columns, (iii) continuous (full base fixity) and (iv) discontinuous (partial base fixity) reinforcement is considered in the critical lower first story columns for the concrete jacketing alternative. Note that full fixity may create foundation problems. Nevertheless, a special connection to the foundation would be required to obtain the increased bending moment capacity.

The initial column stiffnesses used in the analyses are different for the various retrofit techniques and are chosen as 1.0 EI_g and 0.7 EI_g, respectively for the concrete jacketing and masonry retrofit methods. It was shown by Bracci et al. (1992a) that the initial column stiffnesses used in STAAD to match the first period of the R/C model were 0.565 $(EI_{col})_g$. Also to fit the experimental response, the initial column stiffnesses were about 0.60 $(EI_{col})_g$. However since post-tensioning is applied in the proposed retrofit alternatives, the equivalent member stiffnesses are expected to be in the range from 0.8 to 1.0 $(EI_{col})_g$ from the higher axial loads. However since the concrete used in the jacket has superior bond adhesion to the existing column, the full EI_g of the section is used. For the masonry blocks and grout, the bond to the existing column is not as superior and some cracking may still result. Thus 70% of $(EI_{col})_g$ is considered appropriate. These initial member stiffnesses are assumed to be uniform throughout the height of the structure. At the lower first story columns with the partial base fixity (discontinuous rebars and no prestressing), the respective equivalent stiffnesses used are 0.5 EI_g, 0.5 EI_g, and 0.33 EI_g, respectively for the concrete jacketing, masonry jacketing, and partial infills methods. These lower values reflect the more cracked nature of these reinforced sections. Paulay and Priestley (1992) suggest ranges for an effective moment of inertia between 0.7 I_g and 0.9 I_g for heavily loaded columns and between 0.5 I_g and 0.7 I_g for columns with axial loads of about 0.2 $f_c' A_g$. Therefore comparable initial column stiffnesses are approximated for the retrofitted columns.

Since the beams developed only minor damage from the previous shaking, the initial stiffnesses of the beams are about 0.45 $(EI_{bm})_g$ in the analytical study. Note that this beam stiffness is similar to the engineering approximations used for the undamaged building by Bracci et al (1992b). Since the exterior columns were moderately damaged from the previous shaking, the

initial stiffnesses used in the unretrofitted exterior columns are about 0.27 $(EI_{col})_g$. Note that this is a reduction of about 30% from the initial properties used in the experimental fit from the previous shaking.

For development of the hysteretic rule, a post-cracking stiffness of EI/2 is assumed for all retrofit methods. The yield strengths of the beams and columns are computed from basic mechanics principles. Note that the beam moments consider slab steel contributions from the full slab width. Also note that the exterior beam yielding moment in the positive direction considers the effect of slip of the discontinuous bottom beam reinforcement (50% reduction in rebar area based on the prototype ratio of provided and required embedment lengths). However with retrofit, the interior beam moments consider full moment capacity without the pull-out effect. The hysteretic properties for the beams and columns in the analytical modeling for all the retrofit methods are defined based on previous component testing as: (i) 0.3 and 0.8 for the stiffness degradation factor for the columns and beams, respectively; (ii) 0.1 for the strength degradation factor; (iii) 1.0 for the target slip factor; (iv) 1.00 for the slip reduction factor; (v) 1.5% and 1.0% for the post-yielding stiffness ratio for the columns and beams, respectively; and (vi) 2% for the damping ratio.

The platform program IDARC, Kunnath et al. (1990), was used to carry out the inelastic analysis for a severe earthquake (Taft N21E 0.30 g) based on member behavior developed from engineering approximations. The global and local response results for the different retrofit methods are summarized in Table 2-1. The initial first mode periods vary between 0.25 sec. and 0.36 sec. It can be observed from the spectrum in Fig. 2-11 that this period range is in the vicinity of major amplifications from the Taft N21E ground motions (response spectrum of an elastic single degree-of-freedom system for 2% and 5% damping). Although the acceleration amplifications are increased from the added stiffness, a beam-sidesway mechanism, stipulated in the retrofit design, will transfer damage from the columns to the more ductile beams. This can be observed in the redistribution of moment demands versus capacities in the beams and columns.

The resulting demands in the beams for all the retrofit methods are well beyond yield, but not beyond ultimate capacity. Note the large beam moment demands with the retrofit methods as compared to the analytical beam moment demands of the unretrofitted building. Also note that

due to the reinforced fillet and added pressure from prestressing, the positive moment capacity of the beams is stronger and corresponding demands are greater, since the pull-out effect is eliminated.

For the columns, the extent of yielding varies depending on the global retrofit scheme applied. For the schemes using the weak base retrofit (weak link to foundation), some moment demands are slightly above the nominal ultimate capacity (incipient yielding). However, the demands are well within the dynamic ultimate capacity. For the case of strong base retrofit, large moment demands in the lower first story columns are observed, which are well beyond the nominal ultimate capacity. In a prototype structure, these large moment demands would need to be reacted by the existing foundation, if it is strong enough. Otherwise the existing foundation would need to be strengthened.

For the retrofit of the interior columns only, the moments developed in the exterior columns are well below their ultimate capacity, but some incipient yielding occurs in the third story columns. However for the retrofit schemes considering stiffening of all columns, the resulting moment demands in the columns are below yield.

The nominal column to beam strength ratio for the retrofit methods vary between 1.59 and 5.85 for an interior subassemblage. The story strength ratios vary between 1.49 and 4.69. Therefore strong column - weak beam behavior is enforced by the design.

Fig. 2-12 shows the resulting analytical damage states in the model for the different retrofit methods after a severe earthquake (Taft N21E with a PGA of 0.3 g). The resulting failure mechanisms for strengthening all the columns in the model are in the form of the classical beam-sidesway collapse mechanism. Strengthening only the interior columns results in a beam-sidesway mechanism but with added incipient yielding in some interior (retrofitted) and exterior columns. However the resulting moments in these members are well below ultimate capacity and the damage from cracking might be ignored.

It can also be observed from Table 2-1 that all the retrofit methods analyzed provide adequate control of the inter-story drifts, with the largest inter-story drift being less than the recommended by NEHRP (1991). The concrete jacketing of all the columns with the weak base criteria provides the best control of the inter-story drifts for the base motions. The base shear demands are also less than the ultimate capacities determined from a shake-down analysis in all cases.

Note that the greater margin between the base shear demands and capacities for the weak base retrofit as compared to the strong base retrofit. Without retrofit, the base shear demand is either equal to or greater than the capacities.

2.7 Summary Discussions

Three global/local alternatives were suggested for retrofit of R/C frame structures: (i) improved concrete jacketing; (ii) masonry jacketing; and (iii) partial masonry infill. These three techniques were evaluated analytically in global context on the damaged three story R/C model for: (a) retrofitting only the interior columns; (b) retrofitting all columns; (c) partial base fixity (discontinuous added reinforcement at foundation); and (d) full base fixity (continuous added reinforcement into foundation). To ensure an elastic beam-column joint behavior, a reinforced concrete fillet was also provided in the retrofitted joints. Post-tensioning of the added longitudinal reinforcement was proposed to increase the shear strength and thus avoid additional transverse reinforcement to improve the constructability of the retrofit. The post-tensioning also provides an initial uniform strain on the composite section and a compressive pressure on the discontinuous positive beam reinforcement to deter pull-out.

From the analytical evaluation, it was found that:

(1) Stiffening of the structure causes a shift in natural frequency which is in the vicinity of major acceleration amplifications for the Taft N21E accelerogram. An increased base shear demand develops.

(2) A beam-sidesway mechanism after retrofit replaces the column-sidesway collapse mechanism as obtained in the original structure. However some combination mechanisms and incipient member yielding can also be observed from the resulting damage states.

(3) Moment demands in the beams are well beyond yield, but not beyond capacity. An increased positive moment capacity is achieved with the concrete fillet and partly by prestressing, which deters pull-out.

(4) Some incipient yielding in the columns occur for the weak base retrofit. For the full base fixity retrofit, large yielding moments develop in the base columns. These large moments can create foundation problems.

(5) Adequate control according to NEHRP (1991) of the inter-story drifts is obtained by the various methods.

(6) The base shear demands are less than the ultimate capacities determined from a psuedo-static shakedown analysis based on a 2% drift limit and the margin between demand and capacity is slightly expanded.

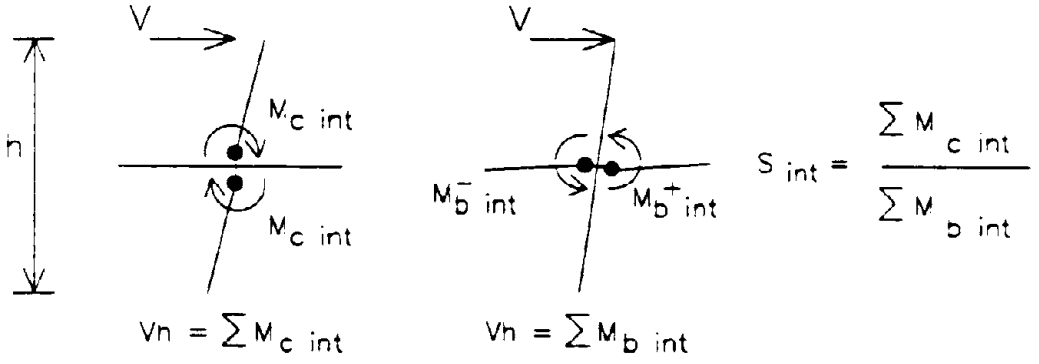

(a) Interior Beam-Column Subassemblage

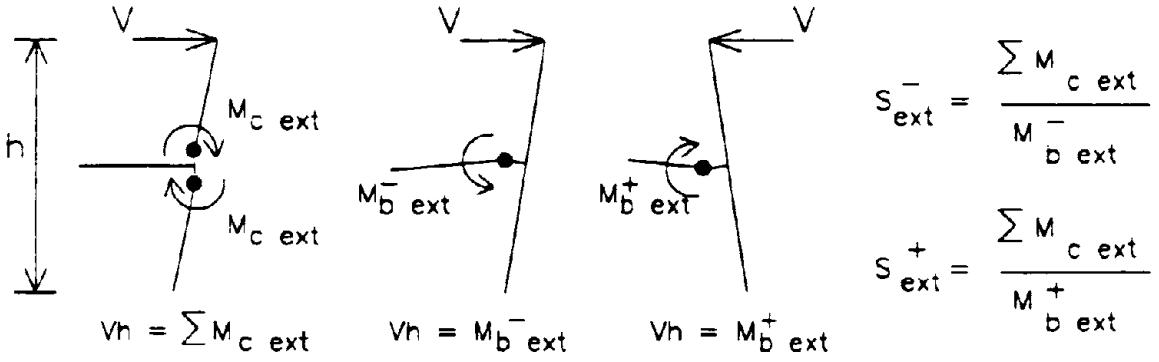

(b) Exterior Beam-Column Subassemblage

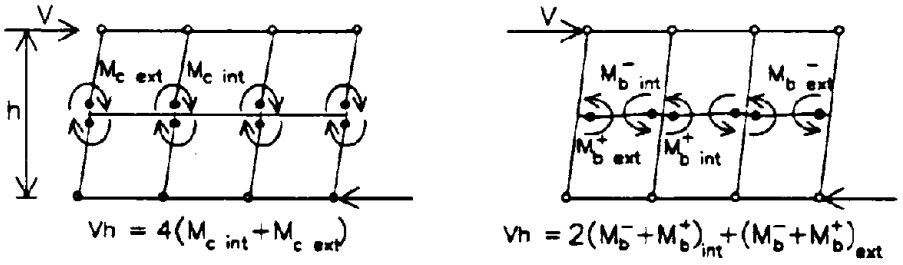

$$S_{story} = \frac{4(M_{c\ int}+M_{c\ ext})}{2(M_b^-+M_b^+)_{int}+(M_b^-+M_b^+)_{ext}}$$

(c) Story Subframe

FIG. 2-10 Nominal Column to Beam Strength Ratio Calculations

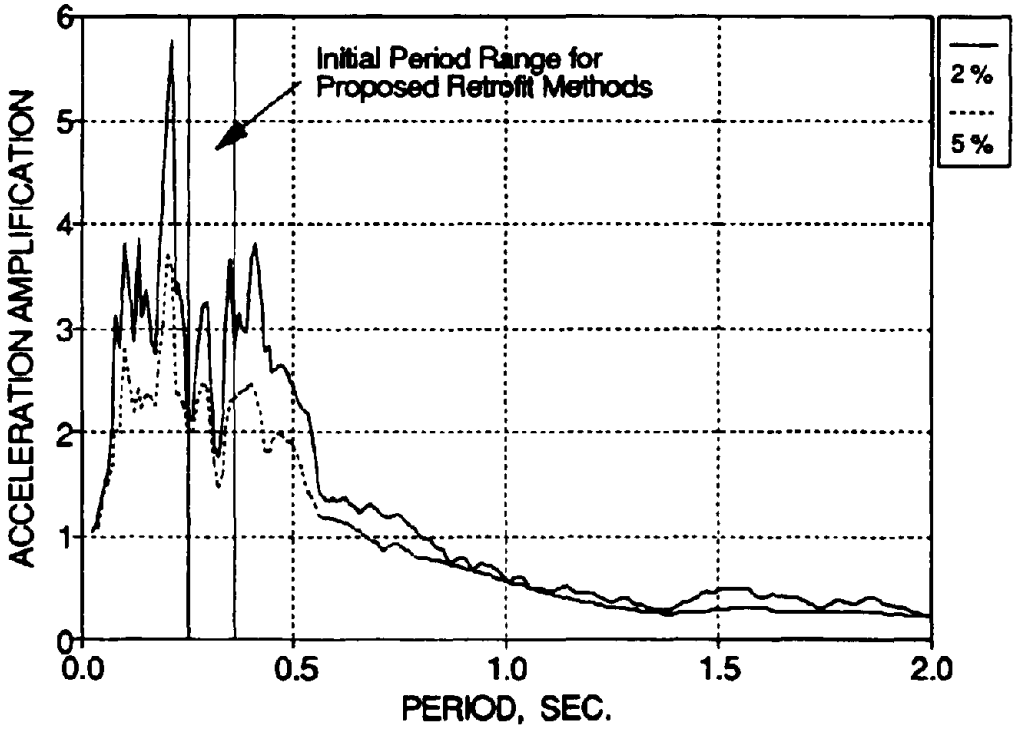

FIG. 2-11 Initial Periods of Retrofitted Buildings - Taft N21E Elastic Response Spectra

TABLE 2-1 Analytical Evaluation of Retrofit Techniques for Taft N21E (PGA 0.3 g)

	Classification	Type	Period (sec)	Maximum Global Response					Interior (kip-in)		Exterior (kip-in)		Column to Beam Strength Ratio		
				Base Shear (%W)	Drift (%) 1st St.	2nd St.	3rd St.	3rd St Disp(in)	Column Moments	Beam Moments	Column Moments	Beam Moments	Interior Comp	Exterior Comp.	Story
EXISTING STRUCTURE	1. Model (Experiment-TFT_30)	Demand Capacity	0.70	15.3	2.03	2.24	0.89	2.35	44.2 38.0	-84.6/+13.1 -98.8/+27.6	39.1 30.0	-39.4/+36.7 -85.3/+24.9	0.60	-0.71/ +2.40	0.75
	2. Model (Analytical-TFT_30)	Demand Capacity	0.70	14.8 15.0	1.81	2.42	0.65	2.28	39.3 38.0	-48.9/+30.2 -98.8/+27.6	30.1 30.0	-55.5/+35.2 -85.3/+24.9	0.60	-0.71/ +2.40	0.75
	3. Model (Future Taft 0.3g)	Demand Capacity	0.83	14.7 15.0	1.82	2.69	0.55	2.39	39.2 38.0	-41.8/+31.0 -98.8/+27.6	31.6 30.0	-42.6/+34.4 -85.3/+24.9	0.60	-0.71/ +2.40	0.75
RETROFIT WITH CONCRETE JACKETING	4. Interior Strengthened, Full Base Fixity	Demand Capacity	0.33	28.9 30.0	1.06	1.00	0.58	1.16	152.3 130.0	-76.2/+47.2 -98.8/+64.9	20.6 30.0	-49.1/+28.2 -85.3/+24.9	1.59	-0.71/ +2.40	1.49
	5. Interior Strengthened, Partial Base Fixity	Demand Capacity	0.36	24.4 28.5	1.24	1.10	0.40	1.30	132.5 130.0	-81.5/+49.7 -98.8/+64.9	20.7 30.0	-50.1/+28.8 -85.3/+24.9	1.59	-0.71/ +2.40	1.49
	6. All Strengthened, Full Base Fixity	Demand Capacity	0.27	36.2 39.0	0.79	1.17	0.89	1.33	135.1 130.0	-78.0/+50.1 -98.8/+64.9	134.8 130.0	-56.1/+37.2 -85.3/+59.7	1.59	-3.06/ +4.33	2.20
	7. All Strengthened, Partial Base Fixity	Demand Capacity	0.30	30.4 34.5	0.91	1.00	0.69	1.21	121.9 130.0	-76.1/+49.9 -98.8/+64.9	86.0 130.0	-54.8/+34.0 -85.3/+59.7	1.59	-3.06/ +4.33	2.20
RETROFIT WITH MASONRY JACKETING	8. Interior Strengthened, Partial Base Fixity	Demand Capacity	0.34	27.5 30.0	1.33	1.36	0.74	1.62	163.0 160.0	-83.3/+51.0 -98.8/+64.9	21.6 30.0	-50.5/+29.4 -85.3/+24.9	1.95	-0.71/ +2.40	1.76
	9. All Strengthened Partial Base Fixity	Demand Capacity	0.28	33.2 36.0	1.20	1.16	0.76	1.49	131.6 160.0	-79.9/+51.6 -98.8/+64.9	97.9 160.0	-55.9/+36.0 -85.3/+59.7	1.95	-3.76/ +5.33	2.71
RETROFIT WITH PARTIAL INFILLS	10. Interior Strengthened, Partial Base Fixity	Demand Capacity	0.25	35.9 37.5	0.78	1.03	0.96	1.33	209.3 480.0	-78.2/+47.2 -98.8/+64.9	22.1 30.0	-50.2/+28.2 -85.3/+24.9	5.85	-0.71/ +2.40	4.69

Note: Base shear capacities determined from a shake-down analysis
Classifications 1 and 2 compare the experimental and analytical results for TFT_30
Column to beam strength ratios based on Nominal Moment Capacities

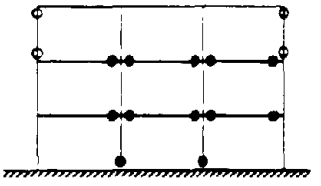

Interior Strengthened, Full Base Fixity

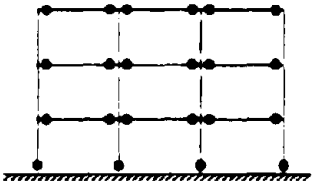

All Strengthened, Full Base Fixity

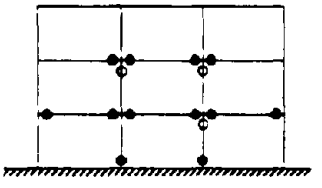

Interior Strengthened, Partial Base Fixity

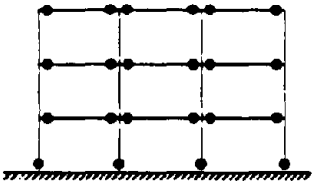

All Strengthened, Partial Base Fixity

(a) Improved Concrete Jacketing Method

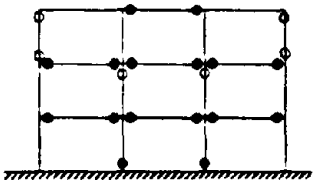

Interior Strengthened, Weak Base

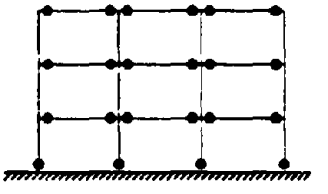

All Strengthened, Weak Base

(b) Masonry Jacketing Method

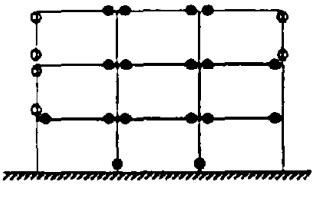

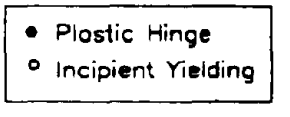

Interior Strengthened, Weak Base

(c) Partial Infill Method

FIG. 2-12 Damage States for the Retrofitted Model (Analytical)

SECTION 3

EXPERIMENTAL STUDY OF RETROFITTED R/C MODEL

3.1 Introduction

In Section 2, the local and global seismic concerns for and expected damage in typical GLD R/C frame buildings were discussed and verified in a previous experimental study (Bracci et al., 1992b). Based on these concerns and the expected damage for such buildings and the previous experimental damage, three seismic retrofit methods were suggested and analytically verified for the 1:3 scale R/C frame model building.

In this section, one of the suggested retrofit techniques is selected to repair and upgrade the 1:3 scale GLD R/C frame model building for an additional experimental shaking table study. Retrofit construction is described and performed on the model. The shaking table testing program for the retrofitted model, along with induced base motions, is presented. The initial dynamic characteristics of the retrofitted model are also identified from an experimental white noise shaking table excitation.

3.2 Selection of Retrofit Method for Experimental Study

It was previously shown that several of the chosen retrofit methods provide adequate control of the story drifts, shears, and damage of the structural system in event of a future strong ground motion. For a prototype structure, the selected retrofit technique would obviously depend on a number of factors such as: costs; amount of time the building (or sections) would remain closed; and the design earthquake zone, etc. However, for the model, other factors had to be considered for determining the retrofit method: the availability of scaled retrofit material (masonry blocks); maintaining proper instrumentation of the model for the experiment (ie. custom made load cells); and construction equipment required for retrofit.

In view of the above considerations, the improved concrete jacketing alternative of the critical interior columns was selected to retrofit the model structure. Although the retrofit of all columns was shown to provide somewhat better control of the inter-story drifts, a minimal retrofit of only the interior columns provides adequate seismic performance, especially for low to moderate

seismicity zones. It was previously shown that the global structural response is adequately controlled with the discontinued reinforcement at the base. To avoid any additional foundation loading, the added reinforcement in the jacketed zone is intentionally discontinued at the rigid base. Fig. 3-1 shows some of the construction stages in the retrofit of the model. The amount of work and structural disturbance is minimal. The completed retrofitted model with the required additional weights for mass similitude are shown on the shaking table in Fig. 3-1c.

3.3 Testing Schedule of Retrofitted Model

Table 3-1 shows the shaking table testing program for the retrofitted model structure. For comparison purposes, the two ground motions are selected using the Taft N21E accelerogram scaled to 0.20 g and 0.30 g, respectively in order to simulate moderate and severe earthquakes. A series of compensated white noise excitations are used before and after every earthquake test for the identification of prevailing dynamic characteristics.

TABLE 3-1 Shaking Table Testing Sequence for the Retrofitted Model

Test #	Date	Test Label	Test Description	Purpose
1	1/28/92	WHNR_B	Compensated White Noise, PGA 0.024 g	Identification
2	1/29/92	WHNR_C	Compensated White Noise, PGA 0.024 g	Identification
3	1/29/92	TFTR_20	Taft N21E, PGA 0.20 g	Moderate Earthquake, Inelastic Response
4	1/29/92	WHNR_D	Compensated White Noise, PGA 0.024 g	Identification
5	1/29/92	TFTR_30	Taft N21E, PGA 0.30 g	Severe Earthquake, Inelastic Response
6	1/29/92	WHNR_E	Compensated White Noise, PGA 0.024 g	Identification

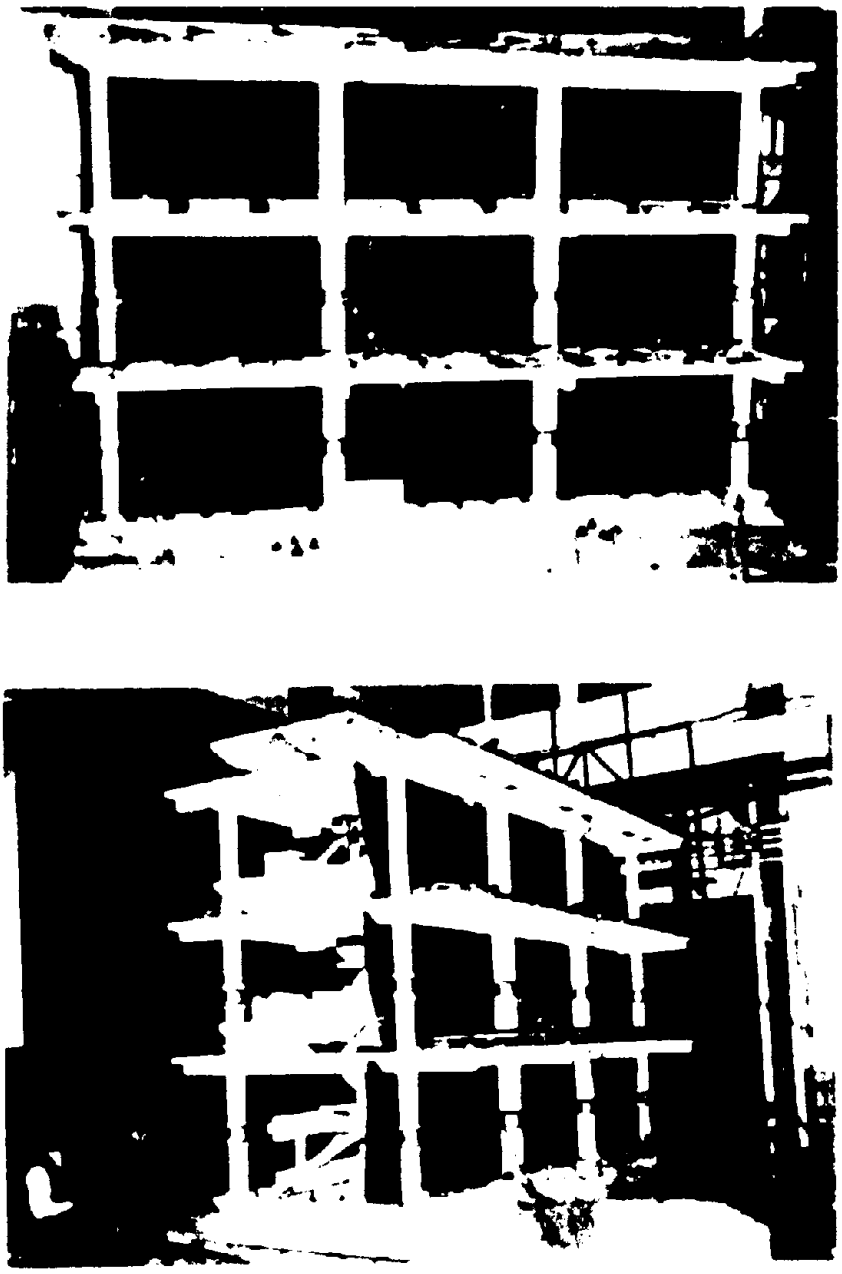

FIG. 3.1a Stages in the Improved Concrete Jacketing Retrofit of the Model.

FIG. 3-1b Stages in the Improved Concrete Jacketing Retrofit of the Model (cont.)

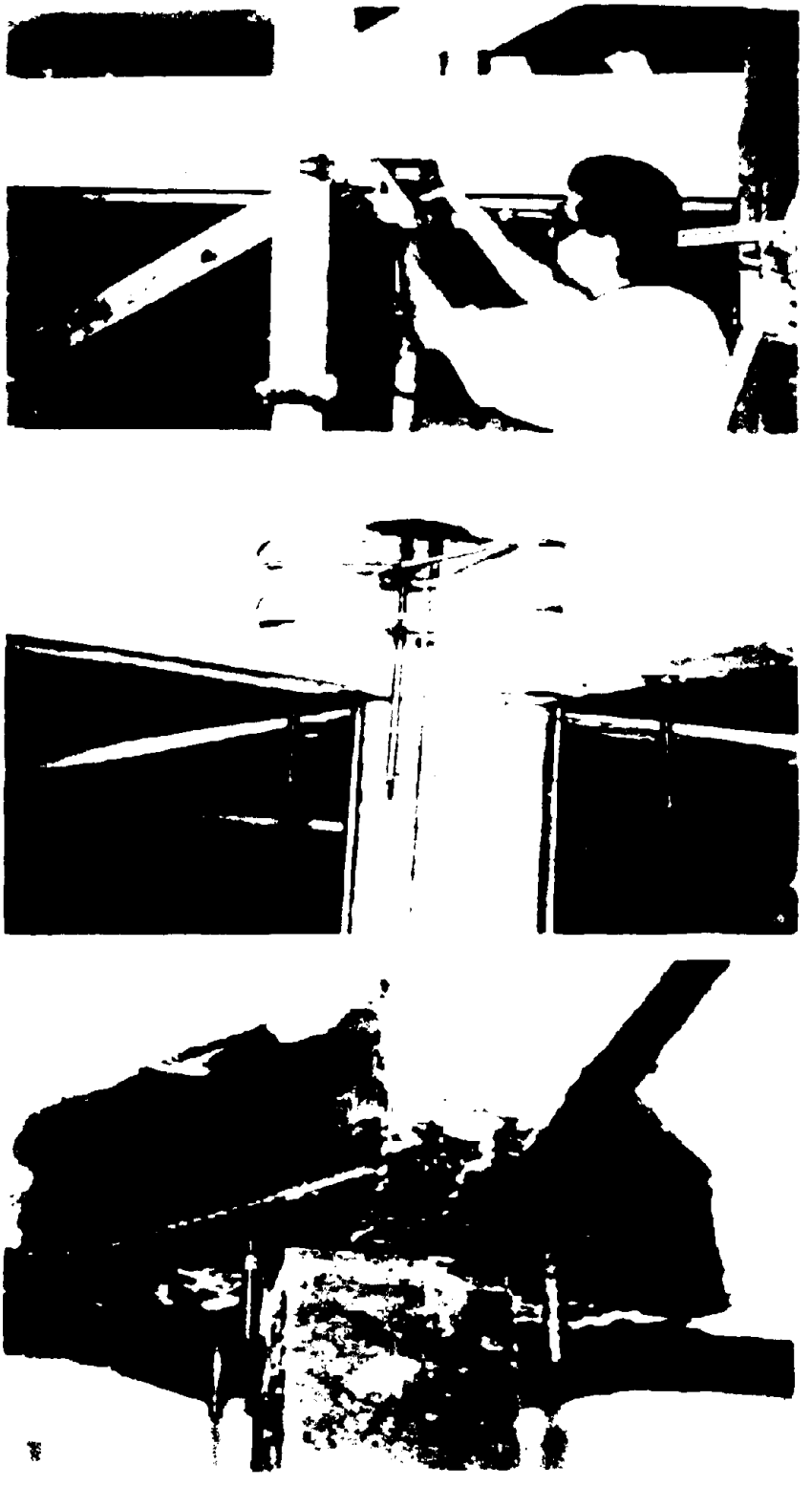

FIG. 3.1c Stages in the Improved Concrete Jacketing Retrofit of the Model (cont'd)

3.4 Dynamic Characteristics of Retrofitted Model - Before Earthquake Shaking

Following the complete retrofit construction and loading of the required weights for mass similitude, a compensated white noise shaking table excitation, WHNR_B, was used for identification of the initial dynamic characteristics of the retrofitted model. The resulting smoothed transfer functions for each floor of the model are shown in Fig. 3-2. The natural frequencies, modal shapes, participation factors, and equivalent viscous damping factors after retrofit (before earthquake shaking) are calculated and tabulated in Table 3-2. It can be observed from comparison to the properties of the original structure that the modal frequencies increase approximately 130%, 150%, and 210%, respectively due to the retrofit. Variations in the modal shapes can be detected before (WHN_F) and after (WHNR_B) retrofit, while the participation factors remain primarily constant. The additional stiffness in the interior columns that change the structural system can be held accountable for these changes. It is also worth noting that some characteristics of non-linear/inelastic response are observed in the transfer functions from the multiplicity of frequency peaks near the main/natural modes of vibration. This non-linear response is primarily attributed to the cracked behavior of the structure, particularly the unretrofitted members.

A large change can be observed in comparing the equivalent viscous damping factors before and after retrofit from Table 3-2. The unretrofitted model experienced large inelastic deformations and had considerable contributions from hysteretic damping during the shaking table tests. Since the retrofit stiffened and repaired the damage to the critical interior columns of the model, the contributions from hysteretic behavior to the "equivalent viscous damping" are significantly reduced. However, the viscous damping is not a suitable model for the energy dissipation and therefore, the equivalent ratios are not used in analysis.

The updated stiffness matrix of the model using the dynamic characteristics of WHNR_B is shown in Table 3-2 along with the corresponding story stiffnesses. It can be observed that the sum of the diagonal terms of the stiffness matrix is increased by about 800% after retrofit. Story stiffness increases of 440%, 1140%, and 860%, respectively for the first, second, and third stories have resulted after retrofit. The different stiffness change of the first story compared to the changes in the second and third stories is due to the discontinuity of the added rebars into the base and lack of prestressing in the lower first story columns. Also note that the stiffness change of the first floor correlates to the change in first mode natural frequency as follows:

$$\frac{f_r}{f_f} = \sqrt{\frac{k_r}{k_f}} \tag{3.1}$$

where f_r = first mode natural frequency from WHNR_B (after retrofit)

f_f = first mode natural frequency from WHN_F (before retrofit)

k_r = first story stiffness from WHNR_B

k_f = first story stiffness from WHN_F

Fig. 3-3 shows the story shear versus inter-story drift histories for WHNR_B. It can be observed that loops occur in these histories mostly due to the equivalent damping present in the structure. The initial stiffnesses for small amplitude displacements are tabulated in Table 3-3 and correspond to increases of about 300%, 600%, and 600%, respectively after retrofit as compared to WHN_F.

At the conclusion of white noise excitation WHNR_B, the table was set down for the day (1/28/92). The next day (1/29/92), the table was again lifted and another white noise excitation, WHNR_C, was performed for identification of the dynamic characteristics of the model. Fig 3-4 shows the smoothed story transfer functions. The natural frequencies, modal shapes, modal participation factors, and equivalent viscous damping factors are calculated and tabulated in Table 3-4. It can be observed that the natural frequencies are reduced by 5.0%, 2.1%, and 0.3%, respectively from the induced white noise shaking table excitation and/or the lowering and lifting of the shaking table. Although it is considered that this reduction is minor. Comparable modal shapes and participation factors can be observed between WHNR_B and WHNR_C. A variation can be observed in comparing the first mode damping factors of WHNR_B and WHNR_C from Table 3-4, which indicates the occurrence of some non-linear cracking behavior in the model due to the white noise excitation.

The updated stiffness matrix and story stiffnesses of the model, using the dynamic characteristics of WHNR_C, is shown in Table 3-4. It can be observed that the sum of the diagonal terms of the stiffness matrix is reduced by 1.6% and a 18.8% story stiffness degradation occurs to the first story due to the movement of the model during the white noise excitation tests and during the lowering and lifting of the shaking table to operating positions.

Fig. 3-5 shows the story shear versus inter-story drift histories for WHNR_C. From Table 3-5, the initial stiffnesses for small amplitude displacements are comparable with the stiffnesses from WHNR_B (Fig. 3-3), but slightly softened.

Therefore it is concluded that the lowering and lifting process and/or the input white noise shaking table excitation inflicts some minor softening to the retrofitted model structure, but is considered insignificant for the strong base motion testing.

TABLE 3-2 Dynamic Properties and Stiffness Matrix before and after Retrofit

	WHN_F (before retrofit)	WHNR_B (after retrofit)
Natural Frequencies (Hz.)	$\mathbf{f}_i = \begin{pmatrix} 1.20 \\ 3.76 \\ 5.27 \end{pmatrix}$	$\mathbf{f}_i = \begin{pmatrix} 2.78 \\ 9.38 \\ 16.75 \end{pmatrix}$
Modal Shapes	$\Phi_{ij} = \begin{pmatrix} 1.00 & -0.86 & -0.46 \\ 0.75 & 0.64 & 1.00 \\ 0.33 & 1.00 & -0.94 \end{pmatrix}$	$\Phi_{ij} = \begin{pmatrix} 1.00 & -0.86 & -0.51 \\ 0.79 & 0.48 & 1.00 \\ 0.42 & 1.00 & -0.89 \end{pmatrix}$
Modal Participation Factors	$\Gamma_i = \begin{pmatrix} 0.43 \\ 0.14 \\ -0.07 \end{pmatrix}$	$\Gamma_i = \begin{pmatrix} 0.44 \\ 0.12 \\ -0.07 \end{pmatrix}$
Damping Ratios (%)	$\xi_i = \begin{pmatrix} 7.0 \\ 2.3 \\ 1.8 \end{pmatrix}$	$\xi_i = \begin{pmatrix} 3.0 \\ 1.9 \\ 1.3 \end{pmatrix}$
Stiffness Matrix (kip/in)	$\mathbf{K}_{ij} = \begin{pmatrix} 23.3 & -24.8 & 0.7 \\ -24.8 & 45.6 & -22.4 \\ 0.7 & -22.4 & 51.0 \end{pmatrix}$	$\mathbf{K}_{ij} = \begin{pmatrix} 205.2 & -238.6 & 71.6 \\ -238.6 & 421.4 & -278.2 \\ 71.6 & -278.2 & 432.7 \end{pmatrix}$
Story Stiffnesses (kip/in)	$\mathbf{k}_i = \begin{pmatrix} 24.8 \\ 22.4 \\ 28.6 \end{pmatrix}$	$\mathbf{k}_i = \begin{pmatrix} 238.6 \\ 278.2 \\ 154.5 \end{pmatrix}$

TABLE 3-3 Low Amplitude Initial Stiffnesses from the Shear versus Inter-Story Drift Histories

Story	WHN_F (kip/in)	WHNR_B (kip/in)
Third	14.3	100.0
Second	14.3	100.0
First	27.8	113.2

TABLE 3-4 Dynamic Properties and Stiffness Matrix of the Retrofitted Structure from WHNR_B and WHNR_C

	WHNR_B	WHNR_C
Natural Frequencies (Hz.)	$\mathbf{f}_i = \begin{pmatrix} 2.78 \\ 9.38 \\ 16.75 \end{pmatrix}$	$\mathbf{f}_i = \begin{pmatrix} 2.64 \\ 9.18 \\ 16.70 \end{pmatrix}$
Modal Shapes	$\Phi_{ij} = \begin{pmatrix} 1.00 & -0.86 & -0.51 \\ 0.79 & 0.48 & 1.00 \\ 0.42 & 1.00 & -0.89 \end{pmatrix}$	$\Phi_{ij} = \begin{pmatrix} 1.00 & -0.86 & -0.49 \\ 0.79 & 0.45 & 1.00 \\ 0.44 & 1.00 & -0.83 \end{pmatrix}$
Modal Participation Factors	$\Gamma_i = \begin{pmatrix} 0.44 \\ 0.12 \\ -0.07 \end{pmatrix}$	$\Gamma_i = \begin{pmatrix} 0.44 \\ 0.11 \\ -0.07 \end{pmatrix}$
Damping Ratios (%)	$\xi_i = \begin{pmatrix} 3.0 \\ 1.9 \\ 1.3 \end{pmatrix}$	$\xi_i = \begin{pmatrix} 4.7 \\ 1.8 \\ 1.6 \end{pmatrix}$
Stiffness Matrix (kip/in)	$\mathbf{K}_{ij} = \begin{pmatrix} 205.2 & -238.6 & 71.6 \\ -238.6 & 421.4 & -278.2 \\ 71.6 & -278.2 & 432.7 \end{pmatrix}$	$\mathbf{K}_{ij} = \begin{pmatrix} 198.9 & -238.2 & 65.2 \\ -238.2 & 438.5 & -279.1 \\ 65.2 & -279.1 & 404.6 \end{pmatrix}$
Story Stiffnesses (kip/in)	$\mathbf{k}_i = \begin{pmatrix} 238.6 \\ 278.2 \\ 154.5 \end{pmatrix}$	$\mathbf{k}_i = \begin{pmatrix} 238.2 \\ 279.1 \\ 125.5 \end{pmatrix}$

TABLE 3-5 Low Amplitude Initial Stiffnesses from the Shear versus Inter-Story Drift Histories

Story	WHNR_B (kip/in)	WHNR_C (kip/in)
Third	100.0	96.8
Second	100.0	96.8
First	113.2	109.1

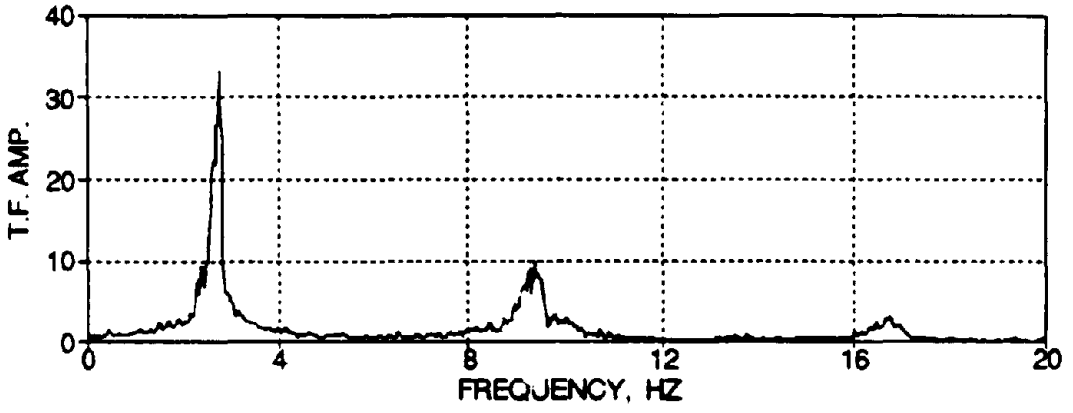

(a) Third Floor

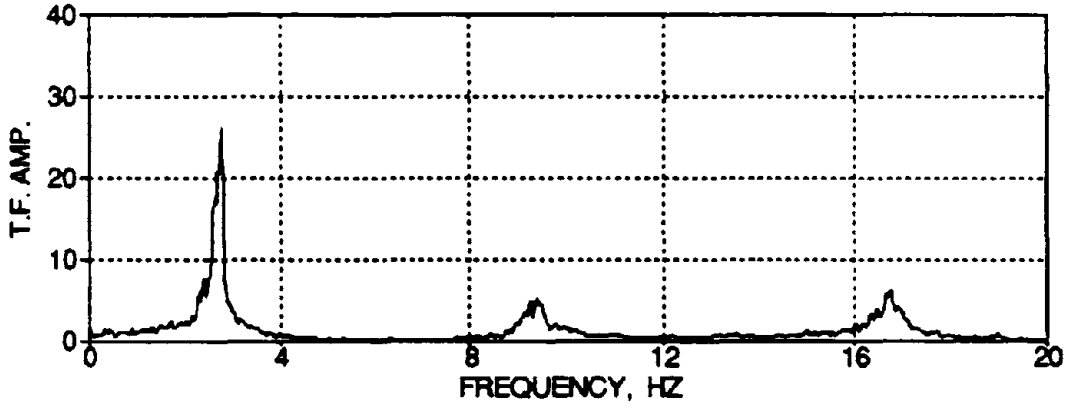

(b) Second Floor

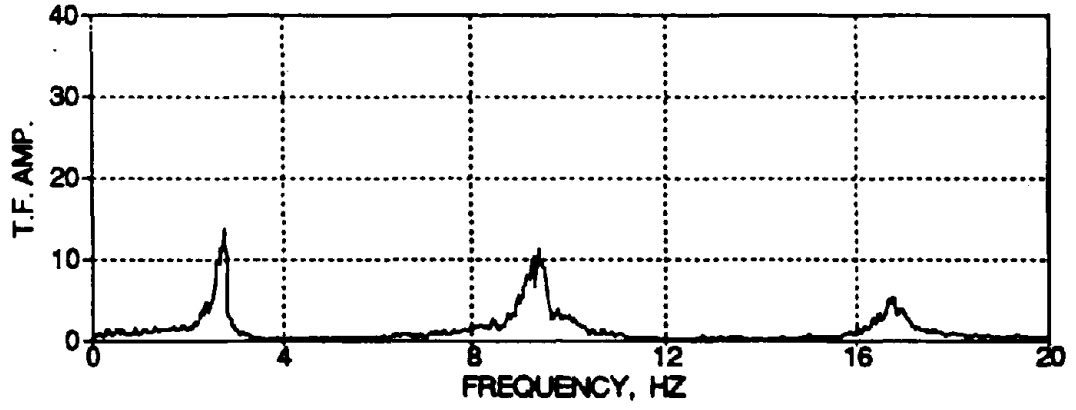

(c) First Floor

FIG. 3-2 Smoothed Transfer Functions from WHNR_B

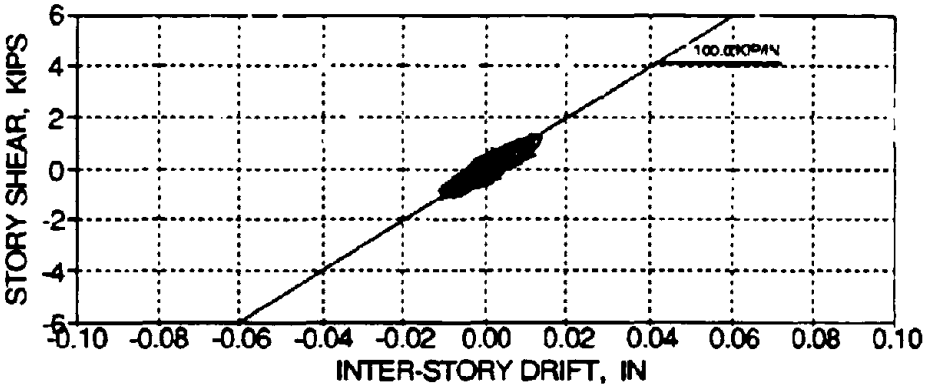

(a) Third Floor

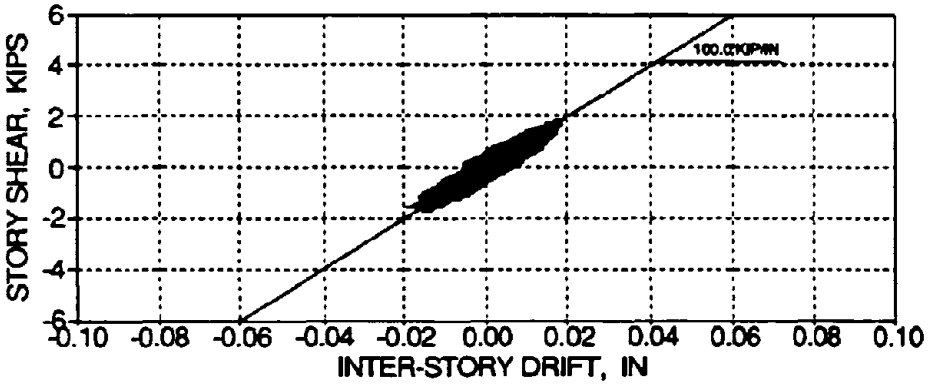

(b) Second Floor

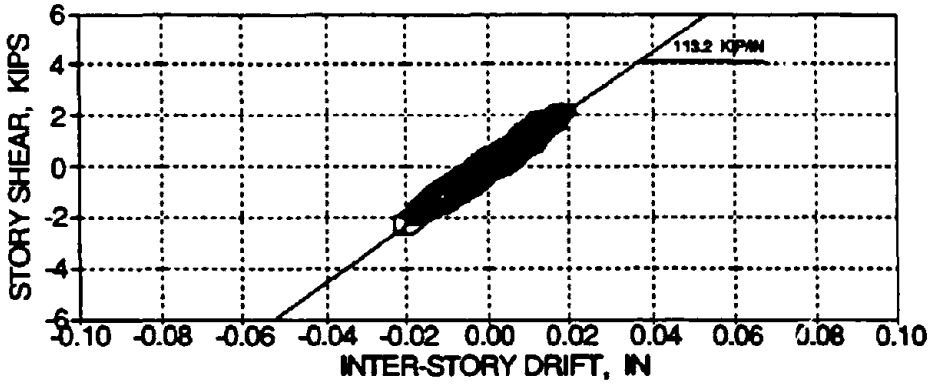

(c) First Floor

FIG. 3-3 Story Shear versus Inter-Story Drift Histories for WHNR_B

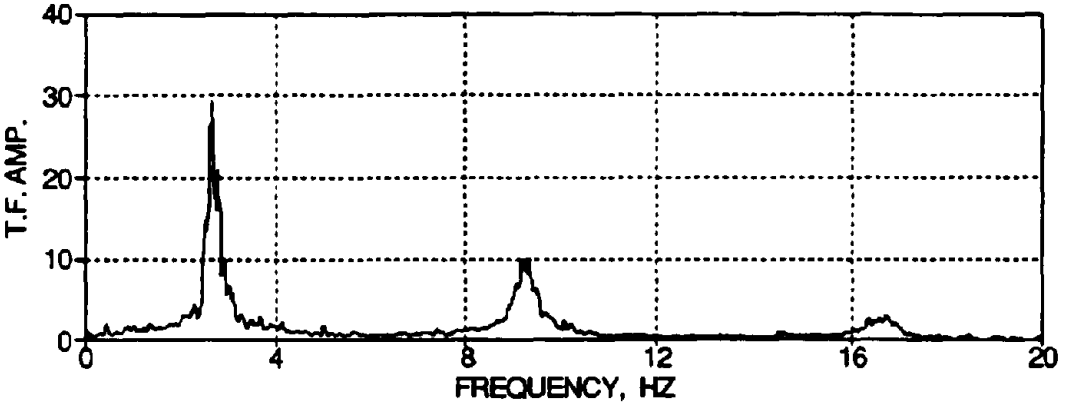

(a) Third Floor

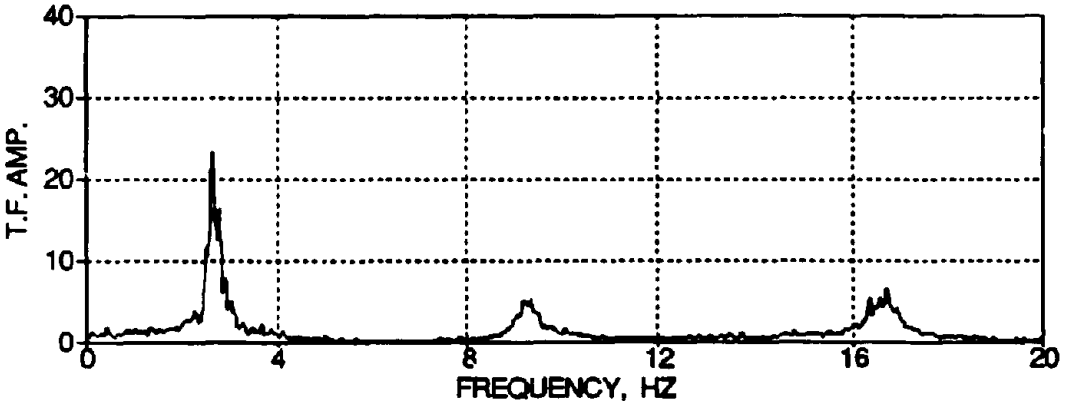

(b) Second Floor

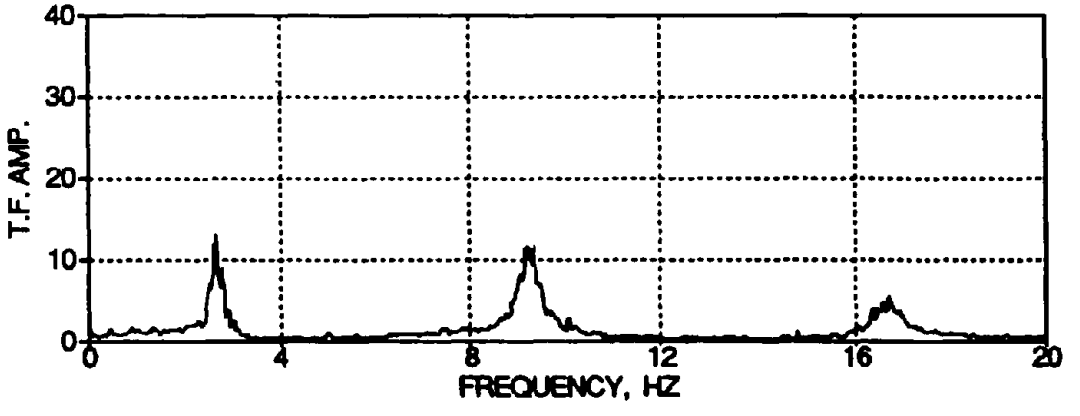

(c) First Floor

FIG. 3-4 Smoothed Transfer Functions from WHNR_C

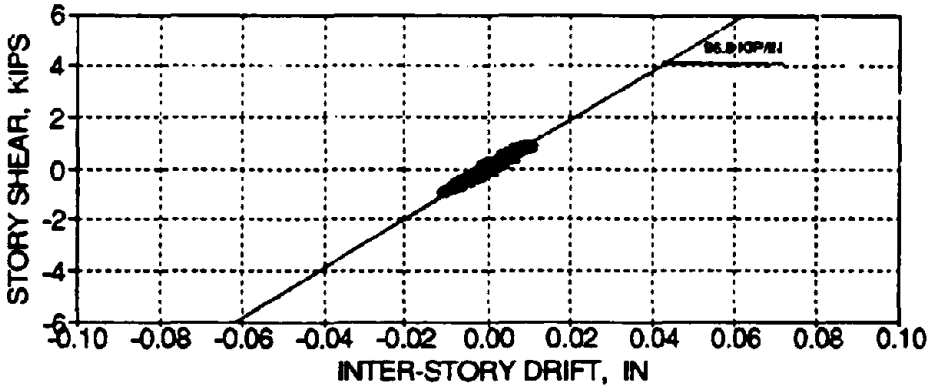

(a) Third Floor

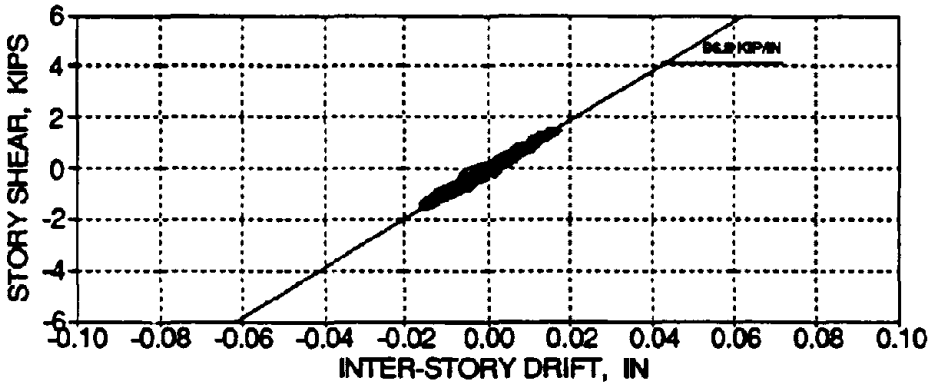

(b) Second Floor

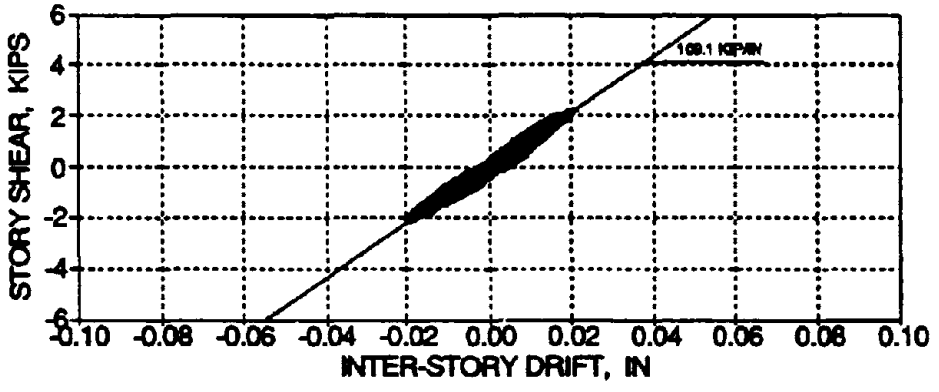

(c) First Floor

FIG. 3-5 Story Shear versus Inter-Story Drift Histories for WHNR_C

3.5 Summary Discussions

The retrofit method selected for the damaged model is the improved concrete jacketing of the interior columns with a weak base retrofit. This retrofit technique: (i) provides satisfactory control of response from seismic forces; (ii) is easy and inexpensive to construct; (iii) requires minimal material that is readily available; and (iv) is a feasible retrofit for the model building.

From the white noise excitation of the retrofitted model, the dynamic properties indicate:

(1) Story stiffness increases of about 440%, 1140%, and 860%, respectively for the first, second, and third floors, as expected. This corresponds to increases in natural frequencies of about 130%, 150%, and 210%, respectively for the first three modes of vibration.

(2) A decrease in equivalent viscous damping from smaller contributions of hysteretic damping after retrofit. This decrease is attributed to the effect of prestressing which ensures the columns behave in an uncracked linear-elastic state.

The testing of the retrofitted model under simulated earthquakes is planned to verify:

(1) A change in formation of the potential collapse mechanism under ultimate load from an undesirable column-sidesway/soft-story mechanism to a more desirable beam-sidesway mechanism.

(2) A reduction of inter-story drifts due to additional stiffening.

(3) A reduction in the expected damage states due to strengthening of the columns.

(4) The use of post-tensioning, to avoid placement of transverse shear steel, leads to a satisfactory structural performance and joint behavior.

(5) Constructability and economical aspects.

SECTION 4

PERFORMANCE OF RETROFITTED R/C MODEL DURING EARTHQUAKES

4.1 Introduction

In Sections 2 and 3, an improved concrete jacketing method was proposed and analyzed for retrofit of the one-third scale three story R/C frame model building. The retrofitted model was tested according to the schedule in Table 3-1.

A moderate base motion, the Taft N21E accelerogram with the peak ground acceleration (PGA) scaled to 0.20 g, was first used to examine the structural response, the damage evaluation, and the identification of the ensuing dynamic characteristics of the retrofitted model.

A more severe shaking was subsequently used (Taft N21E accelerogram with the PGA scaled to 0.30 g). Likewise, the response results, the damage evaluation, and the ensuing dynamic characteristics of the retrofitted model are presented.

A comparison of the above test results with those from the unretrofitted system is presented in this section.

Member behavior parameters are derived from component tests and used to analytically predict the story response during induced base motions. Damage quantifications are obtained analytically for the retrofitted structure for the moderate and severe earthquakes. An elastic analysis is performed for identification of equivalent strength ratios to the inelastic response.

4.2 Response to Moderate Earthquake

A moderate earthquake, the Taft N21E accelerogram scaled for a PGA of 0.20 g, was used to excite the retrofitted model (herein referred to as TFTR_20). Figs. 4-1a and 4-1b show the desired and achieved lateral shaking table acceleration motions for TFTR_20. Fig. 4-1c shows a short segment of the desired and achieved shaking table motions. Initially the desired and achieved motions are similar. However after 11 seconds, the table became erratically unstable causing high frequency accelerations. The excitation gain of the shaking table was immediately

lowered and thereafter the achieved acceleration history shows good agreement with the desired. The instability in the shaking table performance is attributed to some torsional-rocking resonance created by the uneven distribution of damage in the model.

Figs. 4-2a and 4-2b show the vertical table acceleration on the north and south sides of the table. It can be observed that the vertical accelerations are controlled (maintained to zero) except during the table instability The peak vertical acceleration of the table is 0.87 g, which is quite considerable and is closely examined for the effect on the resulting structural response. The vertical response on each side of the table are in-phase, thus implying that the table is uniformly accelerating in the vertical direction. Fig. 4-2c shows the Fourier Transform of the north side vertical table acceleration history. Some frequencies between 10.0 Hz. and 12.0 Hz. and also between 20.0 Hz. and 25.0 Hz. are excited. A point of interest is that the natural frequency of the shaking table with the mass of the structure is in the range of 20.0 Hz. to 25.0 Hz., which explains some of the resonant response.

Fig. 4-3 shows the east and west lateral base acceleration histories along with the corresponding phase angle. Out-of-phase motions can be observed near frequencies of 10.0 Hz. to 12.0 Hz. and higher frequencies, which indicates that the shaking table is yawing (or twisting). Since the response is governed by the first and second modes of vibration, the influence of this out-of-phase input motion is negligible. Fig. 4-4 shows the induced transverse shear forces in the interior and exterior first story east frame columns for table motion TFTR_20. It can be observed from the exterior columns that the transverse shear forces are completely out-of-phase, which implies the building is experiencing torsion. The shear force amplitudes continually increase until the table became unstable. Thereafter the shear forces again can be observed to be out-of-phase. Also a point to note is that the shear forces of interior columns have drifts in the signal at about 3 seconds and then stabilize. This can possibly imply yielding of the load cells and is further examined individually for each load cell in Section 4.2.2.

Therefore it is concluded that the torsional response in the structure due to an uneven distribution of damage was driving the shaking table in a yawing motion during the moderate earthquake and the table control system was not able to control this torsional motion. However the input torsional effects are still minor with respect to the lateral and the overall response is not excessively affected from the instability. To develop meaningful conclusions for the lateral direction, the torsional effects in the building respon· are filtered through an averaging technique as presented in the next section.

4.2.1 Global Response

Fig. 4-5 shows the average story displacement time histories of the east and west sides of the model during moderate earthquake, test TFTR_20. Note that the story displacement histories on the east and west sides of the model are comparable but slightly out-of-phase. The variations of recorded displacements between the east and west frames were within 1%. Fig. 4-6 shows the story shear force time histories identified from the load cells in the first and second story columns and the third story level accelerometers. It can be observed that minor signal drifts of the first and second story shear forces have occurred, which possibly occurs due to some yielding in the load cells. Figs. 4-7a and 4-7b show a magnified overlayed portion of the story displacements and shear forces, respectively. It can be observed that the story displacements and shear forces are moving in phase. Figs. 4-8a and 4-8b show the story displacements, shear forces, and story loads when the maximum first story drifts occurs. The shape of the magnitudes of the story displacements and shears at this point in time resembles the shape caused by the first mode of vibration of the model. Therefore it is concluded that the structural response of the retrofitted building for the moderate earthquake is governed by the first mode of vibration.

Table 4-1 summarizes the maximum results for story displacements, inter-story drifts, story shear forces, story loads, and peak story accelerations for each floor of the model for TFTR_20. It can be observed that the maximum inter-story drifts are 1.37%, 0.80% and 0.33% of the story height, respectively for the first, second and third stories. The maximum inter-story drifts for the unretrofitted building tested by the same moderate earthquake were 1.33%, 1.07%, and 0.54% of the story height, respectively (Bracci et al., 1992b). Therefore the retrofit did not influence the first story drifts, but reduced the second and third story drifts. It will be shown later that the large first story drift of the retrofitted model is a result of the formation of plastic hinges in the lower first story columns and in the first story interior beams. It should be noted that the large first story drift was not predicted in the analytical modeling developed in Section 2. The explanations for this deviation are discussed in Section 4.6. The maximum measured base shear force for the retrofitted model (20.6 kips) is 25.0% of the total structural weight W, whereas the base shear for the unretrofitted model was 15.2% W. Also note in Table 4-1 that there are story acceleration amplifications of 18.2%, 50.0%, and 72.7%, respectively for the first, second, and third stories of the retrofitted building, as compared to the little amplification in the unretrofitted building.

TABLE 4-1 Maximum Response for Moderate Earthquake TFTR_20

Story	Max. Story Displacement (in.)	Max. Inter-Story Drift (percent)	Max. Story Shear (kips)	Max. Story Load (kips)	Peak Story Acceleration (g)
Third	1.18	0.33	10.7	10.7	0.38
Second	1.03	0.80	16.2	9.9	0.33
First	0.66	1.37	20.6 (25.0%W)	8.1	0.26

Fig. 4-9 shows the story shear force versus inter-story drift histories for each floor of the model for test TFTR_20, along with the initial low amplitude story stiffnesses from the previous white noise excitation (WHNR_C). The secondary stiffnesses are also identified for TFTR_20 as 30.2 kip/in for each floor and are compared with the achieved secondary stiffness from the severe shaking to detect any changes due to continued inelastic deformations and strength deterioration in the members of that story. Note that since the third story is primarily governed by elastic response, the secondary stiffness is assumed identical to the first and second stories. It can be observed that considerable inelastic behavior and corresponding stiffness reductions primarily develop on the first and second stories during the moderate earthquake, TFTR_20. The location of member damage can not be distinguished, however its identification is discussed later in this section.

Fig. 4-10a shows the time history of the energy balance for the model during TFTR_20. The total input energy into the model is about 40.0 kip-in, which is 66.7% larger than in the original building for the same motion (TFT_20). The increase in the input energy is a result of the stiffening of the structure from the retrofit. Fig. 4-10b shows the hysteretic and viscous damped energies of each floor of the model as 25.5 kip-in, 15.0, kip-in, and 1.5 kip-in, respectively. This corresponds to percentage ratios of 60.8% : 35.6% : 3.6% of the total, respectively for the first, second, and third stories. In comparison to the original building for the moderate shaking, the percentage ratio of hysteretic and viscous damped energies were 53.2% : 33.2% : 13.6%, respectively. It can be observed that a slightly larger amount of energy is dissipated by the first floor in the retrofitted model. It is interesting to note that the total hysteretic and viscous damped

energies do not exactly equate to that of the input energy. This is a result of the presence of torsion in the structure and of using average story displacements, velocities, and accelerations for the energy balance.

4.2.2 Local Response

Fig. 4-11 shows the induced lateral shear forces in the interior and exterior first story columns (base shear) for the moderate shaking (TFTR_20). For local member designations see Bracci et al. (1992a). It can be observed that the shear forces in the interior columns are approximately five times larger than the exterior columns, which correlates to the ratio of the moments of inertia. Note that both the interior and exterior columns attract higher shear forces when the axial force increases. The shear force signal in column #3 at the end of the motion has an offset. Since the load cells are designed for a shear force capacity of 5 kips, yielding of this load cell may have occurred due to shear force demands near or larger than 5 kips. Also since columns #1, #2, and #4 have no drift in the shear force signals, the drift in the total story shear signal from Fig. 4-6 is a direct result of the signal drift in column #3.

Fig. 4-12 shows the bending moment versus axial load interaction diagrams for the columns of the first and second stories at the beam or slab interfaces. The development of the nominal ultimate surface is presented by Bracci et al. (1992a). The predicted dynamic ultimate surface is developed based on a 30% material strength increase due to strain rate effects and strain hardening of the reinforcement. The surfaces developed for the lower first story columns are based on a 6" square section with the two existing steel layers, since the added reinforcement is discontinued at the base. The surfaces developed for the exterior columns are presented by Bracci et al. (1992a). It can be observed that the bending moment versus axial load history in the columns remain within the nominal ultimate bounds for all columns except that of the lower first story columns. However, note that the lower first story columns are designed as a primary hinge location for the beam-sidesway failure mechanism. Since the retrofit includes transverse hoop steel in the lower first story columns for enhanced shear strength and ductility, these retrofitted columns are in no danger of shear failure. Also note that the interaction history of the unretrofitted exterior columns remain within ultimate bounds. Therefore the retrofit of the interior columns is successful in transferring the induced damage from the vulnerable columns to more safer places in the structure. Also note the greater margin between the seismic loads and the column capacities in the retrofitted columns as compared to the unretrofitted. The

waviness in the interaction histories is a direct result of the table instability. Since the table was accelerating in the vertical direction, additional axial forces are developed in the columns creating distortion in the interaction diagram.

Fig. 4-13a and 4-13b show the first story beam bending moment time histories in the south and north sides of the model at the face of the added joint reinforcement in the fillet along with the ultimate moment surfaces. The development of the ultimate surfaces for the beams considers: (i) the slab reinforcement within the flange width from the ACI-318 (18 in.); and (ii) the slab steel within the full slab width (60 in.). Also the positive ultimate moment (plotted on the negative side) considers tensile contributions from the slab steel, the top reinforcement, and the partially unbonded reinforcement from pull-out of the discontinuous bottom longitudinal reinforcement. However, note that the retrofit of the interior columns provides additional bond and prestressing pressure from the added longitudinal reinforcement to avoid pull-out of these bars. Therefore this surface is only representative for the exterior beams. For the interior beams, both positive nominal ultimate surfaces considering the ACI-318 slab width and the full slab width are representative. It can be observed that the moment demands in the interior beams exceed nominal ultimate bounds, which consider slab steel contributions from the ACI-318 specified slab width and the full slab, in the negative direction. For the positive direction, the measured moments exceed the capacity based on the ACI-318 slab width and are within the capacity based on the full slab width. However, failure does not occur since the moments remain well within the predicted dynamic ultimate surface. Therefore, hinging has developed in the interior beam members of the first story. Also, it is important to note from the measured beam moments that the slab steel from the full slab width contributes to the beam moment capacities. The exterior beam moments remain within the nominal ultimate surfaces and the partially unbonded positive moment surface (since these members were not retrofitted).

The bending moment diagrams for the model are shown in Fig. 4-14 when the first story drift was maximum in each direction, along with the corresponding story displacements. It can be observed that yielding moments have developed in the lower first story columns and in the interior beams of the first floor. However, note that the demands in the exterior beams and possibly the beam moments of the second and third floors are less than capacity. Thus the complete beam-sidesway collapse mechanism has not developed (evident from the test).

The visually observed cracking and measured damage states of the retrofitted model due to the moderate earthquake TFTR_20 are shown in Fig. 4-15. The following points highlight the observed structural damage:

(a) cracking occurred in the lower first story interior columns;

(b) cracking occurred in the beams of the first and second stories near the end of the fillet;

(c) slab cracks were observed along the end of the added fillet primarily throughout the slab width;

(d) additional cracks in the web of the longitudinal beams;

(e) torsional cracks in the south-west transverse beam.

Note that the visual damage and that established by testing do not always correspond, except for the very strongly damaged and worked hinges.

4.3 Dynamic Properties after Moderate Shaking

The dynamic properties of the retrofitted model after the moderate earthquake (TFTR_20) are determined from the white noise excitation labeled as WHNR_D. Since torsion is present in the structure during TFTR_20, the following identifications compare both characteristics of the east and west frames of the model. Figs. 4-16a and 4-16b show the smoothed story transfer functions for the east and west frames of the model, respectively. From the transfer functions, the natural frequencies of the east frame are identified as 1.98 Hz., 8.11 Hz., and 15.33 Hz. and are tabulated in Table 4-2. It can be observed that the natural frequencies of the east frame are reduced by 25.0%, 11.7%, and 8.0%, respectively due to the moderate earthquake. Since a larger reductions in natural frequency occur in the first mode, the table motion largely excites only the first mode of vibration of the model (as was observed in the tests). The modal shapes and participation factors are identified from the story transfer functions and compare with the results before shaking (WHNR_C). Likewise the natural frequencies of the west frame are identified as 1.93 Hz., 7.98 Hz., and 15.48 Hz. and shown in Table 4-3 for comparison with the east frame. It can be observed that the first mode natural frequency of the west frame suffers slightly more deterioration than the east frame. The modal shapes and participation factors of the west frame are comparable with the east frame.

Fig. 4-17 shows the phase angle between the third floor accelerometers on the east and west frames of the model for WHNR_D. It can be observed that the east and west frames are about 20° out-of-phase near the first mode natural frequency, which implies torsion in the model during WHNR_D.

The equivalent viscous damping factors of the east frame are determined from the half-power method as 6.6%, 2.6%, and 1.4%, respectively. The damping factors of the west frame are 8.1%, 2.8%, and 0.8%, respectively. Again since the model experienced inelastic deformations for test TFTR_20, larger damping factors developed due to contributions from hysteretic damping in comparison with the damping factors before shaking (WHNR_C). Since the west frame was previously shown to have suffered more damage, a larger damping factor develops in the west frame.

The updated stiffness matrix of the model, developed from the dynamic characteristics of the east frame from WHNR D, is shown in Table 4-2. It can be observed that the sum of the diagonal terms of the stiffness matrix from the east frame is reduced by 17.7% after the moderate earthquake or a total of 19.0% from the untested retrofitted model (WHNR_B). Story stiffness reductions of 29.1%, 17.8%, and 8.4%, respectively for the first, second, and third stories of the east frame, have resulted from TFTR_20. Therefore the first floor of the model suffered more stiffness deterioration than the others. Table 4-3 shows the stiffness matrix and story stiffness comparisons of the east and west frames of the model. It can be observed that the sum of the diagonal terms of the west frame stiffness matrix is similar to that of the east frame. However a greater stiffness deterioration has occurred to the first floor of the west frame in comparison with the east frame.

Fig. 4-18 shows the story shear versus inter-story drift histories for WHNR_D. The initial stiffnesses for small amplitude displacements are identified as 65.9 kip/in, 55.0 kip/in, and 65.2 kip/in, respectively for the first, second, and third stories. From Table 4-4, this corresponds to stiffness reductions of 39.6%, 43.2%, and 32.6%, respectively after TFTR_20 as compared to before shaking (WHNR_C) or 41.8%, 45.0%, and 34.8%, respectively as compared to WHNR_B (untested).

TABLE 4-2 Dynamic Properties and Stiffness Matrix before and after Moderate Shaking (East Frame)

	WHNR_C (before)	WHNR_D - East (after)
Natural Frequencies (Hz.)	$f_i = \begin{pmatrix} 2.64 \\ 9.18 \\ 16.70 \end{pmatrix}$	$f_i = \begin{pmatrix} 1.98 \\ 8.11 \\ 15.33 \end{pmatrix}$
Modal Shapes	$\Phi_{ij} = \begin{pmatrix} 1.00 & -0.86 & -0.49 \\ 0.79 & 0.45 & 1.00 \\ 0.44 & 1.00 & -0.83 \end{pmatrix}$	$\Phi_{ij} = \begin{pmatrix} 1.00 & -0.86 & -0.56 \\ 0.82 & 0.42 & 1.00 \\ 0.46 & 1.00 & -0.81 \end{pmatrix}$
Modal Participation Factors	$\Gamma_i = \begin{pmatrix} 0.44 \\ 0.11 \\ -0.07 \end{pmatrix}$	$\Gamma_i = \begin{pmatrix} 0.44 \\ 0.11 \\ -0.07 \end{pmatrix}$
Damping Ratios (%)	$\xi_i = \begin{pmatrix} 4.7 \\ 1.8 \\ 1.6 \end{pmatrix}$	$\xi_i = \begin{pmatrix} 6.6 \\ 2.6 \\ 1.4 \end{pmatrix}$
Stiffness Matrix (kip/in)	$\mathbf{K}_{ij} = \begin{pmatrix} 198.9 & -238.2 & 65.2 \\ -238.2 & 438.5 & -279.1 \\ 65.2 & -279.1 & 404.6 \end{pmatrix}$	$\mathbf{K}_{ij} = \begin{pmatrix} 182.7 & -218.2 & 71.9 \\ -218.2 & 356.9 & -229.3 \\ 71.9 & -229.3 & 318.3 \end{pmatrix}$
Story Stiffnesses (kip/in)	$\mathbf{k}_i = \begin{pmatrix} 238.2 \\ 279.1 \\ 125.5 \end{pmatrix}$	$\mathbf{k}_i = \begin{pmatrix} 218.2 \\ 229.3 \\ 89.0 \end{pmatrix}$

TABLE 4-3 Dynamic Properties and Stiffness Matrix Comparison of the East and West Frames after Moderate Shaking

	WHNR_D - East	WHNR_D - West
Natural Frequencies (Hz.)	$f_i = \begin{pmatrix} 1.98 \\ 8.11 \\ 15.33 \end{pmatrix}$	$f_i = \begin{pmatrix} 1.93 \\ 7.98 \\ 15.48 \end{pmatrix}$
Modal Shapes	$\Phi_{ij} = \begin{pmatrix} 1.00 & -0.86 & -0.56 \\ 0.82 & 0.42 & 1.00 \\ 0.46 & 1.00 & -0.81 \end{pmatrix}$	$\Phi_{ij} = \begin{pmatrix} 1.00 & -0.88 & -0.59 \\ 0.82 & 0.38 & 1.00 \\ 0.48 & 1.00 & -0.80 \end{pmatrix}$
Modal Participation Factors	$\Gamma_i = \begin{pmatrix} 0.44 \\ 0.11 \\ -0.07 \end{pmatrix}$	$\Gamma_i = \begin{pmatrix} 0.45 \\ 0.10 \\ -0.07 \end{pmatrix}$
Damping Ratios (%)	$\xi_i = \begin{pmatrix} 6.6 \\ 2.6 \\ 1.4 \end{pmatrix}$	$\xi_i = \begin{pmatrix} 8.1 \\ 2.8 \\ 0.8 \end{pmatrix}$
Stiffness Matrix (kip/in)	$\mathbf{K}_{ij} = \begin{pmatrix} 182.7 & -218.2 & 71.9 \\ -218.2 & 356.9 & -229.3 \\ 71.9 & -229.3 & 318.3 \end{pmatrix}$	$\mathbf{K}_{ij} = \begin{pmatrix} 196.0 & -226.9 & 80.6 \\ -226.9 & 356.5 & -233.8 \\ 80.6 & -233.8 & 311.9 \end{pmatrix}$
Story Stiffnesses (kip/in)	$\mathbf{k}_i = \begin{pmatrix} 218.2 \\ 229.3 \\ 89.0 \end{pmatrix}$	$\mathbf{k}_i = \begin{pmatrix} 226.9 \\ 233.8 \\ 78.1 \end{pmatrix}$

TABLE 4-4 Low Amplitude Initial Stiffnesses from the Shear versus Inter-Story Drift Histories

Story	WHNR_B (kip/in)	WHNR_C (kip/in)	WHNR_D (kip/in)
Third	100.0	96.8	65.2
Second	100.0	96.8	55.0
First	113.2	109.1	65.9

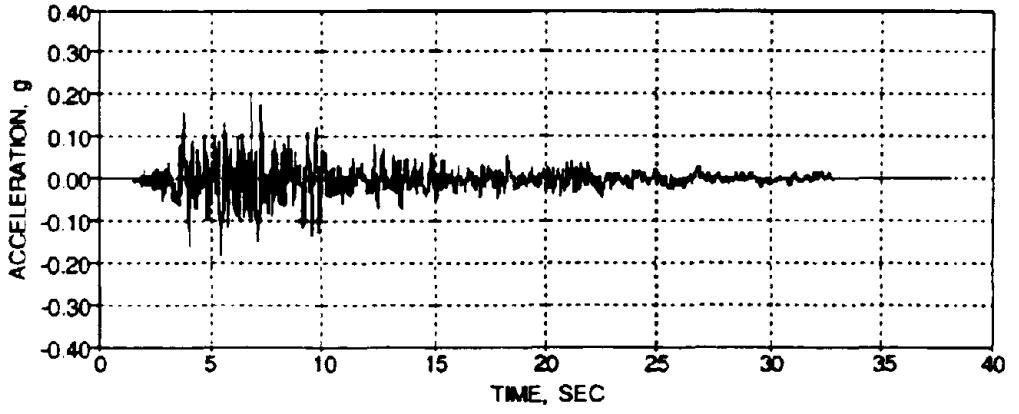

(a) Desired Base Motion

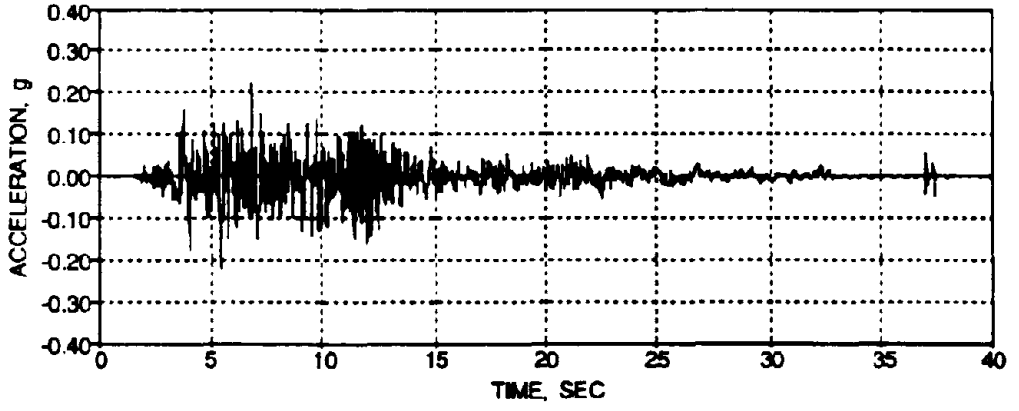

(b) Achieved Base Motion

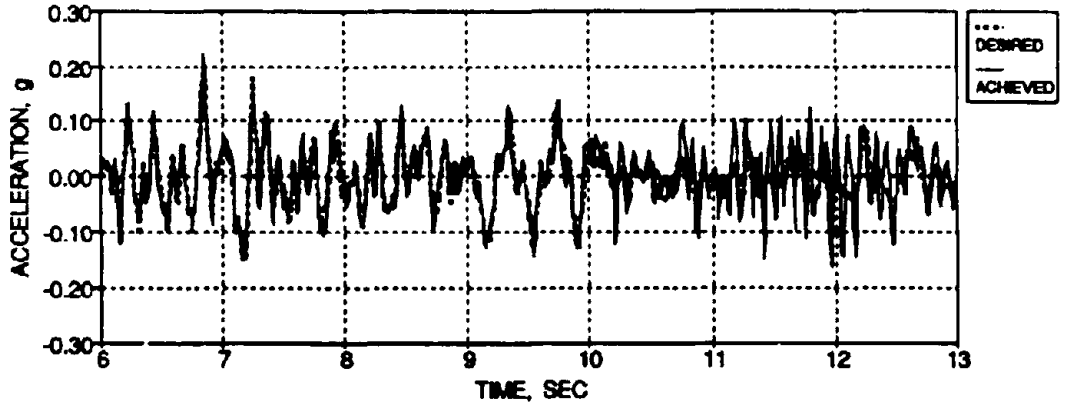

(c) Short Segment Comparison of the Desired and Achieved Base Motions

FIG. 4-1 Lateral Shaking Table Motion for TFTR_20

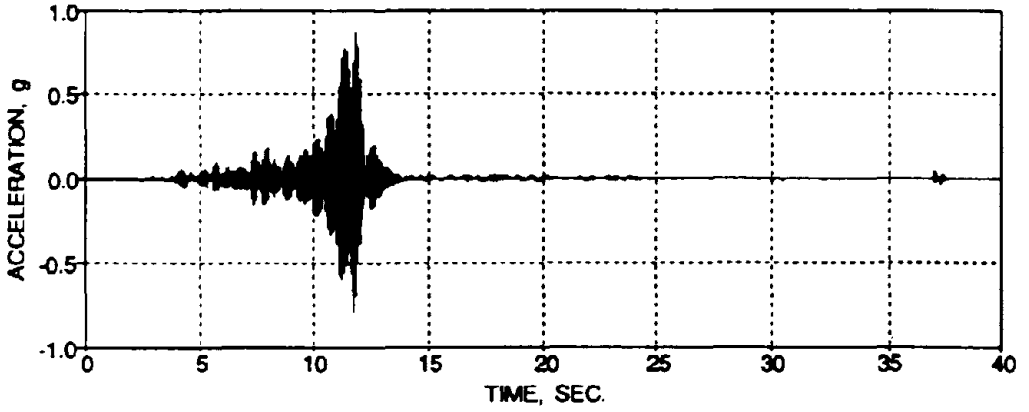

(a) North Side

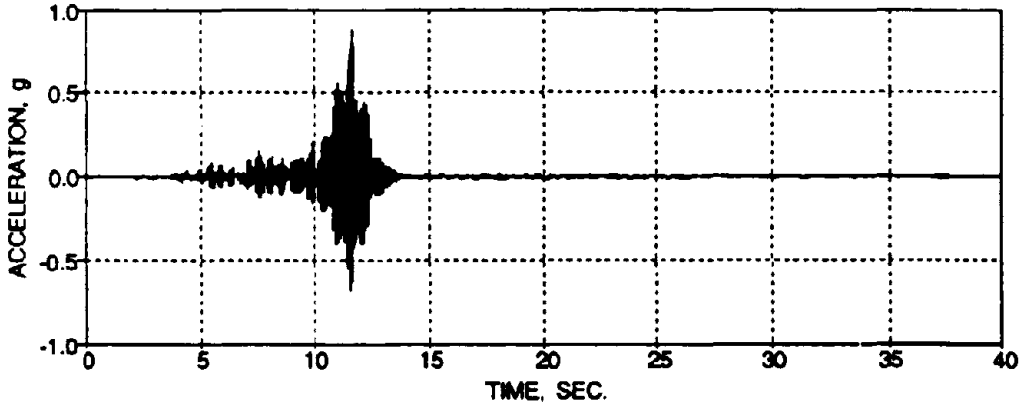

(b) South Side

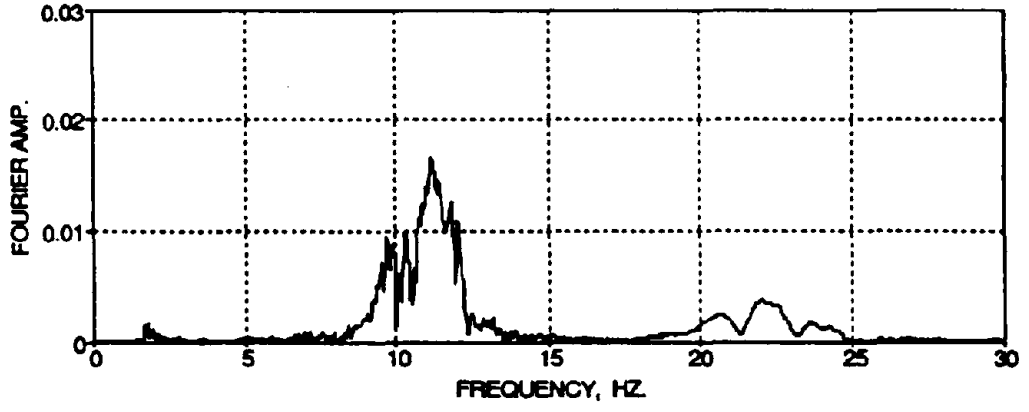

(c) Fourier Transform of the North Side Vertical Acceleration

FIG. 4-2 Vertical Shaking Table Acceleration for TFTR_20

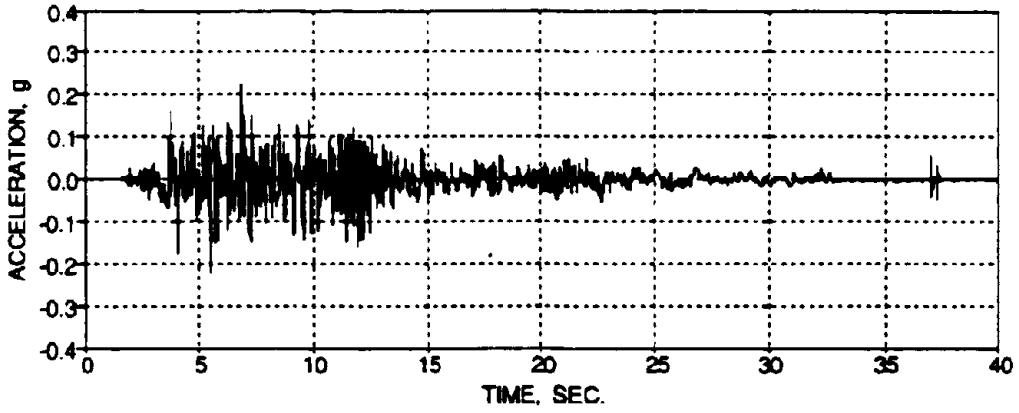

(a) East Side

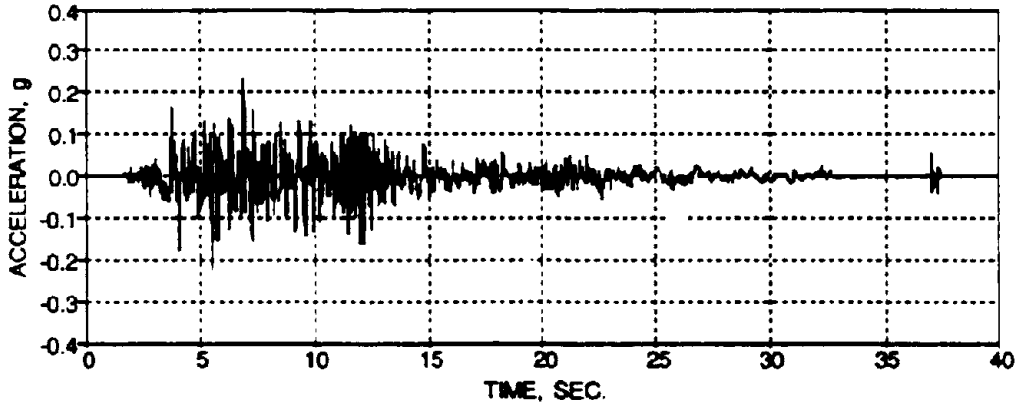

(b) West Side

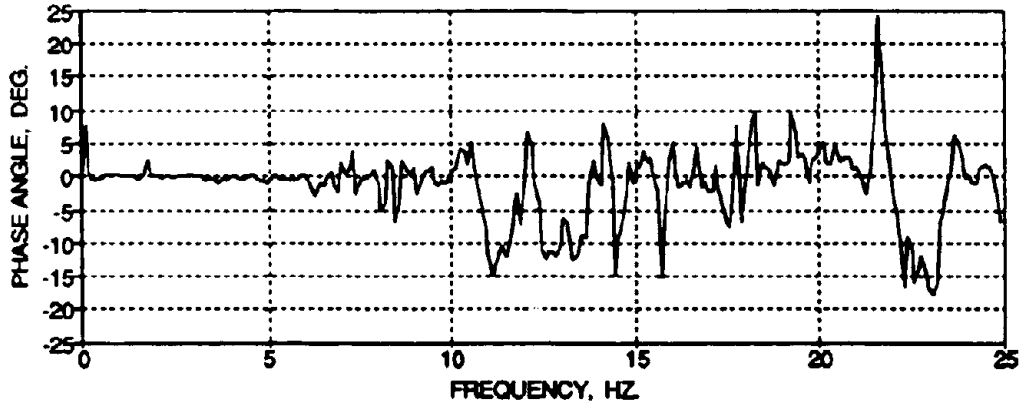

(c) Phase Angle of the East and West Side Accelerations

FIG. 4-3 East and West Lateral Acceleration for TFTR_20 - Torsion

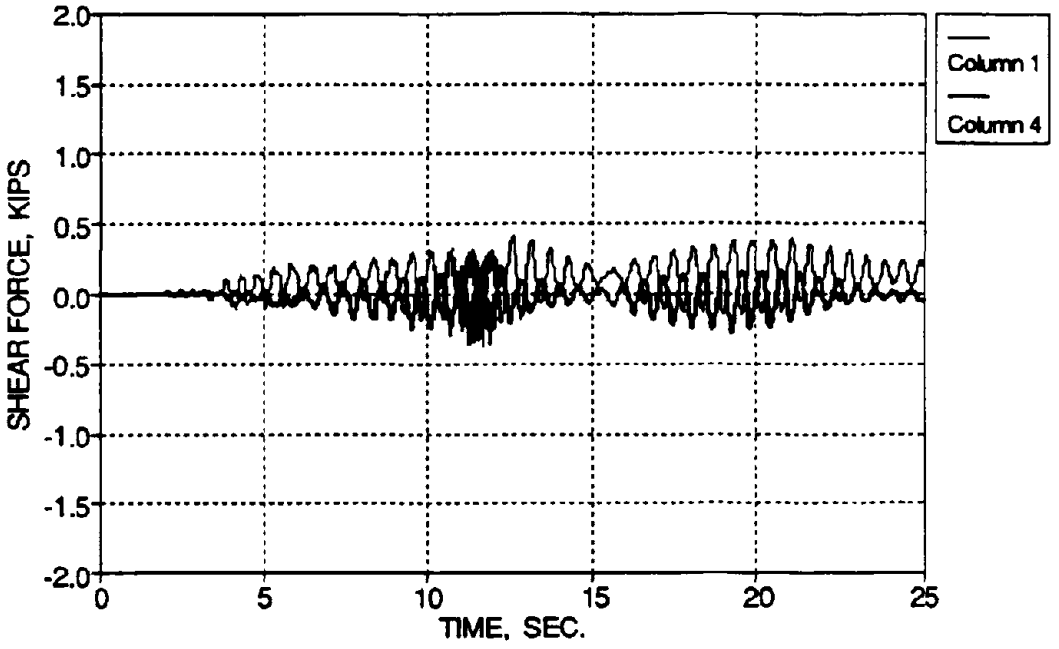

(a) Exterior Columns

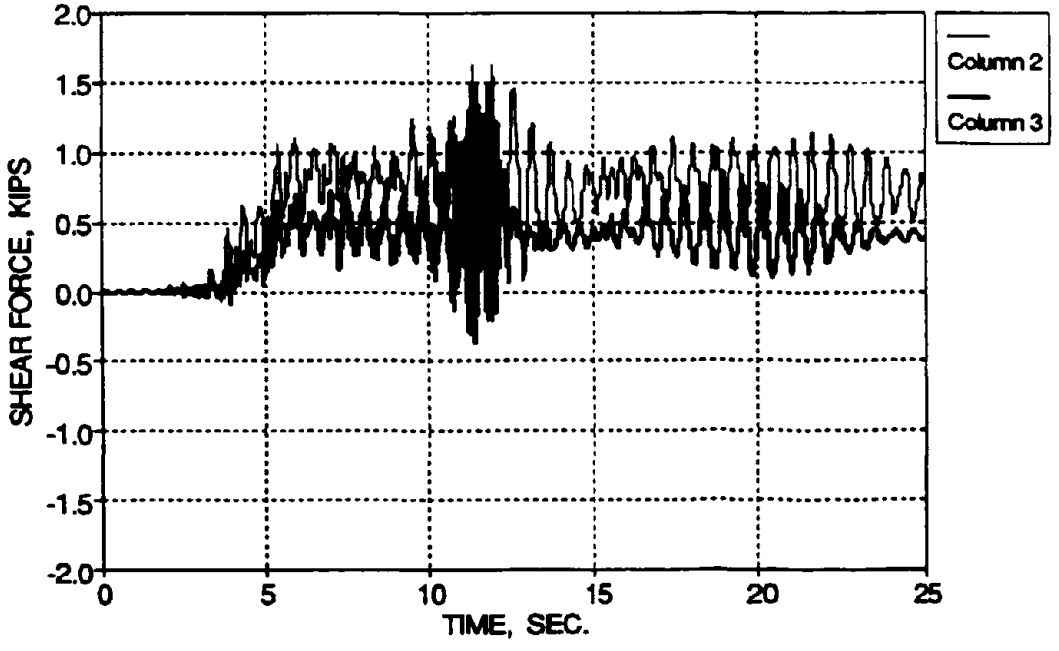

(b) Interior Columns

FIG. 4-4 Transverse Base Column Shear Forces for TFTR_20

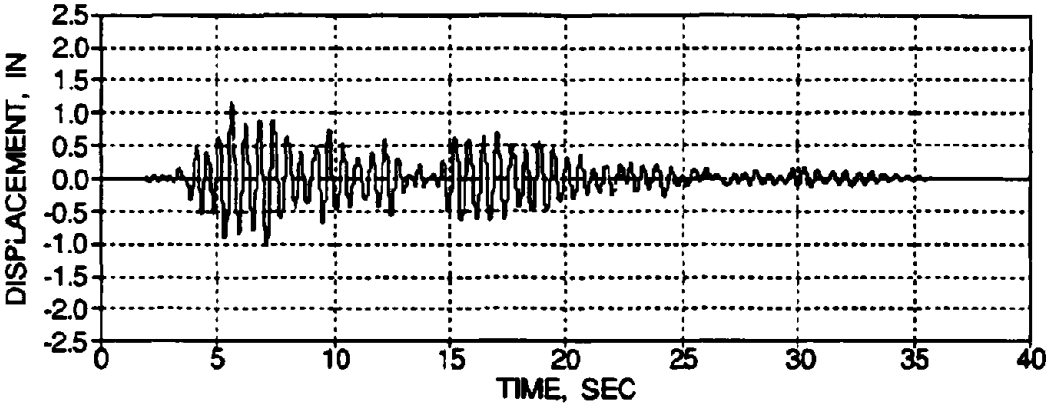

(a) Third Floor

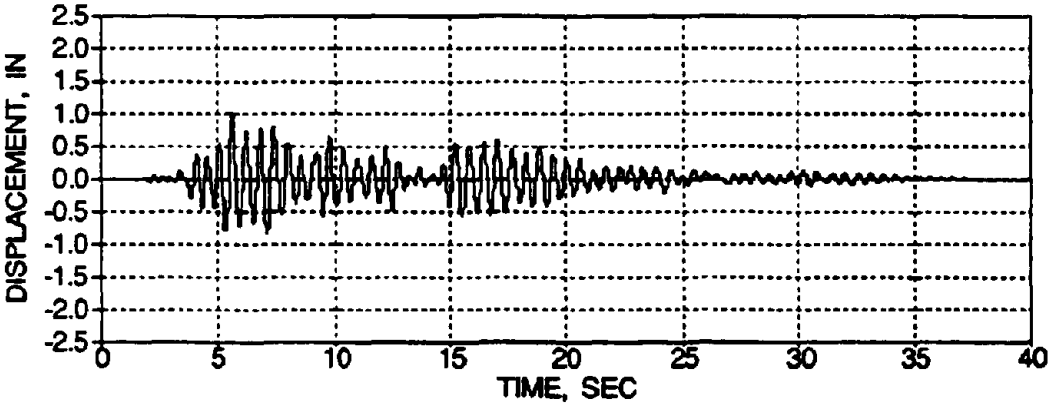

(b) Second Floor

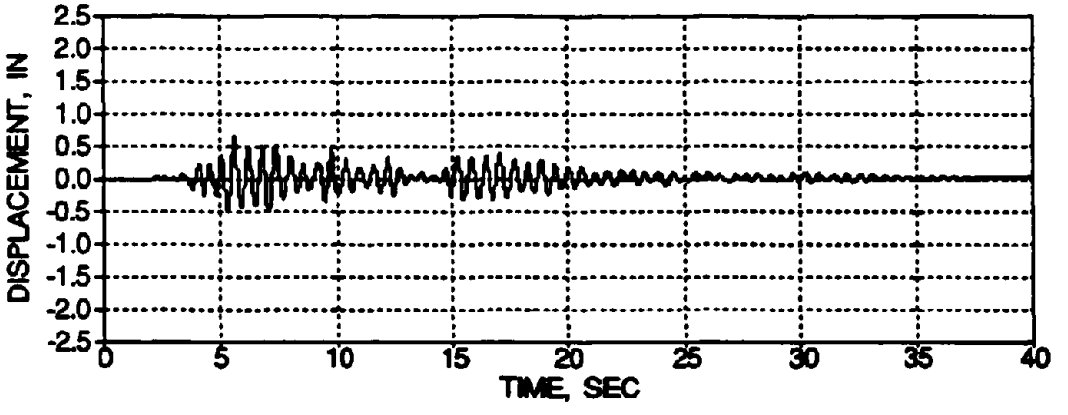

(c) First Floor

FIG. 4-5 Story Displacement Time Histories for TFTR_20

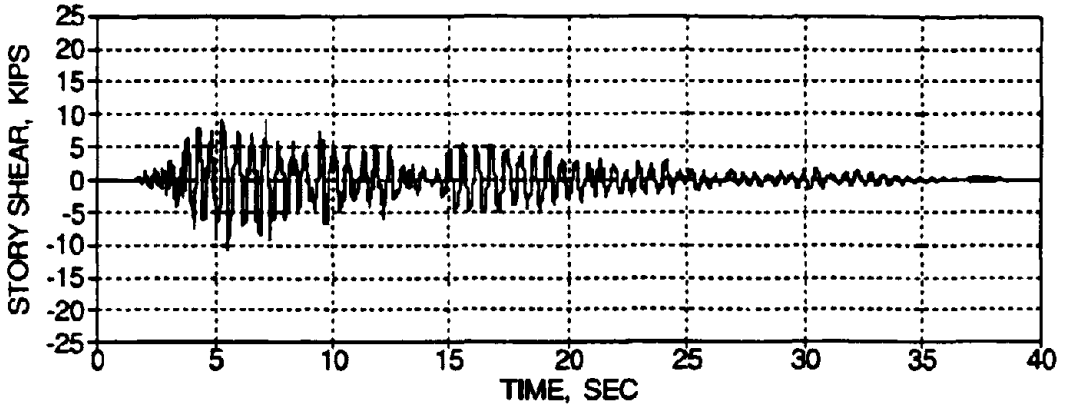

(a) Third Floor

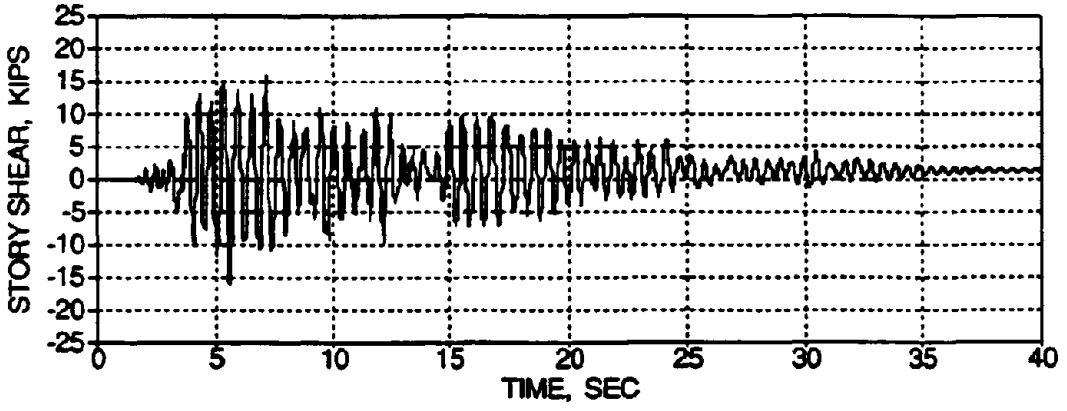

(b) Second Floor

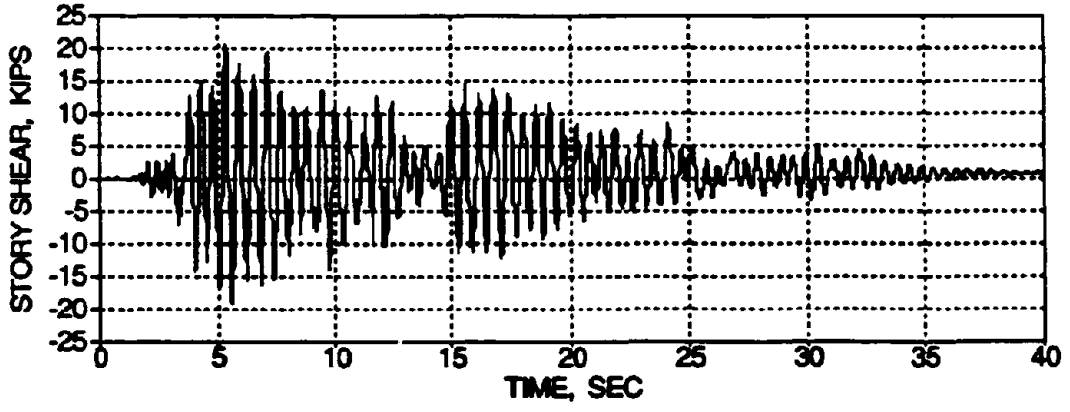

(c) First Floor

FIG. 4-6 Story Shear Time Histories for TFTR_20

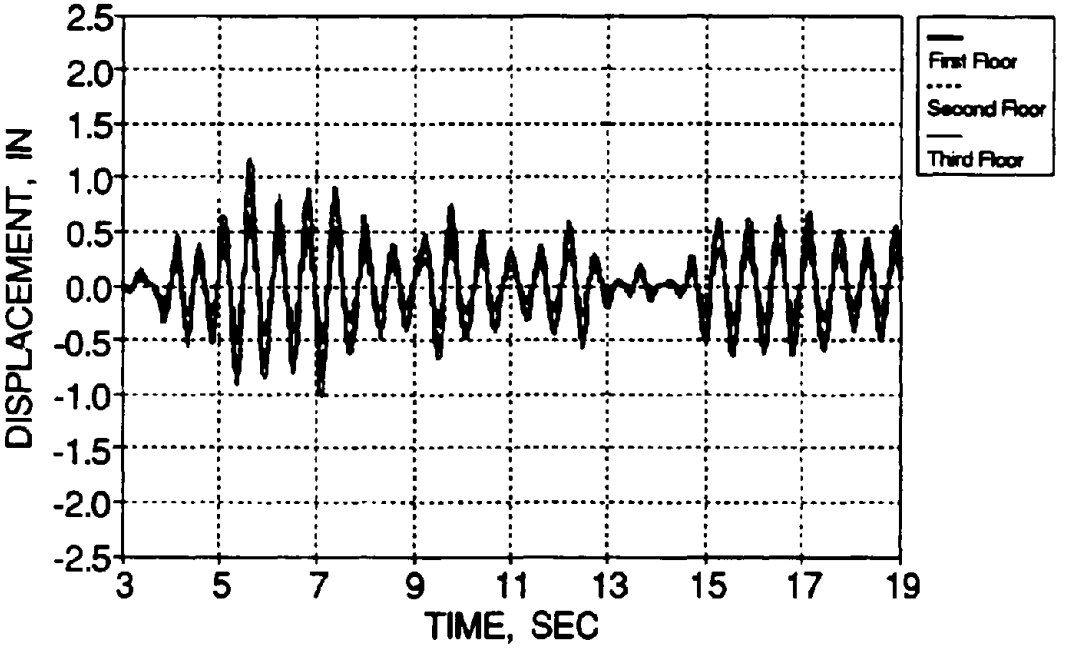

(a) Story Displacements

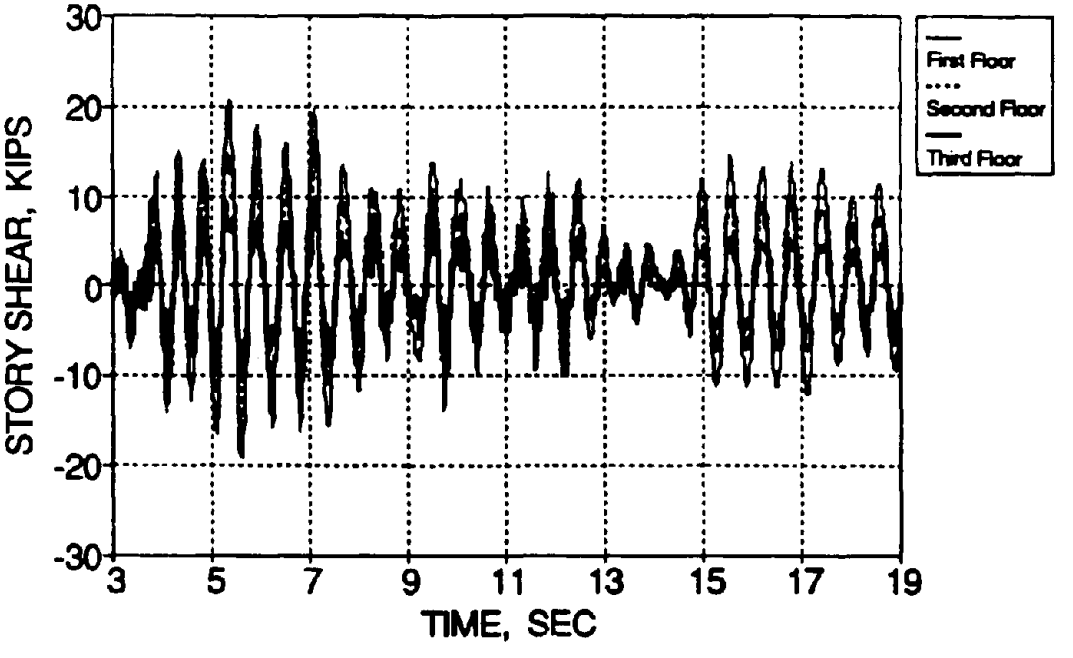

(b) Story Shear Forces

FIG. 4-7 Overlayed Global Response Time History Segments for TFTR_20

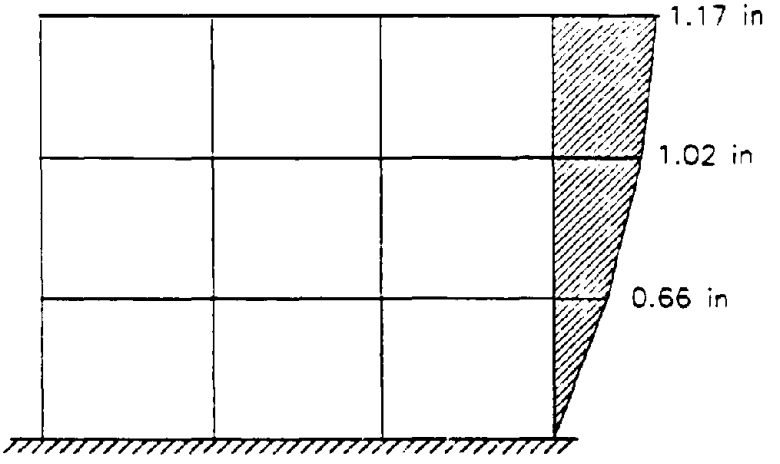

(a) Story Displacements (Time = 5.63 sec.)

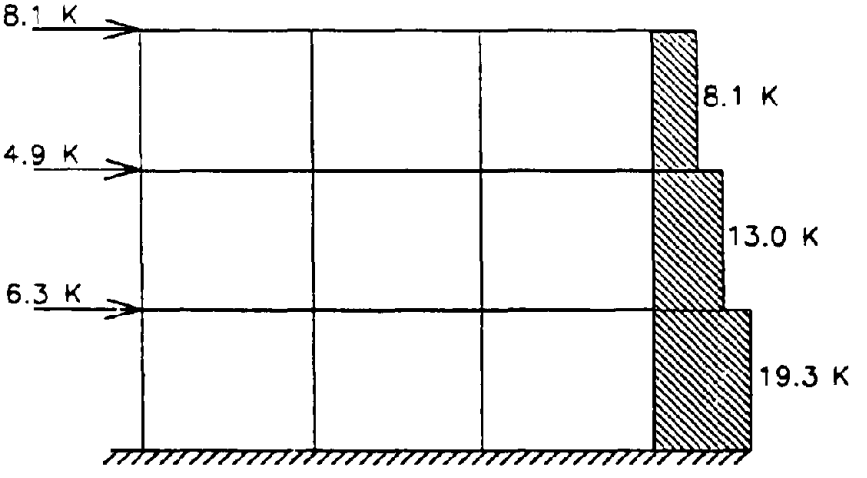

(b) Story Shears (Time = 5.63 sec.)

FIG. 4-8 Story Displacements and Shear Forces at Maximum First Story Drift for TFTR_20

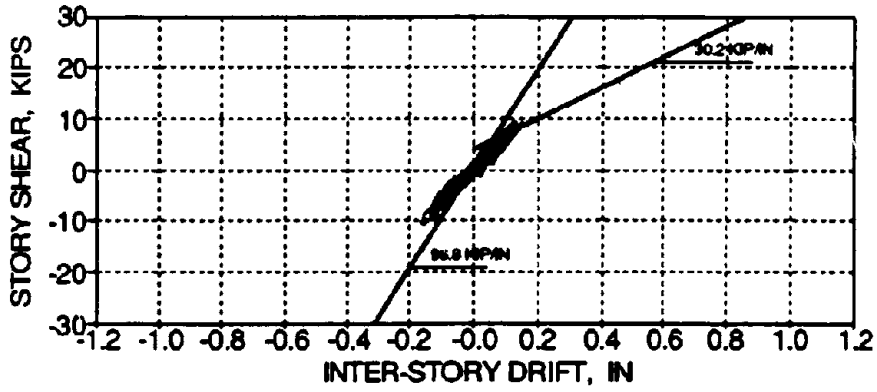

(a) Third Story

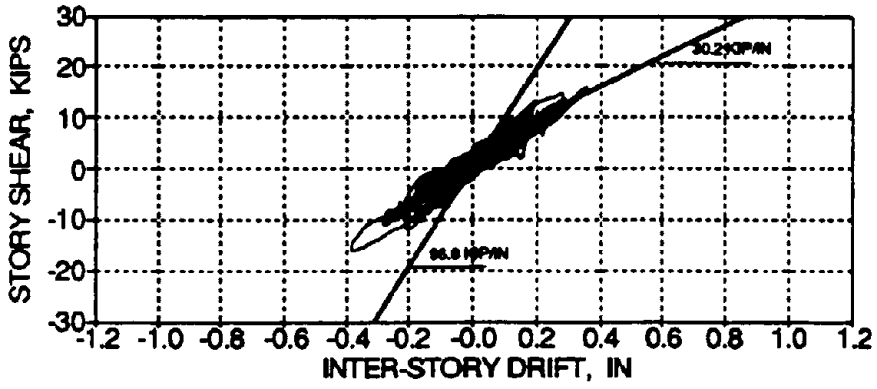

(b) Second Story

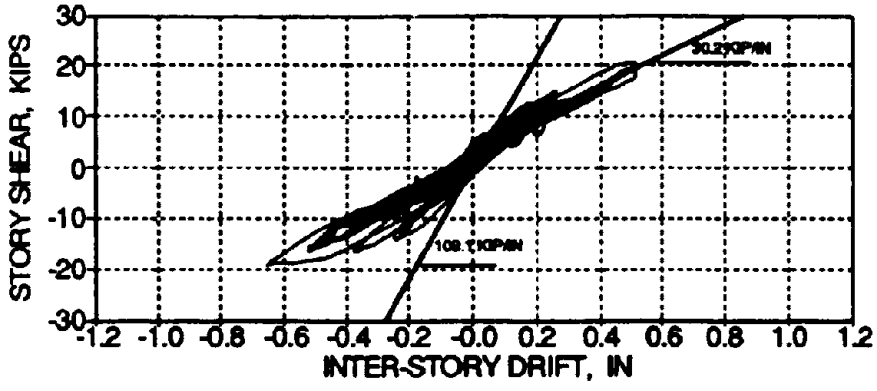

(c) First Story

FIG. 4-9 Story Shear versus Inter-Story Drift Histories for TFTR_20

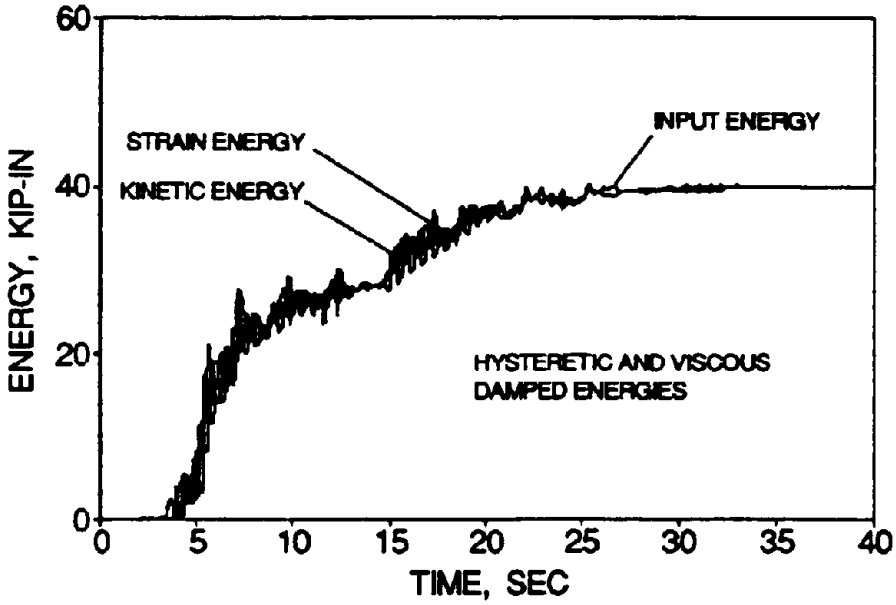

(a) Energy Balance

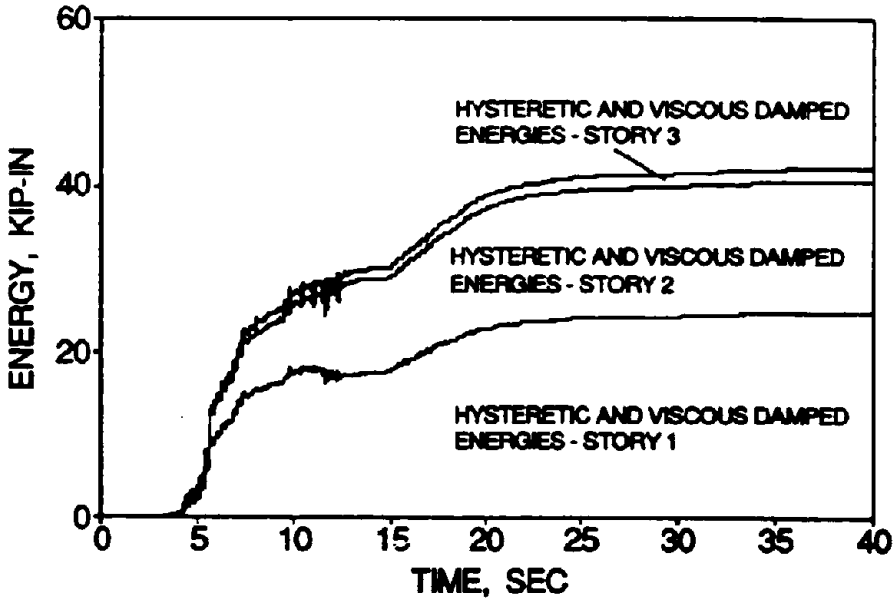

(b) Story Dissipated Energies

FIG. 4-10 Energy Time History for TFTR_20

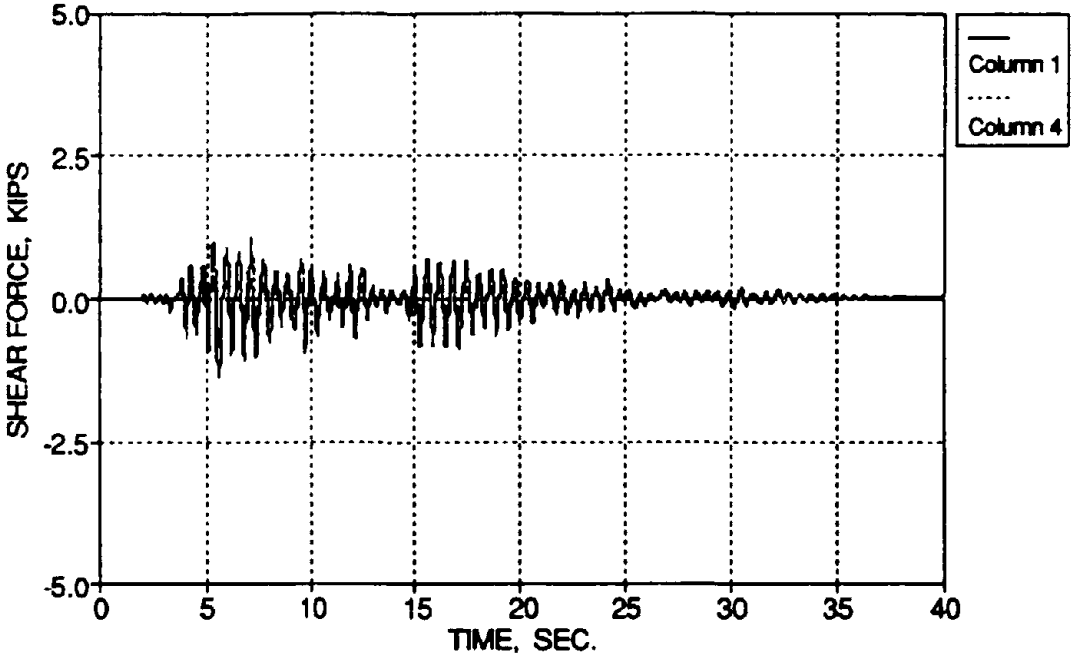

(a) Exterior Columns

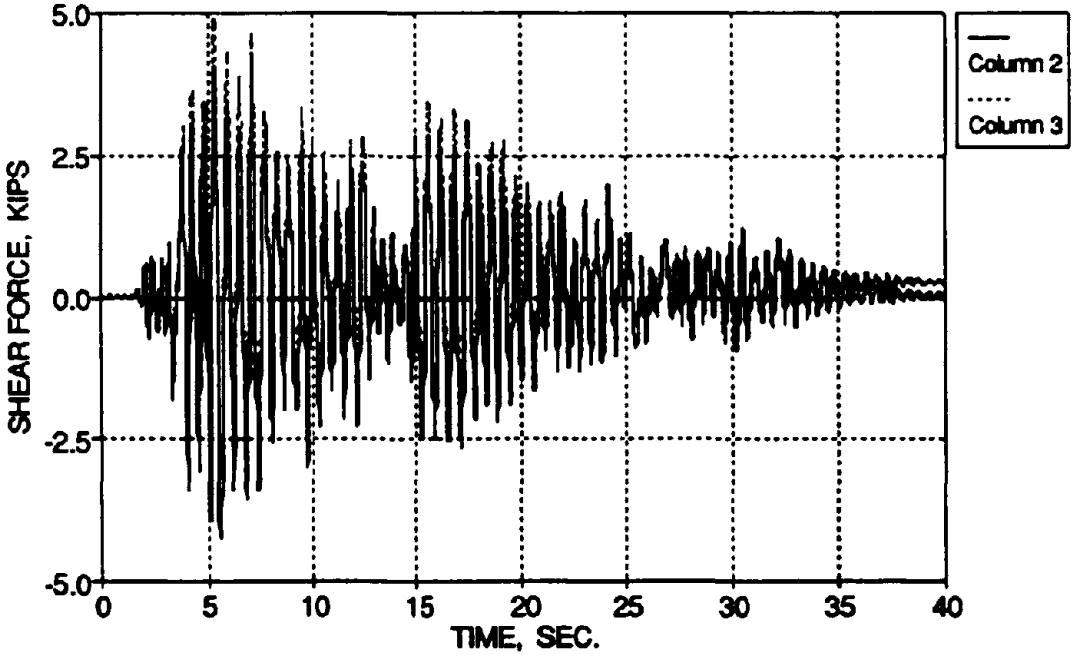

(b) Interior Columns

FIG. 4-11 Base Column Lateral Shear Forces from TFTR_20

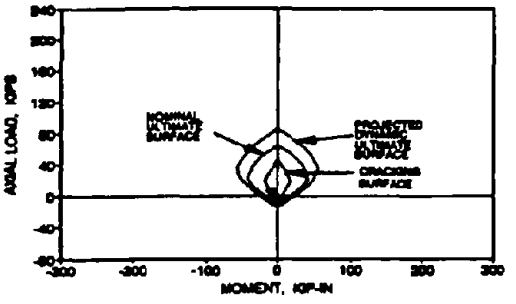

Column 8U

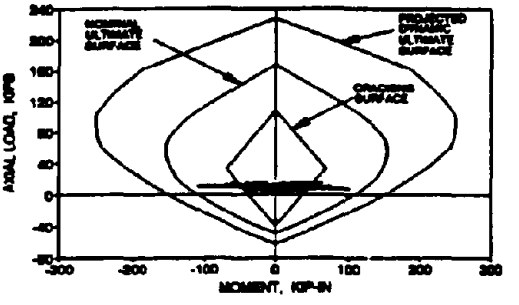

Column 7U

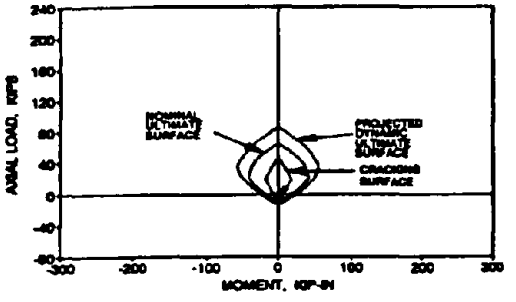

Column 8L

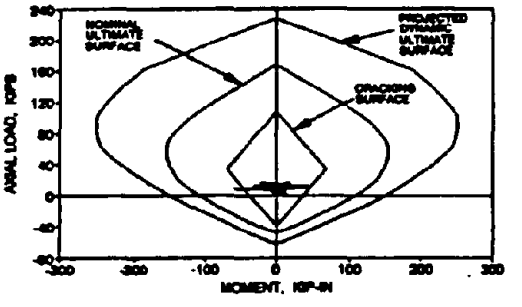

Column 7L

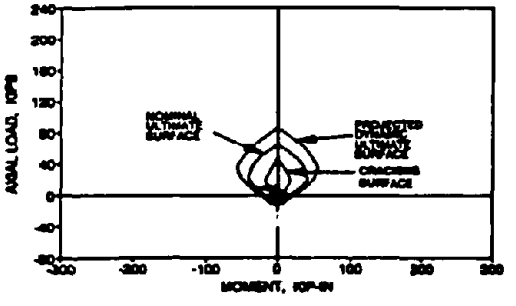

Column 4U

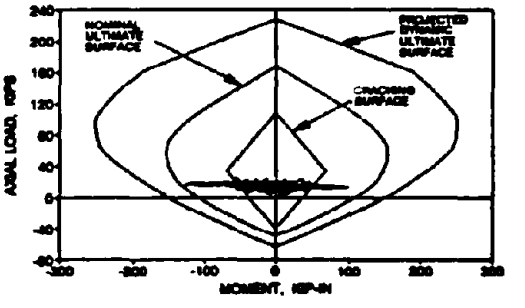

Column 3U

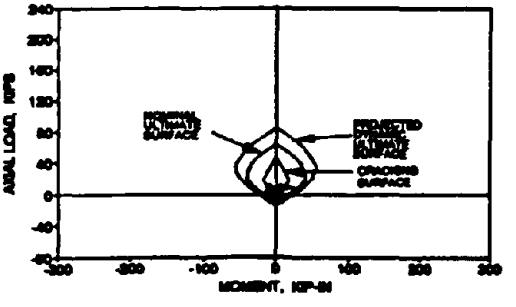

Column 4L

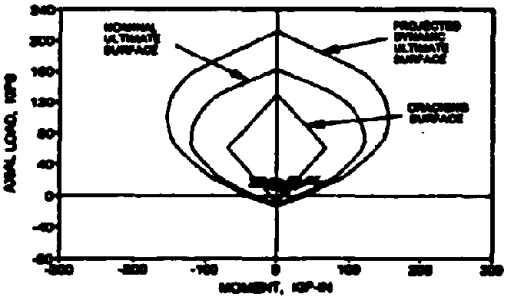

Column 3L

FIG. 4-12a Interaction Diagram for the South-East Columns from TFTR_20

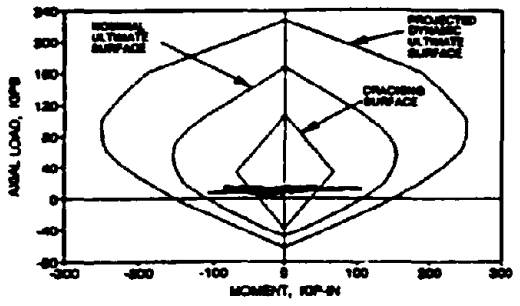

Column 6U

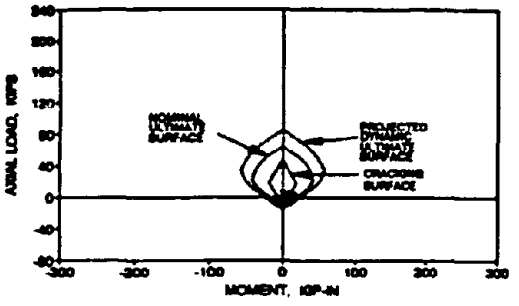

Column 5U

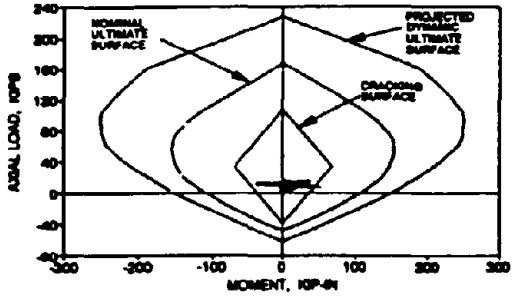

Column 6L

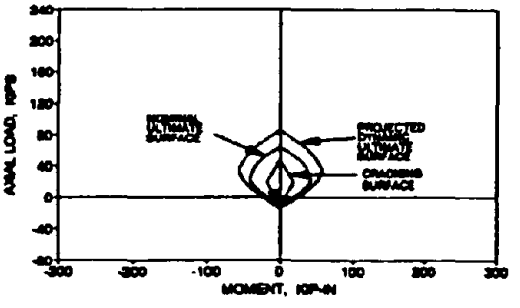

Column 5L

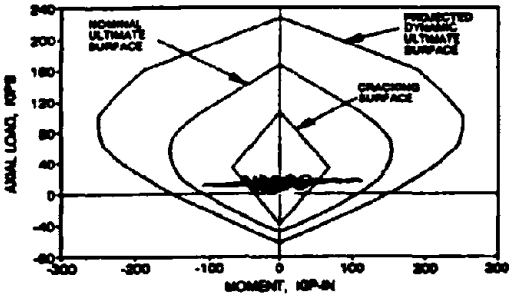

Column 2U

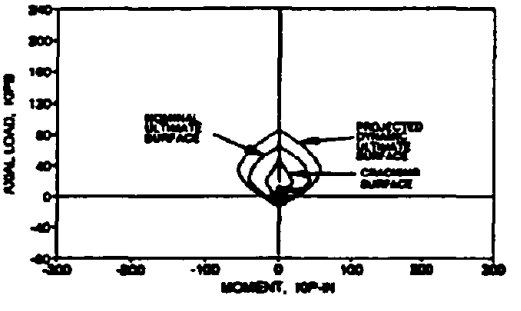

Column 1U

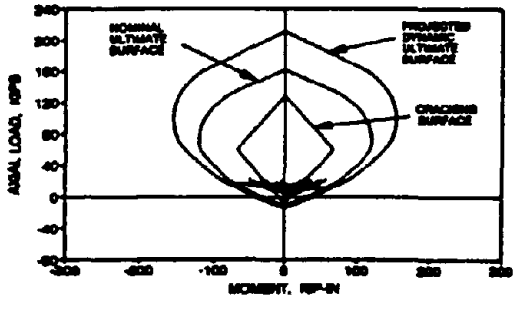

Column 2L

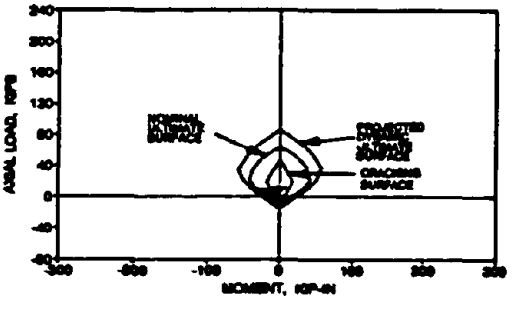

Column 1L

FIG. 4-12b Interaction Diagram for the North-East Columns from TFTR_20

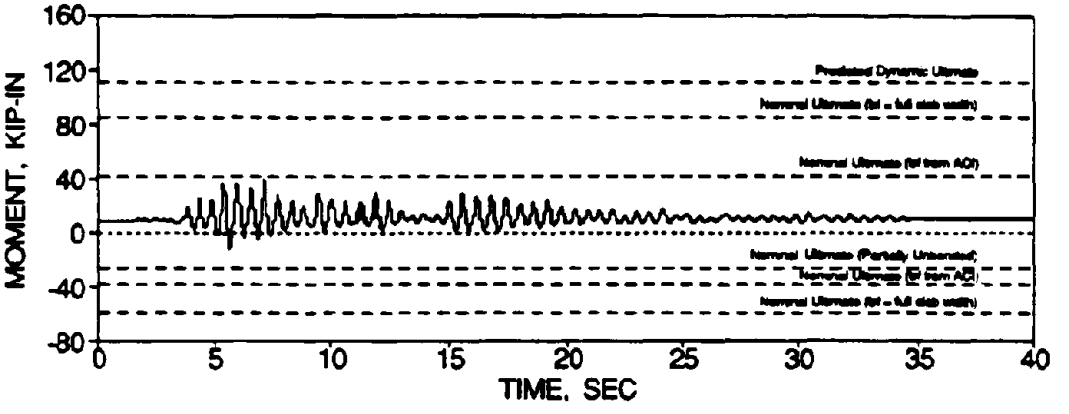

(a) Exbm481

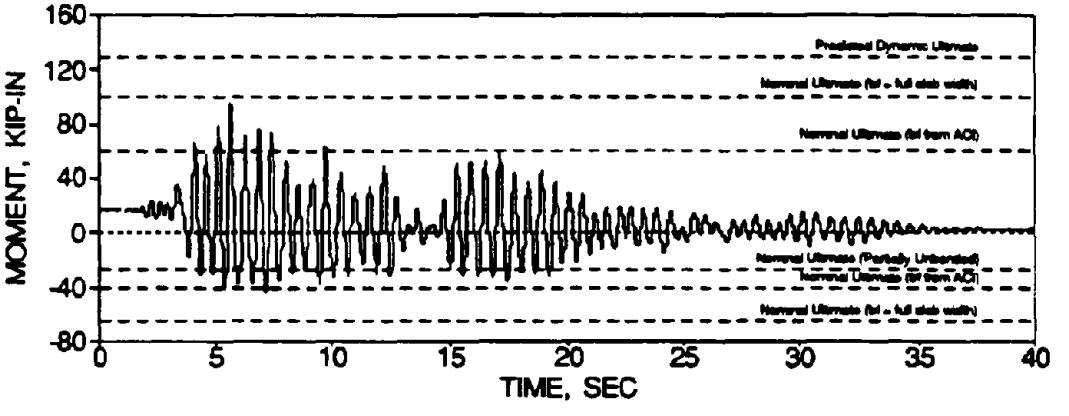

(b) Exbm482

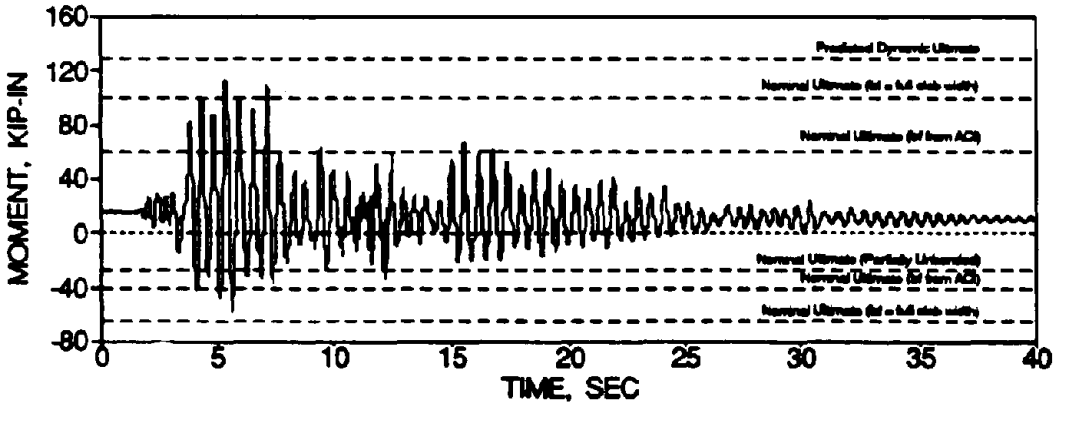

(c) Exbm483

FIG. 4-13a First Story Beam Bending Moment Time Histories for TFTR_20 - South Side

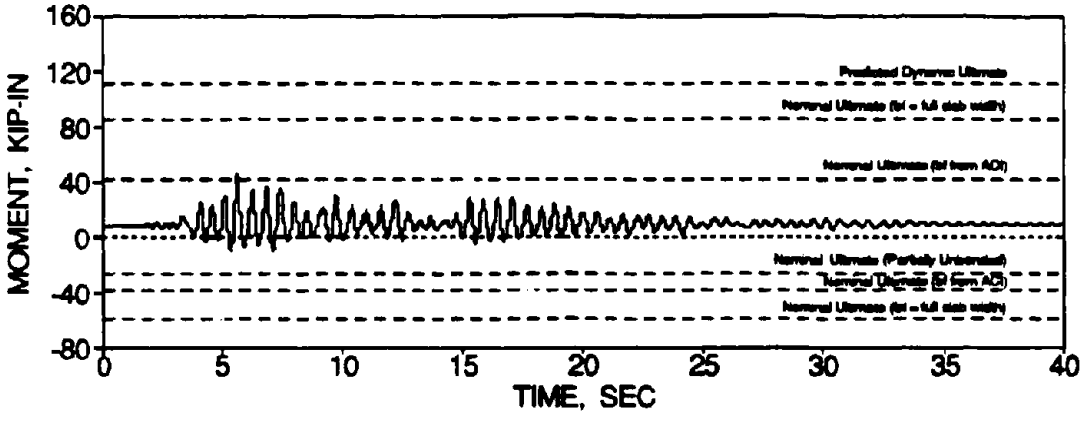

(a) Exbm151

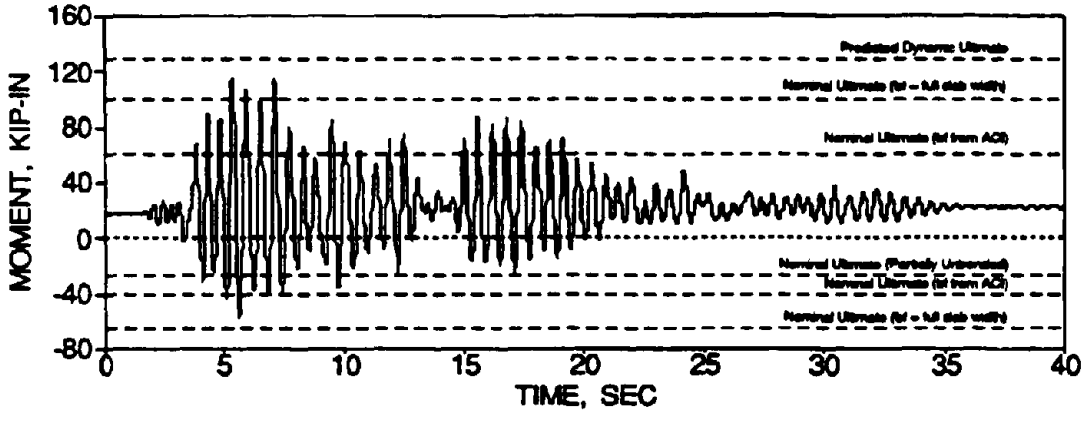

(b) Exbm152

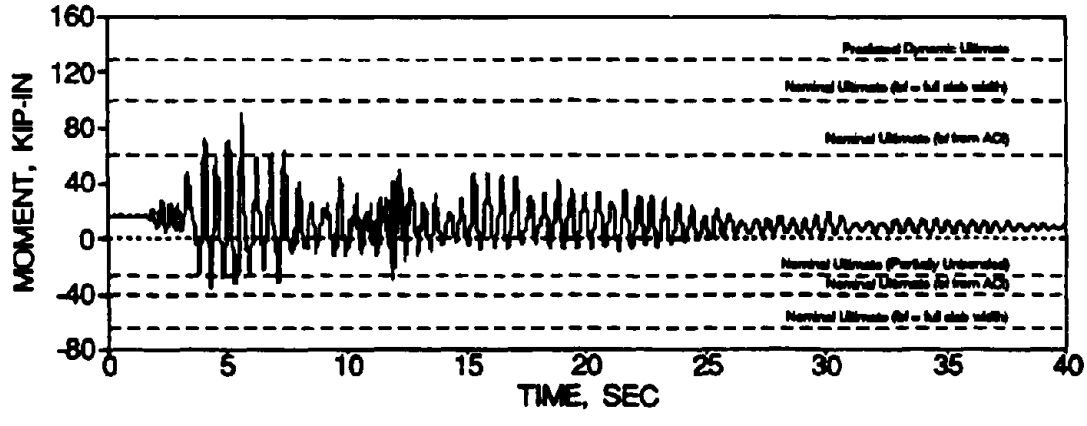

(c) Exbm153

FIG. 4-13b First Story Beam Bending Moment Time Histories for TFTR_20 - North Side

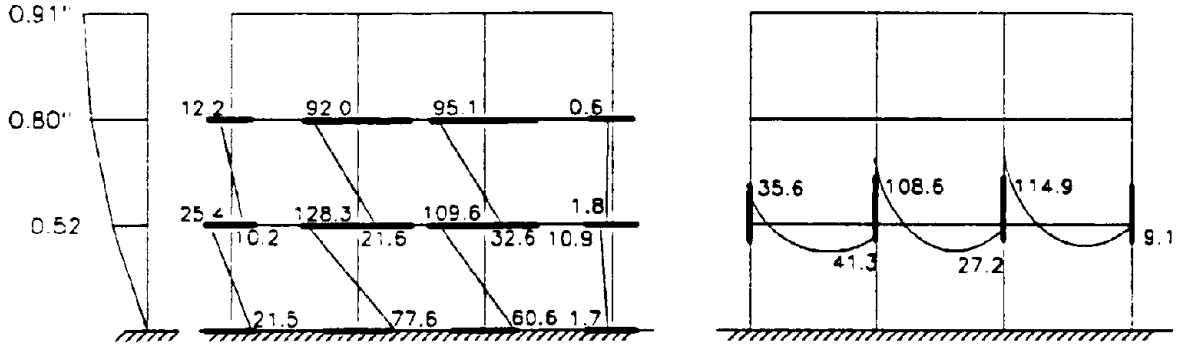

Displacements **Column Moments** **Beam Moments**

(a) Time =5.36 sec.

Moment Capacities

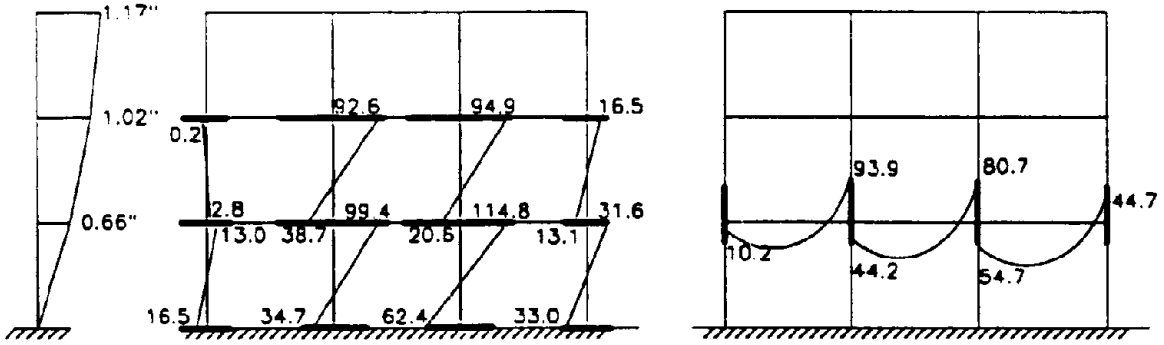

Displacements **Column Moments** **Beam Moments**

(b) Time = 5.63 sec

FIG. 4-14 Moment Diagram at Maximum Story Drifts from TFTR_20

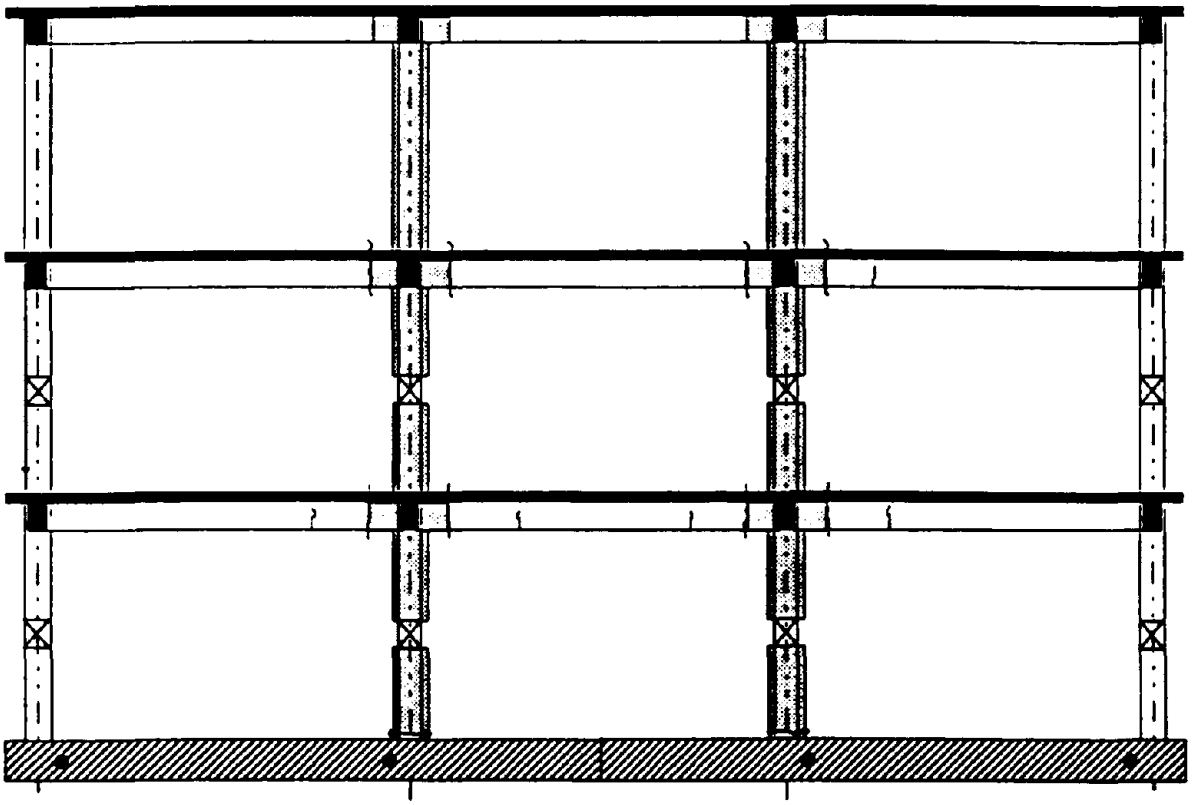

FIG. 4-15a Observed Structural Damage after Moderate Shaking

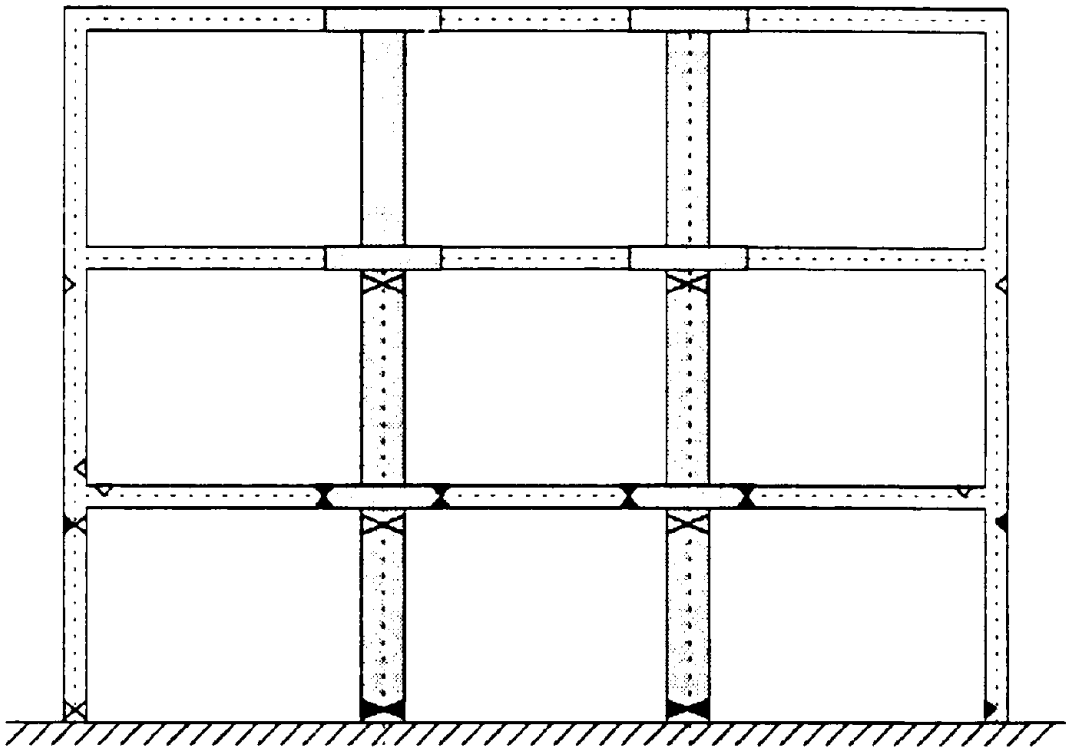

FIG. 4-15b Measured Damage State of Model after Moderate Shaking

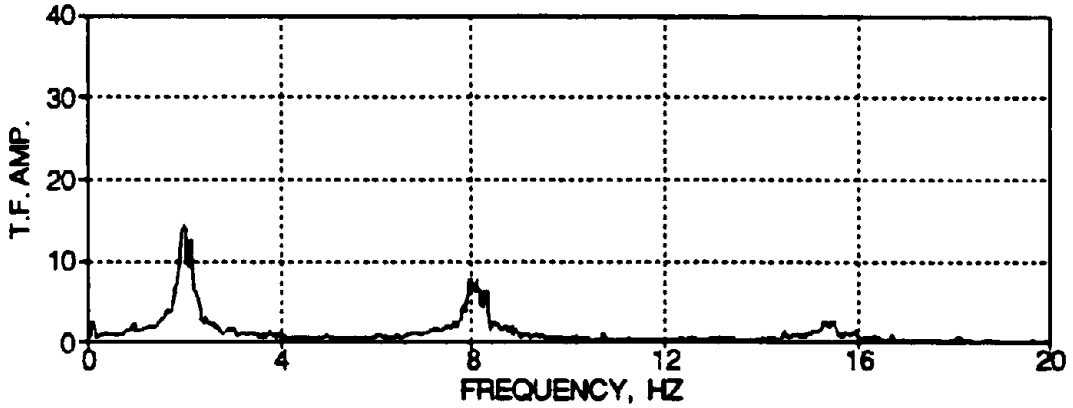

(a) Third Floor

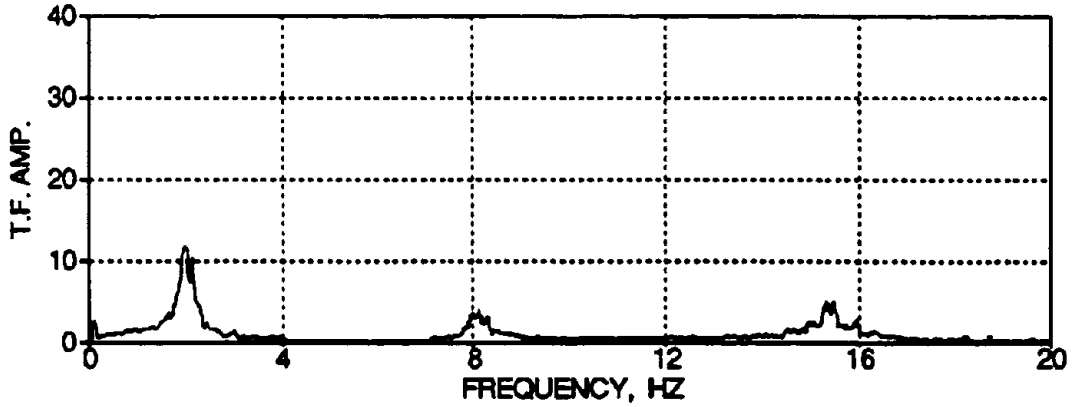

(b) Second Floor

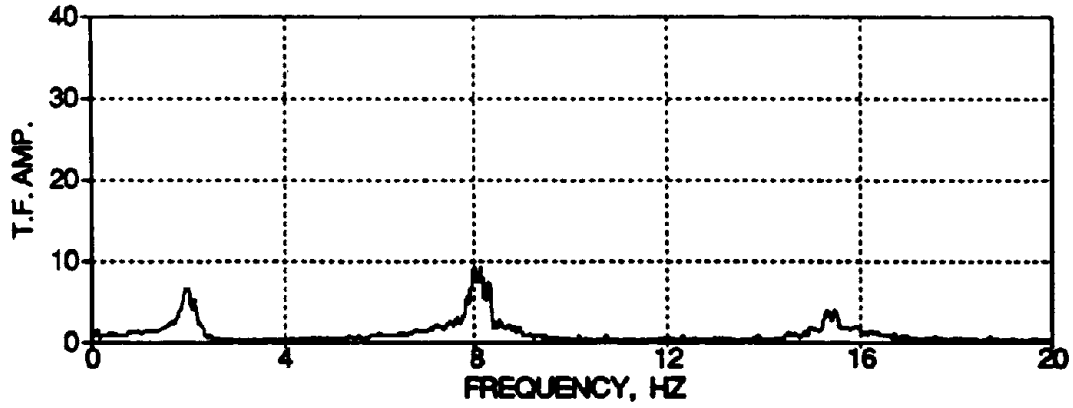

(c) First Floor

FIG. 4-16a Smoothed Transfer Functions from WHNR_D - East Frame

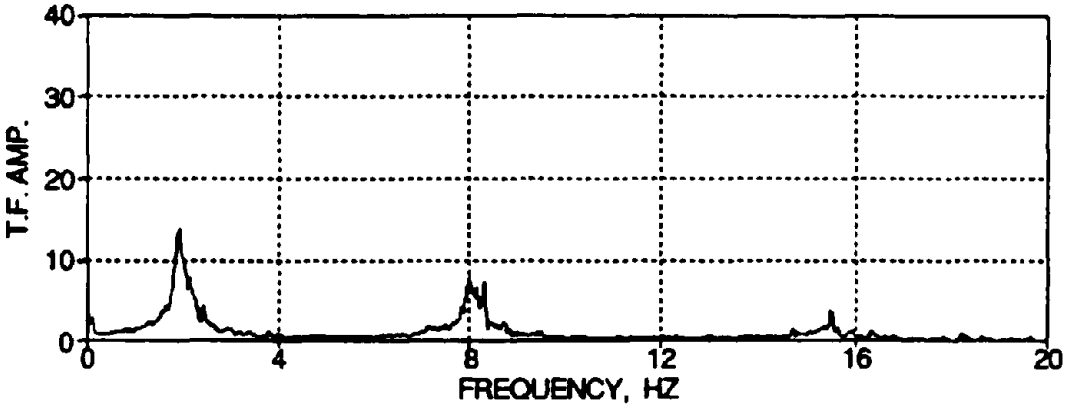

(a) Third Floor

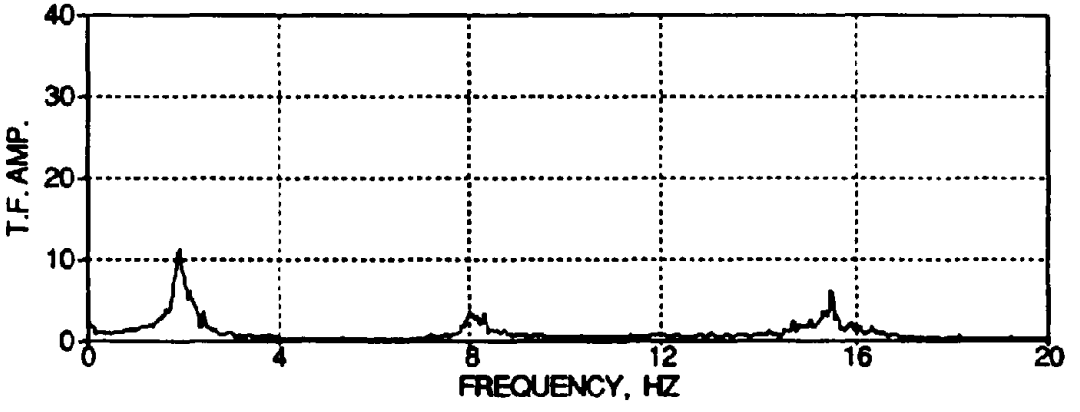

(b) Second Floor

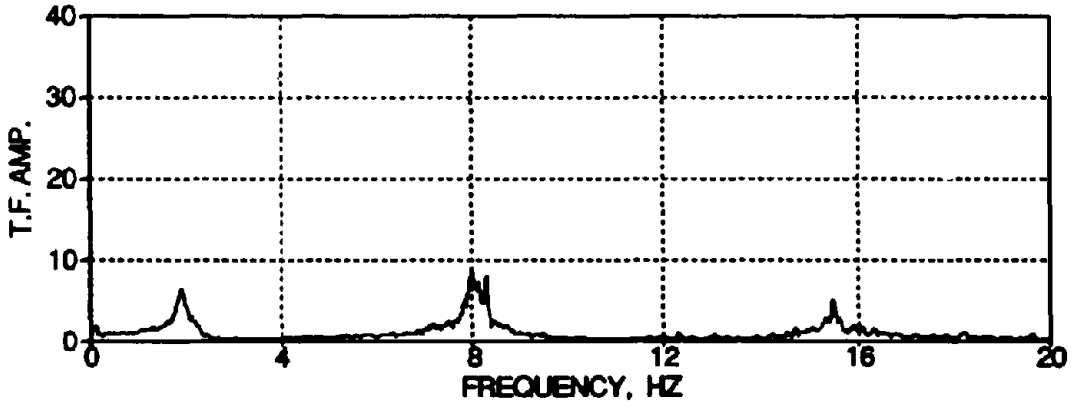

(c) First Floor

FIG. 4-16b Smoothed Transfer Functions from WHNR_D - West Frame

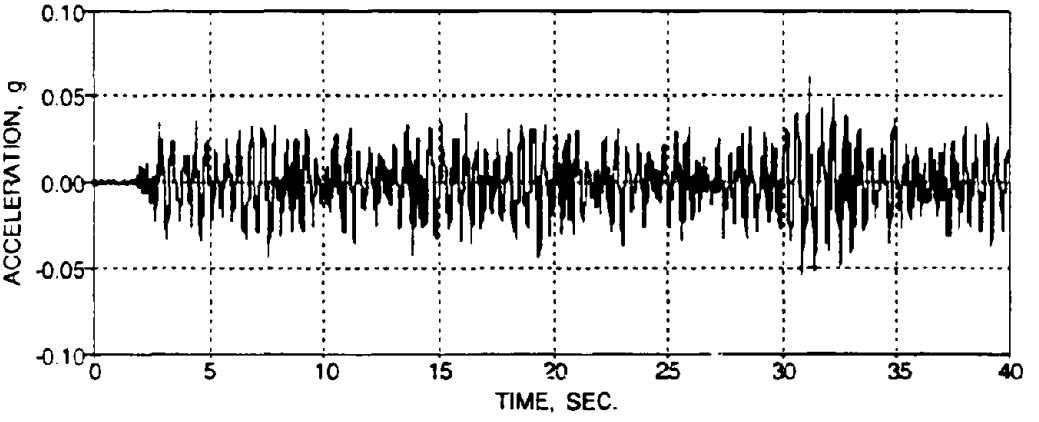

(a) Third Story - East Side Acceleration

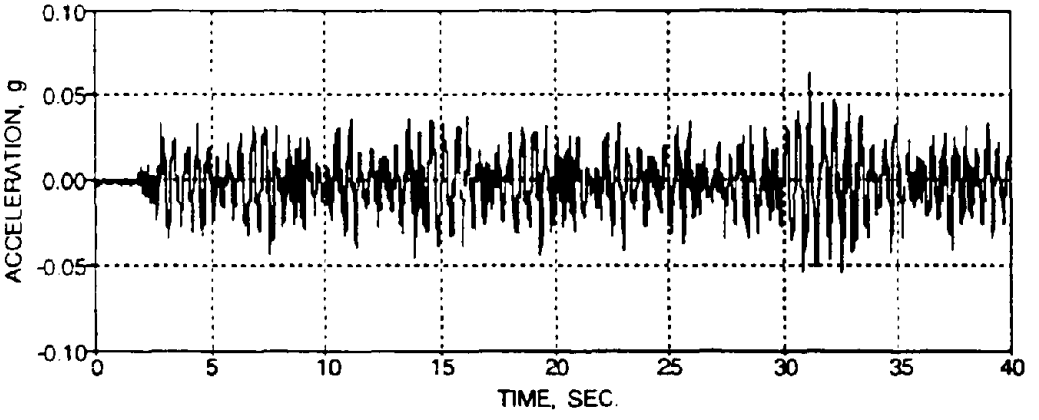

(b) Third Story - West Side Acceleration

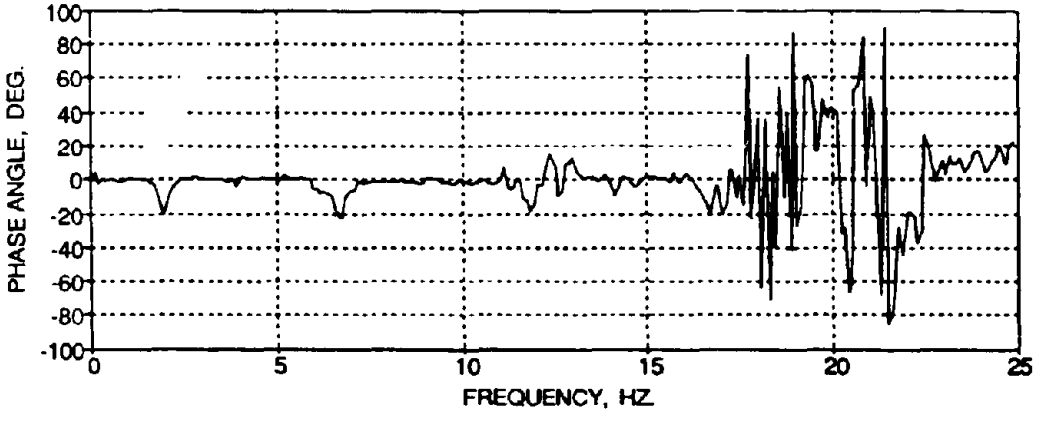

(c) Phase Angle of the East and West Side Accelerations

FIG. 4-17 East and West Lateral Accelerations for WHNR_D - Torsion

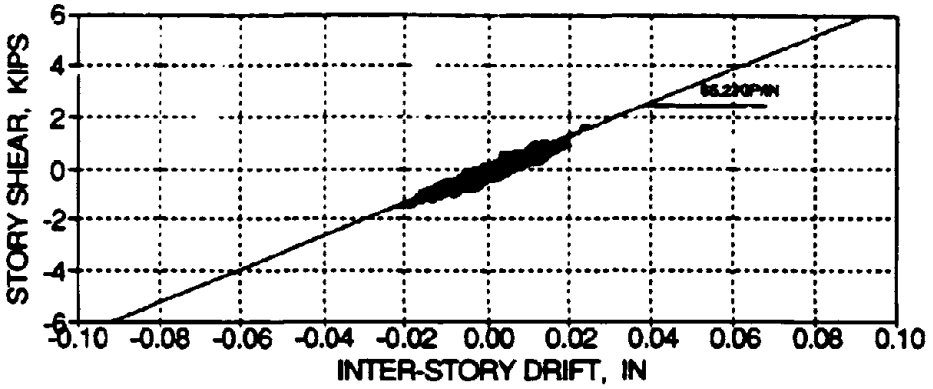

(a) Third Floor

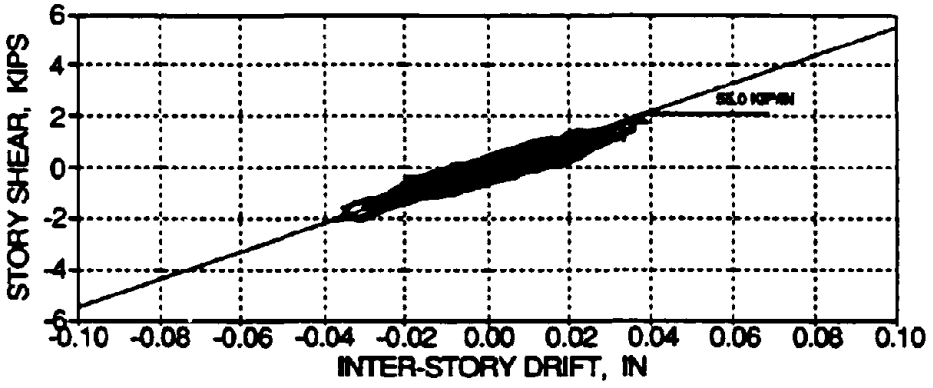

(b) Second Floor

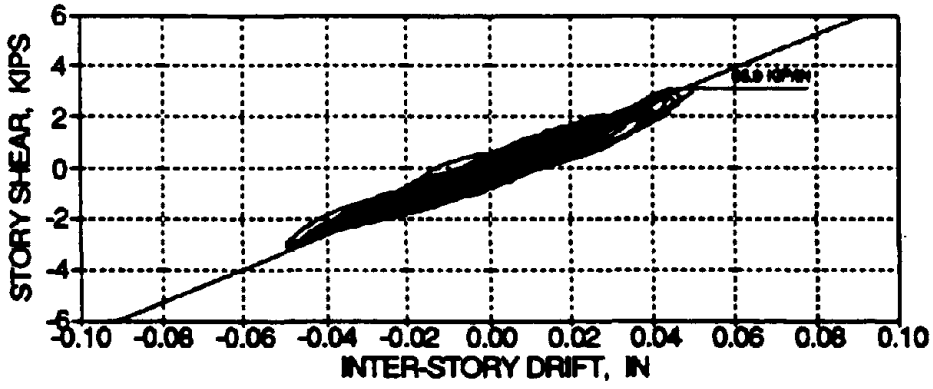

(c) First Floor

FIG. 4-18 Story Shear versus Inter-Story Drift Histories for WHNR_D

4.4 Response to Severe Earthquake

A severe table motion, the Taft N21E accelerogram scaled for a PGA of 0.30 g, was used to excite the model, herein referred to as TFTR_30. Figs. 4-19a and 4-19b show the desired and achieved shaking table acceleration motions for TFTR_30. The achieved PGA is identified as 0.32 g. Fig. 4-19c shows a short segment of the desired and achieved shaking table motions. A high degree of similarity can initially be observed between the desired and achieved motions. But at about 13 seconds, the table motion became erratic. Subsequently, the excitation gain (scale factor) of the shaking table was immediately lowered. Thereafter the achieved acceleration history shows good agreement with the desired. The reasons for this table behavior were discussed in Section 4.2.

Figs. 4-20a and 4-20b show the north and south side vertical table accelerations for TFTR_30. The peak vertical acceleration of the table is 0.87 g and the vertical response on each side of the table are in-phase. Therefore it is concluded that the table is uniformly accelerating in the vertical direction during the instability. Fig. 4-20c shows the Fourier Transform of the north side vertical table acceleration history. Excited frequencies between 10.0 Hz. and 12.0 Hz. and also between 20.0 Hz. and 25.0 Hz. can be observed.

Fig. 4-21 shows the east and west lateral base acceleration histories along with the corresponding phase angle. Out-of-phase motions can be observed near frequencies of 10.0 Hz. to 12.0 Hz. and higher, which indicates that the shaking table is yawing or twisting. Fig. 4-22 shows the induced transverse shear forces in the interior and exterior first story columns for table motion TFTR_30. It can be observed that the transverse shear forces are completely out-of-phase in the exterior columns (presence of torsion).

Therefore it is concluded that the torsional response in the structure was driving the shaking table in a yawing motion during the severe earthquake. However the input torsional effects from the instability are still minor with respect to the lateral and the overall response is not excessively affected. An averaging technique is used to filter out the torsional effects and analyze the lateral direction for meaningful conclusions (as in the moderate shaking).

4.4.1 Global Response

Fig. 4-23 shows the average story displacements time histories of the retrofitted model during the severe earthquake, test TFTR_30. Fig. 4-24 shows the story shear force time histories identified from the load cells in the first and second story columns and the third story level accelerometers, respectively. It can be observed that minor signal drifts of the first and second story shear forces have occurred, possibly a result of some yielding in the load cells. Figs. 4-25a and 4-25b show a magnified overlayed portion of the story displacements and shear forces, respectively. It can be observed that the story displacements and shear forces are moving in phase. Figs. 4-26a and 4-26b show the story displacements, shear forces, and story loads when the maximum first story drift occurs. The shape of the magnitudes of the story displacements and shears at this point in time resembles the shape caused by the first mode of vibration of the model. Therefore it is concluded that the structural response for the severe level earthquake is governed by the first mode of vibration.

Table 4-5 summarizes the maximum results for story displacements, inter-story drifts, story shear forces, story loads, and peak story accelerations for each floor of the model for TFTR_30. It can be observed that the inter-story drifts are 2.13%, 1.19% and 0.49% of the story height, respectively for the first, second, and third floors. The inter-story drift maxima for the unretrofitted building tested by the same severe earthquake (TFT_30) were 2.03%, 2.24%, 0.89%, respe :tively (Bracci et al., 1992b). Therefore the retrofit did not influence the first story drift. However large reductions in the second and third story drifts have occurred. A large inter-story drift of the first floor occurs due to the formation of a plastic hinge at the base, however in no danger of shear failure with the additional confining steel at the base. The analytical study shown in Section 2, grossly underestimated the maximum first story drift. Explanations for this discrepancy are presented in Section 4.6. The maximum measured base shear force for retrofitted model during the severe earthquake (21.8 kips) is 26.4% of the total structural weight W. For comparison, the base shear during moderate shaking of retrofitted model (TFTR_20) was 25.0%. For the unretrofit model test with the same severe earthquake (TFT_30), the base shear was 15.3%, respectively. Therefore a larger shear demand has resulted due to the retrofit and also an increased demand has resulted in comparison with TFTR_20. This implies that base shear capacity for the retrofitted model had not been reached for the moderate shaking and possibly not reached during the severe shaking. Also note that there are

story level acceleration amplifications of about 0.0%, 15.2%, 46.9%, respectively for the first, second, and third stories. These amplifications were less than the moderate shaking, especially on the first story due to inelastic response.

TABLE 4-5 Maximum Response for Severe Earthquake TFTR_30

Story	Max. Story Displacement (in.)	Max. Inter-Story Drift (percent)	Max. Story Shear (kips)	Max. Story Load (kips)	Peak Story Acceleration (g)
Third	1.73	0.49	13.2	13.2	0.47
Second	1.50	1.19	19.5	10.1	0.38
First	1.02	2.13	21.8 (26.4%W)	10.1	0.31

Fig. 4-27 shows the story shear force versus the inter-story drift trajectories for each floor of the model for test TFTR_30. The initial story stiffnesses from WHNR_D (low amplitude before shaking) is shown along with the equivalent slope of the response. It can be observed that considerable inelastic behavior occurred primarily at the first story. The secondary slopes are identified as 21.7 kip/in, 29.8 kip/in, and 30.2 kip/in. This corresponds to reductions of 28.1%, 1.3% and 0.0%, respectively due to the severe shaking. Therefore in addition to the decay of the initial story stiffness, the post-cracking or yielding, story stiffness of the first floor also decays as a result of continued inelastic deformations and strength deterioration in the members of that story. Therefore it is vital in the analytical evaluation not only to correlate the initial period of the structure but also the hysteretic degradation properties.

Fig. 4-28 shows the time history of the energy balance for the model during TFTR_30. The total input energy into the model is about 52.0 kip-in, which is about 30% larger for local member designations see Bracci et al. (1992a) than TFTR_20 and about 40% larger than the unretrofitted building with the same earthquake. The percentage ratio of the viscous damped and dissipated energies by each floor with respect to the total is 55.0% : 38.5% : 6.4%, respectively for the first, second, and third stories. In comparison with TFTR_20, the percentage ratio of viscous damped and hysteretic energies was 60.8% : 35.6% : 3.6%, respectively. It can be observed that similar ratios have resulted in the retrofitted model after the moderate and severe earthquakes. For comparison with the

unretrofitted building with the same earthquake, the percentage ratio of viscous damped and hysteretic energies was 42.6% : 42.1% : 15.2%, respectively. Therefore retrofit of the building was successful in terms of avoiding the soft-story effect on the second floor, which occurred in the unretrofitted building from the severe shaking.

4.4.2 Local Response

Fig. 4-29 shows the induced lateral shear forces in the interior and exterior first story columns (base shear) for table motion TFTR_30. It can be observed that the shears in the interior columns are approximately five times larger than the exterior columns. The shear force signal in column #3 at the end of the motion has a minor offset, which implies some yielding may have occurred in this load cell.

Fig. 4-30 shows the bending moment versus axial load interaction diagrams for the columns of the first and second stories. It can be observed that the interaction history for the retrofitted columns of the upper first and second floors extend to the nominal ultimate bounds. For the second floor lower columns, the history is well below the nominal ultimate bounds and within the cracking surface. However, for the lower first story columns, the moment-axial load history extends beyond the nominal ultimate surface, but remains within the predicted dynamic ultimate surface. This is expected since the lower first story columns are a primary hinge location for the design beam-sidesway failure mechanism. With exception of the lower first story columns, the unretrofitted exterior column interaction histories remain primarily within the nominal ultimate bounds. Also the waviness in the interaction histories is a direct result of the fluctuating axial loads from the table instability.

Fig. 4-31a and 4-31b show the first story beam moment time histories in the south and north sides of the model at the face of the added joint reinforcement in the fillet along with the ultimate moment surfaces. It can be observed that the moment demands in the interior beams exceed the nominal ultimate bounds considering full slab steel contributions in the negative direction. Particularly in beam Exbm152 where the moment history extends beyond the predicted dynamic ultimate surface. Since the slab steel was shown to have a substantial contribution to the moment capacity of the beams, underpredicting the appropriate strain hardening of the rebars and slab steel, along with the additional strain rate effects in these bars, might explain the underestimation of the beam strength. Note that the provided fillet in the retrofitted interior columns and the prestress prevented pull-out of the discontinuous beam reinforcement, thereby enabling higher

positive moment capacity. The exterior beam moment demands remain within the nominal ultimate surfaces and the partially unbonded positive moment surface (since the member was not retrofitted). Therefore it can be concluded that the beams have yielded in test TFTR_30, as expected in the beam-sidesway mechanism. Also the slab steel across the full slab width has a considerable contribution to the ultimate beam moment capacity.

The bending moment diagrams for the model when the first story drift was maximum in each direction, along with the corresponding story displacements, are shown in Fig. 4-32. It is apparent that a beam-sidesway collapse mechanism is developing since that beam moments and the lower first story columns have reached yield strength.

The visually observed structural damage and measured damage state of the retrofitted model from the severe shaking is shown in Fig. 4-33. The following points highlight the observed structural damage:

(a) further cracking occurred in the lower first story interior columns;

(b) further cracking occurred in the beams of the first and second stories near the end of the fillet;

(c) slab cracks were observed along the face of the added fillet throughout the slab width;

(d) additional torsional cracks in the south-west transverse beam.

Except for very strongly damaged and worked hinges, the visual damage and that established by calculating damage indices based on test data do not correspond. This indicates that more often than not visual damage is not accurately describing the structures state.

4.5 Dynamic Properties after Severe Shaking

The dynamic properties of the retrofitted model after the severe earthquake are determined from the white noise WHNR_E. Figs. 4-34a and 4-34b show the smoothed story transfer functions for the east and west frames of the model, respectively. Since small damping and well separated modes can be observed, the natural frequencies of the east frame are identified as 1.88 Hz., 7.50 Hz., and 14.84 Hz. and are tabulated in Table 4-6. It can be observed that the natural frequencies of the east frame are reduced by an additional 5.1%, 7.5%, and 3.2%, respectively from the

severe shaking or 32.4%, 20.0%, and 11.4% from WHNR_B (untested). The modal shapes and modal participation factors are also identified from the story transfer functions and shown in Table 4-6. Slightly varying modal shapes and modal participation factors can be observed. The natural frequencies of the west frame are likewise identified as 1.73 Hz., 7.50 Hz., and 14.84 Hz. and shown in Table 4-7 for comparison with the east frame. It can be observed that the first mode natural frequency of the west frame suffers more deterioration than the east frame. The modal shapes and modal participation factors of the west frame are comparable with the east frame.

Fig. 4-35 shows the phase angle between the third floor accelerometers on the east and west frames of the model. It can be observed that the east and west frames are about 22° out-of-phase near the first mode natural frequency, which implies torsion is present in the model during WHNR_E.

The equivalent viscous damping factors of the east frame are determined from the half-power method as 5.5%, 1.9%, and 1.5%, respectively. Likewise the modal damping factors of the west frame are identified as 6.7%, 1.9%, and 1.2%, respectively. Since the west frame was previously shown to have suffered more damage during the moderate and severe earthquakes, a large damping factor was expected in the west frame. Note that the damping factors after the severe shaking were less than the factors after the moderate shaking. These damping factors indicate energy dissipation in various modes. These factors cannot be used for equivalent analyses since the energy dissipation is hysteretic and not viscous.

The updated stiffness matrix of the model, developed from the dynamic characteristics of the east frame from WHNR_E, is shown in Table 4-6. It can be observed that the sum of the diagonal terms of the stiffness matrix is reduced by an additional 8.1% after the severe shaking or a total of 25.6% from WHNR_B (untested). Story stiffness reductions of 30.7%, 5.9%, and 1.1%, respectively for the first, second, and third stories have resulted after TFTR_30 or 60.1%, 22.4%, and 14.0% as compared to WHNR_B (original). Therefore it can be observed that considerable stiffness deterioration has primarily occurred to the first story of the retrofitted model, similar to the behavior after the moderate shaking. Table 4-7 shows the stiffness matrix comparisons of the east and west frames of the model. It can be observed that the sum of the stiffness matrix of the west frame of the model is similar to that of the east frame. Also the corresponding stiffness reductions for the west frame are similar to the east frame.

Fig. 4-36 shows the story shear versus inter-story drift histories for WHNR_E. The story stiffnesses for small amplitude displacements are identified as 54.0 kip/in, 46.0 kip/in, and 62.5 kip/in, respectively for the first, second, and third stories. From Table 4-8, this corresponds to stiffnesses reductions of 18.1%, 16.4%, and 4.1%, respectively after TFTR_30 as compared to WHNR_D (before shaking) or about 52%, 54%, and 38% as compared to WHNR_B (untested). Therefore further stiffness deterioration is evident from TFTR_30.

TABLE 4-6 Dynamic Properties and Stiffness Matrix before and after Severe Shaking (East Frame)

	WHNR_D - East (before)	WHNR_E - East (after)
Natural Frequencies (Hz.)	$f_i = \begin{pmatrix} 1.98 \\ 8.11 \\ 15.33 \end{pmatrix}$	$f_i = \begin{pmatrix} 1.88 \\ 7.50 \\ 14.84 \end{pmatrix}$
Modal Shapes	$\Phi_{ij} = \begin{pmatrix} 1.00 & -0.86 & -0.56 \\ 0.82 & 0.42 & 1.00 \\ 0.46 & 1.00 & -0.81 \end{pmatrix}$	$\Phi_{ij} = \begin{pmatrix} 1.00 & -0.83 & -0.56 \\ 0.82 & 0.36 & 1.00 \\ 0.45 & 1.00 & -0.76 \end{pmatrix}$
Modal Participation Factors	$\Gamma_i = \begin{pmatrix} 0.44 \\ 0.11 \\ -0.07 \end{pmatrix}$	$\Gamma_i = \begin{pmatrix} 0.44 \\ 0.10 \\ -0.07 \end{pmatrix}$
Damping Ratios (%)	$\xi_n = \begin{pmatrix} 6.6 \\ 2.6 \\ 1.4 \end{pmatrix}$	$\xi_n = \begin{pmatrix} 5.5 \\ 1.9 \\ 1.5 \end{pmatrix}$
Stiffness Matrix (kip/in)	$\mathbf{K}_{ij} = \begin{pmatrix} 182.7 & -218.2 & 71.9 \\ -218.2 & 356.9 & -229.3 \\ 71.9 & -229.3 & 318.3 \end{pmatrix}$	$\mathbf{K}_{ij} = \begin{pmatrix} 168.1 & -205.3 & 69.6 \\ -205.3 & 342.7 & -215.8 \\ 69.6 & -215.8 & 277.5 \end{pmatrix}$
Story Stiffnesses (kip/in)	$\mathbf{k}_i = \begin{pmatrix} 218.2 \\ 229.3 \\ 89.0 \end{pmatrix}$	$\mathbf{k}_i = \begin{pmatrix} 205.3 \\ 215.8 \\ 61.7 \end{pmatrix}$

TABLE 4-7 Dynamic Properties and Stiffness Matrix Comparison of the East and West Frames after Severe Shaking

	WHNR_E - East	WHNR_E - West
Natural Frequencies (Hz.)	$f_i = \begin{pmatrix} 1.88 \\ 7.50 \\ 14.84 \end{pmatrix}$	$f_i = \begin{pmatrix} 1.73 \\ 7.50 \\ 14.84 \end{pmatrix}$
Modal Shapes	$\Phi_y = \begin{pmatrix} 1.00 & -0.83 & -0.56 \\ 0.82 & 0.36 & 1.00 \\ 0.45 & 1.00 & -0.76 \end{pmatrix}$	$\Phi_y = \begin{pmatrix} 1.00 & -0.84 & -0.55 \\ 0.83 & 0.36 & 1.00 \\ 0.49 & 1.00 & -0.76 \end{pmatrix}$
Modal Participation Factors	$\Gamma_i = \begin{pmatrix} 0.44 \\ 0.10 \\ -0.07 \end{pmatrix}$	$\Gamma_i = \begin{pmatrix} 0.44 \\ 0.10 \\ -0.06 \end{pmatrix}$
Damping Ratios (%)	$\xi_i = \begin{pmatrix} 5.5 \\ 1.9 \\ 1.5 \end{pmatrix}$	$\xi_i = \begin{pmatrix} 6.7 \\ 1.9 \\ 1.2 \end{pmatrix}$
Stiffness Matrix (kip/in)	$\mathbf{K}_y = \begin{pmatrix} 168.1 & -205.3 & 69.6 \\ -205.3 & 342.7 & -215.8 \\ 69.6 & -215.8 & 277.5 \end{pmatrix}$	$\mathbf{K}_y = \begin{pmatrix} 165.0 & -203.8 & 67.5 \\ -203.8 & 344.0 & -217.8 \\ 67.5 & -217.8 & 277.8 \end{pmatrix}$
Story Stiffnesses (kip/in)	$\mathbf{k}_i = \begin{pmatrix} 205.3 \\ 215.8 \\ 61.7 \end{pmatrix}$	$\mathbf{k}_i = \begin{pmatrix} 203.8 \\ 217.8 \\ 60.0 \end{pmatrix}$

TABLE 4-8 Low Amplitude Initial Stiffnesses from the Shear versus Inter-Story Drift Histories

Story	WHNR_B (kip/in)	WHNR_D (kip/in)	WHNR_E (kip/in)
Third	100.0	65.2	62.5
Second	100.0	55.0	46.0
First	113.2	65.9	54.0

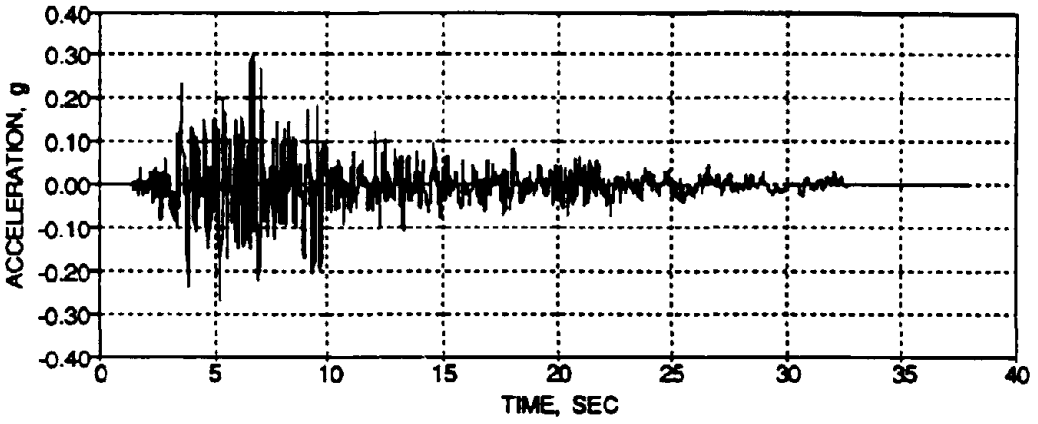

(a) Desired Base Motion

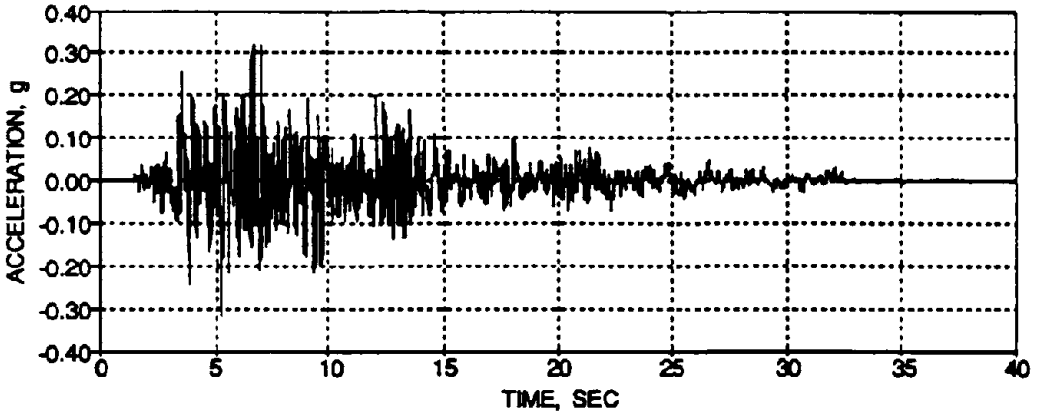

(b) Achieved Base Motion

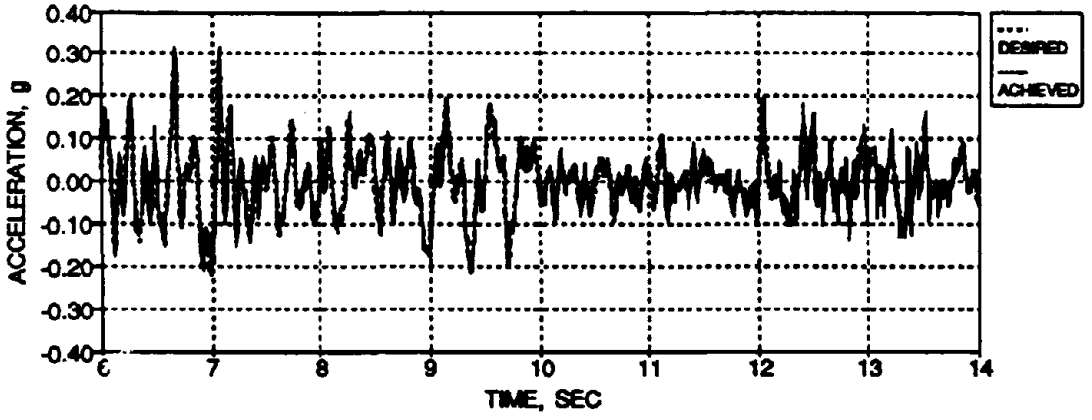

(c) Short Segment Comparison of the Desired and Achieved Base Motions

FIG. 4-19 Lateral Shaking Table Motion for TFTR_30

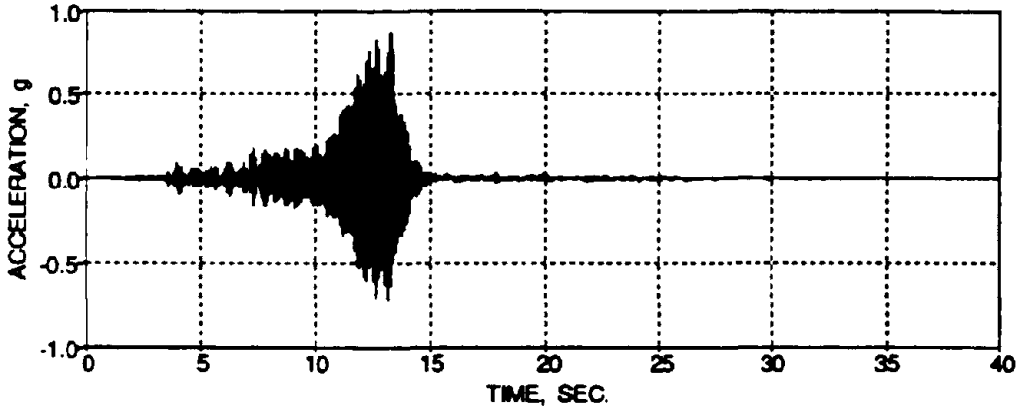

(a) North Side

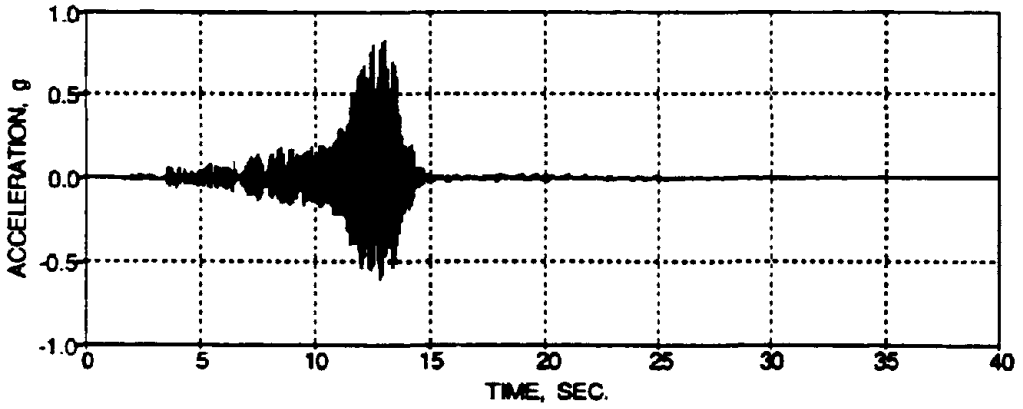

(b) South Side

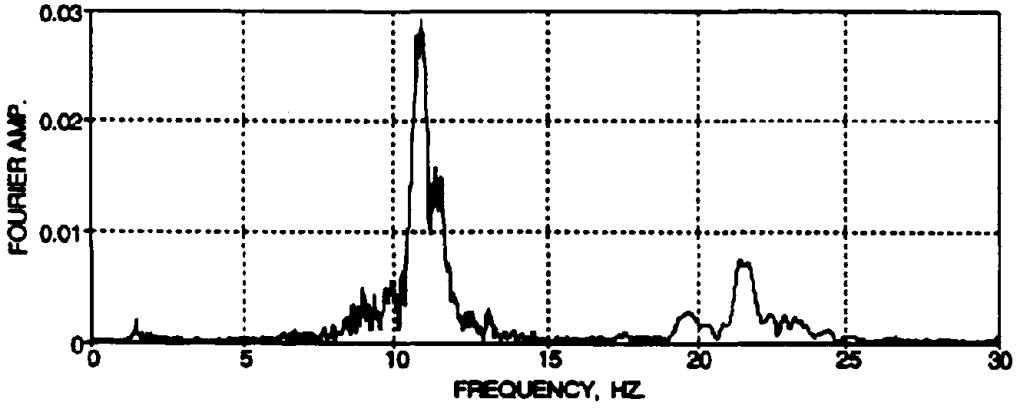

(c) Fourier Transform Amplitude of North Side Vertical Acceleration

FIG. 4-20 Vertical Shaking Table Acceleration for TFTR_30

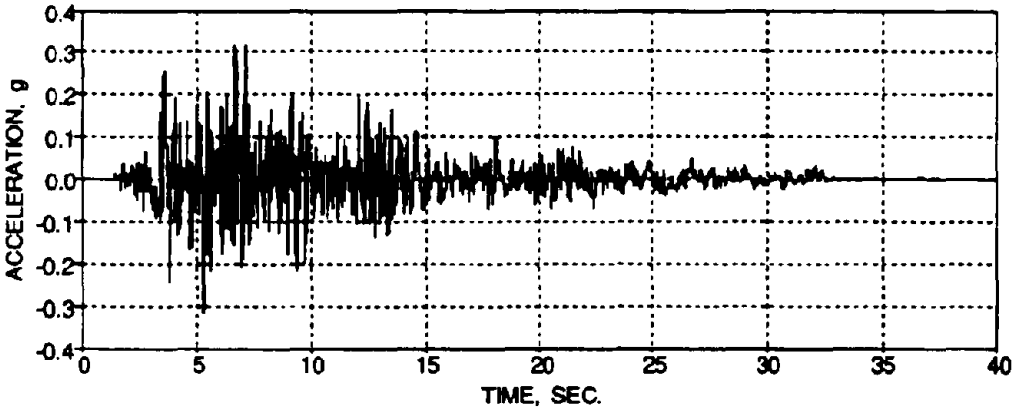

(a) East Side

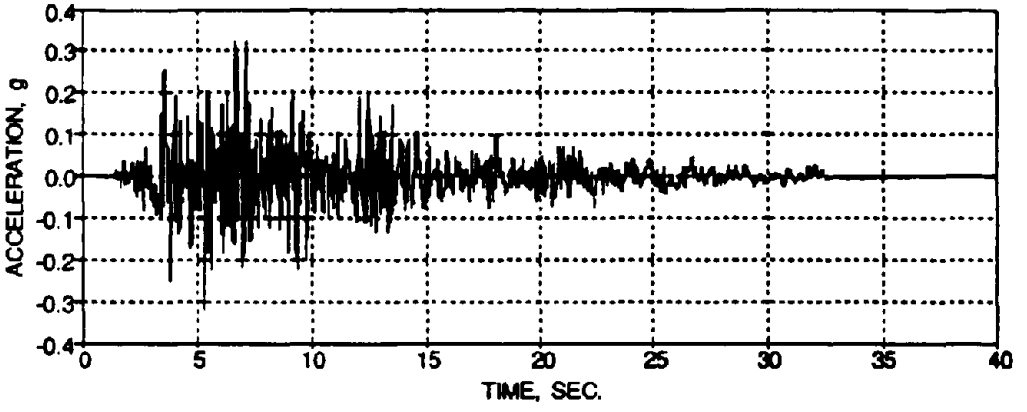

(b) West Side

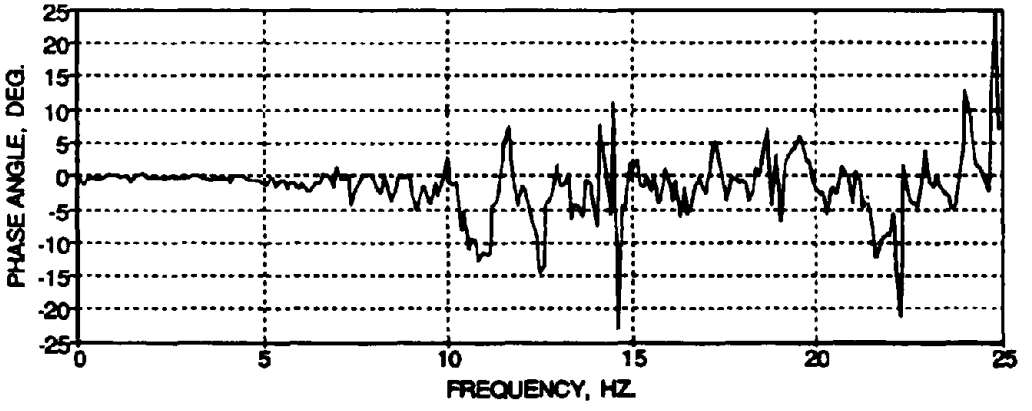

(c) Phase Angle of the East and West Side Acceleration

FIG. 4-21 East and West Lateral Acceleration for TFTR_30 - Torsion

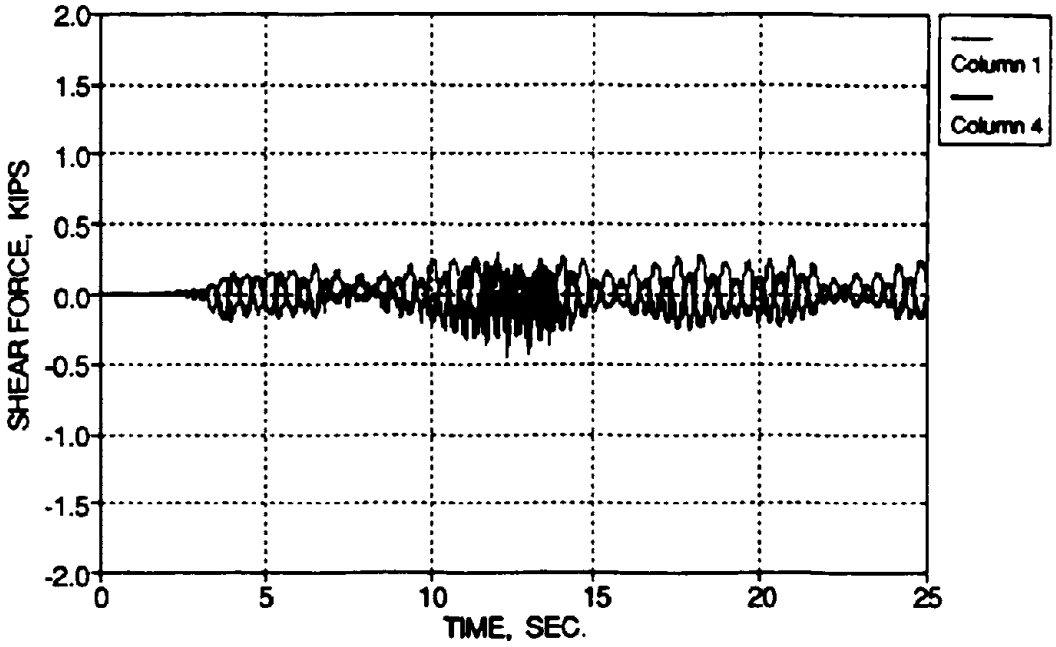

(a) Exterior Columns

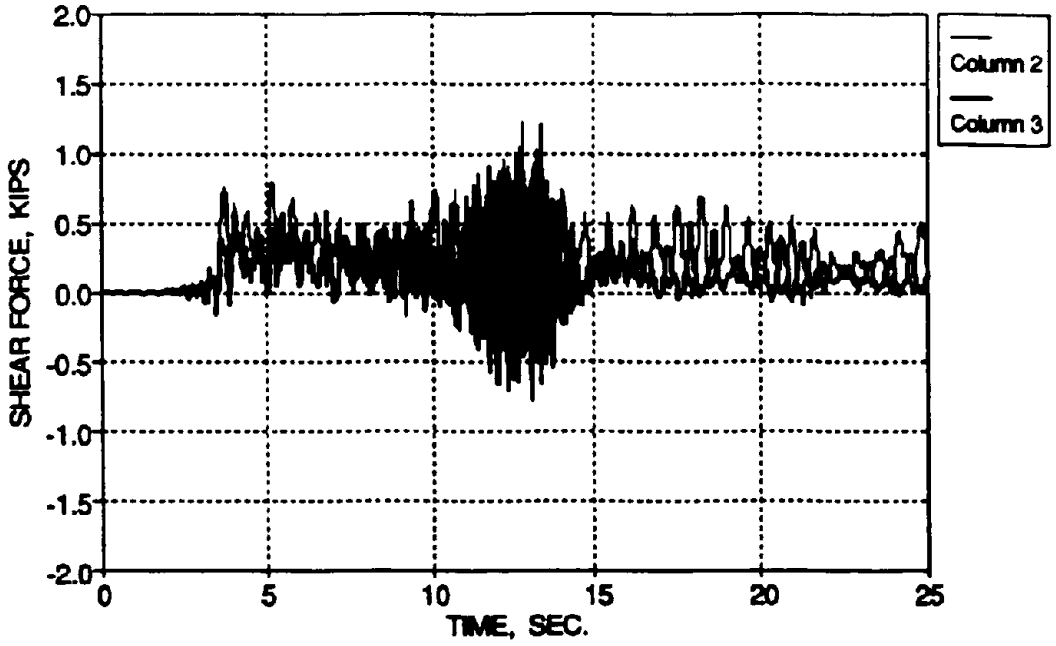

(b) Interior Columns

FIG. 4-22 Transverse Base Column Shear Forces for TFTR_30

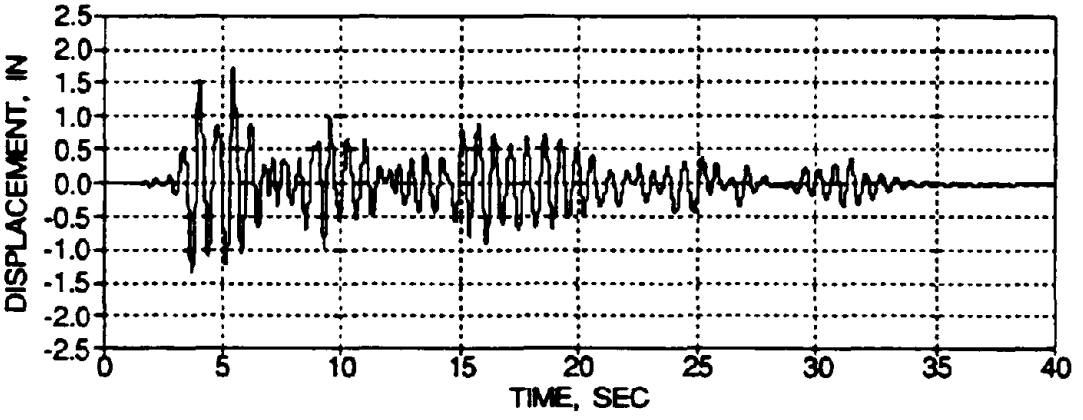

(a) Third Floor

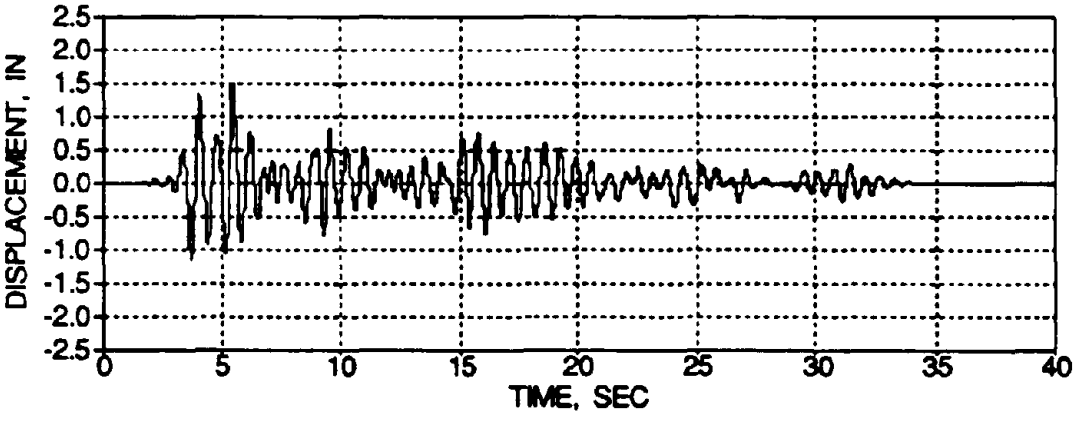

(b) Second Floor

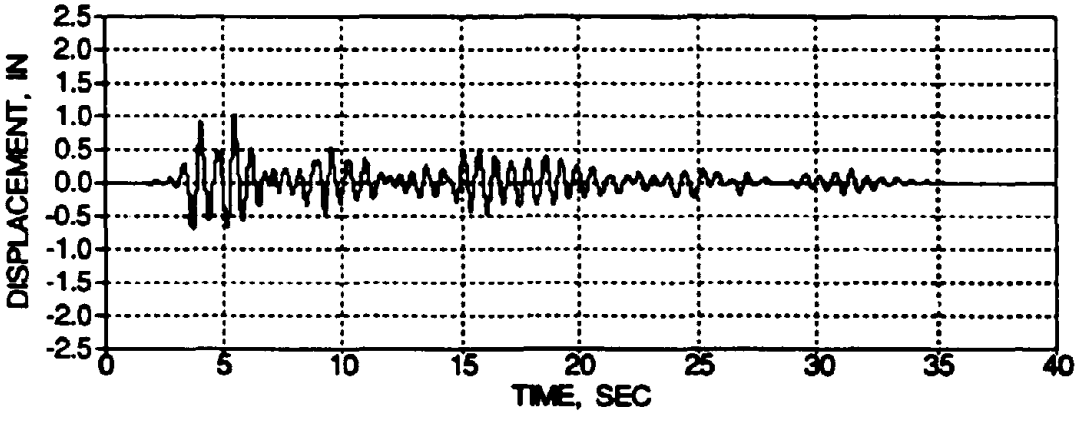

(c) First Floor

FIG. 4-23 Story Displacement Time Histories for TFTR_30

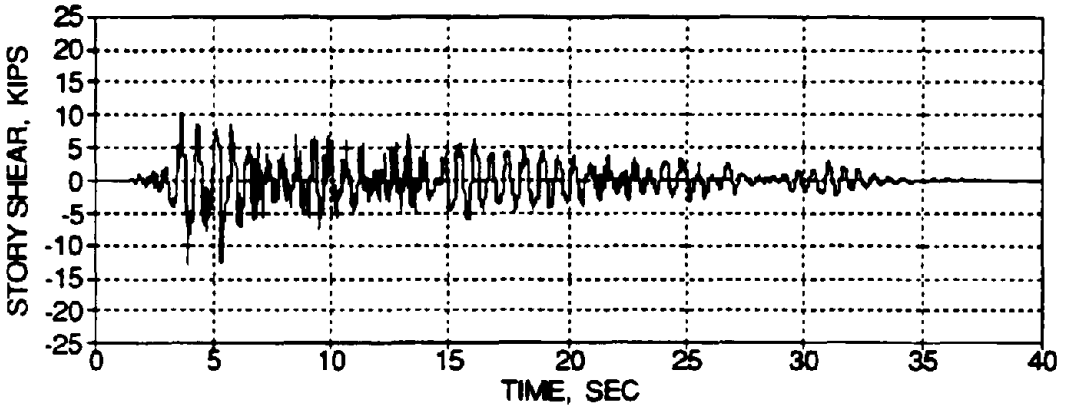

(a) Third Floor

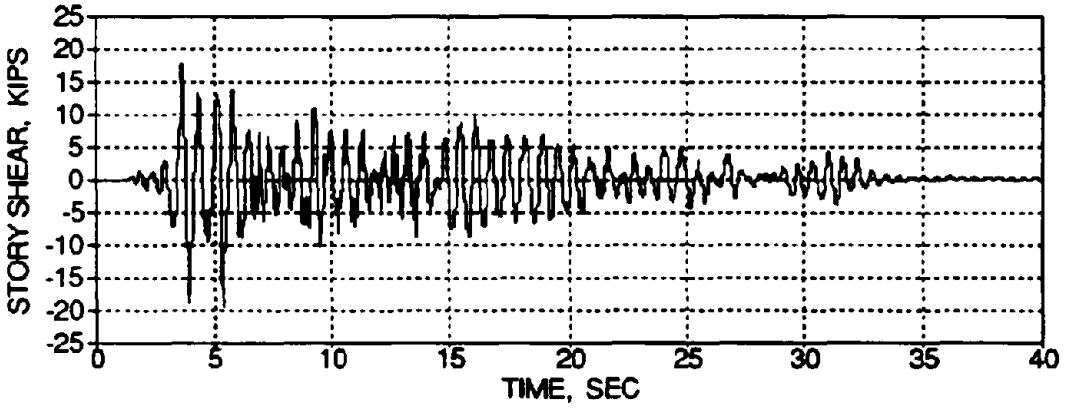

(b) Second Floor

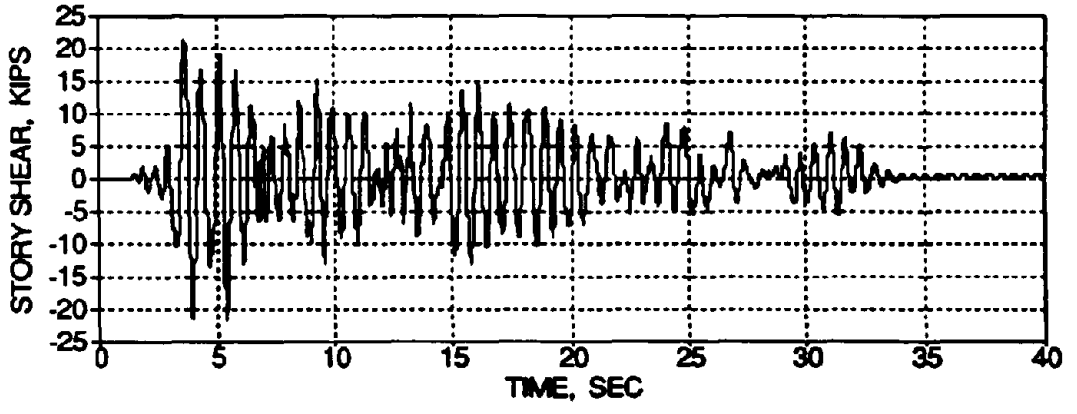

(c) First Floor

FIG. 4-24 Story Shear Time Histories for TFTR_30

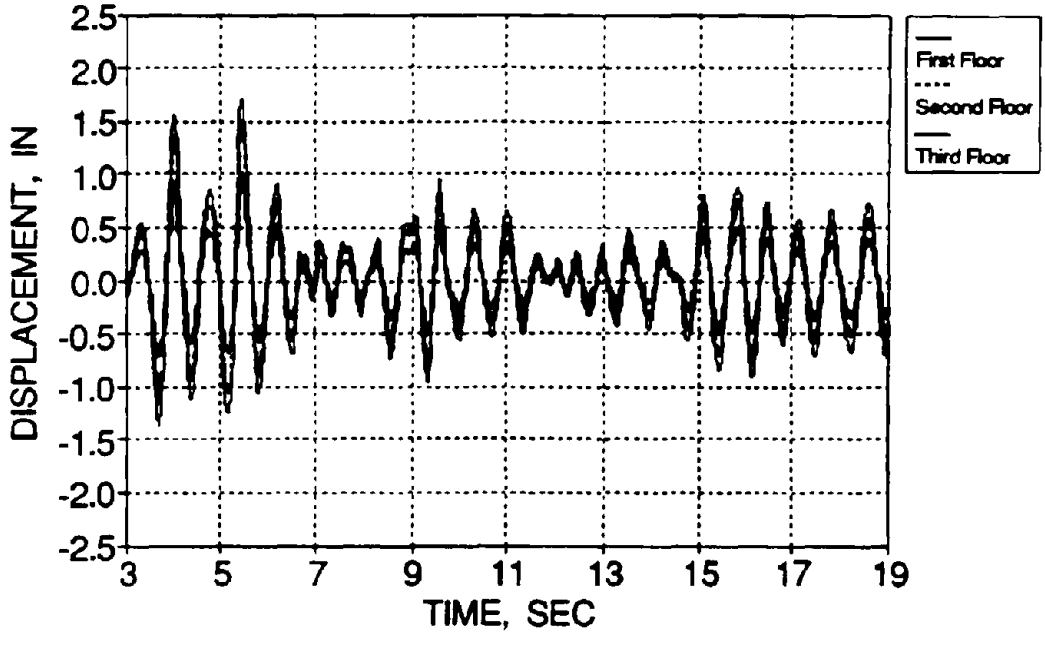

(a) Story Displacements

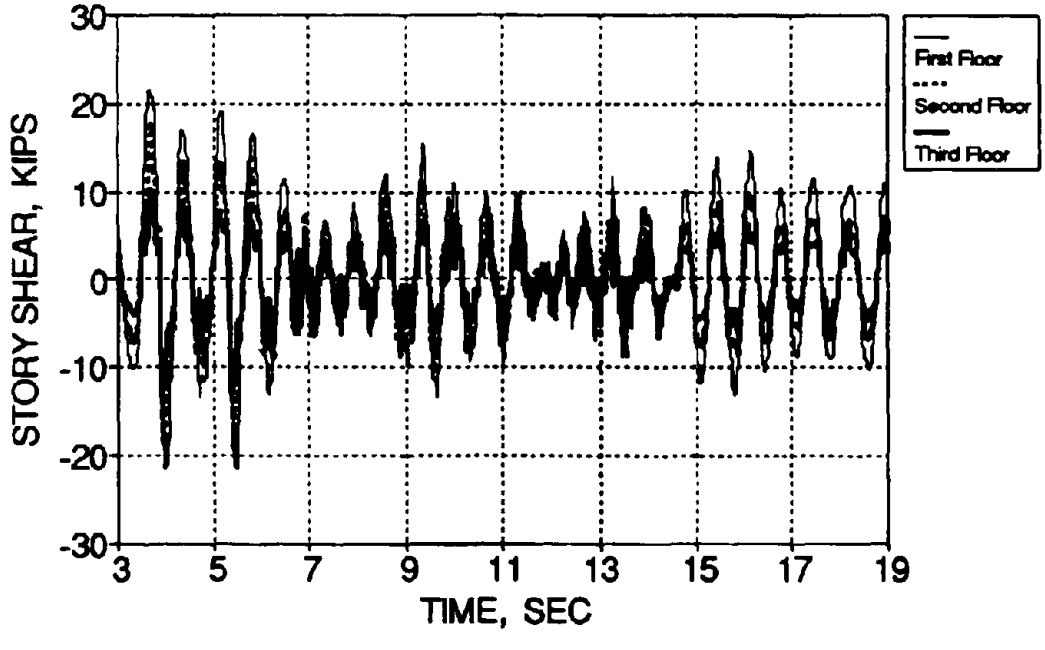

(b) Story Shear Forces

FIG. 4-25 Overlayed Global Response Time History Segments for TFTR_30

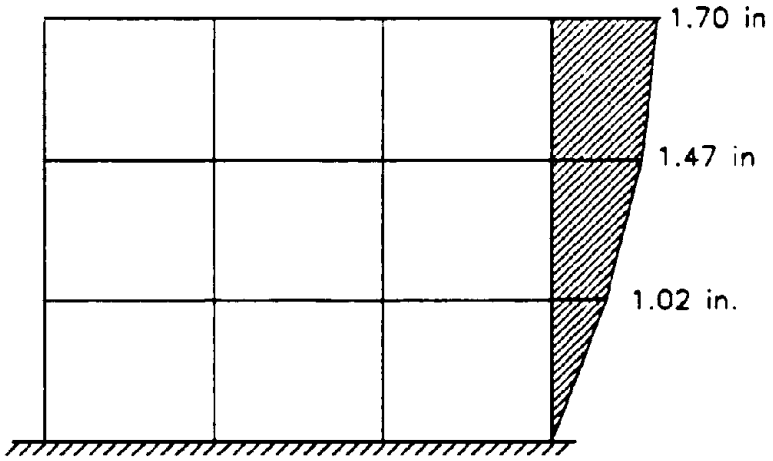

(a) Story Displacements (Time = 5.47 sec.)

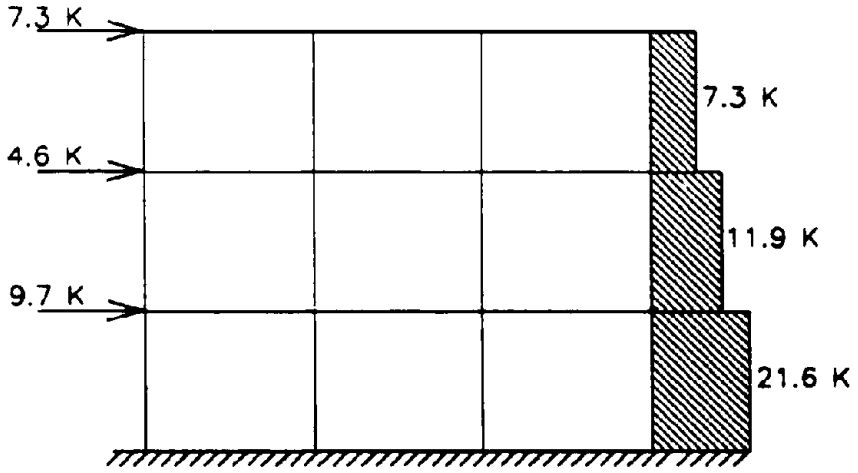

(b) Story Shears (Time = 5.47 sec.)

FIG. 4-26 Story Displacements and Shear Forces at Maximum First Story Drift for TFTR_30

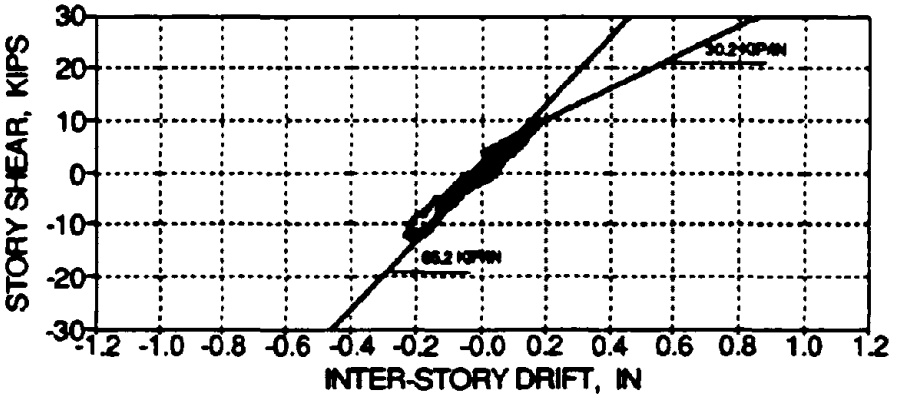

(a) Third Story

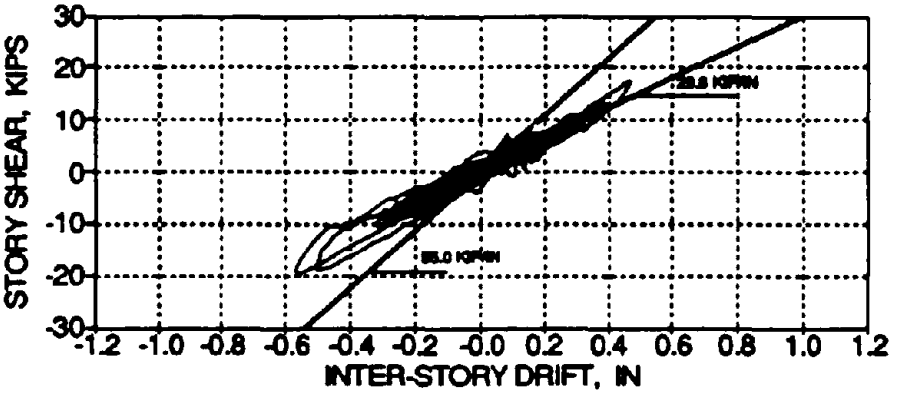

(b) Second Story

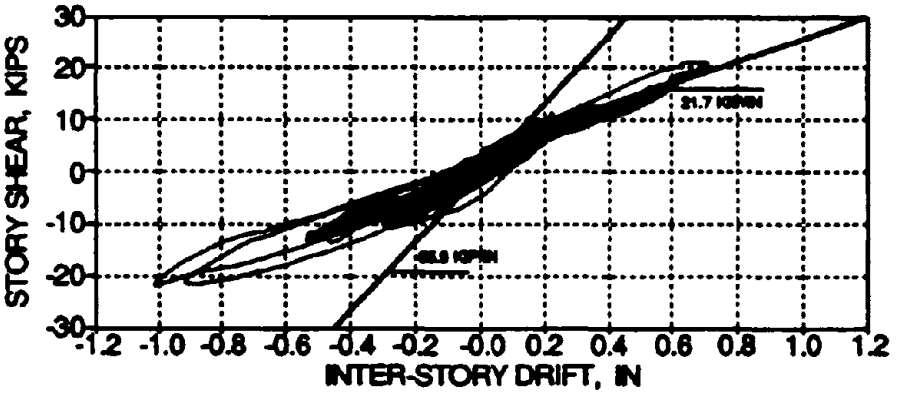

(c) First Story

FIG. 4-27 Story Shear versus Inter-Story Drift Histories for TFTR_30

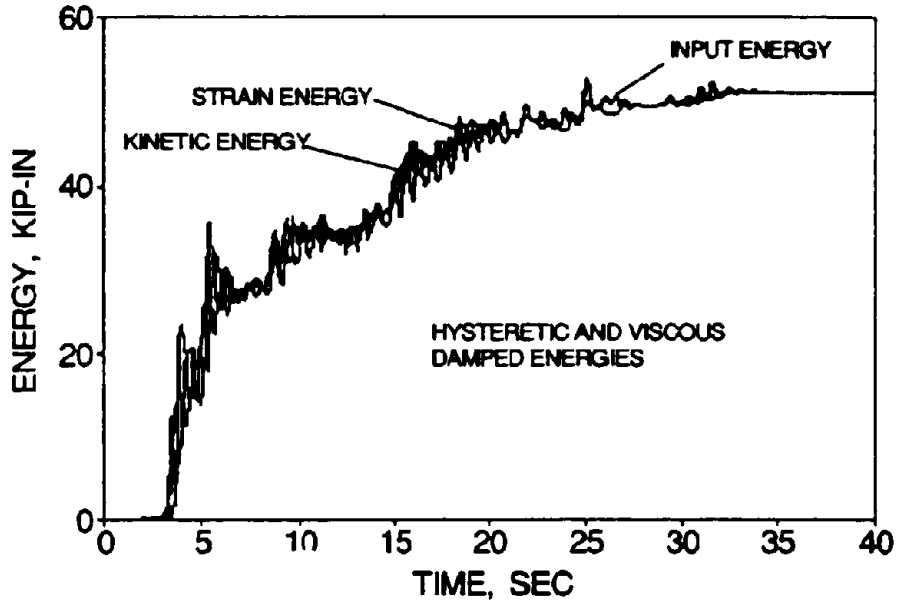

(a) Energy Balance

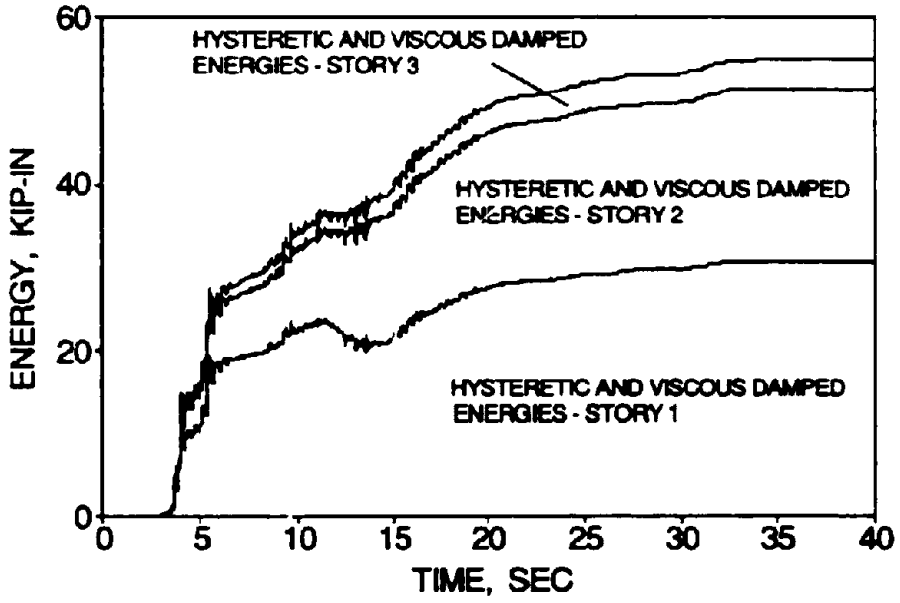

(b) Story Dissipated Energies

FIG. 4-28 Energy Time History for TFTR_30

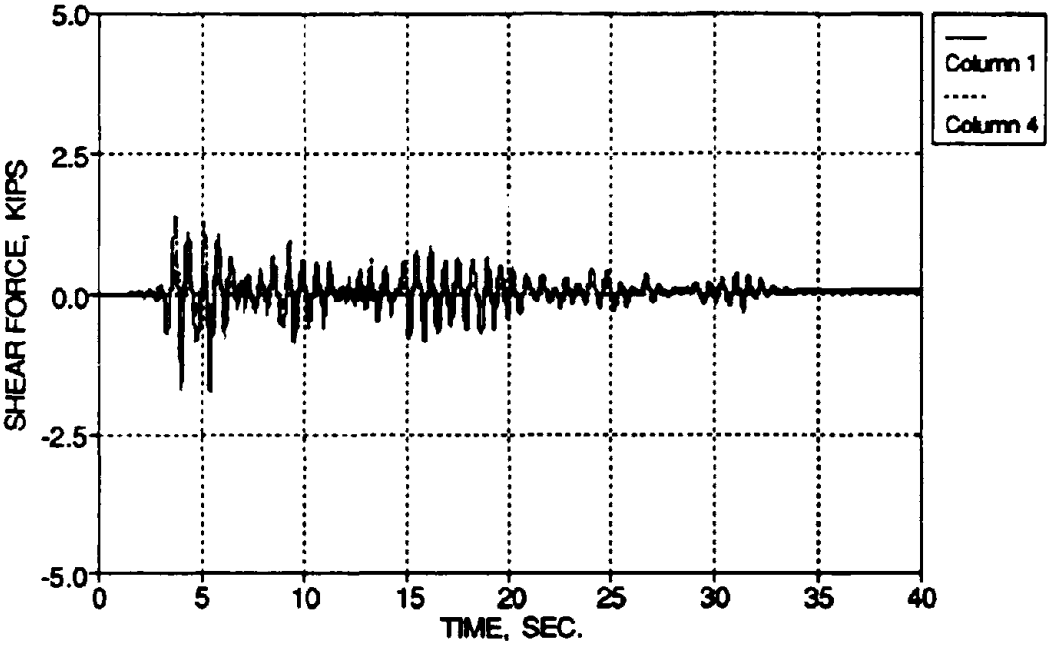

(a) Exterior Columns

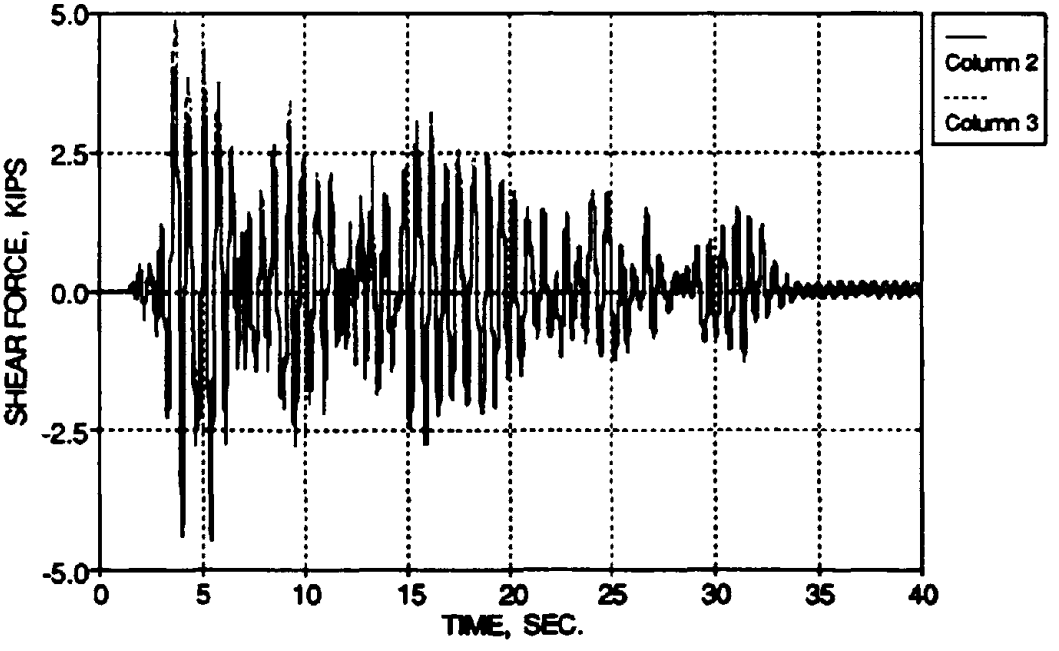

(b) Interior Columns

FIG. 4-29 **Base Column Lateral Shear Forces for TFTR_30**

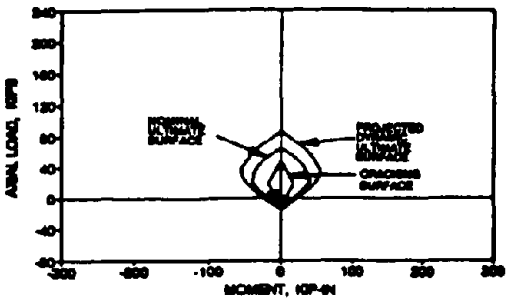

Column 8U

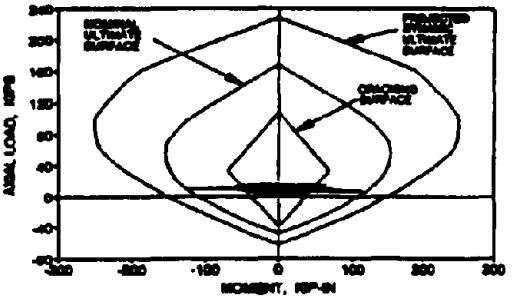

Column 7U

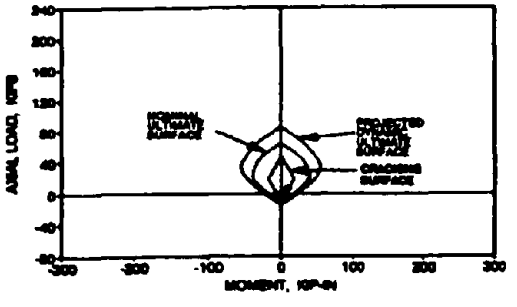

Column 8L

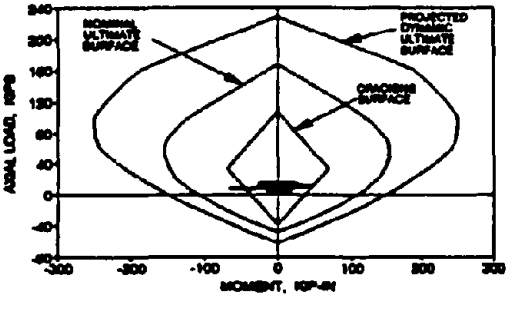

Column 7L

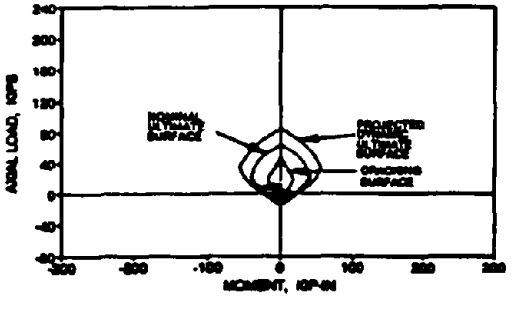

Column 4U

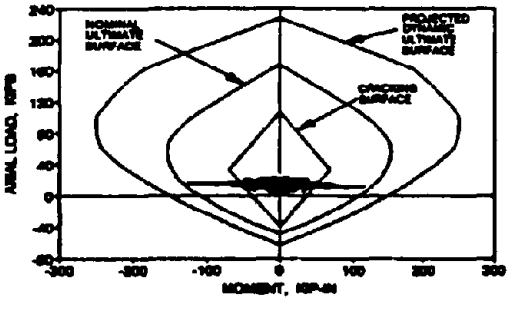

Column 3U

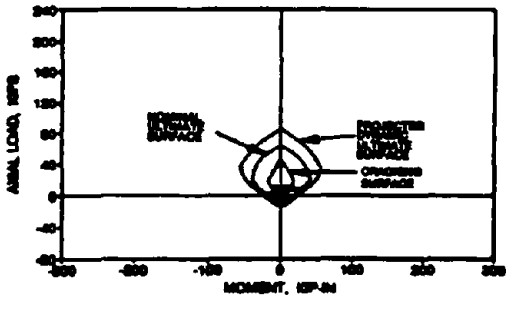

Column 4L

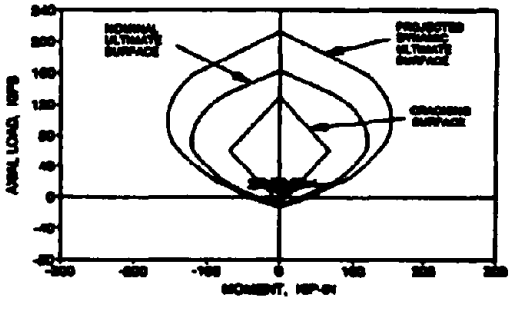

Column 3L

FIG. 4-30a Interaction Diagram for the South-East Columns from TFTR_30

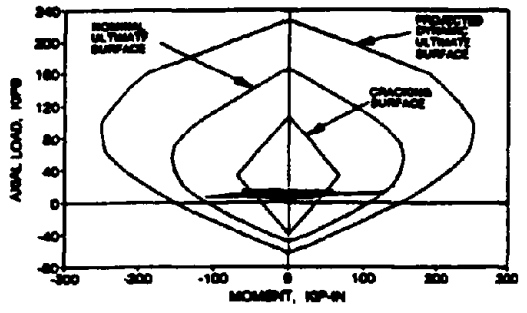

Column 6U

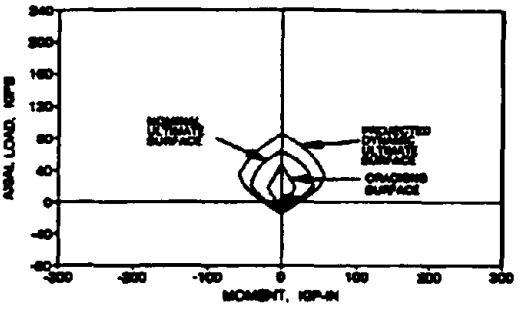

Column 5U

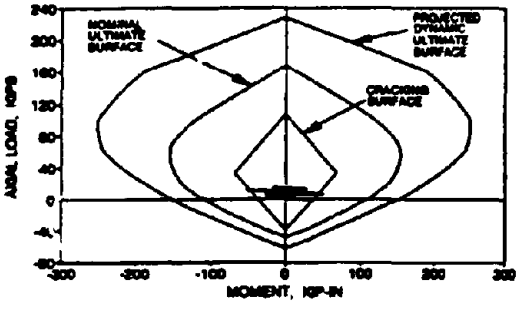

Column 6L

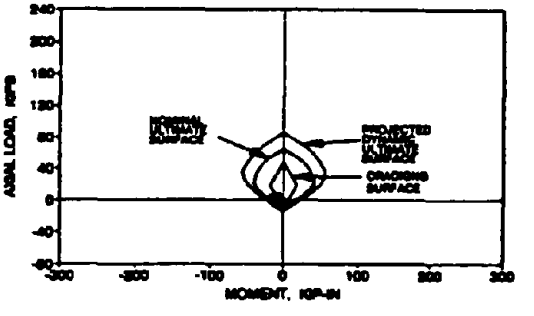

Column 5L

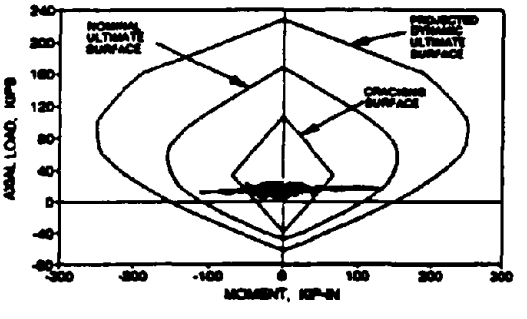

Column 2U

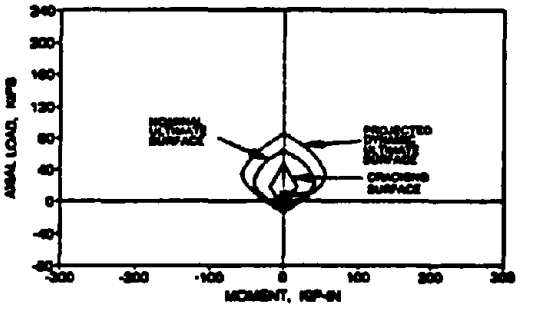

Column 1U

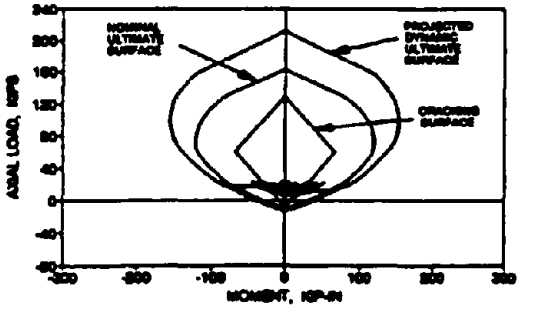

Column 2L

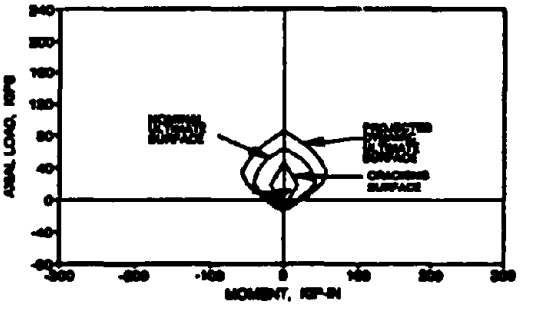

Column 1L

FIG. 4-30b Interaction Diagram for the North-East Columns from TFTR_30

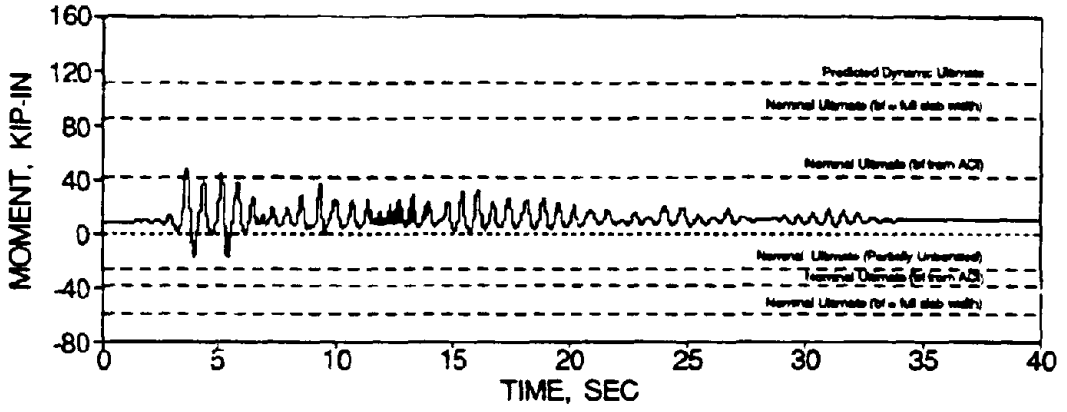

(a) Exbm481

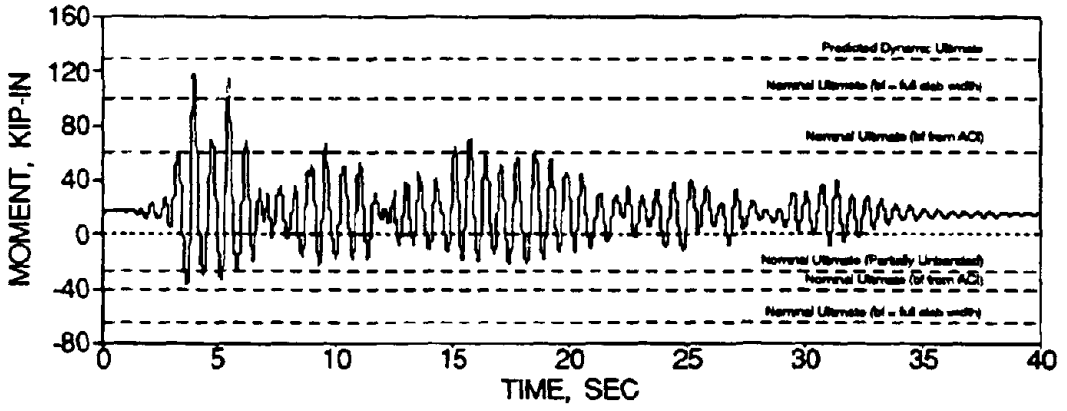

(b) Exbm482

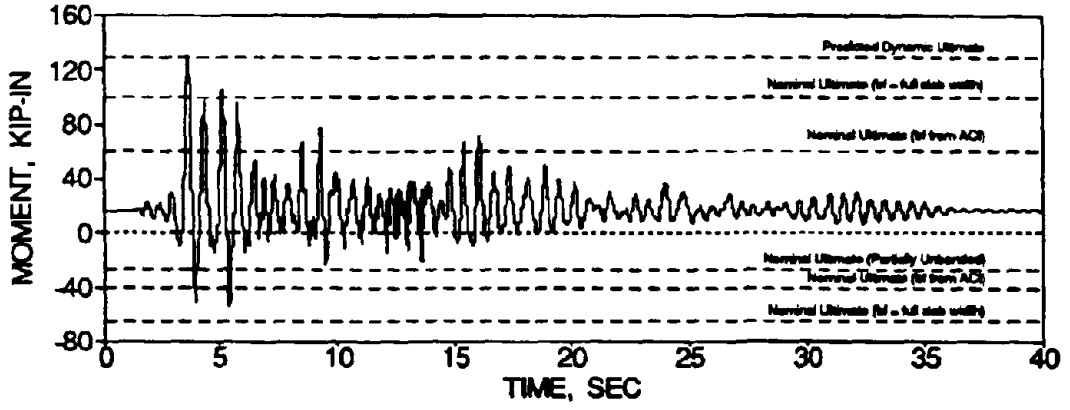

(a) Exbm483

FIG. 4-31a First Story Beam Bending Moment Time Histories for TFTR_30 - South Side

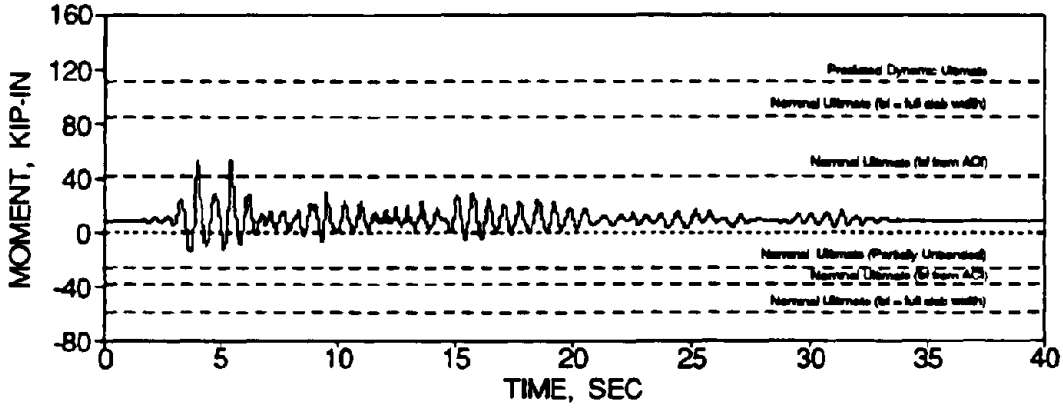

(a) Exbm151

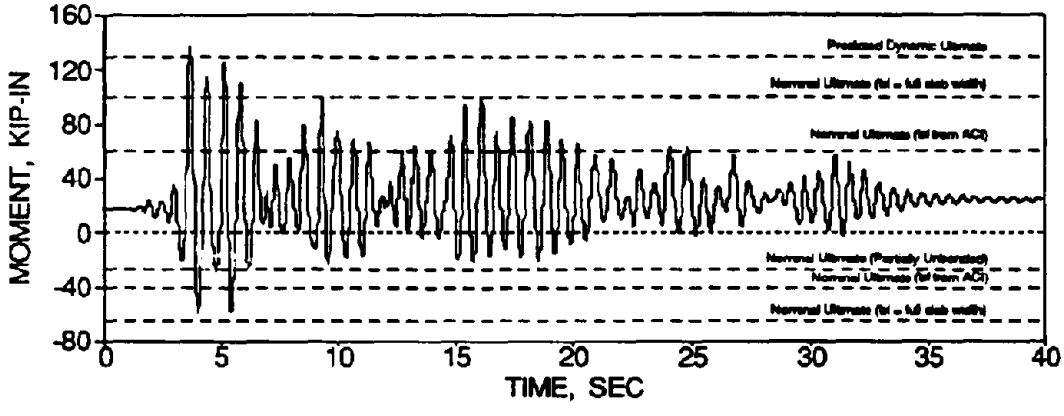

(b) Exbm152

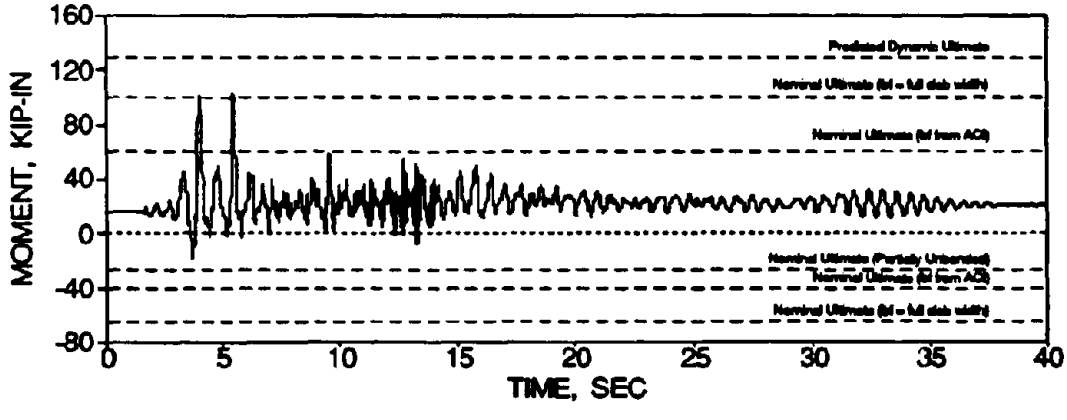

(c) Exbm153

FIG. 4 31b First Story Beam Bending Moment Time Histories for TFTR_30 - North Side

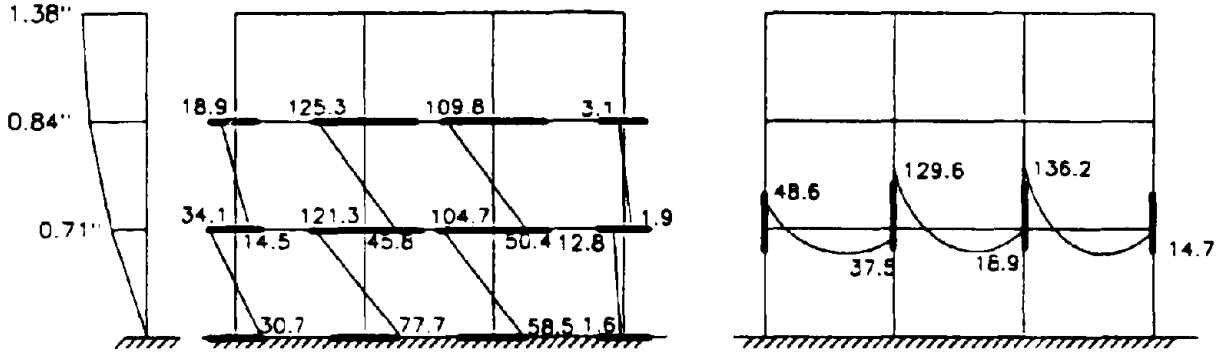

Displacements **Column Moments** **Beam Moments**

(a) Time =3.70 sec.

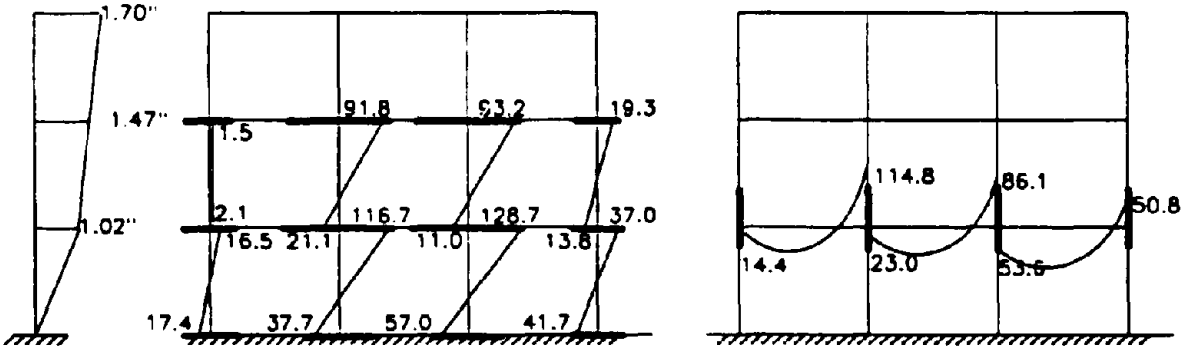

Displacements **Column Moments** **Beam Moments**

(b) Time = 5.47 sec.

FIG. 4-32 Moment Diagram at Maximum Story Drifts from TFTR_30

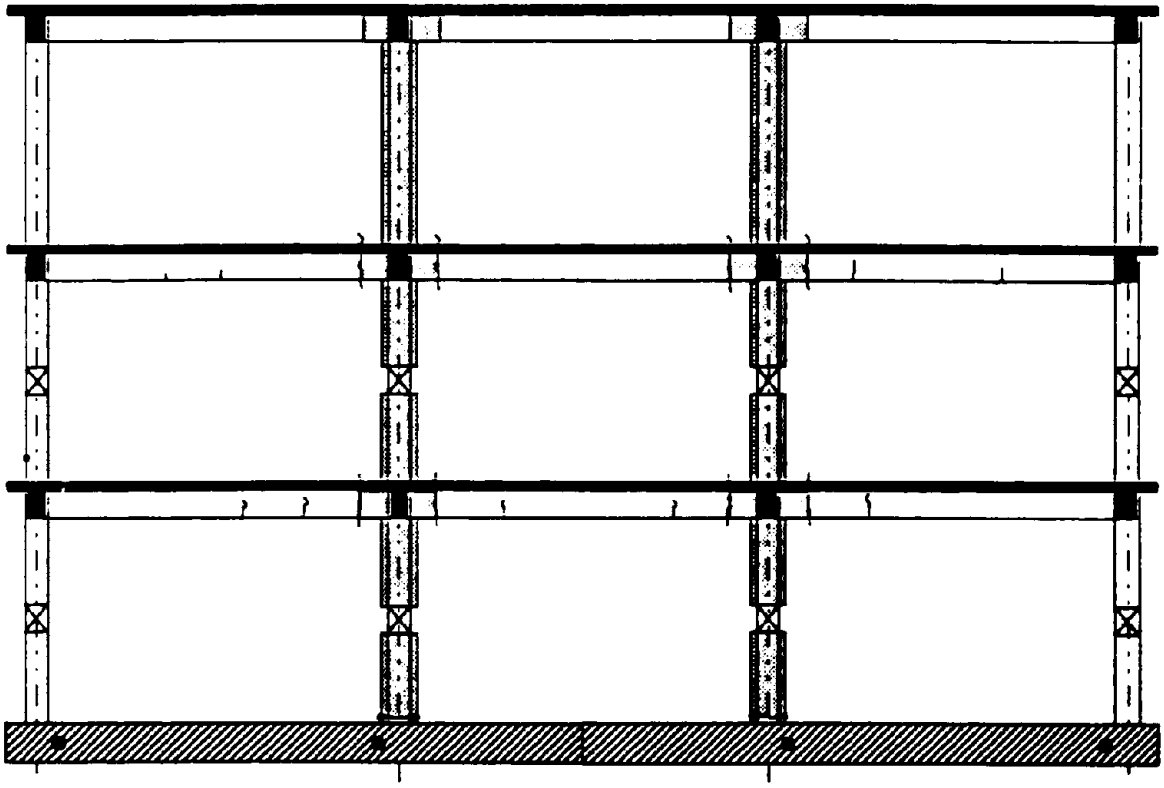

FIG. 4-33a Observed Structural Damage after Severe Shaking

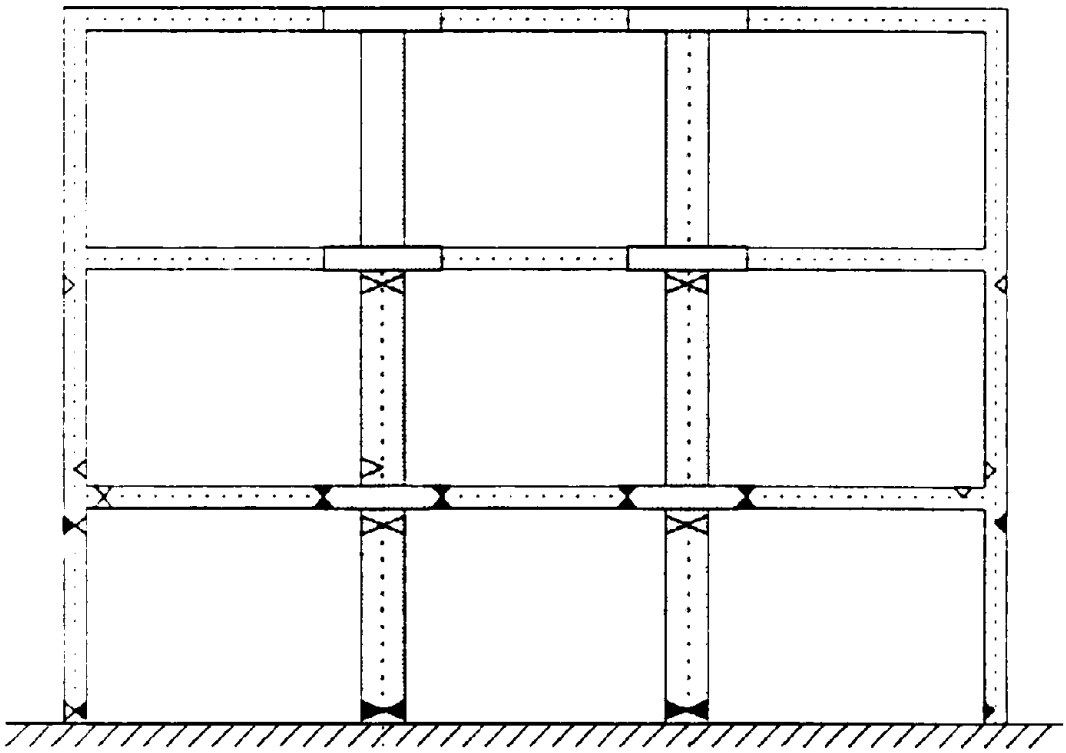

FIG. 4-33b Measured Damage State of the Model after Severe Shaking

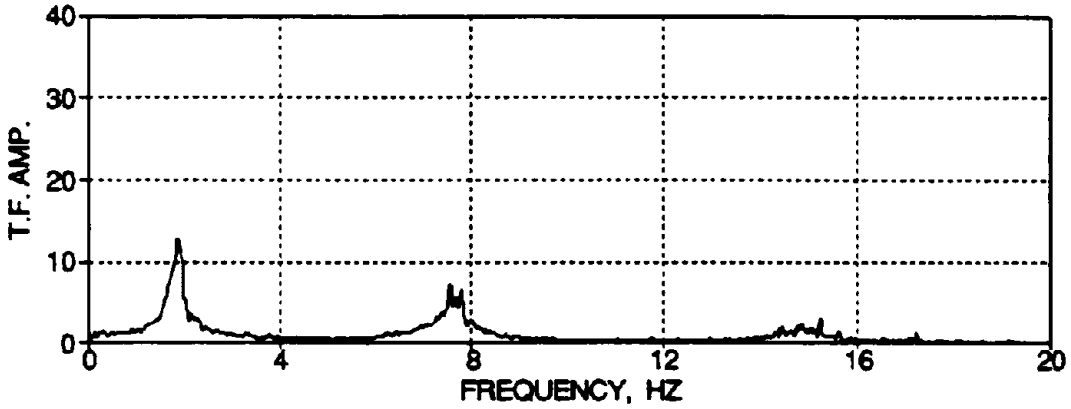

(a) Third Floor

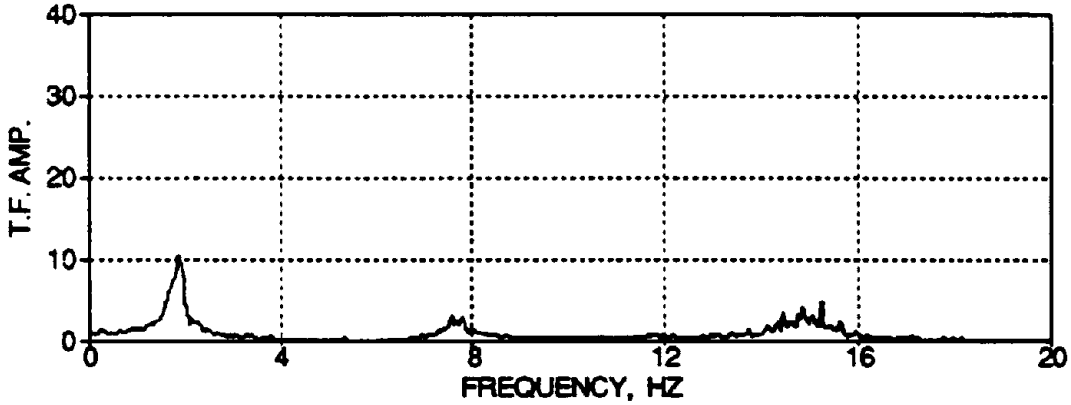

(b) Second Floor

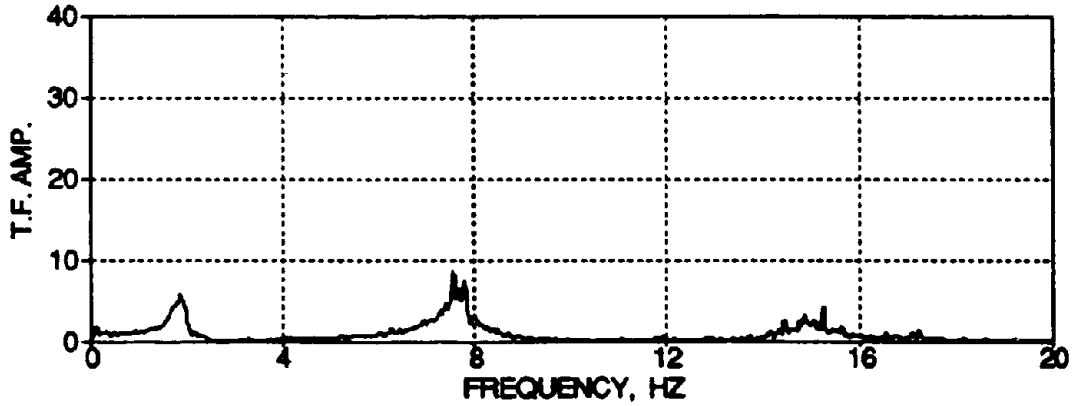

(c) First Floor

FIG. 4-34a Smoothed Transfer Functions from WHNR_E - East Frame

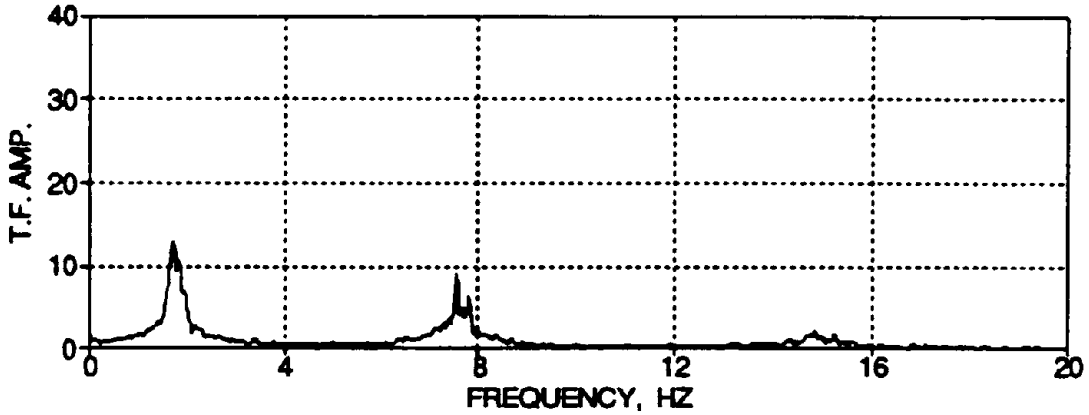

(a) Third Floor

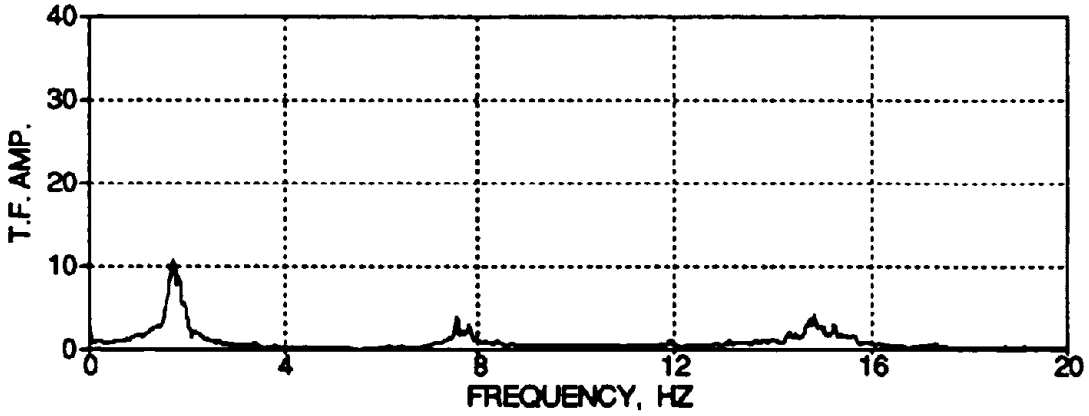

(b) Second Floor

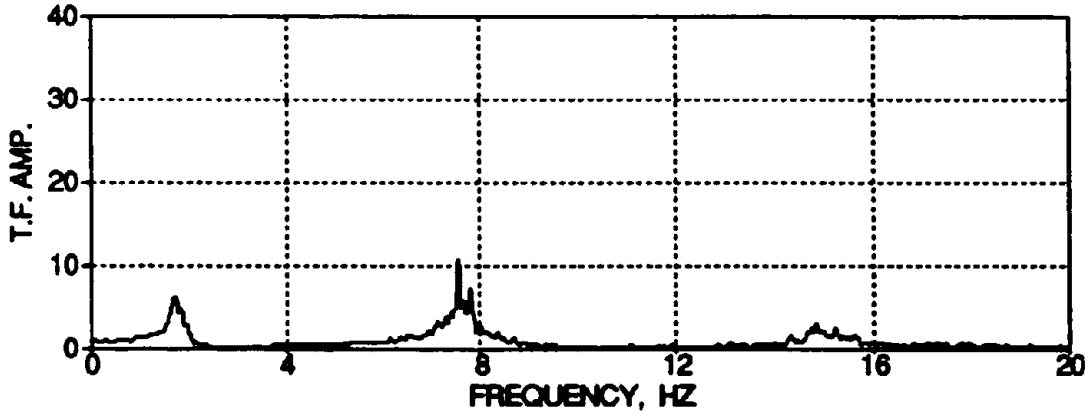

(c) First Floor

FIG. 4-34b Smoothed Transfer Functions from WHNR_E - West Frame

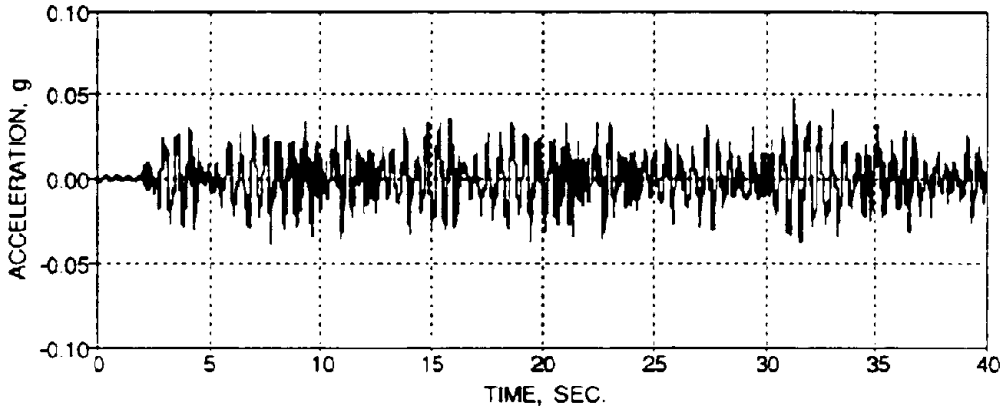

(a) Third Story - East Side Acceleration

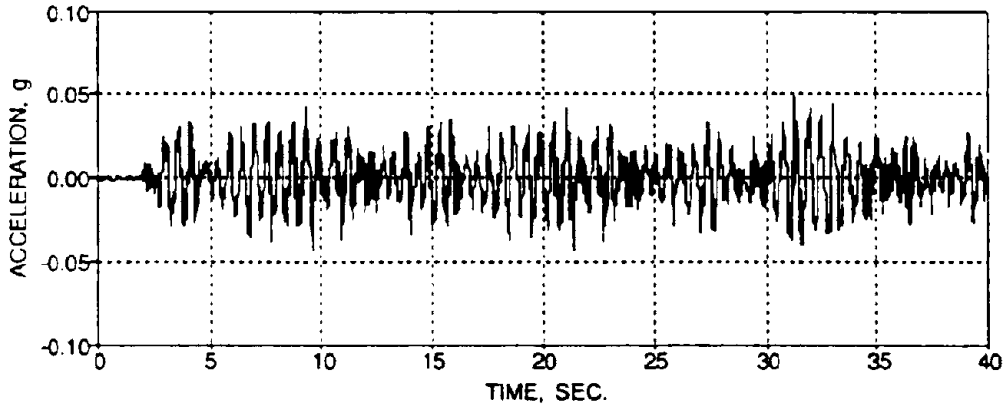

(b) Third Story - West Side Acceleration

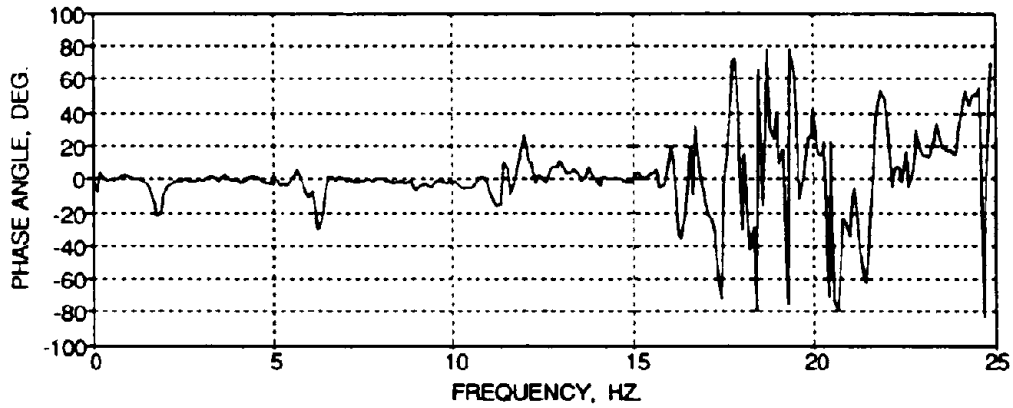

(c) Phase Angle of the East and West Side Accelerations

FIG. 4-35 East and West Lateral Accelerations for WHNR_E

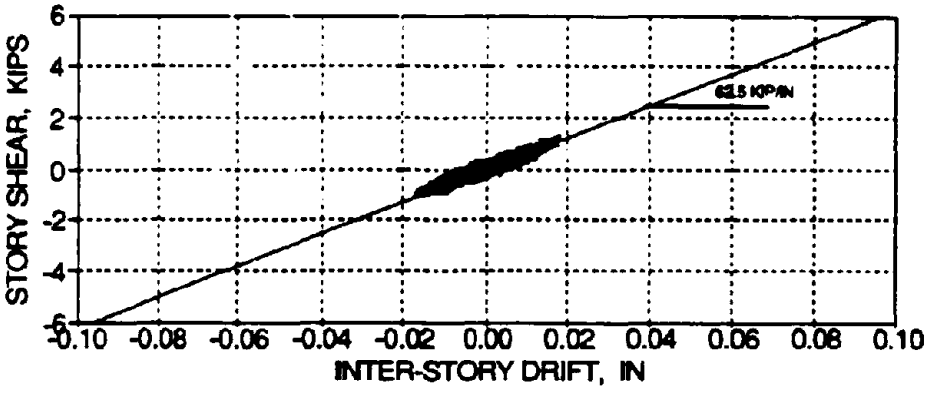

(a) Third Floor

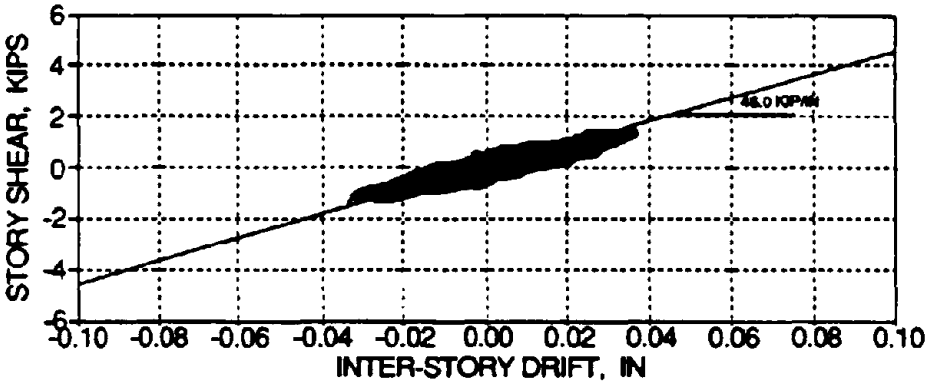

(b) Second Floor

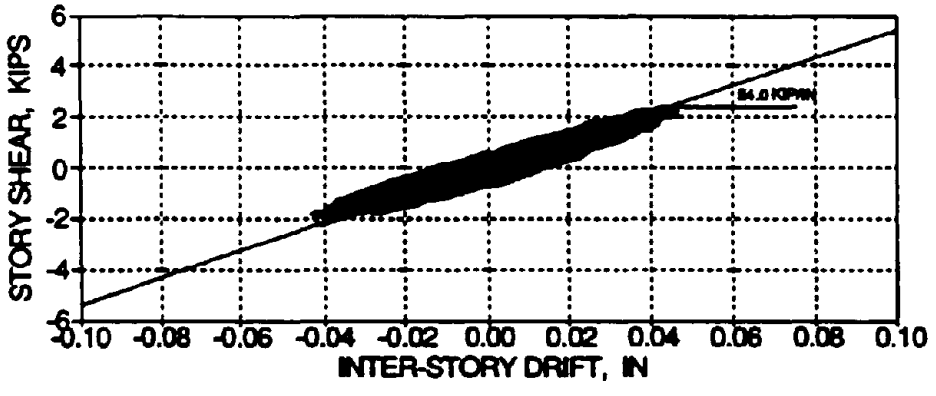

(c) First Floor

FIG. 4-36 Story Shear versus Inter-Story Drift Histories for WHNR_E

4.6 Analytical Modeling and Response Comparison

The experimental response results of the retrofitted model from the moderate (0.20 g) and severe (0.30 g) earthquakes were presented in Sections 4.2 and 4.4, respectively. In this sub-section, an inelastic analysis, using analytical modeling with member parameters developed from component tests, is presented and used to predict the story response of the retrofitted model from the induced earthquake simulations. The damage to the individual members, story levels, and overall structure from the shaking is quantified analytically in terms of damage indices according to modified Park et al. (1985) damage model. A discussion of this damage model was presented by Bracci et al. (1992b).

A collapse mode (shakedown) analysis of the retrofitted model is presented for sequential hinge formation and the base shear capacity. An elastic analysis of the retrofitted model is also performed for identification of equivalent strength ratios due to inelastic behavior for the moderate and severe earthquakes.

4.6.1 Analytical Simulation

4.6.1.1 Engineering Approximations

In Section 2, analytical modeling, based on approximate structural parameters, was used to predict the response of the retrofitted model structure. These structural parameters were: (i) the initial, post-cracking, and post-yielding stiffnesses; (ii) the cracking and yielding moments; and (iii) the hysteretic properties. Since the retrofitted columns were prestressed from the midheight of the first story to the roof, an initial stiffness of 1.0 EI_g was used. At the retrofitted base column with discontinuous reinforcement and no prestressing, an initial stiffness of 0.5 EI_g was used. Paulay and Priestley (1992) suggest ranges for an effective moment of inertia between 0.7 I_g and 0.9 I_g for heavily loaded columns and between 0.5 I_g and 0.7 I_g for columns with axial loads of about 0.2 $f_c' A_g$. The initial stiffness for the beams is suggested to be 0.45 EI_g.

For development of the hysteretic rule, a post-cracking stiffness of EI/2 was assumed. The yield strengths of the beams and columns were computed from basic principles. Note that the beam moments considered slab steel contributions from the full slab width. Also note that the exterior beam yielding moment in the positive direction considered the effect of pull-out of the discontinuous bottom beam reinforcement (50% reduction in rebar area based on the prototype ratio of provided and required embedment lengths). However with retrofit, the interior beam

moments considered full moment capacity without pull-out. The hysteretic properties for analytical modeling of the beams and columns were defined based on previous component testing as: (i) 0.3 and 0.8 for the stiffness degradation factor for the columns and beams, respectively; (ii) 0.1 for the strength degradation factor; (iii) 1.0 for the target slip factor; (iv) 1.00 for the slip reduction factor; and 1.5%; (v) 1.0% for the post-yielding stiffness ratio for the columns and beams, respectively; and (vi) 2% for the damping ratio.

The platform program IDARC, Kunnath et al. (1990), was used to carry out the inelastic analysis for a severe earthquake (Taft N21E 0.30 g) based on the structural member parameters from engineering approximations. From Table 2-1, the predicted maximum first story drift was 1.24% of the story height. However from Tables 4-1 and 4-5 for the moderate (0.20 g) and severe (0.30 g) shaking, the maximum measured first story drifts are 1.37% and 2.13%, respectively. Obviously a gross error was made with the approximations since the measured story drift was approximately double the estimated drift for the severe shaking. However the estimated maximum base shear demand of 20.1 kips (24.5% of the structural weight W) reasonably predicts the measured base shears of 20.6 kips (25.0% W) and 21.8 kips (26.4% W) from the moderate and severe shaking.

4.6.1.2 Component Tests

Choudhuri et al. (1992) (in Part I of the Retrofit Report Series) tested quasi-statically the retrofitted interior subassemblage component by concrete jacketing. The original subassemblage component was built and tested by Aycardi et al. (1992) (in Part II of the Evaluation Retrofit Series). The initial stiffness of the retrofitted column with applied prestressing was identified as.

$$EI_{ini\ col} = 0.71\ (EI_{col})_g \tag{4.1}$$

At the base retrofitted columns of the model where the longitudinal rebars are discontinuous and not prestressed, the initial stiffnesses are assumed based on previous tests as:

$$EI_{ini\ base} = 0.50\ (EI_{col})_g \tag{4.2}$$

Aycardi et al. (1992) (in Part II of the Evaluation Report Series) also built and quasi-statically tested the original (unretrofitted) column and subassemblage components. Since the model

structure previously experienced story drifts of about 2% of the story height, the unloading stiffness from the column components at 2% drift is used as the initial stiffness of the exterior columns and identified as follows:

$$EI_{ext.\,col} = 0.22\,(EI_{col})_g \tag{4.3}$$

From the subassemblage tests at 2% drift, the unloading of the interior and exterior beams is used for the initial stiffness of the beams in the analytical modeling as follows:

$$EI_{int.\,bm} = 0.32\,(EI_{bm})_g \tag{4.4}$$
$$EI_{ext.\,bm} = 0.23\,(EI_{bm})_g$$

Note that the stiffness of the interior beam is identical to the initial stiffness used in the undamaged building.

A post-cracking stiffness of about EI/2 is identified from the component tests and used for each member. The member strengths are identified from the component tests and are similar to those from basic principles. The hysteretic properties for analytical modeling of the beams and columns are defined as: (i) 0.5 for the stiffness degradation factor; (ii) 0.04 for the strength degradation factor; (iii) 0.7 for the target slip factor; (iv) 1.0 for the slip reduction factor; (v) 1.5% for the post-yielding stiffness ratio; and (vi) 2% for the damping ratio.

Table 4-9 summarizes the member parameters from engineering approximations and component tests used for the analytical modeling of the retrofitted model with concrete jacketing of the interior columns and partial base fixity.

The platform program IDARC is used to carry out the analytical modeling based on member parameters identified from component tests. From static computations, the first natural frequency is determined to be 2.24 Hz. Note from the experimental white noise test before the moderate shaking that the first natural frequency was determined to be 2.64 Hz. (see Table 2-5). Therefore the analytical modeling predicts a slightly softer structure.

A collapse mode (shakedown) analysis is performed in IDARC by statically increasing the lateral loads on the model according to a inverted triangular loading distribution. The sequence of hinge formation in the model is shown in Fig. 4-37. It can be observed that yielding first occurs in the lower first story interior columns (with discontinuous added rebars). Yielding then propagates to the interior beam members and then throughout the structure. The static

loading is continually increased until the top story displacement exceeds 2% of the building height. At this drift limit, the base shear ca, acity of the retrofitted model is determined as 25.5% of the total structural weight (21.1 kips). From Tables 4-1 and 4-5, the maximum measured base shears during the moderate and severe earthquakes are 25.0% W and 26.4% W. Therefore the analytical base shear capacity slightly underpredicts the actual base shear capacity.
Figs. 4-38 and 4-39 show the comparisons of the predicted story displacements and shear forces of the retrofitted model from the analytical modeling based on component tests with the experimentally measured response for the moderate (0.20 g), and severe (0.30 g) earthquake simulations, respectively. Sequential runs of the moderate and severe motions are used to capture the degradations of both elastic and inelastic hysteretic properties. It can be observed that the predicted story response adequately correlates to the experimentally obtained results.

Fig. 4-40 shows the resulting damage states of the model predicted analytically in comparison with the experimental measured damage states of the simulated earthquakes. It can be observed that yielding has occurred in the lower first story interior columns (base) and the upper first and second story interior columns for the moderate shaking using IDARC. However the hinges in the upper first and second stories are in the incipient stages. Yielding was not measured experimentally in these sections. Yielding has also developed in some of the beam members of the first and second stories for the moderate earthquake both experimentally and analytically. The unretrofitted exterior columns and exterior beams result in a cracked damage state from IDARC. However experimentally, some yielding was also observed in the first story exterior columns. For the severe shaking in IDARC, yielding occurs in the same members as the moderate shaking with additional hinging in the exterior columns of the first story. Experimentally, the measured damage state of the retrofitted model after the severe shaking was also similar to the moderate shaking. It can be observed that the correlation exists between the analytically predicted and experimentally measured damage states for both earthquakes. Since yielding has occurred in the base columns and first and second story beams, the apparent collapse mechanism for the retrofitted model under ultimate load is a beam-sidesway failure mechanism. In comparison, the unretrofitted model shows (see Bracci et al., 1992b), a resulting damaged state of a column-sidesway mechanism type under ultimate load.

4.6.2 Damage Evaluation

Fig. 4-41 shows the quantified member damages in the retrofitted model building for the moderate and severe earthquakes computed from the modified Park's damage model in IDARC.

TABLE 4-9 Summary of Member Parameters for Analytical Modeling of Retrofitted Model

Modeling Type	Initial Stiffness, EI				Post-Cracking Stiffness		Hysteretic Properties [F]					
	Interior Base Column (%EIg)	Interior Upper Column (%EIg)	Exterior Column (%EIg)	Beams [A] (%EIg)	Column (%EI)	Beam (%EI)	Stiffness Deter. Factor	Strength Deter. Factor	Target Slip Factor	Crack Closing Factor [X]	Post-Yield Stiffness (%)	Damping Ratio (%)
(1)	(2)	(3)	(4)	(5)	(6)	(7)	(8)	(9)	(10)	(11)	(12)	(13)
1. Engineering Approximations	50 [B]	100 [C]	27 [B]	45 [D]	50	50	0.3 - 0.8	0.1	1.0	1.0	1.0 - 1.5	2.0
2. Component Tests [E]	50	71	22	23 - 32	50	50	0.5	0.04	0.7	1.0	1.5	2.0

[A] Based on gross section properties with full slab width contributions.
[B] Suggested by Paulay and Priestley (1992).
[C] Approximately 10% greater than suggested by Paulay and Priestley (1992).
[D] Approximately 50% greater than suggested by Paulay and Priestley (1992).
[E] Based on subassemblage tests by Aycardi et al. (1992).
[F] Refer to Bracci et al. (1992b) for notation.

For the moderate shaking, the damage indices in the first story interior and exterior columns reach values of 0.17 and 0.11, respectively. Therefore the damage to the first story columns after the moderate shaking is within the *minor - "serviceable"* damage state (DI<0.33). However note that the resulting damage to the retrofitted interior columns occur as a result of a hinge formation at the base. Since transverse reinforcement was added in the base column sections, the corresponding damage index is small. The damage indices for the interior and exterior beam members of the first story (DI = 0.26 and 0.18) are also within the *"serviceable"* damage state. It can be observed from the story level damage indices that most of the resulting damage occurs to the members of the first story and that the larger damage results in the beams members. The overall structural damage index is 0.14 after the moderate shaking, which implies a *minor/moderate* damage state ($DI_{structure} < 0.40$). In comparison with the unretrofitted building tested under the same moderate earthquake, a damage index of 0.36 (*moderate - "repairable"* damage state) resulted for the first story interior columns. However damage to the beams was minimal, except in the exterior beams due to reinforcement slip. The overall structure damage index was 0.23. Therefore the damage from the moderate shaking was significantly reduced in the retrofitted building and damage is transferred from the columns to the beams.

For the severe shaking, the damage indices in the first story interior and exterior columns reach values of 0.31 and 0.18, respectively. Note that the damage associated with the interior columns is a result to damage at the base only. Therefore the first story columns are barely within the *minor - "serviceable"* damage state. The damage indices of the column in the second and third floors are minimal. The damage indices for the exterior beam members of the first story (DI = 0.44 and 0.37) are also within the *moderate - "repairable"* damage state. However the first story interior beam (DI = 0.67) is categorized as just beyond the *moderate - "repairable"* damage state. It can be observed from the story level damage indices that most of the resulting damage occurs to the members of the first story and larger damage results in the beams. The overall structural damage index is 0.32, which implies a *minor/moderate* damage state ($DI_{structure} < 0.40$). In comparison with the unretrofitted building tested under the same severe earthquake, damage indices of 0.72 and 0.67 (*severe - "irrepairable"* damage state) resulted for the first and second story interior columns. The exterior columns remained in the *"repairable"* damage state. Damage to the first story exterior beams was 0.46 from the pull-out demands and was minimal for the interior beams. The overall structure damage index was 0.49. Therefore the overall structural damage index was significantly reduced after retrofit and damage is transferred from the columns to the beams from retrofit (same results as the moderate shaking).

Therefore from the damage evaluations of the retrofitted model building, it can be concluded that: (i) the first story beams have a *moderate - "repairable"* damage state after the moderate and severe shaking. For the shaking of the original model, the only significant beam damage was in the first story exterior beam in the pull-out direction; (ii) the retrofitted interior and unretrofitted exterior base columns develop only *minor - "serviceable"* damage from the earthquakes, while the remaining columns develop negligible damage. For the shaking of the original model, *severe* damage occurred to the interior columns and *moderate* damage to the exterior columns of the first and second floors; (iii) the resulting damage distribution is typical of strong column - weak beam behavior in structure (beam-sidesway mechanism). In contrast with the original building where a column-sidesway mechanism was evident; and (iv) a significant decrease in column damage indices and overall structural damage index results for retrofitted model after the moderate and severe shaking in comparison with the original model.

4.6.3 Damage with P-delta Effect

The proposed damage index for including damage associated with the P-delta effect (see Bracci et al., 1992b) is used to evaluate the damage of a first story retrofitted interior column under various levels of peak ground accelerations (PGA). Firstly the column yield displacement, yield force, and ultimate displacement are found using IDARC by statically loading each story of the retrofitted model with forces proportional to the inverted triangular loading. Fig. 4-42 shows the first story shear force of a retrofitted interior column versus inter-story drift under increasing static loads. It can be observed that yielding occurs at about 1% of the story height (0.45 in.). The yielding shear force for the column is about 5.0 kips. The post-yielding shear force continually increases with displacement from the input strain hardening without a loss in strength. However the ultimate monotonic displacement is conservatively considered to be 3% of the story height based on a loss in strength determined from component tests.

Fig. 4-43 shows the retrofitted column damage index as a function of time, displacement ductility (δ_a/δ_y), and deformation damage ($[\delta_m - \delta_y]/[\delta_u - \delta_y]$) for the various PGAs. It can be observed that the resulting damage index is relatively small (DI < 0.20) for PGAs up to and including the 0.40 g motion. Note that this is considerably less than for unretrofitted columns previously tested (see Bracci et al., 1992b). At a PGA of 0.70 g, the damage index with and without the P-delta effect approaches 1.0 (collapse). However note that other members of the building, particularly the beams, may have collapsed under smaller levels of PGA , (evaluation which was not in the objective in this analysis). For the original building, the unretrofitted columns

approached collapse at a PGA between 0.30 g and 0.35 g. It can also be observed from Fig. 4-43 that the damage contribution from P-delta effect in the retrofitted columns is relatively small and significantly less as compared to the unretrofitted columns.

4.6.4 Elastic Analysis and Equivalent Strength Ratios

An elastic analysis is performed on the retrofitted model for the shaking motions with analytical modeling developed based on component test results (see Section 4.6.1.2). Fig. 4-44 shows the elastic base shear histories for the moderate and severe shaking motions. The peak base shears from these elastic analyses are identified as 44.6 kips (54.1% of the total structural weight W) and 78.0 kips (94.5% W), respectively. From the inelastic analyses in Section 4.6.1.2, the analytical base shear demands were identified as 21.0 kips (25.5% W), and 20.9 kips (25.3% W), respectively. This corresponds to an equivalent strength ratio (reduction from the elastic force level to the inelastic strength level) of 2.12 and 3.73, respectively. This equivalent strength ratio is compared to the ductility based reduction factor (R_μ) in the discussions concerning UBC (1991). Refer to Bracci et al. (1992b) for more details.

According to the provisions in UBC (1991) for an intermediate moment resisting R/C frame (since the model was retrofitted), the total strength reduction factor (R_w) is 7. For the retrofitted model building, a dynamic amplification factor (overstrength reduction factor, Ω) of 1.3 and an allowable stress factor (Y) of 1.4 are used. Therefore the corresponding ductility based reduction factor (R_μ) according to UBC (1991) is 3.85 ($R_\mu = R_w/\Omega Y$).

Table 4-10 summarizes the equivalent strength ratios for the original and retrofitted models both analytically and from UBC (1991) along with the corresponding structural damage indices, displacement ductility ratios, and the base shear demands and capacities computed analytically. It can be observed that comparable ratios to UBC reduction factors result when the base shear approaches ultimate load for the severe shaking and deviations occur under the minor and moderate shaking. This variation occurs since UBC (1991) specifies only one design earthquake for the ultimate limit state. The lower equivalent ratios for moderate motions are associated also with lower damage states. The retrofit reduces the damage levels as compared with the unretrofitted structure although larger strength ratios are obtained. The ductility demand (first story displacement ductility) for the retrofitted model is greater than for the original model since the retrofit provided additional stiffness. However note that the first story ductility capacity

of the retrofitted model far exceeds the ductility capacity of the original model. The base shear demands reach the analytical capacities during the moderate and severe shaking for both the retrofitted and unretrofitted models.

TABLE 4-10 Equivalent Strength Ratio (R)

			Minor (0.05 g)	Moderate (0.20 g)	Severe (0.30 g)
Analytical (Original Bldg.)	[1] Equivalent Strength Ratio *R*		1.15	1.89	2.77
	Structural Damage Index		0.04	0.23	0.49
	Ductility Demand		0.45[4]	1.38	1.96
	Inelastic Base Shear (% of Structural Weight)	Demand (Capacity)	8.8% (15.0%)	14.7% (15.0%)	14.6% (15.0%)
Code	[2] UBC (1991) - Ductility Reduction Factor, R_μ		2.75	2.75	2.75
Analytical (Retrofitted Bldg.)	Equivalent Strength Ratio *R*			2.12	3.73
	Structural Damage Index			0.14	0.32
	Ductility Demand			2.19	3.44
	Inelastic Base Shear (% of Structural Weight)	Demand (Capacity)		25.5% (25.5%)	25.3% (25.5%)
Code	[3] UBC (1991) - Ductility Reduction Factor, R_μ			3.85	3.85

[1] Equivalent strength ratio computed from the ratio of the analytical elastic and inelastic base shears.

[2] Ordinary Moment Resisting Concrete Frame: $R_w = 5$, $\Omega = 1.3$, and $Y = 1.4$.

[3] Intermediate Moment Resisting Concrete Frame: $R_w = 7$, $\Omega = 1.3$, and $Y = 1.4$.

[4] Ductility under 1.0 indicate elastic behavior.

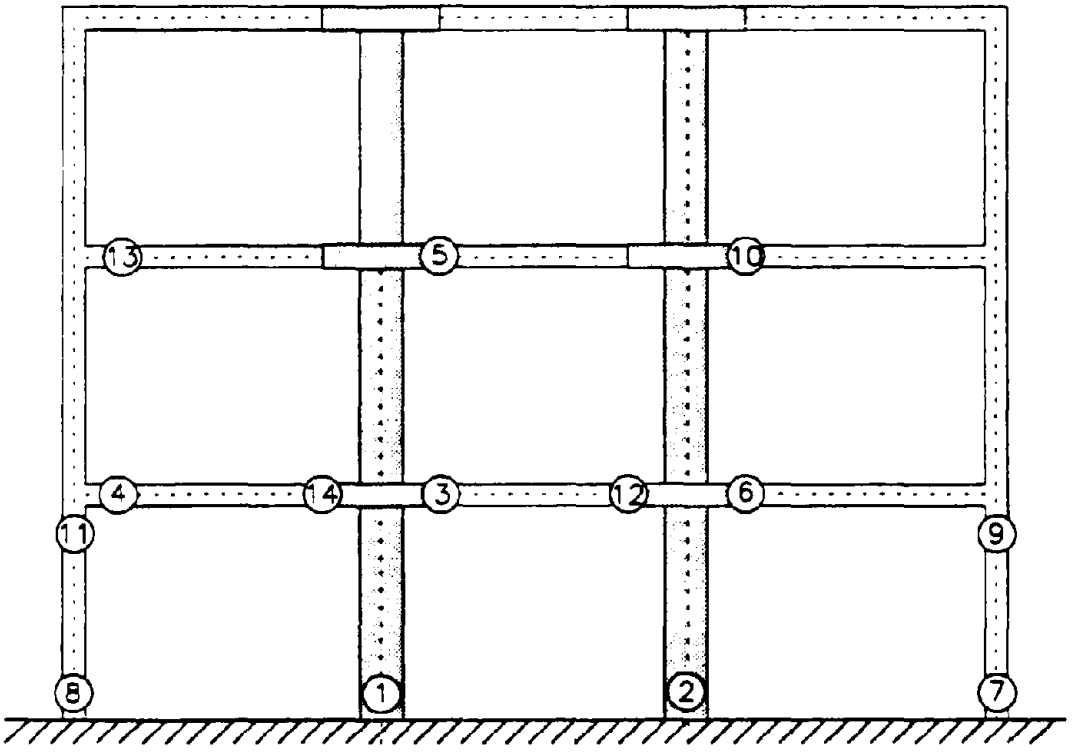

(#) – Signifies sequence of yielding

FIG. 4-37 Collapse Mode (Shakedown) Analysis

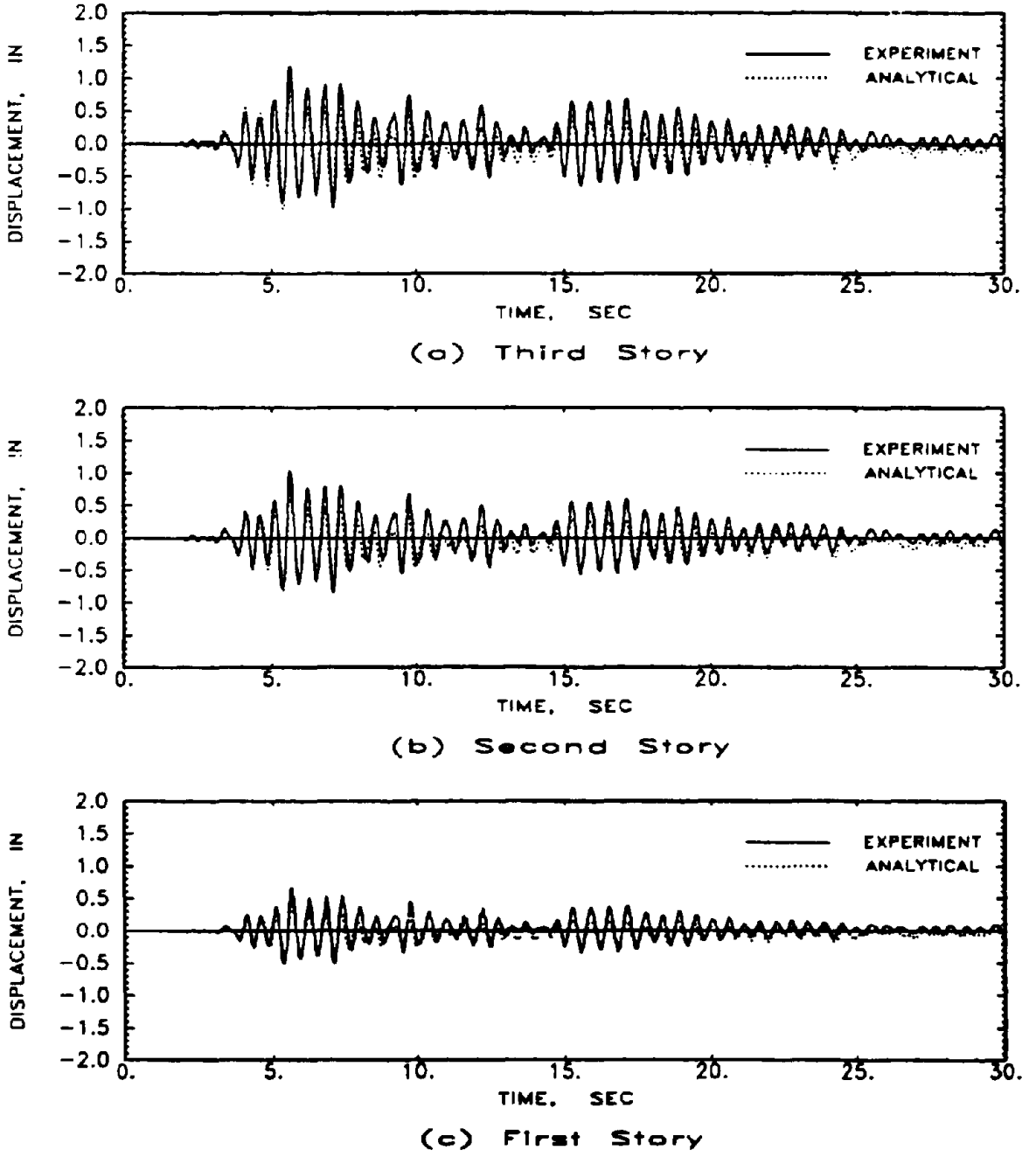

FIG. 4-38a Displacement Comparisons for Moderate Shaking - Component Tests

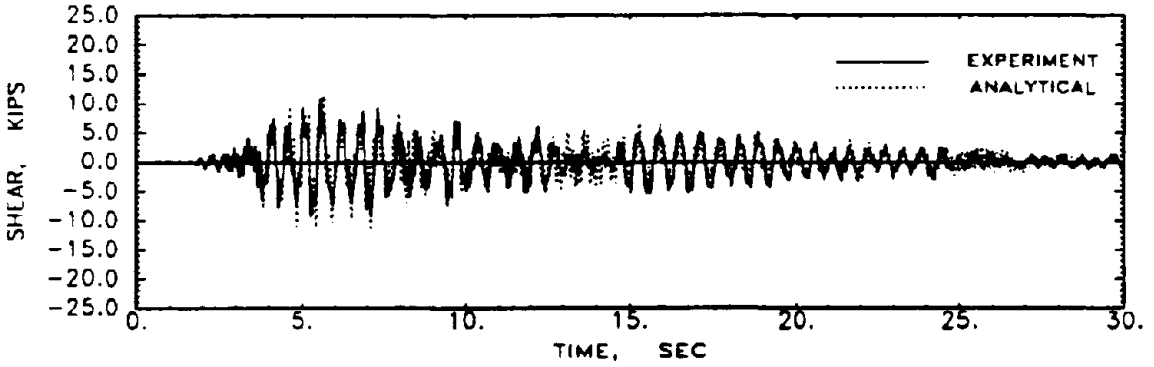

(a) Third Story

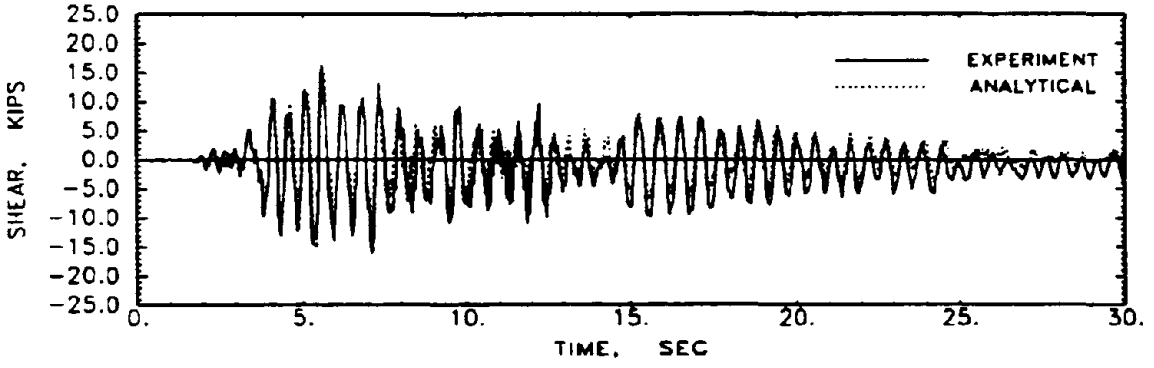

(b) Second Story

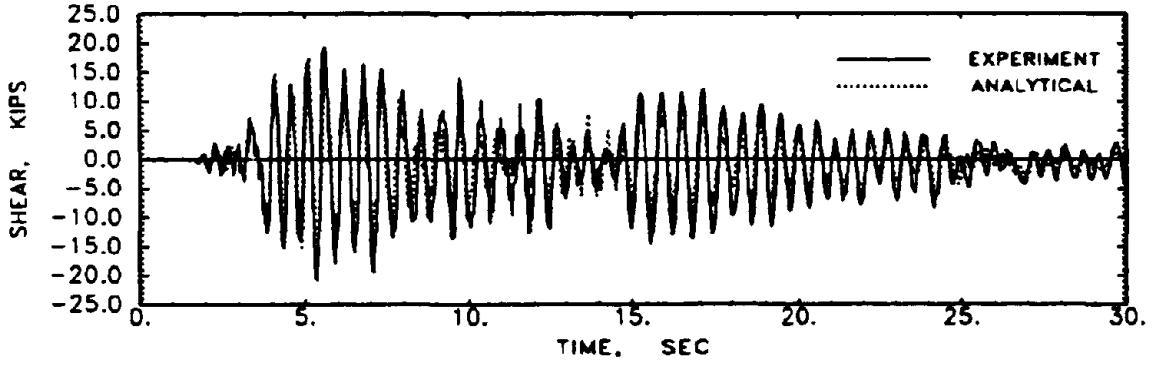

(c) First Story

FIG. 4-38b Shear Force Comparisons for Moderate Shaking - Component Tests

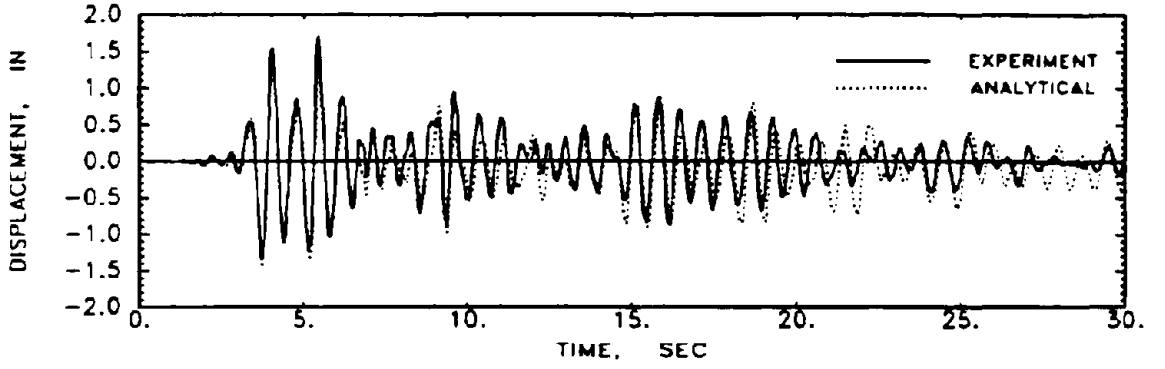

(a) Third Story

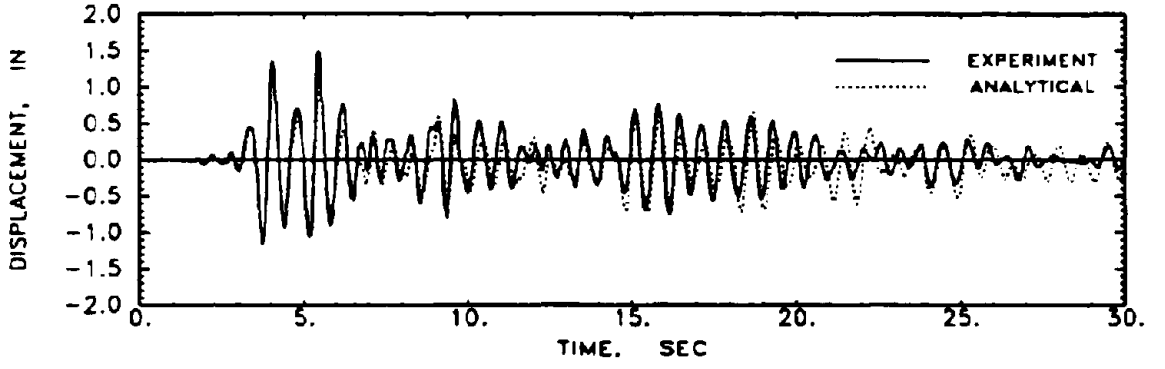

(b) Second Story

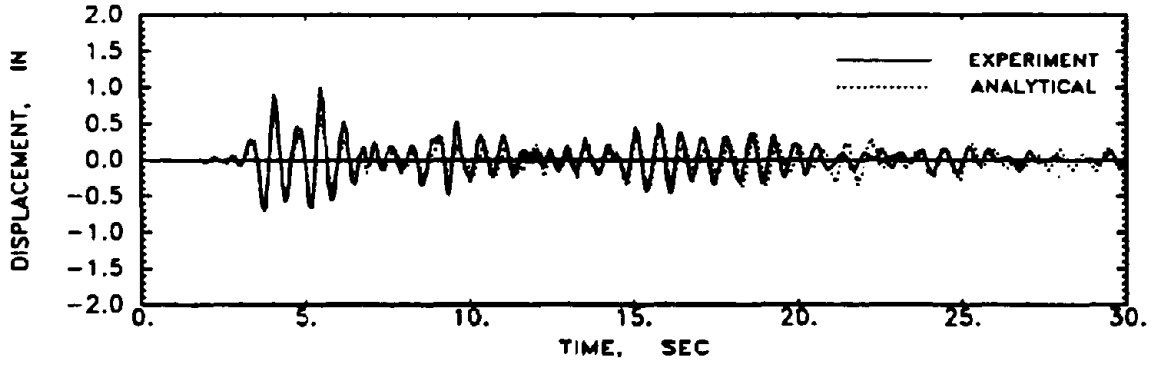

(c) First Story

FIG. 4-39a Displacement Comparisons for Severe Shaking - Component Tests

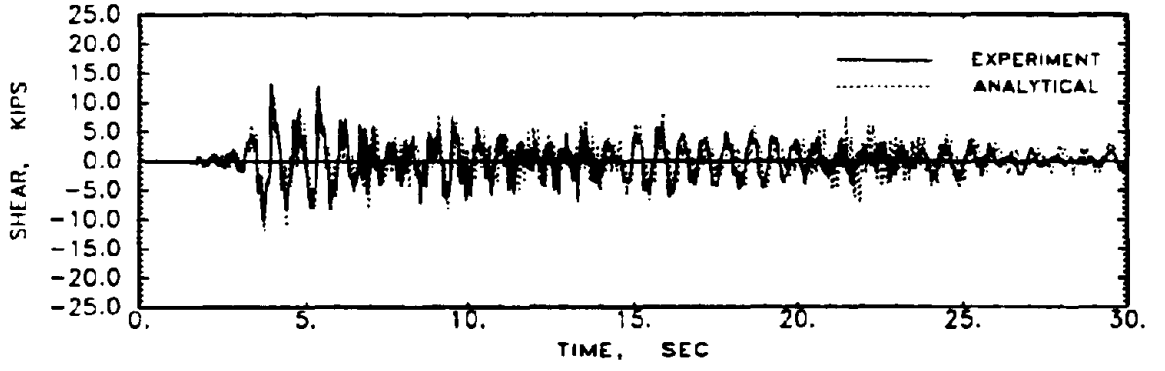

(a) Third Story

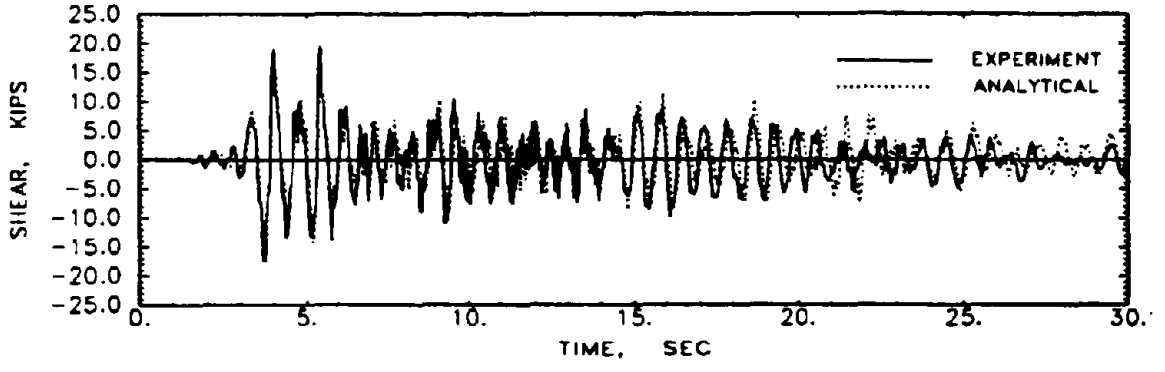

(b) Second Story

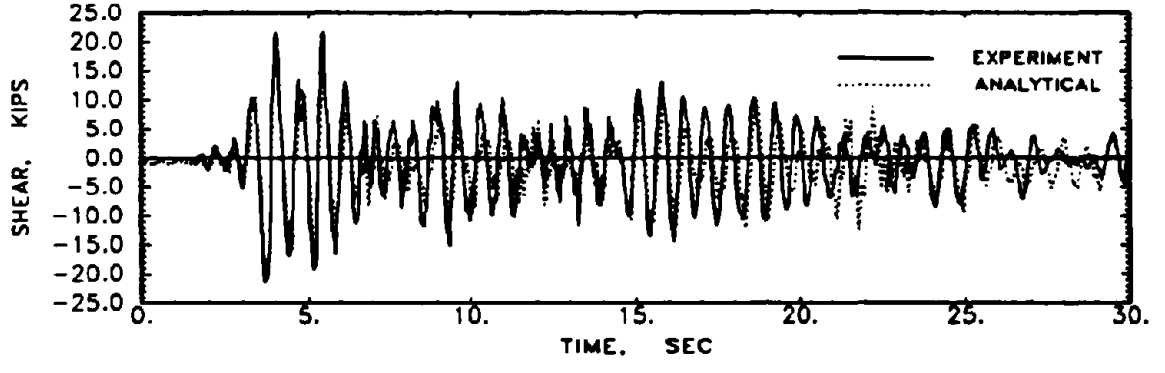

(c) First Story

FIG. 4-39b Shear Force Comparisons for Severe Shaking - Component Tests

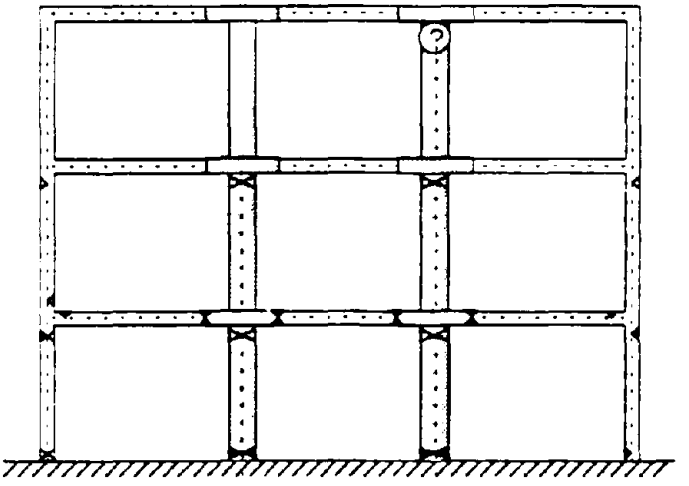

(a) Experimental

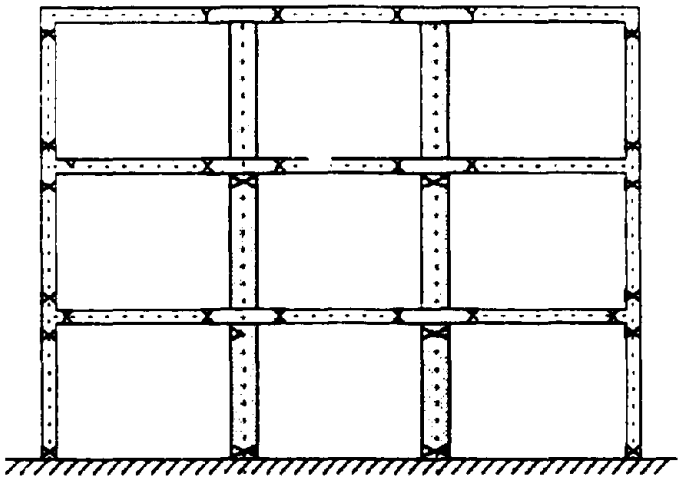

(b) Analytical

▷ Cracked
▶ Yielded

? NOTE: 2nd story beams and above were not quantitatively observed

FIG. 4-40a Comparison of Damage State after Moderate Shaking

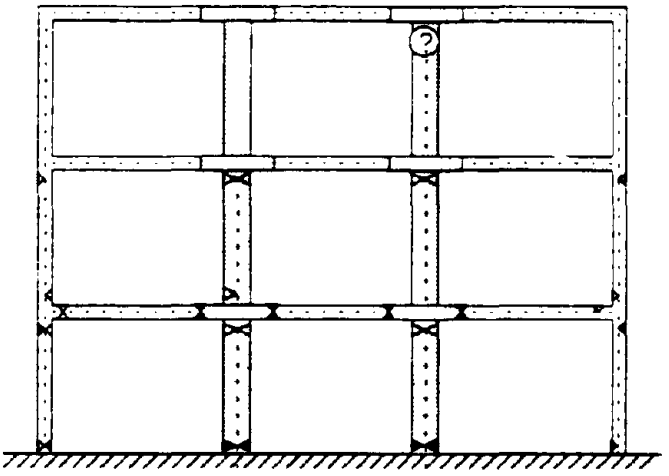

(a) Experimental

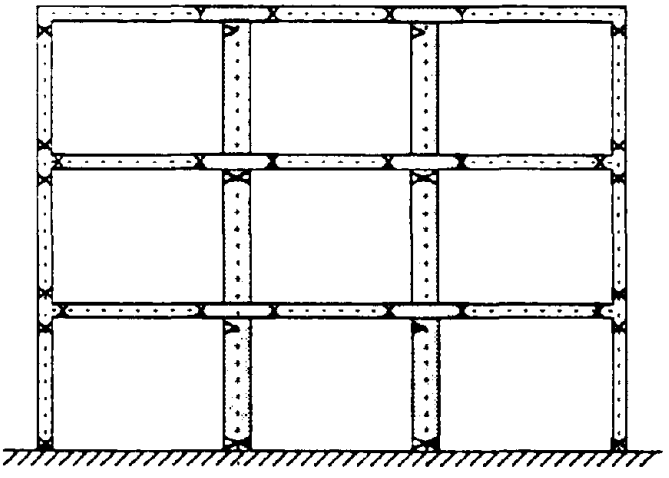

(b) Analytical

▷ Cracked
▶ Yielded

? NOTE: 2nd story beams and above were not quantitatively observed

FIG. 4-40b Comparison of Damage State after Severe Shaking

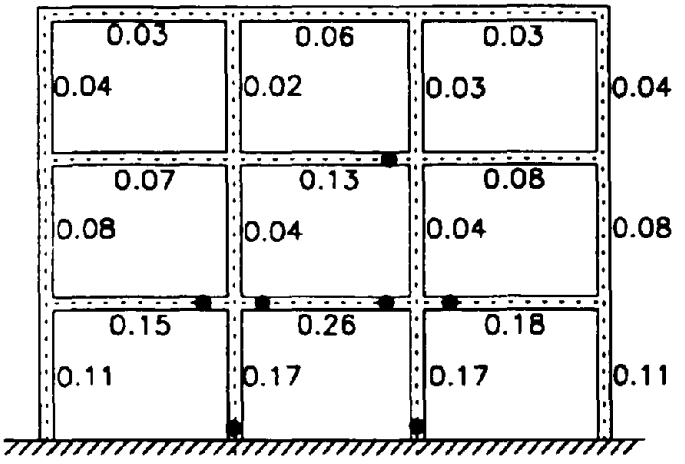

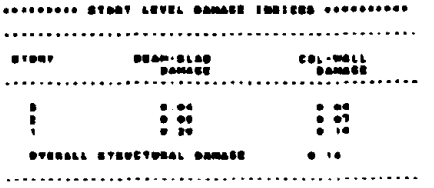

(a) Moderate Shaking

● Signifies Yielding

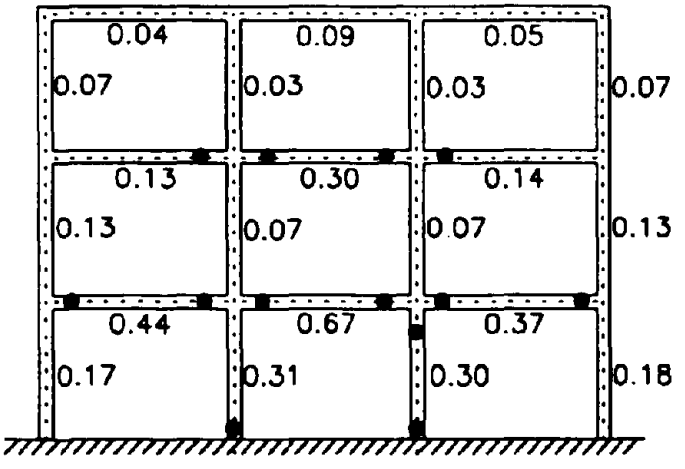

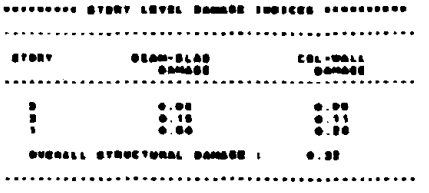

(b) Severe Shaking

FIG. 4-41 Damage Quantifications of the Retrofitted Model

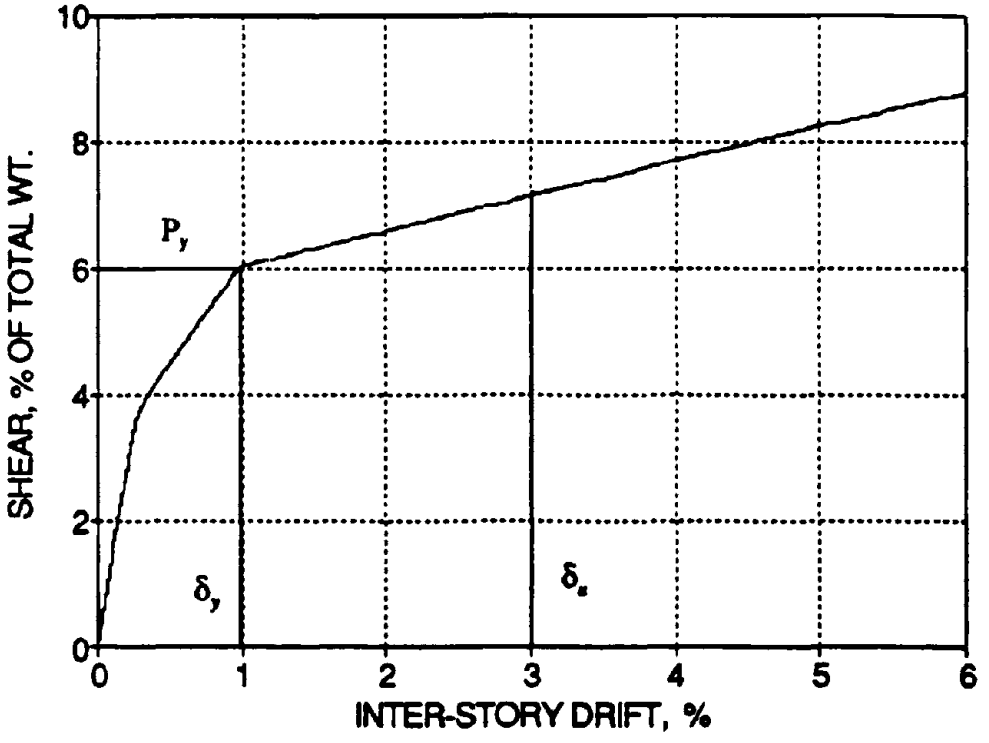

FIG. 4-42 Static Monotonic Analysis of the Model

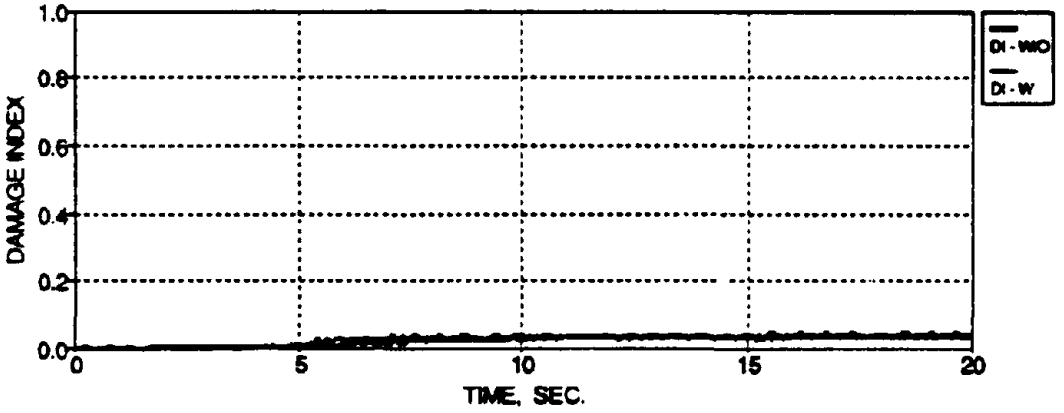

(a) Time History

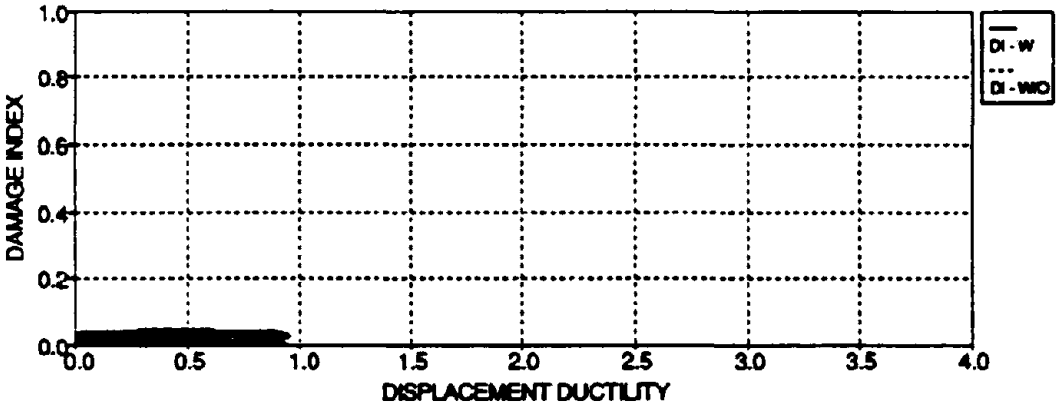

(b) Displacement Ductility History

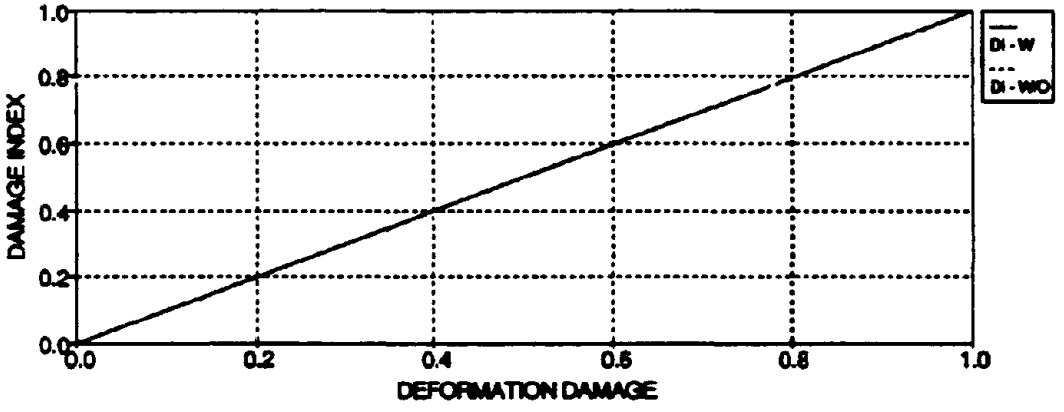

(c) Deformation Damage History

FIG. 4-43a Damage Index History - First Story Retrofitted Interior Column - PGA 0.20 g

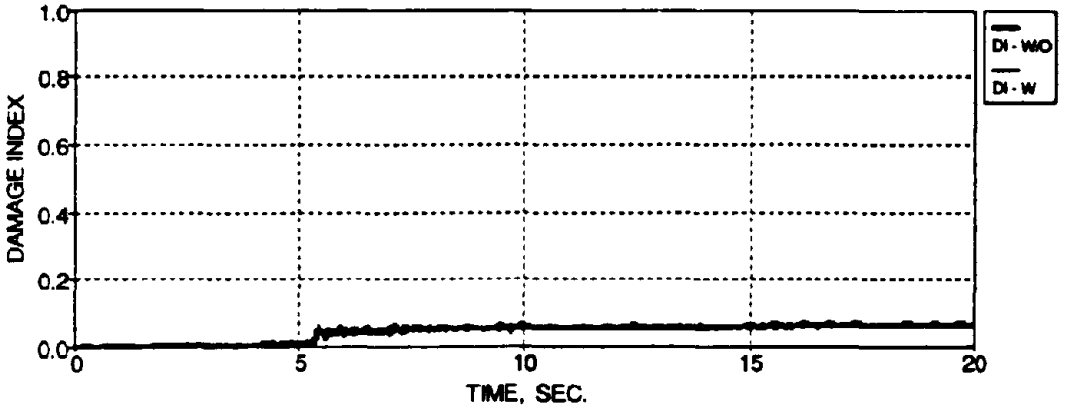

(a) Time History

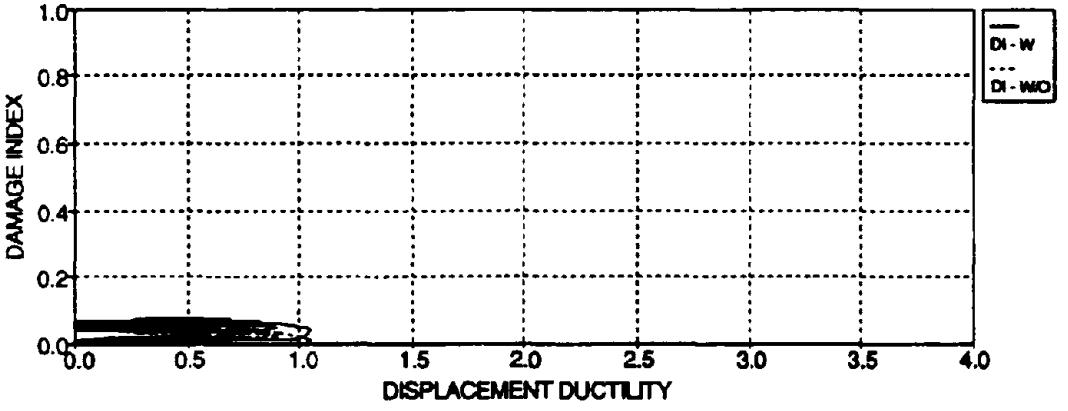

(b) Displacement Ductility History

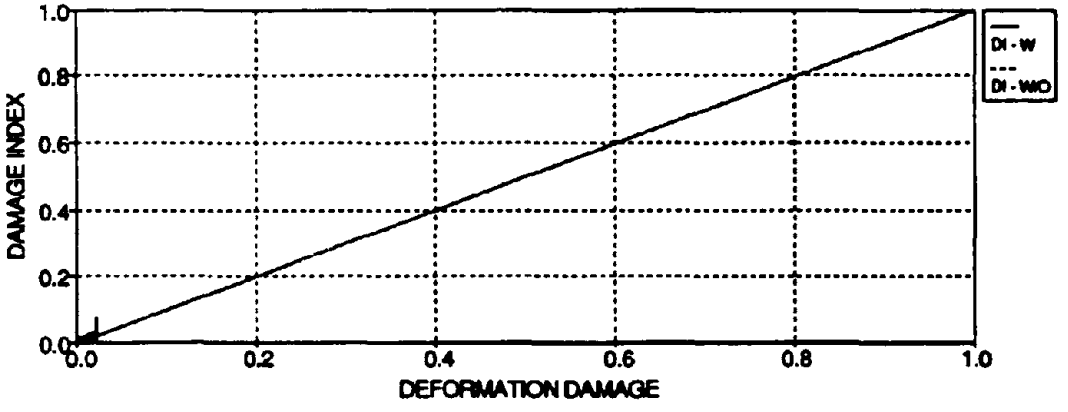

(c) Deformation Damage History

FIG. 4-43b Damage Index History - First Story Retrofitted Interior Column - PGA 0.25 g

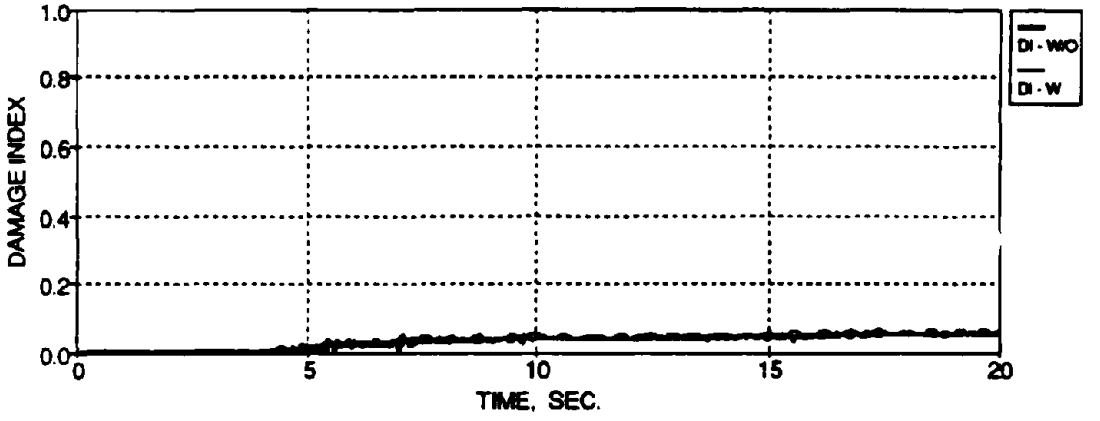

(a) Time History

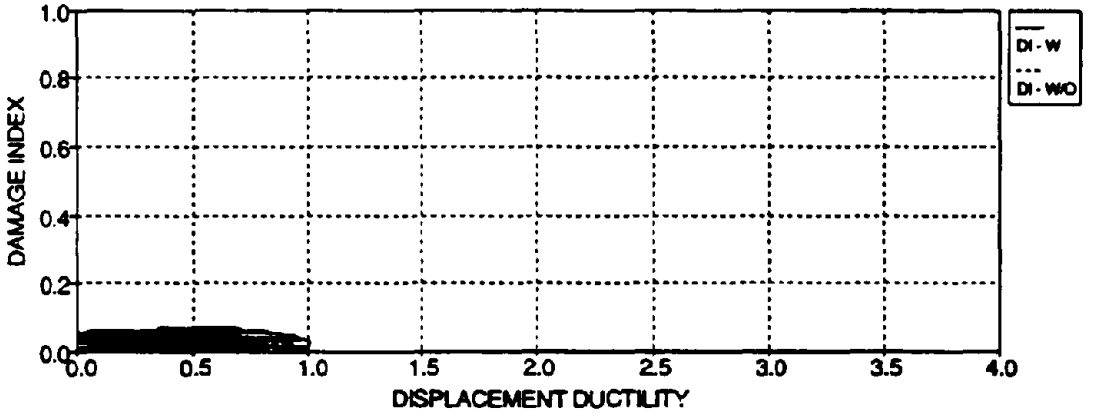

(b) Displacement Ductility History

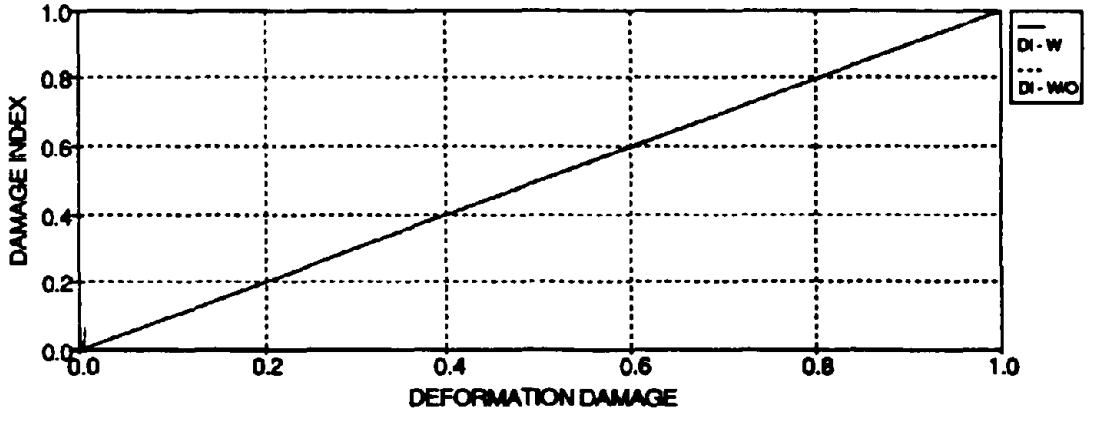

(c) Deformation Damage History

FIG. 4-43c Damage Index History - First Story Retrofitted Interior Column - PGA 0.30 g

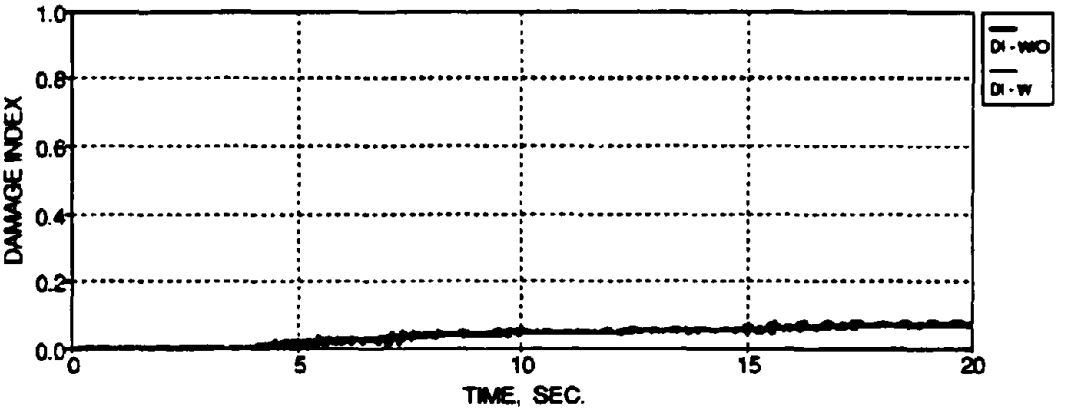

(a) Time History

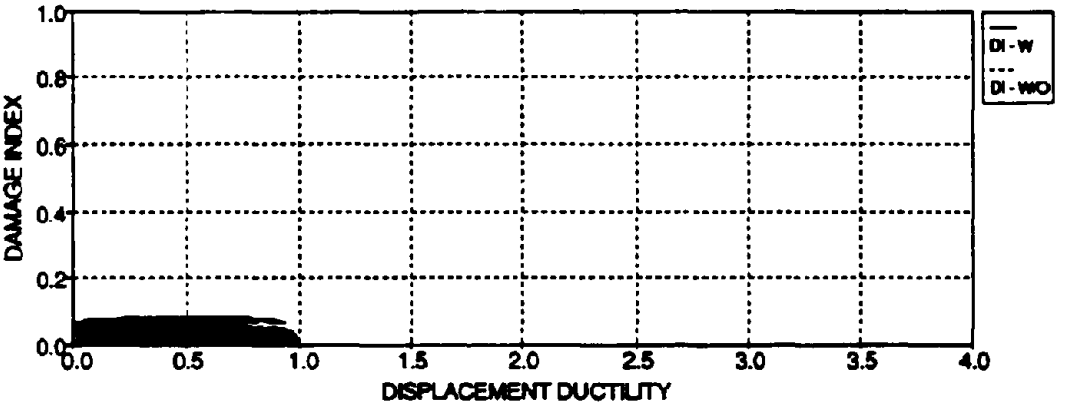

(b) Displacement Ductility History

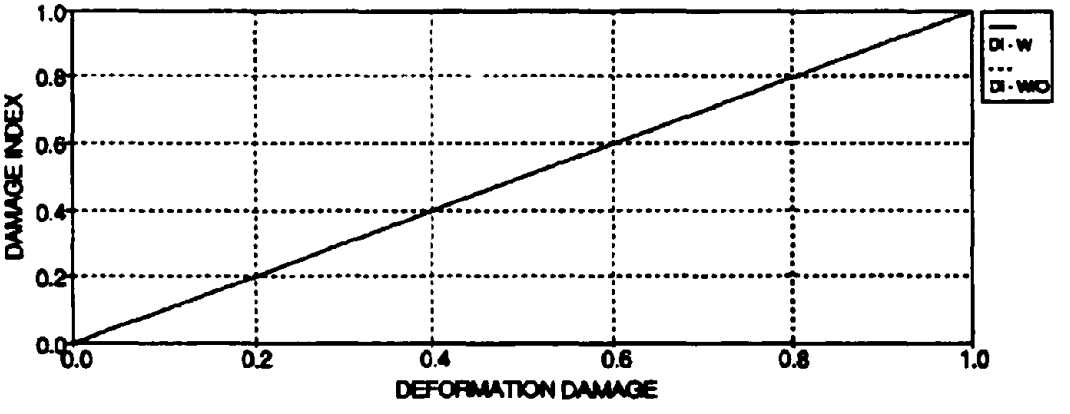

(c) Deformation Damage History

FIG. 4-43d Damage Index History - First Story Retrofitted Interior Column - PGA 0.35 g

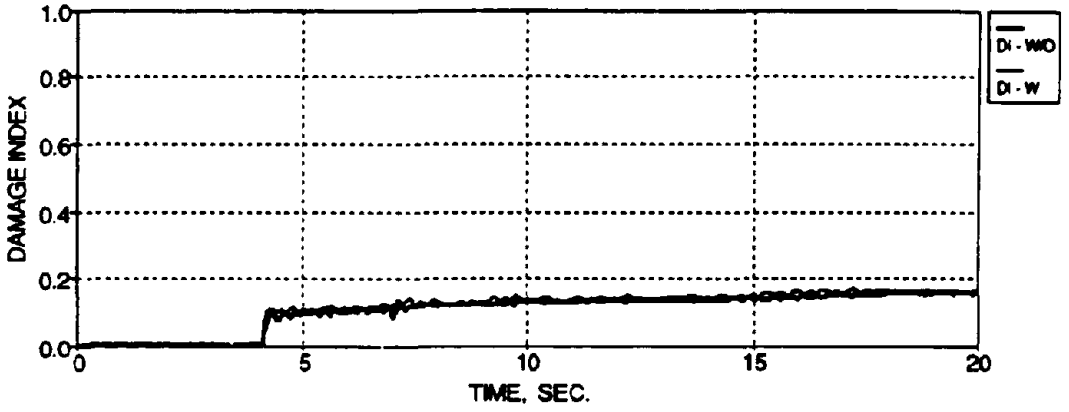

(a) Time History

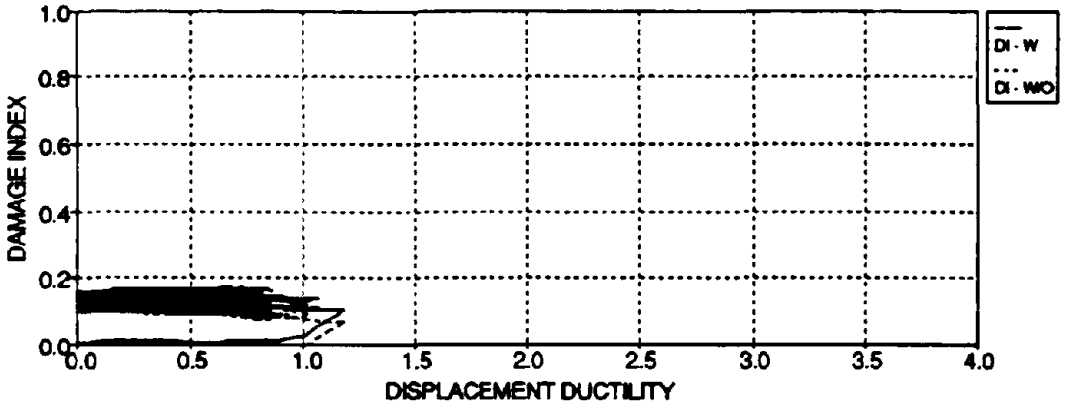

(b) Displacement Ductility History

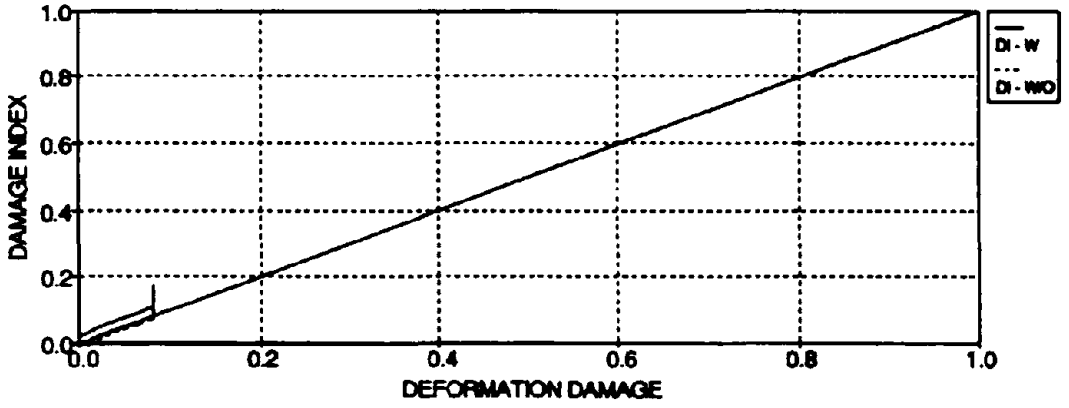

(c) Deformation Damage History

FIG. 4-43e Damage Index History - First Story Retrofitted Interior Column - PGA 0.40 g

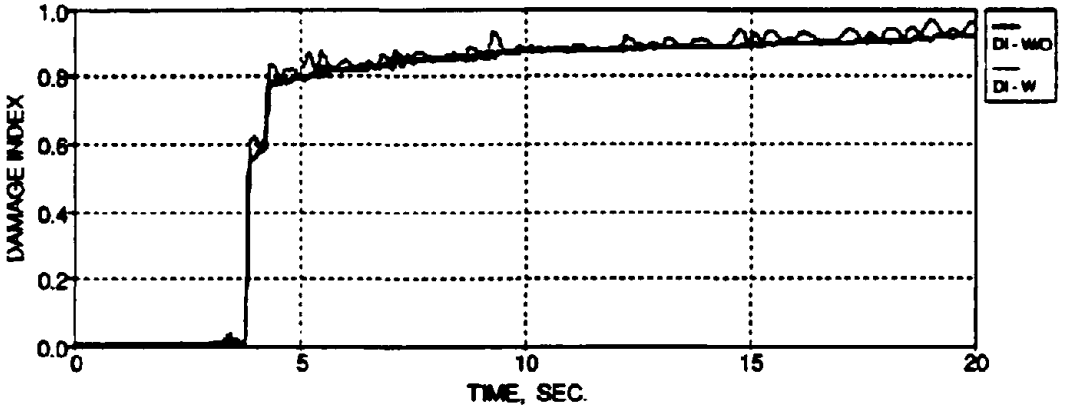

(a) Time History

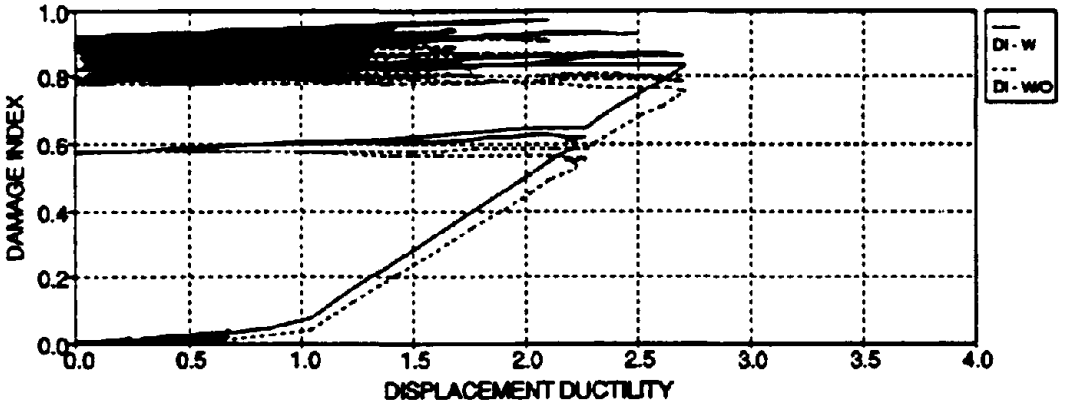

(b) Displacement Ductility History

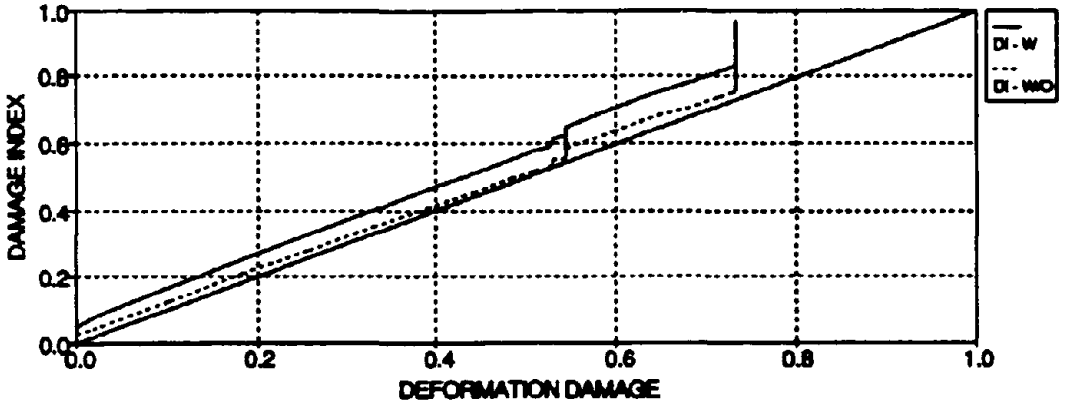

(c) Deformation Damage History

FIG. 4-43f Damage Index History - First Story Retrofitted Interior Column - PGA 0.70 g

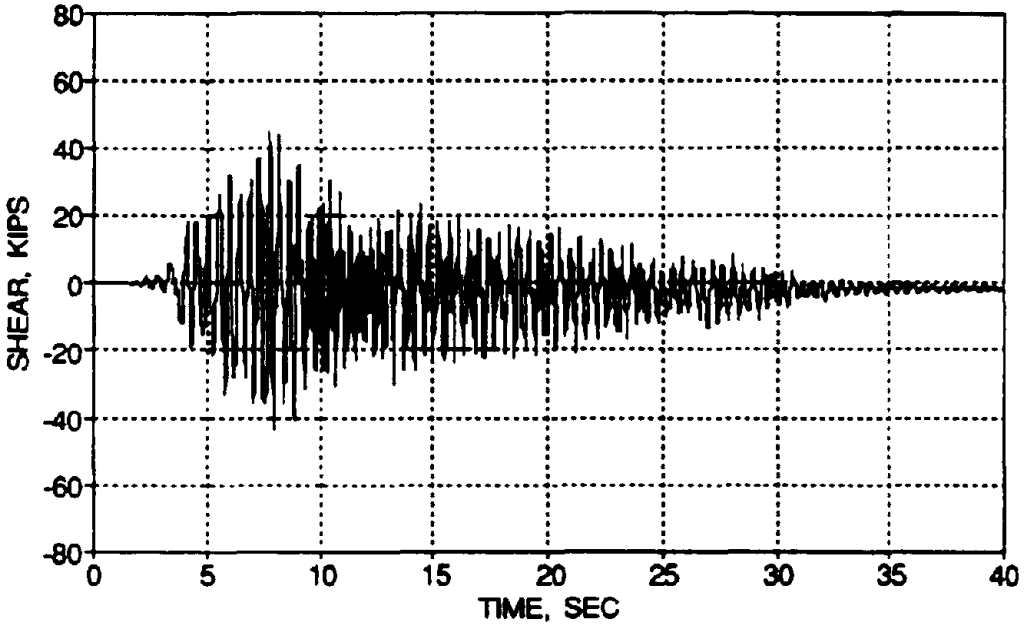

(a) Moderate Shaking

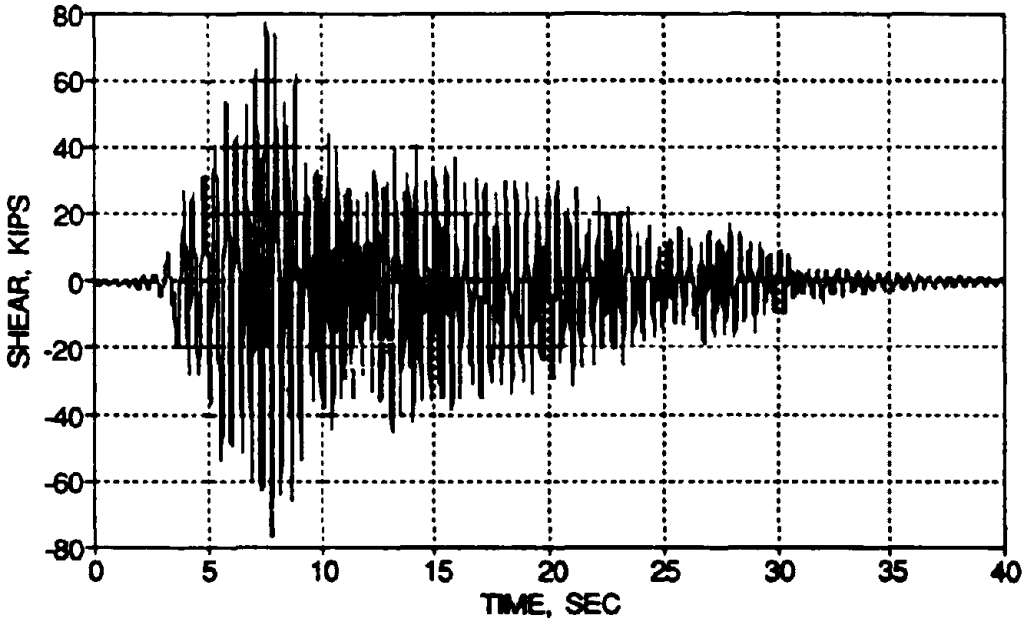

(b) Severe Shaking

FIG. 4-44 Elastic Base Shear Response - Retrofitted Model

4.7 Summary Discussions

The local and global response of the retrofitted model from the moderate and severe simulated earthquakes (Taft N21E, PGA 0.20 g and 0.30 g, respectively) are presented in this section. The following summarize the maximum response of the retrofitted model during the earthquake tests, the dynamic characteristic history throughout the testing, and the resulting conclusions.

4.7.1 Maximum Story Response of Retrofitted Model

The maximum response of the retrofitted R/C frame model for the moderate and severe shaking table motions are presented in a Table 4-11 for comparison.

TABLE 4-11 Maximum Response for the Retrofitted Model

Test	Story	Max. Story Displacement (in.)	Max. Inter-Story Drift (%)	Max. Story Shear (kips)	Peak Story Acceleration (g)
Taft N21E	Third	**1.18**	0.33	10.7	0.38
PGA 0.20 g	Second	1.03	0.80	16.2	0.33
(TFTR_20)	First	0.66	**1.37**	20.6 (25.0%)	0.26
Taft N21E	Third	**1.73**	0.49	13.2	0.47
PGA 0.30 g	Second	1.50	1.19	19.5	0.38
TFTR_30	First	1.02	**2.13**	21.8 (26.4%)	0.31

It can be observed that: (i) large story drifts occur on the first story (1.37% and 2.13% of the story height, respectively for the moderate and severe shaking). The maximum drifts on the second and third stories are smaller. The increase in drift is almost proportional to the level of excitation; (ii) the top story displacement for the moderate and severe shaking is 1.18 in. and 1.73 in., respectively. This corresponds to displacements in the prototype building of 3.54 in. and 5.19 in.; (iii) the measured base shear is 25.0% of the total weight for the moderate shaking (PGA 0.20 g) and increases slightly to 26.4% for the severe shaking (PGA 0.30 g). From a shakedown analysis, the analytical base shear capacity is 25.5% of the total structural weight. Therefore the base shear capacity is slightly underpredicted by the analytical modeling developed from component tests. Based on an elastic analysis, the corresponding equivalent

strength ratios of elastic to inelastic base shear demands are 2.12 and 3.73, respectively. According to UBC (1991), the ductility reduction factor is 3.85 ($R_w = 7$, $\Omega = 1.3$, and $Y = 1.4$) ; (iv) the peak story accelerations show amplifications for the moderate and severe shaking, except for the first story of the severe shaking (no amplification).

4.7.2 Summary of Dynamic Characteristics of Retrofitted Model

The natural frequencies, modal shapes, stiffness matrix, and damping characteristics of the retrofitted model throughout the shaking testing program are summarized in Table 4-12.

Table 4-12 Dynamic Characteristic History of the Retrofitted Model

Test	Frequency	Modal Shapes	Stiffness Matrix	Story Stiffnesses	Equivalent Viscous Damping
	f_i (Hz.)	Φ_{ij}	K_{ij} (kip/in)	k_i (kip/in)	ξ_m (%)
WHNR_B	$\begin{pmatrix} 2.78 \\ 9.38 \\ 16.75 \end{pmatrix}$	$\begin{pmatrix} 1.00 & -0.86 & -0.51 \\ 0.79 & 0.48 & 1.00 \\ 0.42 & 1.00 & -0.89 \end{pmatrix}$	$\begin{pmatrix} 205.2 & -238.6 & 71.6 \\ -238.6 & 421.4 & -278.2 \\ 71.6 & -278.2 & 432.7 \end{pmatrix}$	$\begin{pmatrix} 238.6 \\ 278.2 \\ 154.5 \end{pmatrix}$	$\begin{pmatrix} 3.0 \\ 1.9 \\ 1.3 \end{pmatrix}$
WHNR_C	$\begin{pmatrix} 2.64 \\ 9.18 \\ 16.70 \end{pmatrix}$	$\begin{pmatrix} 1.00 & -0.86 & -0.49 \\ 0.79 & 0.45 & 1.00 \\ 0.44 & 1.00 & -0.83 \end{pmatrix}$	$\begin{pmatrix} 198.9 & -238.2 & 65.2 \\ -238.2 & 438.5 & -279.1 \\ 65.2 & -279.1 & 404.6 \end{pmatrix}$	$\begin{pmatrix} 238.2 \\ 279.1 \\ 125.5 \end{pmatrix}$	$\begin{pmatrix} 4.7 \\ 1.8 \\ 1.6 \end{pmatrix}$
Taft N21E PGA 0.20 g					
WHNR_D (East)	$\begin{pmatrix} 1.98 \\ 8.11 \\ 15.33 \end{pmatrix}$	$\begin{pmatrix} 1.00 & -0.86 & -0.56 \\ 0.82 & 0.42 & 1.00 \\ 0.46 & 1.00 & -0.81 \end{pmatrix}$	$\begin{pmatrix} 182.7 & -218.2 & 71.9 \\ -218.2 & 356.9 & -229.3 \\ 71.9 & -229.3 & 318.3 \end{pmatrix}$	$\begin{pmatrix} 218.2 \\ 229.3 \\ 89.0 \end{pmatrix}$	$\begin{pmatrix} 6.6 \\ 2.6 \\ 1.4 \end{pmatrix}$
WHNR_D (West)	$\begin{pmatrix} 1.93 \\ 7.98 \\ 15.48 \end{pmatrix}$	$\begin{pmatrix} 1.00 & -0.88 & -0.59 \\ 0.82 & 0.38 & 1.00 \\ 0.48 & 1.00 & -0.80 \end{pmatrix}$	$\begin{pmatrix} 196.0 & -226.9 & 80.6 \\ -226.9 & 356.5 & -233.8 \\ 80.6 & -233.8 & 311.9 \end{pmatrix}$	$\begin{pmatrix} 226.9 \\ 233.8 \\ 78.1 \end{pmatrix}$	$\begin{pmatrix} 8.1 \\ 2.8 \\ 0.8 \end{pmatrix}$
Taft N21E PGA 0.30 g					
WHNR_E (East)	$\begin{pmatrix} 1.88 \\ 7.50 \\ 14.84 \end{pmatrix}$	$\begin{pmatrix} 1.00 & -0.83 & -0.56 \\ 0.82 & 0.36 & 1.00 \\ 0.45 & 1.00 & -0.76 \end{pmatrix}$	$\begin{pmatrix} 168.1 & -205.3 & 69.6 \\ -205.3 & 342.7 & -215.8 \\ 69.6 & -215.8 & 277.5 \end{pmatrix}$	$\begin{pmatrix} 205.3 \\ 215.8 \\ 61.7 \end{pmatrix}$	$\begin{pmatrix} 5.5 \\ 1.9 \\ 1.5 \end{pmatrix}$
WHNR_E (West)	$\begin{pmatrix} 1.73 \\ 7.50 \\ 14.84 \end{pmatrix}$	$\begin{pmatrix} 1.00 & -0.84 & -0.55 \\ 0.83 & 0.36 & 1.00 \\ 0.49 & 1.00 & -0.76 \end{pmatrix}$	$\begin{pmatrix} 165.0 & -203.8 & 67.5 \\ -203.8 & 344.0 & -217.8 \\ 67.5 & -217.8 & 277.8 \end{pmatrix}$	$\begin{pmatrix} 203.8 \\ 217.8 \\ 60.0 \end{pmatrix}$	$\begin{pmatrix} 6.7 \\ 1.9 \\ 1.2 \end{pmatrix}$

It can be observed that: (i) a minor reduction in the first mode natural frequency occurs after white noise WHNR_C (5.0%), a larger reduction in first mode natural frequency occurs after the moderate shaking (28.8%), and only a slight additional reduction after the severe shaking (5.1%). The frequency reductions for the second and third modes are considerable smaller; (ii) large story stiffness reductions occur primarily on the first story after the moderate and severe shaking (total reduction of 61.2%). Small stiffness reductions occur on the second and third floors; (iii) the change in first mode natural frequency is approximately proportional to the square root of the ratio of first story stiffnesses; (iv) the mode shapes vary slightly after the moderate and severe shaking; (v) the equivalent viscous damping factor for the first mode increases by 56.6% from white noise WHNR_C (reduction based only on the white noise excitation). After the moderate shaking, the damping factors for the east and west frames approximately double. This increased equivalent damping is due to inelastic contributions from hysteretic (non-linear) behavior. After the severe shaking, the damping factors actually decrease. However this variation is primarily due to numerical errors and smoothing.

4.7.3 Concluding Remarks on Testing of Retrofitted Model

The following are the overall results, conclusions, and remarks from the shaking table testing of the retrofitted R/C frame model:

(a) Inter-Story Drifts

It was previously mentioned that the maximum first story drifts of the model for the moderate (0.2 g) and severe (0.3 g) earthquakes are 1.37% and 2.13% of the story heights, respectively. For comparison with the unretrofitted (original) model, the maximum first story drifts were 1.33% and 2.03%, respectively for the moderate and severe motions. Therefore the first story drift maxima of the retrofitted model are similar to those from the original model. However the second and third floor drifts are considerably smaller and within recommended limits. For the severe base motion, the first story drift exceeds the recommended limits of NEHRP (1991) and UBC (1991). Therefore the suggested retrofit method provided limited control of the first story drifts. From Table 2-1, the analytical evaluation of the retrofitted model using the suggested concrete jacketing (based on approximate structural parameters) predicted only a maximum first story drift of 1.24% for a severe shaking (0.30 g). The variations in predicted story drifts results from inaccurate member properties initially selected in the evaluation. However the analytical modeling, developed from component testing by Choudhuri et al. in Part I of the

Retrofit Report Series (1992) and Aycardi et al. in Part II of the Evaluation Report Series (1992), predicts story response that are similar to the measured experimental response. The variation in the structural parameters between the two analytical modeling types are: (i) a softer initial stiffness in the beams of the component test model; (ii) a slightly softer initial column stiffness in the retrofitted (prestressed) columns of the component test model; and (iii) slight variations of member hysteretic parameters.

But even with the relatively high first story drifts, the model was in no danger of collapse since the base columns have adequate ductility capacity from the added transverse reinforcement and the beams have greater hinge rotation capacities from the large quantities of slab steel. Furthermore, the full collapse mechanism did not developed in the earthquake tests.

(b) Damage to Beam-Column Joints

The retrofitted beam-column joints with the reinforced fillet remained primarily elastic during the shaking as the design mandated. In the unretrofitted exterior joints, the resulting damage was also minimal since the interior columns absorbed most of the seismic forces.

(c) Beam and Column Damage

It was observed that the interior beams cracked and yielded near the ends of the fillets from the earthquake motions (with visual cracks appearing). Large positive and negative moments (reaching capacity) were recorded in the interior beams of the first floor from the shaking. Since pull-out of the discontinuous beam reinforcement was prevented with the retrofit, the full positive moment capacity was achieved. The slab steel from the full bay width dramatically contributes to the flexural strength of the beams. The moment demands in the exterior beams remained primarily elastic with only some slight additional cracking. However for the columns, the only substantial damage occurred in the base columns. The remainder of the columns remained primarily undamaged. Therefore with the suggested concrete jacketing retrofit of the interior columns, hinges developed in the beam members at the ends of the fillets, primarily on the first floor, and at the base columns.

(d) Damage Evaluation

From the damage evaluations of the retrofitted model building, it can be concluded that: (i) the first story beams develop a considerable amount damage from the moderate and severe shaking (*moderate* damage state). For the shaking of the original model, the only significant beam damage was in the first story exterior beam in the pull-out (windward) direction; (ii) the retrofitted interior and unretrofitted exterior base columns develop only *minor* damage from the earthquakes, while the remaining columns develop negligible damage. For the shaking of the original model, *severe* damage was inflicted to the interior columns and *moderate* damage to the exterior columns of the first and second floors; (iii) the resulting damage distribution of the retrofitted model was typical of strong column - weak beam behavior (beam-sidesway mechanism). In contrast with the original building where a column-sidesway (or soft-story) mechanism was evident; and (iv) a significant decrease in overall structural damage index results for retrofitted model after the moderate and severe shaking in comparison with the original model.

(e) Apparent Collapse Mechanism

ACI-318 specifies that the design column strengths should be greater than 20% of the beam strengths to ensure a strong column - weak beam behavior. Note that a dramatic increase in moment capacity results in the beams which consider slab steel contributions from the full slab width. For a typical beam-slab-column component, the nominal moment capacity of the retrofitted columns were about 55% stronger than the nominal capacity of the beams with slab steel contributions from the full slab width. Thus a strong column - weak beam behavior exists. For the shaking tests, hinging in the base columns of the first story and hinging in the interior beams were measured. Thus as the retrofit design stipulates, a desirable beam-sidesway mechanism (refer to Fig. 4-40) was apparently in development for the model. It should also be noted that this behavior was achieved by strengthening only the interior columns.

(f) "Second Mode" Effect

Second mode contributions were observed in the original (unretrofitted) model. However for the retrofitted model, only first mode contributions occur during the moderate and severe base motions. Intentionally, the base columns were designed to have a smaller moment capacity

than the rest of the columns and the columns were designed stronger than the beams. Therefore the retrofitted columns remain relatively rigid throughout the height of the building and rotate about the weak base, rather than deflecting as a flexural element between floors.

(g) Story Stiffness and Natural Frequency Deteriorations

Due to the large resulting damage in the base columns and first story beams, first story stiffness (60.5%) and natural frequency deteriorations (35.3%) have occurred (see Table 4-12). However only slight stiffness deterioration have resulted in the upper stories. The second and third story columns and beams remain primarily within yielding bounds throughout the testing. Therefore only first mode behavior was observed and corresponding first story stiffness and first mode natural frequency deteriorations occur.

(h) Story Shear Force Demands

It can be observed from Table 4-11 that the base shear force demands were 25.0% and 26.4% of the total structural weight for the moderate and severe base motions, respectively. This increase in demand implies that the base shear capacity has not been attained during the moderate base motion. However from a shakedown analysis with analytical modeling based on component tests, the base shear capacity at 2% drift limits was 25.5% of the total structural weight. Also note the story shear force demands were relatively proportional to the first mode of vibration. In comparison with the original model, the base shear coefficients were 15.2% and 15.3% for the moderate and severe motions, respectively. Therefore a large increase in base shear demand and also capacity has developed after retrofit. From an elastic analysis, the corresponding base shear force reductions (ductility reduction factors) were determined to be 2.12 and 3.73 for the moderate and severe shaking, respectively. These reductions were the result of inelastic member behavior. UBC (1991) specifies a strength reduction factor for such a structure (R_w = 7) to account for the inelastic behavior for the design base shear. The corresponding ductility reduction factor was 3.85 (see Section 4.6.4). Therefore for the retrofit model during the severe earthquake, the measured strength reductions were similar to the UBC (1991).

(i) Presence of Torsion

It was shown that torsion developed in the model during the moderate shaking due to the uneven distribution of damage between bays and exacerbated by uncompensated table-structure interaction. Some of the various reasons are the following: (i) the retrofit strength of the frames may have been unsymmetrical, possibly due to varying concrete strengths or applied prestressing force; (ii) the moment capacities of the beams may have varied due to placement (location) of the longitudinal and slab steel reinforcements during construction.

SECTION 5

CONCLUDING REMARKS

5.1 Remarks on Testing of Retrofitted Model

5.1.1 Retrofit Design

For typical low-rise and for upper stories of higher-rise GLD R/C frame structures, the seismic response of the structure is governed by weak column - strong beam behavior, which can lead to an undesirable column-sidesway/soft-story collapse mechanism under severe earthquake loadings. A retrofit design should seek to strengthen the vulnerable columns for strong column - weak beam behavior. Global seismic retrofits are required for improved overall structural performance. Seismic retrofit can be used to upgrade existing structures or to repair previously damaged structures for improved behavior during earthquakes.

Since the GLD R/C model was categorized as in a *moderate - "repairable"* damage state from the previous earthquakes (Bracci et al., 1992b), retrofit was required to reinstate a *"serviceable"* condition. The retrofit considered not only to repair the previous seismic damage but also to upgrade the structural strength to resist any future earthquakes or large lateral loads. Several retrofit methods were presented and analyzed in various global arrangements for a future strong ground motion. Based on response behavior and several factors concerning modeling, the improved concrete jacketing alternative of the critical interior columns with discontinuous added rebars at the foundation was selected to retrofit the model structure. Prestressing of the added reinforcement was applied to enhance the shear strength of the columns and beam-column joints, to supply a compressive pressure on the discontinuous beam reinforcement in the joints to deter pull-out, and provide an initial strain in the new composite section. A reinforced fillet was also used in the beam-column joints to ensure elastic joint behavior and to provide additional embedment length for the discontinuous beam reinforcement.

5.1.2 Experimental Studies

The characteristics of the retrofitted model in comparison with the original damaged model can be summarized:

1. Large story stiffness and corresponding natural frequency increases after retrofit from column strengthening and stiffening.

2. Decreased "equivalent viscous damping" factors from smaller contributions from hysteretic damping. Post-tensioning reduces the degree of cracking in the structure and thus lowers the equivalent damping.

The seismic behavior of the retrofitted model during the moderate (Taft N21E, PGA 0.20 g) and severe (Taft N21E, PGA 0.30 g) earthquakes can be summarized:

1. Large first story drifts of 1.37% and 2.13% of the story height, respectively. However the second and third story drifts were considerably smaller.

2. The retrofit beam-column joints (R/C fillet) remained primarily elastic throughout the shaking.

3. Cracking and yielding was observed in the interior beams at the ends of the fillet. The moment demands in the exterior beams remained primarily below yielding. The interior beam moment demands exceeded moment capacities that considered slab steel contributions from the full slab width. Strength increases in excess of 30% were observed due to strain hardening of the rebars and dynamic strain rate effects.

4. The columns remained primarily undamaged with exceptions to the lower first story columns. A desirable beam-sidesway mechanism was apparently in development, however beam hinging was not observed in the upper stories. Thus the complete beam-sideway collapse mechanism had not formed.

5. For a typical beam-column-slab component, the nominal moment capacity of the retrofitted columns were about 59% stronger than the nominal strength capacity of the beams that considered slab steel contributions from the full slab width.

6. The response was governed by the first mode of vibration.

7. Large reduction in first story stiffness (60%) and corresponding first natural frequencies (about 35%) occurred after the moderate and severe shaking.

8. The equivalent viscous damping factors were determined to have doubled after the moderate and severe earthquakes due to contributions from hysteretic damping.

9. The measured base shear force demands were 25.0% and 26.4% of the total structural weight for the moderate and severe shaking, respectively. Note that base shear demands were increased about 70% after retrofit as compared to before retrofit from the same earthquakes.

5.1.3 Analytical Studies

Analytical modeling, with structural parameters determined from: (i) engineering approximations; and (ii) component tests, was used to simulate the seismic response of the model.

It can be concluded that:

1. The inelastic analytical modeling based on stiffnesses obtained from engineering approximations grossly underpredicted the first story drift for the moderate and severe earthquakes by about 50%.

2. The inelastic analytical modeling based on stiffnesses obtained from component tests had different initial member values that better fit the experimental response. For the moderate and severe shaking (consecutive runs), the initial stiffness of the retrofitted columns were 0.71 $(EI_{col})_g$ with prestressing and 0.50 $(EI_{col})_g$ at the base columns (no prestressing and discontinuous added reinforcement). The initial stiffness of the interior and exterior beams were 0.32 $(EI_{bm})_g$ and 0.23 $(EI_{bm})_g$, respectively. The analytically predicted damage state was similar to the experimentally measured and observed.

3. The damage evaluation indicated *moderate - "repairable"* damage to the first story beams. The retrofitted interior and unretrofitted exterior columns of the first floor remained within a *minor - "serviceable"* damage state. The overall damage indices were 0.14 and 0.32, respectively after the moderate and severe earthquakes, which imply *minor/moderate* damage states. These are considerably less than the original building under the same earthquakes.

4. The strength reduction factors from inelastic response were comparable to the inelastic design values from UBC (1991) for the severe shaking only (near ultimate strength capacity). However for the moderate earthquake, the code based design reduction factors from UBC (1991) do not relate well with the experimentally observed.

5.2 Conclusions on Retrofit of GLD R/C Structures

Based on the proposed concrete jacketing retrofit of the critical interior columns, the following conclusions can be made about the behavior of this particular type of retrofit for GLD R/C frame structures during earthquakes:

1. Structural retrofits can be designed to successfully enforce strong column - weak beam behavior.

2. Damage can be significantly reduced in the columns by transferring the inelastic behavior to beam hinging.

3. To minimize additional foundation loads, the strengthening should seek to toughen rather than stiffen the base columns. Thus the added rebars in the columns can be discontinued at the foundation leading to only a slight increase moment demand at the foundation.

4. Inaccurate identifications of member properties in non-linear time history analyses can lead to large deviations in response predictions. Since experimental data are not available in actual structures, in extreme uses, component testing can be used to identify the initial member properties for analytical models. In other cases rational proportions of virgin properties may produce satisfactory results.

5. Stiffening and strengthening only selected critical columns can provide adequate control of the response behavior. However the integration of locally retrofitted members must be such to control the overall global response.

6. Repair and seismic retrofit of a moderately damage structure is a viable economic and structural alternative as compared to demolition and reconstruction of another. However, economical aspects must be carefully checked.

SECTION 6

REFERENCES

ACI Committee 318 (1989). "Building Code Requirements for Reinforced Concrete (ACI 318-89)", ACI, Detroit.

Al-Haddad, M.S. and Wight, J.K. (1986). "Feasibility and Consequences of Moving Beam Plastic Hinging Zones for Earthquake Resistant Design of R/C Buildings", University of Michigan/Ann Arbor, Report No. UMCE 86-1.

Applied Technology Council ATC-14 (1987). *Evaluating the Seismic Resistance of Existing Buildings*, Redwood City, California.

Aycardi, L.E., Mander, J.B., and Reinhorn, A.M. (1992). "Seismic Resistance of Reinforced Concrete Frame Structures Designed only for Gravity Loads: Part II - Experimental Performance of Subassemblages", Technical Report NCEER-92-0028, National Center for Earthquake Engineering Research, SUNY/Buffalo.

Benjamin, J. and Williams, H. (1958). "The Behavior Of One-Story Brick Shear Walls", *Proceedings*, American Society of Civil Engineers (ASCE), Vol. 84, ST4, July, 1723-1 - 1723-30.

Beres, A., El-Borgi, S., White, R.N., and Gergely, P. (1992), "Full-Scale Tests of Retrofitted Beam-Column Joints in Lightly Reinforced Concrete Frame Buildings", NIST Project 50SBNB1C6543, Report #2 (of 3).

Bertero, V.V. and Brokken, S. (1983). "Infills In Seismic Resistant Buildings", *Proceedings, Journal of Structural Engineering*, ASCE, Vol. 109, No. ST6, June, 1337-1361.

Bett, B.J., Klinger, R.E., and Jirsa, J.O. (1985), "Behavior of Strengthened and Repaired Reinforced Concrete Columns under Cyclic Deformations", University of Texas at Austin, PMFSEL Report No. 85-3.

Bracci, J.M., Reinhorn, A.M., and Mander, J.B. (1992a). "Seismic Resistance of Reinforced Concrete Frame Structures Designed only for Gravity Loads: Part I - Design and Properties of a One-Third Scale Model Structure", Technical Report NCEER-92-0027, National Center for Earthquake Engineering Research, SUNY/Buffalo.

Bracci, J.M., Reinhorn, A.M., and Mander, J.B. (1992b). "Seismic Resistance of Reinforced Concrete Frame Structures Designed only for Gravity Loads: Part III - Experimental Performance and Analytical Study of Structural Model", Technical Report NCEER-92-0029, National Center for Earthquake Engineering Research, SUNY/Buffalo. (submitted)

Buchanan, A.H. (1979). "Diagonal Beam Reinforcing for Ductile Frames", *Bulletin of the New Zealand National Society for Earthquake Engineering*, Vol. 12, No. 4, December, 346-356.

Chai, Y.H., Priestley, M.J.N., and Seible, F. (1991). "Seismic Retrofit of Circular Bridge Columns for Enhanced Flexural Performance", *ACI Structural Journal*, Vol. 88, No. 5, September-October, 572-584.

Choudhuri, D., Mander, J.B., and Reinhorn, A.M. (1992). "Evaluation of Seismic Retrofit of Reinforced Concrete Frame Structures: Part I - Experimental Performance of Retrofitted Subassemblages", Technical Report NCEER-92-0030, National Center for Earthquake Engineering Research, SUNY/Buffalo.

El-Attar, A.G., White, R.N., and Gergely, P. (1991a). "Shaking Table Test of a 1/6 Scale Two-Story Lightly Reinforced Concrete Building", Technical Report NCEER-91-0017, National Center for Earthquake Engineering Research, SUNY/Buffalo.

El-Attar, A.G., White, R.N., and Gergely, P. (1991b). "Shaking Table Test of a 1/8 Scale Three-Story Lightly Reinforced Concrete Building", Technical Report NCEER-91-0018, National Center for Earthquake Engineering Research, SUNY/Buffalo.

Esteva, L. (1966). "Behavior Under Alternating Loads Of Masonry Diaphrams Framed by Reinforced Concrete Members", *Proceedings, The International Symposium On the Effects Of Repeated Loading On Materials and Structural Systems (RILEM)*, Vol. 5, Mexico.

Fiorato, A., Sozen, M., and Gamble, W. (1970). "An Investigation Of The Interaction Of Reinforced Concrete Frames With Masonry Filler Walls", University of Illinois, Report No. UILU-ENG-70-100, November.

Iglesias, J. (1986). "Repairing and Strengthening of Reinforced Concrete Buildings Damaged in 1985 Mexico City Earthquakes", *Proceedings, The Mexico Earthquakes 1985: Factors Involved and Lessons Learned*, ASCE, September.

Kahn, L. and Hanson, R. (1976). "Reinforced Concrete Infilled Shear Walls For Aseismic Strengthening", University of Michigan/Ann Arbor, Report No. UMEE 76S1, January.

Klinger, R.E. and Bertero, V.V. (1976). "Infilled Frames In Earthquake Resistant Construction", Earthquake Engineering Research Center, University of California/Berkeley, California, Report No. EERC 76-32, December.

Krause, G.L. and Wight, J.K. (1990). "Strengthening and Modeling of Reinforced Concrete Frames for Seismic Forces", University of Michigan/Ann Arbor, Report No. UMCE 90-23.

Kunnath, S.K., Reinhorn, A.M., and Park, Y.J. (1990). "Analytical Modeling of Inelastic Seismic Response of R/C Structures", *Journal of Structural Engineering*, ASCE, Vol. 116, No. 4, April, 996-1017.

Lao, Larry F. (1990). "The Effect of Detailing on the Seismic Performance of Gravity Load Dominated Reinforced Concrete Frames", MS Thesis, State University of New York at Buffalo.

Mander, J.B., Priestley, M.J.N., and Park, R. (1988a). "Observed Stress-Strain Behavior of Confined Concrete", *Journal of Structural Engineering*, ASCE, Vol. 114, No. 8, August, 1827-1849.

Mander, J.B., Priestley, M.J.N., and Park, R. (1988b). "Theoretical Stress-Strain Model for Confined Concrete", *Journal of Structural Engineering*, ASCE, Vol. 114, No. 8, August, 1804-1826.

Parducci, A. and Mezzi, M. (1980). "Repeated Horizontal Displacements Of Infilled Frames Having Different Stiffnesses and Connection Systems: Experimental Analysis", *Proceedings, Seventh WCEE*, Vol. 7, 193-198, Istanbul, Turkey.

Park, R. and Milburn, J.R. (1983). "Comparison of Recent New Zealand and United States Seismic Design Provisions fro Reinforced Concrete Beam-Column Joints and Test Results for Four Units Designed According to the New Zealand Code", *Bulletin of the New Zealand National Society of Earthquake Engineering*, Vol .16, No. 1, March, 21-42.

Park, R. and Paulay, T. (1975). *Reinforced Concrete Structures*, John Wiley and Sons, Inc.

Park, Y.J., Ang, A. H-S., and Wen, Y.K. (1985). "Mechanistic Seismic Damage Model for Reinforced Concrete", *Journal of Structural Engineering*, ASCE, Vol. 111, No. 4, 722-739.

Paulay, T. (1989). "Equilibrium Criteria for Reinforced Concrete Beam-Column Joints", *ACI Structural Journal*, Vol. 86, No. 6, November-December, 635-643.

Paulay, T. and Bull, I.N. (1979). "Shear Effect on Plastic Hinges of Earthquake Resisting Reinforced Concrete Frames", *Bulletin D'Information 132*, Comite Euro-International du Beton, April, 165-172.

Paulay, T. and Priestley, M.J.N. (1992). *Seismic Design of Reinforced Concrete and Masonry Buildings*, John Wiley and Sons, Inc., New York.

Priestly, M. (1980). "Masonry Structural Systems For Regions Of High Seismicity", *Proceedings, Seventh WCEE*, Vol. 4, 441-448, Istanbul, Turkey.

Recommended Provisions for the Development of Seismic Regulations for New Buildings, NEHRP 1991 Edition, FEMA 222/January 1992, Washington D.C.

STAAD™ (1989). *Integrated Structural Design System*, Research Engineers, Inc., New Jersey.

Stafford Smith, B. and Carter, C. (1969). "A Method Of Analysis For Infilled Frames", *Proceedings, Institution of Civil Engineers (London)*, Vol. 44, September, 31-48.

Stoppenhagen, D.R. and Jirsa, J.O. (1987). "Seismic Repair of a Reinforced Concrete Frame Using Encased Columns", University of Texas at Austin, PMFSEL Report No. 87-2.

Uniform Building Code (UBC) (1991). International Conference of Building Officials, Whittier, California.

Wolfgram-French, C., Thorp, G.A., and Tsai, W.J. (1990). "Epoxy Repair Techniques for Moderate Earthquake Damage", *ACI Structural Journal*, July-August, 416-424.

NATIONAL CENTER FOR EARTHQUAKE ENGINEERING RESEARCH
LIST OF TECHNICAL REPORTS

The National Center for Earthquake Engineering Research (NCEER) publishes technical reports on a variety of subjects related to earthquake engineering written by authors funded through NCEER. These reports are available from both NCEER's Publications Department and the National Technical Information Service (NTIS). Requests for reports should be directed to the Publications Department, National Center for Earthquake Engineering Research, State University of New York at Buffalo, Red Jacket Quadrangle, Buffalo, New York 14261. Reports can also be requested through NTIS, 5285 Port Royal Road, Springfield, Virginia 22161. NTIS accession numbers are shown in parenthesis, if available.

NCEER-87-0001 "First-Year Program in Research, Education and Technology Transfer," 3/5/87, (PB88-134275/AS).

NCEER-87-0002 "Experimental Evaluation of Instantaneous Optimal Algorithms for Structural Control," by R.C. Lin, T.T. Soong and A.M. Reinhorn, 4/20/87, (PB88-134341/AS).

NCEER-87-0003 "Experimentation Using the Earthquake Simulation Facilities at University at Buffalo," by A.M. Reinhorn and R.L. Ketter, to be published.

NCEER-87-0004 "The System Characteristics and Performance of a Shaking Table," by J.S. Hwang, K.C. Chang and G.C. Lee, 6/1/87, (PB88-134259/AS). This report is available only through NTIS (see address given above).

NCEER-87-0005 "A Finite Element Formulation for Nonlinear Viscoplastic Material Using a Q Model," by O. Gyebi and G. Dasgupta, 11/2/87, (PB88-213764/AS).

NCEER-87-0006 "Symbolic Manipulation Program (SMP) - Algebraic Codes for Two and Three Dimensional Finite Element Formulations," by X. Lee and G. Dasgupta, 11/9/87, (PB88-219522/AS).

NCEER-87-0007 "Instantaneous Optimal Control Laws for Tall Buildings Under Seismic Excitations," by J.N. Yang, A. Akbarpour and P. Ghaemmaghami, 6/10/87, (PB88-134333/AS).

NCEER-87-0008 "IDARC: Inelastic Damage Analysis of Reinforced Concrete Frame - Shear-Wall Structures," by Y.J. Park, A.M. Reinhorn and S.K. Kunnath, 7/20/87, (PB88-134325/AS).

NCEER-87-0009 "Liquefaction Potential for New York State: A Preliminary Report on Sites in Manhattan and Buffalo," by M. Budhu, V. Vijayakumar, R.F. Giese and L. Baumgras, 8/31/87, (PB88-163704/AS). This report is available only through NTIS (see address given above).

NCEER-87-0010 "Vertical and Torsional Vibration of Foundations in Inhomogeneous Media," by A.S. Veletsos and K.W. Dotson, 6/1/87, (PB88-134291/AS).

NCEER-87-0011 "Seismic Probabilistic Risk Assessment and Seismic Margins Studies for Nuclear Power Plants," by Howard H.M. Hwang, 6/15/87, (PB88-134267/AS).

NCEER-87-0012 "Parametric Studies of Frequency Response of Secondary Systems Under Ground-Acceleration Excitations," by Y. Yong and Y.K. Lin, 6/10/87, (PB88-134309/AS).

NCEER-87-0013 "Frequency Response of Secondary Systems Under Seismic Excitation," by J.A. HoLung, J. Cai and Y.K. Lin, 7/31/87, (PB88-134317/AS).

NCEER-87-0014 "Modelling Earthquake Ground Motions in Seismically Active Regions Using Parametric Time Series Methods," by G.W. Ellis and A.S. Cakmak, 8/25/87, (PB88-134283/AS).

NCEER-87-0015 "Detection and Assessment of Seismic Structural Damage," by E. DiPasquale and A.S. Cakmak, 8/25/87, (PB88-163712/AS).

NCEER-87-0016 "Pipeline Experiment at Parkfield, California," by J. Isenberg and E. Richardson, 9/15/87, (PB88-163720/AS). This report is available only through NTIS (see address given above).

NCEER-87-0017 "Digital Simulation of Seismic Ground Motion," by M. Shinozuka, G. Deodatis and T. Harada, 8/31/87, (PB88-155197/AS). This report is available only through NTIS (see address given above).

NCEER-87-0018 "Practical Considerations for Structural Control: System Uncertainty, System Time Delay and Truncation of Small Control Forces," J.N. Yang and A. Akbarpour, 8/10/87, (PB88-163738/AS).

NCEER-87-0019 "Modal Analysis of Nonclassically Damped Structural Systems Using Canonical Transformation," by J.N. Yang, S. Sarkani and F.X. Long, 9/27/87, (PB88-187851/AS).

NCEER-87-0020 "A Nonstationary Solution in Random Vibration Theory," by J.R. Red-Horse and P.D. Spanos, 11/3/87, (PB88-163746/AS).

NCEER-87-0021 "Horizontal Impedances for Radially Inhomogeneous Viscoelastic Soil Layers," by A.S. Veletsos and K.W. Dotson, 10/15/87, (PB88-150859/AS).

NCEER-87-0022 "Seismic Damage Assessment of Reinforced Concrete Members," by Y.S. Chung, C. Meyer and M. Shinozuka, 10/9/87, (PB88-150867/AS). This report is available only through NTIS (see address given above).

NCEER-87-0023 "Active Structural Control in Civil Engineering," by T.T. Soong, 11/11/87, (PB88-187778/AS).

NCEER-87-0024 "Vertical and Torsional Impedances for Radially Inhomogeneous Viscoelastic Soil Layers," by K.W. Dotson and A.S. Veletsos, 12/87, (PB88-187786/AS).

NCEER-87-0025 "Proceedings from the Symposium on Seismic Hazards, Ground Motions, Soil-Liquefaction and Engineering Practice in Eastern North America," October 20-22, 1987, edited by K.H. Jacob, 12/87, (PB88-188115/AS).

NCEER-87-0026 "Report on the Whittier-Narrows, California, Earthquake of October 1, 1987," by J. Pantelic and A. Reinhorn, 11/87, (PB88-187752/AS). This report is available only through NTIS (see address given above).

NCEER-87-0027 "Design of a Modular Program for Transient Nonlinear Analysis of Large 3-D Building Structures," by S. Srivastav and J.F. Abel, 12/30/87, (PB88-187950/AS).

NCEER-87-0028 "Second-Year Program in Research, Education and Technology Transfer," 3/8/88, (PB88-219480/AS).

NCEER-88-0001 "Workshop on Seismic Computer Analysis and Design of Buildings With Interactive Graphics," by W. McGuire, J.F. Abel and C.H. Conley, 1/18/88, (PB88-187760/AS).

NCEER-88-0002 "Optimal Control of Nonlinear Flexible Structures," by J.N. Yang, F.X. Long and D. Wong, 1/22/88, (PB88-213772/AS).

NCEER-88-0003 "Substructuring Techniques in the Time Domain for Primary-Secondary Structural Systems," by G.D. Manolis and G. Juhn, 2/10/88, (PB88-213780/AS).

NCEER-88-0004 "Iterative Seismic Analysis of Primary-Secondary Systems," by A. Singhal, L.D. Lutes and P.D. Spanos, 2/23/88, (PB88-213798/AS).

NCEER-88-0005 "Stochastic Finite Element Expansion for Random Media," by P.D. Spanos and R. Ghanem, 3/14/88, (PB88-213806/AS).

NCEER-88-0006 "Combining Structural Optimization and Structural Control," by F.Y. Cheng and C.P. Pantelides, 1/10/88, (PB88-213814/AS).

NCEER-88-0007 "Seismic Performance Assessment of Code-Designed Structures," by H.H-M. Hwang, J-W. Jaw and H-J. Shau, 3/20/88, (PB88-219423/AS).

NCEER-88-0008 "Reliability Analysis of Code-Designed Structures Under Natural Hazards," by H.H-M. Hwang, H. Ushiba and M. Shinozuka, 2/29/88, (PB88-229471/AS).

NCEER-88-0009 "Seismic Fragility Analysis of Shear Wall Structures," by J-W Jaw and H.H-M. Hwang, 4/30/88, (PB89-102867/AS).

NCEER-88-0010 "Base Isolation of a Multi-Story Building Under a Harmonic Ground Motion - A Comparison of Performances of Various Systems," by F-G Fan, G. Ahmadi and I.G. Tadjbakhsh, 5/18/88, (PB89-122238/AS).

NCEER-88-0011 "Seismic Floor Response Spectra for a Combined System by Green's Functions," by F.M. Lavelle, L.A. Bergman and P.D. Spanos, 5/1/88, (PB89-102875/AS).

NCEER-88-0012 "A New Solution Technique for Randomly Excited Hysteretic Structures," by G.Q. Cai and Y.K. Lin, 5/16/88, (PB89-102883/AS).

NCEER-88-0013 "A Study of Radiation Damping and Soil-Structure Interaction Effects in the Centrifuge," by K. Weissman, supervised by J.H. Prevost, 5/24/88, (PB89-144703/AS).

NCEER-88-0014 "Parameter Identification and Implementation of a Kinematic Plasticity Model for Frictional Soils," by J.H. Prevost and D.V. Griffiths, to be published.

NCEER-88-0015 "Two- and Three- Dimensional Dynamic Finite Element Analyses of the Long Valley Dam," by D.V. Griffiths and J.H. Prevost, 6/17/88, (PB89-144711/AS).

NCEER-88-0016 "Damage Assessment of Reinforced Concrete Structures in Eastern United States," by A.M. Reinhorn, M.J. Seidel, S.K. Kunnath and Y.J. Park, 6/15/88, (PB89-122220/AS).

NCEER-88-0017 "Dynamic Compliance of Vertically Loaded Strip Foundations in Multilayered Viscoelastic Soils," by S. Ahmad and A.S.M. Israil, 6/17/88, (PB89-102891/AS).

NCEER-88-0018 "An Experimental Study of Seismic Structural Response With Added Viscoelastic Dampers," by R.C. Lin, Z. Liang, T.T. Soong and R.H. Zhang, 6/30/88, (PB89-122212/AS). This report is available only through NTIS (see address given above).

NCEER-88-0019 "Experimental Investigation of Primary - Secondary System Interaction," by G.D. Manolis, G. Juhn and A.M. Reinhorn, 5/27/88, (PB89-122204/AS).

NCEER-88-0020 "A Response Spectrum Approach For Analysis of Nonclassically Damped Structures," by J.N. Yang, S. Sarkani and F.X. Long, 4/22/88, (PB89-102909/AS).

NCEER-88-0021 "Seismic Interaction of Structures and Soils: Stochastic Approach," by A.S. Veletsos and A.M. Prasad, 7/21/88, (PB89-122196/AS).

NCEER-88-0022 "Identification of the Serviceability Limit State and Detection of Seismic Structural Damage," by E. DiPasquale and A.S. Cakmak, 6/15/88, (PB89-122188/AS). This report is available only through NTIS (see address given above).

NCEER-88-0023 "Multi-Hazard Risk Analysis: Case of a Simple Offshore Structure," by B.K. Bhartia and E.H. Vanmarcke, 7/21/88, (PB89-145213/AS).

NCEER-88-0024 "Automated Seismic Design of Reinforced Concrete Buildings," by Y.S. Chung, C. Meyer and M. Shinozuka, 7/5/88, (PB89-122170/AS). This report is available only through NTIS (see address given above)

NCEER-88-0025 "Experimental Study of Active Control of MDOF Structures Under Seismic Excitations," by L.L. Chung, R.C. Lin, T.T. Soong and A.M. Reinhorn, 7/10/88, (PB89-122600/AS).

NCEER-88-0026 "Earthquake Simulation Tests of a Low-Rise Metal Structure," by J.S. Hwang, K.C. Chang, G.C. Lee and R.L. Ketter, 8/1/88, (PB89-102917/AS).

NCEER 88-0027 "Systems Study of Urban Response and Reconstruction Due to Catastrophic Earthquakes," by F. Kozin and H.K. Zhou, 9/22/88, (PB90-162348/AS).

NCEER-88-0028 "Seismic Fragility Analysis of Plane Frame Structures," by H.H-M. Hwang and Y.K. Low, 7/31/88, (PB89-131445/AS).

NCEER-88-0029 "Response Analysis of Stochastic Structures," by A. Kardara, C. Bucher and M. Shinozuka, 9/22/88, (PB89-174429/AS).

NCEER-88-0030 "Nonnormal Accelerations Due to Yielding in a Primary Structure," by D.C.K. Chen and L.D. Lutes, 9/19/88, (PB89-131437/AS).

NCEER 88-0031 "Design Approaches for Soil-Structure Interaction," by A.S. Veletsos, A.M. Prasad and Y. Tang, 12/30/88, (PB89-174437/AS). This report is available only through NTIS (see address given above).

NCEER-88-0032 "A Re-evaluation of Design Spectra for Seismic Damage Control," by C.J. Turkstra and A.G. Tallin, 11/7/88, (PB89-145221/AS).

NCEER-88-0033 "The Behavior and Design of Noncontact Lap Splices Subjected to Repeated Inelastic Tensile Loading," by V.E. Sagan, P. Gergely and R.N. White, 12/8/88, (PB89-163737/AS).

NCEER-88-0034 "Seismic Response of Pile Foundations," by S.M. Mamoon, P.K. Banerjee and S. Ahmad, 11/1/88, (PB89-145239/AS).

NCEER-88-0035 "Modeling of R/C Building Structures With Flexible Floor Diaphragms (IDARC2)," by A.M. Reinhorn, S.K. Kunnath and N. Panahshahi, 9/7/88, (PB89-207153/AS).

NCEER-88-0036 "Solution of the Dam-Reservoir Interaction Problem Using a Combination of FEM, BEM with Particular Integrals, Modal Analysis, and Substructuring," by C-S. Tsai, G.C. Lee and R.L. Ketter, 12/31/88, (PB89-207146/AS).

NCEER-88-0037 "Optimal Placement of Actuators for Structural Control," by F.Y. Cheng and C.P. Pantelides, 8/15/88, (PB89-162846/AS).

NCEER-88-0038 "Teflon Bearings in Aseismic Base Isolation: Experimental Studies and Mathematical Modeling," by A. Mokha, M.C. Constantinou and A.M. Reinhorn, 12/5/88, (PB89-218457/AS). This report is available only through NTIS (see address given above).

NCEER-88-0039 "Seismic Behavior of Flat Slab High-Rise Buildings in the New York City Area," by P. Weidlinger and M. Ettouney, 10/15/88, (PB90-145681/AS).

NCEER-88-0040 "Evaluation of the Earthquake Resistance of Existing Buildings in New York City," by P. Weidlinger and M. Ettouney, 10/15/88, to be published.

NCEER-88-0041 "Small-Scale Modeling Techniques for Reinforced Concrete Structures Subjected to Seismic Loads," by W. Kim, A. El-Attar and R.N. White, 11/22/88, (PB89-189625/AS).

NCEER-88-0042 "Modeling Strong Ground Motion from Multiple Event Earthquakes," by G.W. Ellis and A.S. Cakmak, 10/15/88, (PB89-174445/AS).

NCEER-88-0043 "Nonstationary Models of Seismic Ground Acceleration," by M. Grigoriu, S.E. Ruiz and E. Rosenblueth, 7/15/88, (PB89-189617/AS).

NCEER-88-0044 "SARCF User's Guide: Seismic Analysis of Reinforced Concrete Frames," by Y.S. Chung, C. Meyer and M. Shinozuka, 11/9/88, (PB89-174452/AS).

NCEER-88-0045 "First Expert Panel Meeting on Disaster Research and Planning," edited by J. Pantelic and J. Stoyle, 9/15/88, (PB89-174460/AS).

NCEER-88-0046 "Preliminary Studies of the Effect of Degrading Infill Walls on the Nonlinear Seismic Response of Steel Frames," by C.Z. Chrysostomou, P. Gergely and J.F. Abel, 12/19/88, (PB89-208383/AS).

NCEER-88-0047 "Reinforced Concrete Frame Component Testing Facility - Design, Construction, Instrumentation and Operation," by S.P. Pessiki, C. Conley, T. Bond, P. Gergely and R.N. White, 12/16/88, (PB89-174478/AS).

NCEER-89-0001 "Effects of Protective Cushion and Soil Compliancy on the Response of Equipment Within a Seismically Excited Building," by J.A. HoLung, 2/16/89, (PB89-207179/AS).

NCEER-89-0002 "Statistical Evaluation of Response Modification Factors for Reinforced Concrete Structures," by H.H-M. Hwang and J-W. Jaw, 2/17/89, (PB89-207187/AS).

NCEER-89-0003 "Hysteretic Columns Under Random Excitation," by G-Q. Cai and Y.K. Lin, 1/9/89, (PB89-196513/AS).

NCEER-89-0004 "Experimental Study of 'Elephant Foot Bulge' Instability of Thin-Walled Metal Tanks," by Z-H. Jia and R.L. Ketter, 2/22/89, (PB89-207195/AS).

NCEER-89-0005 "Experiment on Performance of Buried Pipelines Across San Andreas Fault," by J. Isenberg, E. Richardson and T.D. O'Rourke, 3/10/89, (PB89-218440/AS).

NCEER-89-0006 "A Knowledge-Based Approach to Structural Design of Earthquake-Resistant Buildings," by M. Subramani, P. Gergely, C.H. Conley, J.F. Abel and A.H. Zaghw, 1/15/89, (PB89-218465/AS).

NCEER-89-0007 "Liquefaction Hazards and Their Effects on Buried Pipelines," by T.D. O'Rourke and P.A. Lane, 2/1/89, (PB89-218481).

NCEER-89-0008 "Fundamentals of System Identification in Structural Dynamics," by H. Imai, C-B. Yun, O. Maruyama and M. Shinozuka, 1/26/89, (PB89-207211/AS).

NCEER-89-0009 "Effects of the 1985 Michoacan Earthquake on Water Systems and Other Buried Lifelines in Mexico," by A.G. Ayala and M.J. O'Rourke, 3/8/89, (PB89-207229/AS).

NCEER-89-R010 "NCEER Bibliography of Earthquake Education Materials," by K.E.K. Ross, Second Revision, 9/1/89, (PB90-125352/AS).

NCEER-89-0011 "Inelastic Three-Dimensional Response Analysis of Reinforced Concrete Building Structures (IDARC-3D), Part I - Modeling," by S.K. Kunnath and A.M. Reinhorn, 4/17/89, (PB90-114612/AS).

NCEER-89-0012 "Recommended Modifications to ATC-14," by C.D. Poland and J.O. Malley, 4/12/89, (PB90-108648/AS).

NCEER-89-0013 "Repair and Strengthening of Beam-to-Column Connections Subjected to Earthquake Loading," by M. Corazao and A.J. Durrani, 2/28/89, (PB90-109885/AS).

NCEER-89-0014 "Program EXKAL2 for Identification of Structural Dynamic Systems," by O. Maruyama, C-B. Yun, M. Hoshiya and M. Shinozuka, 5/19/89, (PB90-109877/AS).

NCEER-89-0015 "Response of Frames With Bolted Semi-Rigid Connections, Part I - Experimental Study and Analytical Predictions," by P.J. DiCorso, A.M. Reinhorn, J.R. Dickerson, J.B. Radziminski and W.L. Harper, 6/1/89, to be published.

NCEER-89-0016 "ARMA Monte Carlo Simulation in Probabilistic Structural Analysis," by P.D. Spanos and M.P. Mignolet, 7/10/89, (PB90-109893/AS).

NCEER-89-P017 "Preliminary Proceedings from the Conference on Disaster Preparedness - The Place of Earthquake Education in Our Schools," Edited by K.E.K. Ross, 6/23/89

NCEER-89-0017 "Proceedings from the Conference on Disaster Preparedness - The Place of Earthquake Education in Our Schools," Edited by K.E.K. Ross, 12/31/89, (PB90-207895). This report is available only through NTIS (see address given above).

NCEER-89-0018 "Multidimensional Models of Hysteretic Material Behavior for Vibration Analysis of Shape Memory Energy Absorbing Devices, by E.J. Graesser and F.A. Cozzarelli, 6/7/89, (PB90-164146/AS).

NCEER-89-0019 "Nonlinear Dynamic Analysis of Three-Dimensional Base Isolated Structures (3D-BASIS)," by S. Nagarajaiah, A.M. Reinhorn and M.C. Constantinou, 8/3/89, (PB90-161936/AS). This report is available only through NTIS (see address given above).

NCEER-89-0020 "Structural Control Considering Time-Rate of Control Forces and Control Rate Constraints," by F.Y. Cheng and C.P. Pantelides, 8/3/89, (PB90-120445/AS).

NCEER-89-0021 "Subsurface Conditions of Memphis and Shelby County," by K.W. Ng, T-S. Chang and H-H.M. Hwang, 7/26/89, (PB90-120437/AS)

NCEER-89-0022 "Seismic Wave Propagation Effects on Straight Jointed Buried Pipelines," by K. Elhmadi and M.J. O'Rourke, 8/24/89, (PB90-162322/AS).

NCEER-89-0023 "Workshop on Serviceability Analysis of Water Delivery Systems," edited by M. Grigoriu, 3/6/89, (PB90-127424/AS).

NCEER-89-0024 "Shaking Table Study of a 1/5 Scale Steel Frame Composed of Tapered Members," by K.C. Chang, J.S. Hwang and G.C. Lee, 9/18/89, (PB90-160169/AS).

NCEER-89-0025 "DYNA1D: A Computer Program for Nonlinear Seismic Site Response Analysis - Technical Documentation," by Jean H. Prevost, 9/14/89, (PB90-161944/AS). This report is available only through NTIS (see address given above).

NCEER-89-0026 "1:4 Scale Model Studies of Active Tendon Systems and Active Mass Dampers for Aseismic Protection," by A.M. Reinhorn, T.T. Soong, R.C. Lin, Y.P. Yang, Y. Fukao, H. Abe and M. Nakai, 9/15/89, (PB90-173246/AS).

NCEER-89-0027 "Scattering of Waves by Inclusions in a Nonhomogeneous Elastic Half Space Solved by Boundary Element Methods," by P.K. Hadley, A. Askar and A.S. Cakmak, 6/15/89, (PB90-145699/AS).

NCEER-89-0028 "Statistical Evaluation of Deflection Amplification Factors for Reinforced Concrete Structures," by H.H.M. Hwang, J-W. Jaw and A.L. Ch'ng, 8/31/89, (PB90-164633/AS).

NCEER-89-0029 "Bedrock Accelerations in Memphis Area Due to Large New Madrid Earthquakes," by H.H.M. Hwang, C.H.S. Chen and G. Yu, 11/7/89, (PB90-162330/AS).

NCEER-89-0030 "Seismic Behavior and Response Sensitivity of Secondary Structural Systems," by Y.Q. Chen and T.T. Soong, 10/23/89, (PB90-164658/AS).

NCEER-89-0031 "Random Vibration and Reliability Analysis of Primary-Secondary Structural Systems," by Y. Ibrahim, M. Grigoriu and T.T. Soong, 11/10/89, (PB90-161951/AS).

NCEER-89-0032 "Proceedings from the Second U.S. - Japan Workshop on Liquefaction, Large Ground Deformation and Their Effects on Lifelines, September 26-29, 1989," Edited by T.D. O'Rourke and M. Hamada, 12/1/89, (PB90-209388/AS).

NCEER-89-0033 "Deterministic Model for Seismic Damage Evaluation of Reinforced Concrete Structures," by J.M. Bracci, A.M. Reinhorn, J.B. Mander and S.K. Kunnath, 9/27/89.

NCEER-89-0034 "On the Relation Between Local and Global Damage Indices," by E. DiPasquale and A.S. Cakmak, 8/15/89, (PB90-173865).

NCEER-89-0035 "Cyclic Undrained Behavior of Nonplastic and Low Plasticity Silts," by A.J. Walker and H.E. Stewart, 7/26/89, (PB90-183518/AS).

NCEER-89-0036 "Liquefaction Potential of Surficial Deposits in the City of Buffalo, New York," by M. Budhu, R. Giese and L. Baumgrass, 1/17/89, (PB90-208455/AS).

NCEER-89-0037 "A Deterministic Assessment of Effects of Ground Motion Incoherence," by A.S. Veletsos and Y. Tang, 7/15/89, (PB90-164294/AS).

NCEER-89-0038 "Workshop on Ground Motion Parameters for Seismic Hazard Mapping," July 17-18, 1989, edited by R.V. Whitman, 12/1/89, (PB90-173923/AS).

NCEER-89-0039 "Seismic Effects on Elevated Transit Lines of the New York City Transit Authority," by C.J. Costantino, C.A. Miller and E. Heymsfield, 12/26/89, (PB90-207887/AS).

NCEER-89-0040 "Centrifugal Modeling of Dynamic Soil-Structure Interaction," by K. Weissman, Supervised by J.H. Prevost, 5/10/89, (PB90-207879/AS).

NCEER-89-0041 "Linearized Identification of Buildings With Cores for Seismic Vulnerability Assessment," by I-K. Ho and A.E. Aktan, 11/1/89, (PB90-251943/AS).

NCEER-90-0001 "Geotechnical and Lifeline Aspects of the October 17, 1989 Loma Prieta Earthquake in San Francisco," by T.D. O'Rourke, H.E. Stewart, F.T. Blackburn and T.S. Dickerman, 1/90, (PB90-208596/AS).

NCEER-90-0002 "Nonnormal Secondary Response Due to Yielding in a Primary Structure," by D.C.K. Chen and L.D. Lutes, 2/28/90, (PB90-251976/AS).

NCEER-90-0003 "Earthquake Education Materials for Grades K-12," by K.E.K. Ross, 4/16/90, (PB91-113415/AS).

NCEER-90-0004 "Catalog of Strong Motion Stations in Eastern North America," by R.W. Busby, 4/3/90, (PB90-251984)/AS.

NCEER-90-0005 "NCEER Strong-Motion Data Base: A User Manual for the GeoBase Release (Version 1.0 for the Sun3)," by P. Friberg and K. Jacob, 3/31/90 (PB90-258062/AS).

NCEER-90-0006 "Seismic Hazard Along a Crude Oil Pipeline in the Event of an 1811-1812 Type New Madrid Earthquake," by H.H.M. Hwang and C-H.S. Chen, 4/16/90(PB90-258054).

NCEER-90-0007 "Site-Specific Response Spectra for Memphis Sheahan Pumping Station," by H.H.M. Hwang and C.S. Lee, 5/15/90, (PB91-108811/AS).

NCEER-90-0008 "Pilot Study on Seismic Vulnerability of Crude Oil Transmission Systems," by T. Ariman, R. Dobry, M. Grigoriu, F. Kozin, M. O'Rourke, T. O'Rourke and M. Shinozuka, 5/25/90, (PB91-108837/AS).

NCEER-90-0009 "A Program to Generate Site Dependent Time Histories: EQGEN," by G.W. Ellis, M. Srinivasan and A.S. Cakmak, 1/30/90, (PB91-108829/AS).

NCEER-90-0010 "Active Isolation for Seismic Protection of Operating Rooms," by M.E. Talbott, Supervised by M. Shinozuka, 6/8/9, (PB91-110205/AS).

NCEER 90-0011 "Program LINEARID for Identification of Linear Structural Dynamic Systems," by C-B. Yun and M. Shinozuka, 6/25/90, (PB91-110312/AS).

NCEER-90-0012 "Two-Dimensional Two-Phase Elasto-Plastic Seismic Response of Earth Dams," by A.N. Yiagos, Supervised by J.H. Prevost, 6/20/90, (PB91-110197/AS).

NCEER-90-0013 "Secondary Systems in Base-Isolated Structures: Experimental Investigation, Stochastic Response and Stochastic Sensitivity," by G.D. Manolis, G. Juhn, M.C. Constantinou and A.M. Reinhorn, 7/1/90, (PB91-110320/AS).

NCEER-90-0014 "Seismic Behavior of Lightly-Reinforced Concrete Column and Beam-Column Joint Details," by S.P. Pessiki, C.H. Conley, P. Gergely and R.N. White, 8/22/90, (PB91-108795/AS).

NCEER-90-0015 "Two Hybrid Control Systems for Building Structures Under Strong Earthquakes," by J.N. Yang and A. Danielians, 6/29/90, (PB91-125393/AS).

NCEER-90-0016 "Instantaneous Optimal Control with Acceleration and Velocity Feedback," by J.N. Yang and Z. Li, 6/29/90, (PB91-125401/AS).

NCEER-90-0017 "Reconnaissance Report on the Northern Iran Earthquake of June 21, 1990," by M. Mehrain, 10/4/90, (PB91-125377/AS).

NCEER-90-0018 "Evaluation of Liquefaction Potential in Memphis and Shelby County," by T.S. Chang, P.S. Tang, C.S. Lee and H. Hwang, 8/10/90, (PB91-125427/AS).

NCEER-90-0019 "Experimental and Analytical Study of a Combined Sliding Disc Bearing and Helical Steel Spring Isolation System," by M.C. Constantinou, A.S. Mokha and A.M. Reinhorn, 10/4/90, (PB91-125385/AS).

NCEER-90-0020 "Experimental Study and Analytical Prediction of Earthquake Response of a Sliding Isolation System with a Spherical Surface," by A.S. Mokha, M.C. Constantinou and A.M. Reinhorn, 10/11/90, (PB91-125419/AS).

NCEER-90-0021 "Dynamic Interaction Factors for Floating Pile Groups," by G. Gazetas, K. Fan, A. Kaynia and E. Kausel, 9/10/90, (PB91-170381/AS).

NCEER-90-0022 "Evaluation of Seismic Damage Indices for Reinforced Concrete Structures," by S. Rodriguez-Gomez and A.S. Cakmak, 9/30/90, PB91-171322/AS).

NCEER-90-0023 "Study of Site Response at a Selected Memphis Site," by H. Desai, S. Ahmad, E.S. Gazetas and M.R. Oh, 10/11/90, (PB91-196857/AS).

NCEER-90-0024 "A User's Guide to Strongmo: Version 1.0 of NCEER's Strong-Motion Data Access Tool for PCs and Terminals," by P.A. Friberg and C.A.T. Susch, 11/15/90, (PB91-171272/AS).

NCEER-90-0025 "A Three-Dimensional Analytical Study of Spatial Variability of Seismic Ground Motions," by L-L. Hong and A.H.-S. Ang, 10/30/90, (PB91-170399/AS).

NCEER-90-0026 "MUMOID User's Guide - A Program for the Identification of Modal Parameters," by S. Rodriguez-Gomez and E. DiPasquale, 9/30/90, (PB91-171298/AS).

NCEER-90-0027 "SARCF-II User's Guide - Seismic Analysis of Reinforced Concrete Frames," by S. Rodriguez-Gomez, Y.S. Chung and C. Meyer, 9/30/90, (PB91-171280/AS).

NCEER-90-0028 "Viscous Dampers: Testing, Modeling and Application in Vibration and Seismic Isolation," by N. Makris and M.C. Constantinou, 12/20/90 (PB91-190561/AS).

NCEER-90-0029 "Soil Effects on Earthquake Ground Motions in the Memphis Area," by H. Hwang, C.S. Lee, K.W. Ng and T.S. Chang, 8/2/90, (PB91-190751/AS).

NCEER-91-0001 "Proceedings from the Third Japan-U.S. Workshop on Earthquake Resistant Design of Lifeline Facilities and Countermeasures for Soil Liquefaction, December 17-19, 1990," edited by T.D. O'Rourke and M. Hamada, 2/1/91, (PB91-179259/AS).

NCEER-91-0002 "Physical Space Solutions of Non-Proportionally Damped Systems," by M. Tong, Z. Liang and G.C. Lee, 1/15/91, (PB91-179242/AS).

NCEER-91-0003 "Seismic Response of Single Piles and Pile Groups," by K. Fan and G. Gazetas, 1/10/91, (PB92-174994/AS).

NCEER-91-0004 "Damping of Structures: Part 1 - Theory of Complex Damping," by Z. Liang and G. Lee, 10/10/91, (PB92-197235/AS).

NCEER-91-0005 "3D-BASIS - Nonlinear Dynamic Analysis of Three Dimensional Base Isolated Structures: Part II," by S. Nagarajaiah, A.M. Reinhorn and M.C. Constantinou, 2/28/91, (PB91-190553/AS).

NCEER-91-0006 "A Multidimensional Hysteretic Model for Plasticity Deforming Metals in Energy Absorbing Devices," by E.J. Graesser and F.A. Cozzarelli, 4/9/91, (PB92-108364/AS).

NCEER-91-0007 "A Framework for Customizable Knowledge-Based Expert Systems with an Application to a KBES for Evaluating the Seismic Resistance of Existing Buildings," by E.G. Ibarra-Anaya and S.J. Fenves, 4/9/91, (PB91-210930/AS).

NCEER-91-0008 "Nonlinear Analysis of Steel Frames with Semi-Rigid Connections Using the Capacity Spectrum Method," by G.G. Deierlein, S-H. Hsieh, Y-J. Shen and J.F. Abel, 7/2/91, (PB92-113828/AS).

NCEER-91-0009 "Earthquake Education Materials for Grades K-12," by K.E.K. Ross, 4/30/91, (PB91-212142/AS).

NCEER-91-0010 "Phase Wave Velocities and Displacement Phase Differences in a Harmonically Oscillating Pile," by N. Makris and G. Gazetas, 7/8/91, (PB92-108356/AS).

NCEER-91-0011 "Dynamic Characteristics of a Full-Size Five-Story Steel Structure and a 2/5 Scale Model," by K.C. Chang, G.C. Yao, G.C. Lee, D.S. Hao and Y.C. Yeh," 7/2/91.

NCEER-91-0012 "Seismic Response of a 2/5 Scale Steel Structure with Added Viscoelastic Dampers," by K.C. Chang, T.T. Soong, S-T. Oh and M.L. Lai, 5/17/91 (PB92-110816/AS).

NCEER-91-0013 "Earthquake Response of Retaining Walls; Full-Scale Testing and Computational Modeling," by S. Alampalli and A-W.M. Elgamal, 6/20/91, to be published.

NCEER-91-0014 "3D-BASIS-M: Nonlinear Dynamic Analysis of Multiple Building Base Isolated Structures," by P.C. Tsopelas, S. Nagarajaiah, M.C. Constantinou and A.M. Reinhorn, 5/28/91, (PB92-113885/AS).

NCEER-92-0007 "Engineering Evaluation of Permanent Ground Deformations Due to Seismically-Induced Liquefaction," by M.H. Baziar, R. Dobry and A-W.M. Elgamal, 3/24/92, (PB92-222421/AS).

NCEER-92-0008 "A Procedure for the Seismic Evaluation of Buildings in the Central and Eastern United States," by C.D. Poland and J.O. Malley, 4/2/92, (PB92-222439/AS).

NCEER-92-0009 "Experimental and Analytical Study of a Hybrid Isolation System Using Friction Controllable Sliding Bearings," by M.Q. Feng, S. Fuji and M. Shinozuka, 5/15/92, (PB93-150282/AS).

NCEER-92-0010 "Seismic Resistance of Slab-Column Connections in Existing Non-Ductile Flat-Plate Buildings," by A.J. Durrani and Y. Du, 5/18/92.

NCEER-92-0011 "The Hysteretic and Dynamic Behavior of Brick Masonry Walls Upgraded by Ferrocement Coatings Under Cyclic Loading and Strong Simulated Ground Motion," by H. Lee and S.P. Prawel, 5/11/92, to be published.

NCEER-92-0012 "Study of Wire Rope Systems for Seismic Protection of Equipment in Buildings," by G.F. Demetriades, M.C. Constantinou and A.M. Reinhorn, 5/20/92.

NCEER-92-0013 "Shape Memory Structural Dampers: Material Properties, Design and Seismic Testing," by P.R. Witting and F.A. Cozzarelli, 5/26/92

NCEER-92-0014 "Longitudinal Permanent Ground Deformation Effects on Buried Continuous Pipelines," by M.J. O'Rourke, and C. Nordberg, 6/15/92.

NCEER-92-0015 "A Simulation Method for Stationary Gaussian Random Functions Based on the Sampling Theorem," by M. Grigoriu and S. Balopoulou, 6/11/92, (PB93-127496/AS).

NCEER-92-0016 "Gravity-Load-Designed Reinforced Concrete Buildings: Seismic Evaluation of Existing Construction and Detailing Strategies for Improved Seismic Resistance," by G.W. Hoffmann, S.K. Kunnath, J.B. Mander and A.M. Reinhorn, 7/15/92, to be published.

NCEER-92-0017 "Observations on Water System and Pipeline Performance in the Limón Area of Costa Rica Due to the April 22, 1991 Earthquake," by M. O'Rourke and D. Ballantyne, 6/30/92, (PB93-126811/AS).

NCEER-92-0018 "Fourth Edition of Earthquake Education Materials for Grades K-12," Edited by K.E.K. Ross, 8/10/92.

NCEER-92-0019 "Proceedings from the Fourth Japan-U.S. Workshop on Earthquake Resistant Design of Lifeline Facilities and Countermeasures for Soil Liquefaction," Edited by M. Hamada and T.D. O'Rourke, 8/12/92.

NCEER-92-0020 "Active Bracing System: A Full Scale Implementation of Active Control," by A.M. Reinhorn, T.T. Soong, R.C. Lin, M.A. Riley, Y.P. Wang, S. Aizawa and M. Higashino, 8/14/92, (PB93-127512/AS).

NCEER-92-0021 "Empirical Analysis of Horizontal Ground Displacement Generated by Liquefaction-Induced Lateral Spreads," by S.F. Bartlett and T.L. Youd, 8/17/92.

NCEER-92-0022 "IDARC Version 3.0: Inelastic Damage Analysis of Reinforced Concrete Structures," by S.K. Kunnath, A.M. Reinhorn and R.F. Lobo, 8/31/92, to be published.

NCEER-92-0023 "A Semi-Empirical Analysis of Strong-Motion Peaks in Terms of Seismic Source, Propagation Path and Local Site Conditions, by M. Kamiyama, M.J. O'Rourke and R. Flores-Berrones, 9/9/92, (PB93-150266/AS).

NCEER-92-0024 "Seismic Behavior of Reinforced Concrete Frame Structures with Nonductile Details, Part I: Summary of Experimental Findings of Full Scale Beam-Column Joint Tests," by A. Beres, R.N. White and P. Gergely, 9/30/92, to be published.

NCEER-92-0025 "Experimental Results of Repaired and Retrofitted Beam-Column Joint Tests in Lightly Reinforced Concrete Frame Buildings," by A. Beres, S. El-Borgi, R.N. White and P. Gergely, 10/29/92, to be published.

NCEER-92-0026 "A Generalization of Optimal Control Theory: Linear and Nonlinear Structures," by J.N. Yang, Z. Li and S. Vongchavalitkul, 11/2/92.

NCEER-92-0027 "Seismic Resistance of Reinforced Concrete Frame Structures Designed Only for Gravity Loads: Part I - Design and Properties of a One-Third Scale Model Structure," by J.M. Bracci, A.M. Reinhorn and J.B. Mander, 12/1/92, to be published.

NCEER-92-0028 "Seismic Resistance of Reinforced Concrete Frame Structures Designed Only for Gravity Loads: Part II - Experimental Performance of Subassemblages," by L.E. Aycardi, J.B. Mander and A.M. Reinhorn, 12/1/92, to be published.

NCEER-92-0029 "Seismic Resistance of Reinforced Concrete Frame Structures Designed Only for Gravity Loads: Part III - Experimental Performance and Analytical Study of a Structural Model," by J.M. Bracci, A.M. Reinhorn and J.B. Mander, 12/1/92, to be published.

NCEER-92-0030 "Evaluation of Seismic Retrofit of Reinforced Concrete Frame Structures: Part I - Experimental Performance of Retrofitted Subassemblages," by D. Choudhuri, J.B. Mander and A.M. Reinhorn, 12/8/92.

NCEER-92-0031 "Evaluation of Seismic Retrofit of Reinforced Concrete Frame Structures: Part II - Experimental Performance and Analytical Study of a Retrofitted Structural Model," by J.M. Bracci, A.M. Reinhorn and J.B. Mander, 12/8/92.